NASA CONTRACTOR REPORT

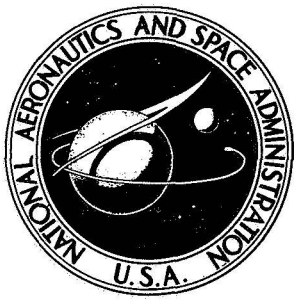

NASA CR-2300

NASA CR-2300

NONLINEAR TRANSIENT ANALYSIS OF MULTI-MASS FLEXIBLE ROTORS THEORY AND APPLICATIONS

by R. Gordon Kirk and Edgar J. Gunter

Prepared by
UNIVERSITY OF VIRGINIA
Charlottesville, Va. 22904
for Lewis Research Center

NATIONAL AERONAUTICS AND SPACE ADMINISTRATION • WASHINGTON, D. C. • SEPTEMBER 1973

1. Report No. NASA CR-2300	2. Government Accession No.	3. Recipient's Catalog No.
4. Title and Subtitle NONLINEAR TRANSIENT ANALYSIS OF MULTI-MASS FLEXIBLE ROTORS - THEORY AND APPLICATIONS		5. Report Date September 1973 6. Performing Organization Code
7. Author(s) R. Gordon Kirk and Edgar J. Gunter		8. Performing Organization Report No. ME-4040-112-72U 10. Work Unit No.
9. Performing Organization Name and Address University of Virginia Charlottesville, Virginia 22904		11. Contract or Grant No. NGL 47-005-050
12. Sponsoring Agency Name and Address National Aeronautics and Space Administration Washington, D.C. 20546		13. Type of Report and Period Covered Contractor Report 14. Sponsoring Agency Code

15. Supplementary Notes

Project Manager, Robert E. Cunningham, Fluid System Components Division, NASA Lewis Research Center, Cleveland, Ohio

16. Abstract

The equations of motion necessary to compute the transient response of multi-mass flexible rotors are formulated to include unbalance, rotor acceleration, and flexible damped nonlinear bearing stations. A method of calculating the unbalance response of flexible rotors from a modified Myklestad-Prohl technique is discussed in connection with the method of solution for the transient response. Several special cases of simplified rotor-bearing systems are presented and analyzed for steady-state response, stability, and transient behavior. These simplified rotor models produce extensive design information necessary to insure stable performance of elastic mounted rotor-bearing systems under varying levels and forms of excitation. The nonlinear journal bearing force expressions derived from the short bearing approximation are utilized in the study of the stability and transient response of the floating bush squeeze damper support system. Both rigid and flexible rotor models are studied, and results indicate that the stability of flexible rotors supported by journal bearings can be greatly improved by the use of squeeze damper supports. Results from linearized stability studies of flexible rotors indicate that a tuned support system can greatly improve the performance of the units from the standpoint of unbalance response and impact loading. Extensive stability and design charts may be readily produced for given rotor specifications by the computer codes presented in this analysis.

17. Key Words (Suggested by Author(s))	18. Distribution Statement
Rotor dynamics, Flexible rotors, Flexible shafts, Damped supports, Rotor response, Rotor stability	Unclassified - unlimited

19. Security Classif. (of this report)	20. Security Classif. (of this page)	21. No. of Pages	22. Price*
Unclassified	Unclassified	264	$3.00

* For sale by the National Technical Information Service, Springfield, Virginia 22151

TABLE OF CONTENTS

TABLE OF CONTENTS (Continued)

TABLE OF CONTENTS (Contents)

LIST OF FIGURES

LIST OF FIGURES (Continued)

LIST OF FIGURES (Continued)

LIST OF FIGURES (Continued)

LIST OF FIGURES (Continued)

LIST OF FIGURES (Continued)

LIST OF FIGURES (Continued)

LIST OF FIGURES (Continued)

LIST OF FIGURES (Continued)

LIST OF FIGURES (Continued)

LIST OF TABLES

NOMENCLATURE

SYMBOL	DESCRIPTION	UNITS
a	length from left end of rotor to first major bearing station	in.
$\vec{a}$	acceleration	in./sec.^{2}
A	critical amplitude on rigid support	---
A_i	coefficient for steady-state solution	in.
ACX	amplification factor in x-dir. for rigid supports	---
ACY	amplification factor in y-dir. for rigid supports	---
b	length from left end of rotor to second major bearing	in.
$(B.F.)_x$	total bearing force in x-dir.	lb.
$(B.F.)_y$	total bearing force in y-dir.	lb.
c	radial clearance of journal	
c	ratio of damping values, $= c_1/c_2$	---
c_i	damping at major mass stations	lb.-sec./in.
c_i	internal damping	lb.-sec./in.
c_s	rotor shaft damping	lb.-sec./in.
c_{xx}, c_{xy} c_{yx}, c_{yy}	bearing damping	lb.-sec./in.
c_{1xx}, c_{1xy} c_{1yx}, c_{1yy}	support damping	lb.-sec./in.
C	radial clearance of journal	in.
C_1	support damping	
C_2	rotor damping	lb.-sec./in.

NOMENCLATURE (Continued)

SYMBOL	DESCRIPTION	UNITS
CIX,CIY	support damping	lb.-sec./in.
CBX,CBY	bearing damping	lb.-sec./in.
C_B	bearing damping	lb.-sec./in.
$\overline{C}_B$	dimensionless bearing damping = $C_B/m_2\omega_g$	---
C_i	internal damping	lb.-sec./in.
CI	internal damping	lb.-sec./in.
CI_i	internal damping at i^{th} major mass station	lb.-sec./in.
C_{i_x}, C_{i_y}	couple acting at i^{th} major mass station	in.-lb.
C_o	damping for squeeze damper from circular synchronous precession	---
C_s	rotor shaft damping	lb.-sec./in.
CL	journal clearance	in.
CS	rotor shaft damping	lb.-sec./in.
C_{xx}, C_{xy} } C_{yx}, C_{yy}	bearing damping	lb.-sec./in.
C_{1xx}, C_{1xy} } C_{1yx}, C_{1yy}	support damping	lb.-sec./in.
D	journal diameter	in.
e	journal radial displacement from bearing center	in.
e_μ	unbalance eccentricity	in.
E_μ	unbalance eccentricity ratio, = e_μ/c	---
EMU	unbalance eccentricity	---

SYMBOL	DESCRIPTION	UNITS
ENX,ENY	percent synchronous speed of harmonic force	---
ES	equilibrium eccentricity	in.
ESU	equilibrium eccentricity calculated from unbalance load	in.
EU	unbalance eccentricity	mils.
$\vec{F}_i^{(inertia)}$	inertia load at i^{th} station	lb.
F_o	rotating load on journal	lb.
F_{s_x}, F_{s_y}	support force	lb.
F_x, F_y	force components	lb.
F_{x_1}, F_{x_2}	bearing forces at major bearing locations	lb.
$\hat{F}_x, \hat{F}_y$	fluid-film bearing forces	lb.
FHX,FHY	harmonic force on journal	lb.
FMAX	maximum force	lb.
FMAXB	maximum force to bearing	lb.
FMAXS	maximum force to support	lb.
FU	rotating unbalance load	lb.
FURATIO	ratio of unbalance to weight	---
F_{x_i}, F_{y_i}	total unidirectional load at i^{th} station with exception of absolute inertia load $(m\ddot{q})_i$	lb.
H_{x_i}, H_{y_i}	total torque at i^{th} rotor station with exception of inertia torque $(I_T\ddot{q})_i$	in.-lb.

NOMENCLATURE (Continued)

SYMBOL	DESCRIPTION	UNITS
$\vec{i},\vec{j},\vec{k}$	unit vector set in fixed reference coordinates	---
I_{ij}	moment of inertia	lb.-in.-sec.^{2}
I_p	polar moment of inertia	lb.-in.-sec.^{2}
I_T	transverse moment of inertia	lb.-in.-sec.^{2}
I_{p_i}	polar moment of inertia of i^{th} major mass station	lb.-in.-sec.^{2}
I_{T_i}	transverse moment of inertia of i^{th} major mass station	lb.-in.-sec.^{2}
IC	internal damping	lb.-sec. /in.
JC	journal radial clearance	in.
JL	journal length	in.
JMU@5	journal bearing fluid vicosity x 10^5	reyns
JR	journal radius	in.
K_B	bearing housing stiffness	lb./in.
$\overline{K}_B$	dimensionless housing stiffness	---
K_{s_i}	external shaft stiffness at i^{th} major mass station	lb./in.
K_{xx}, K_{xy} K_{yx}, K_{yy}	bearing stiffness	lb./in.
K_{1xx}, K_{1xy} K_{1yx}, K_{1yy}	support stiffness	lb./in.
K	ratio of support to rotor shaft stiffness, = K_1/K_2	---

NOMENCLATURE (Continued)

SYMBOL	DESCRIPTION	UNIT
K_1	support stiffness	lb./in.
K_2	rotor shaft stiffness	lb./in.
K_o	pseudo stiffness of damper journal bearing	lb./in.
KBX,KBY	support stiffness	lb./in.
KS	rotor shaft stiffness	lb./in.
KIX,KIY	support stiffness	lb./in.
K	torsional stiffness	in.-lb.
ℓ_i	length to rotor stations from left end of shaft	in.
L	bearing span of major bearing stations	in.
L	length of journal bearing	in.
m_i	mass of i^{th} major mass station	lb.-sec.^{2}/in.
m_1	support mass	lb.-sec.^{2}/in.
m_2	rotor mass	lb.-sec.^{2}/in.
m_J	journal mass	lb.-sec.^{2}/in.
m_{J_1}	1^{st} major journal station mass	lb.-sec.^{2}/in.
m_{J_2}	2^{nd} major journal station mess	lb.-sec.^{2}/in.
m_{s_1}	support mass at 1^{st} major bearing	lb.-sec.^{2}/in.
m_{s_2}	support mass at 2^{nd} major bearing	lb.-sec.^{2}/in.
M	ratio of support to rotor mass	---
M_1	support mass	lb.-sec.^{2}/in.
M_2	rotor mass	lb.-sec.^{2}/in.

NOMENCLATURE (Continued)

SYMBOL	DESCRIPTION	UNIT
M_n	moment at n^{th} station for steady state analysis	in.-lb.
M'_n	moment referred to right side of n^{th} station	in.-lb.
M_x, M_y, M_z	torque	in.-lb.
MU@5	viscosity x 10^5	reyns
N	rotor speed	RPM
$\vec{P}$	position vector	in.
P_{x_i}, P_{y_i}	total transverse load at i^{th} major mass station	lb.
Q	aerodynamic cross-coupling	lb./in.
Q_i	aerodynamic cross-coupling at i^{th} major mass station	lb./in.
R	radius of journal	in.
$\vec{R}_i$	position vector to i^{th} major mass station	in.
RPMB	speed of bush damper	RPM
S	Sommerfeld number	---
SC	damper clearance	in.
SL	damper length	in.
SMU@5	damper fluid viscosity x 10^5	reyns
SS	short bearing Sommerfeld number	---
$(S.F.)_x, (S.F.)_y$	support force	lb.
SU	Sommerfeld number based on unbalance load	---
t	time	sec.

NOMENCLATURE (Continued)

SYMBOL	DESCRIPTION	UNIT
T	dimensionless time, = ωt	rad.
T_1	kinetic energy of translation	lb.-in.
T_2	kinetic energy of rotation	lb.-in.
TRDB	transmissibility of bearing	---
TRDS	transmissibility of support	---
TRSMAX	maximum dimensionless force to support	---
TRDMAX	maximum force divided by unbalance load	---
u_i, v_i	relative shaft deflection at i^{th} major mass station	in.
V	potential energy	lb.-in.
$\vec{V}$	velocity	in./sec.
V_n	shear at n^{th} station	lb.
W	load parameter = $\frac{2\pi W_j}{\mu LD} \left(\frac{2c}{L}\right)^2 \sqrt{c/g}$	...
W_1	support weight	lb.
W_2, W	rotor weight	lb.
W_j	journal weight	lb.
WB	bearing support weight	lb.
WCX, WCY	critical speed of flexible rotor on rigid housing	RPM
WJ	journal weight	lb.
WS	stability speed parameter, = $\omega/\sqrt{g/c}$	---
WT	total load on journal	lb.
x,y,z	body fixed coordinate system	---

NOMENCLATURE (Continued)

SYMBOL	DESCRIPTION	UNIT
x_1, y_1	support displacement	in.
x_2, y_2	rotor displacement (single mass model)	in.
x_j, y_j	journal relation displacement	in.
x_s, y_s	rotor relative displacement	in.
X,Y	dimensionless displacement	---
X,Y,Z	fixed reference set	---
$\overline{X}_i, \overline{Y}_i$	rigid rotor deflection at i^{th} major mass station	in.
$\overline{X}_{s_i}, \overline{Y}_{s_i}$	support displacement referred to i^{th} mass station	in.
α_{ij}	deflection at station i due to a unit load at station j	in.
β_{ij}	deflection at station i due to a unit couple at station j	in.
γ_{ij}	angular rotation at station i due to a unit couple at station j	rad.
δ	static deflection of rotor station	in.
ε	eccentricity, = e/c	---
ε_o	equilibrium eccentricity for given journal properties	---
η	fraction of synchronous speed of an external rotating load	---
$\vec{n}_x, \vec{n}_y, \vec{n}_z$	unit vector set fixed in rotating rigid body	---
θ_x	rotation in x-z plane about y-axis	rad.
θ_y	rotation in x-z plane about negative x-axis	rad.

NOMENCLATURE (Continued)

SYMBOL	DESCRIPTION	UNIT
θ,ϕ,ψ	Eulerian angles	rad.
$\theta_{x_i},\theta_{y_i}$	relative rotations of i^{th} station	rad.
$\Theta_{x_i},\Theta_{y_i}$	absolute rotation of i^{th} station	rad.
λ	assumed complex root solution of differential equations	---
ϕ	phase angle of unbalance from reference mark	rad.
ϕ_i	phase angle of unbalance at i^{th} station from reference	rad.
ϕ_{ij}	angular rotation at station i due to a unit load at station j	rad.
ω	angular velocity	$sec.^{-1}$
ω_b	damper bush spin rate	$sec.^{-1}$
ω_c	critical speed	$sec.^{-1}$
ω_g	defined as $\sqrt{g/c}$	$sec.^{-1}$
ω_s	stability parameter, $= \omega/\omega_g$	---
ω_j	journal angular speed	$sec.^{-1}$
$\vec{\Omega}$	total angular velocity vector	$sec.^{-1}$

CHAPTER I

ROTOR DYNAMICS: BACKGROUND AND STATEMENT OF THE PROBLEM

I.I Introduction

From the time the wheel was invented man has been plagued with problems of bearing lubrication and shaft dynamics. His ingenuity has produced the high-speed turbine rotors that power the giant jet liners of the present age and the vast array of process machinery that the American industrial community must keep in operation to meet the demands of our society.

A typical example of a small high-speed rotating unit is shown in Fig. I.I. This is a cut-away of the Brayton-cycle turbine-generator unit that has a design speed of 50,000 RPM and is being developed for the NASA space program. The six-stage axial compressor and single stage drive turbine compose one integral shaft system with the generator rotor and drive turbine composing the second integral rotor-bearing system. Of great importance in such a unit is the design of the bearings and bearing housing mount structures. The present analysis will be concentrating on methods of coupling bearing and rotor-shaft dynamics.

A vast amount of information has been developed to date concerning the problems of lubrication or separately the kinematics and dynamics of machinery. The interest and means of solution for the combined problem of rotor-bearing system dynamics has been evolving since the early 1960's. The earliest works in the fields of shaft vibrations and bearing whirl are important to the overall understanding of the scope of the problems of rotating equipment. The following background section will briefly

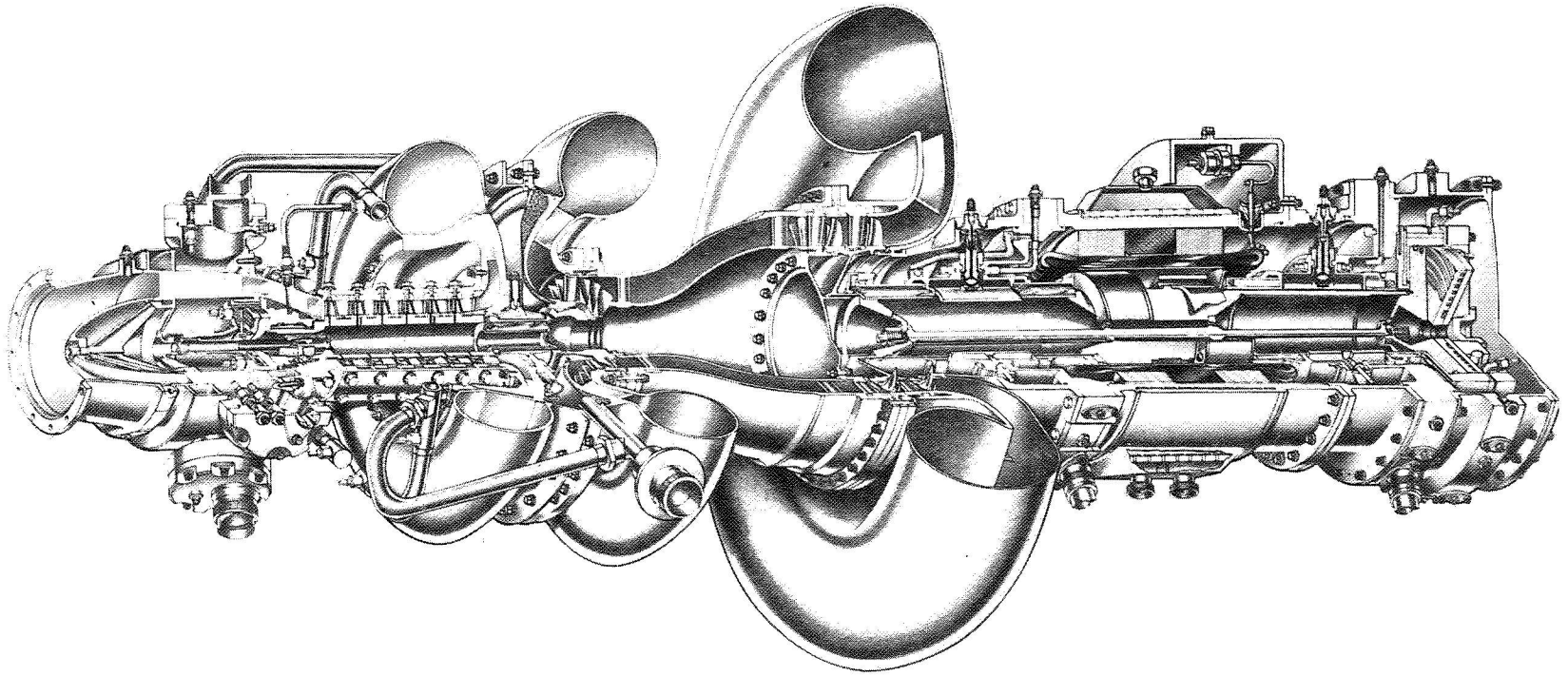

FIG. 1.1 CUT-AWAY VIEW OF BRAYTON-CYCLE TURBO-GENERATOR SET

review a portion of the earliest work but will concentrate on the present state of the art in the field of rotor-bearing dynamics.

1.2 Background

The study of rotor dynamics may be broken down into four distinct areas which have been treated in the literature. These are as follows:

1) Critical speed analysis

2) Unbalance response and the inverse problem, balancing

3) Analysis of self-excited instabilities resulting from:

   a. Fluid-film bearings

   b. Internal friction damping

   c. Aerodynamic and hydraulic cross-coupling

4) Time-transient simulation

The well-known method of Holzer for finding the torsional natural frequencies was extended by Myklestad (1) for application to the analysis of aircraft wing structures and separately by Prohl (2) who formulated the problem specifically for flexible rotors. A tabular approach as advanced in their original works has been formulated for solution on digital computers and is currently being widely used for critical speed analysis of rotating shafts.

One other major paper of the 1940's concerning critical speeds was the work of Green (3) which presented much data on the effect of gyroscopics on the single overhung disk, simply supported single disk and double disk rotors, and finally the infinite disk case. His work indicated the presence of both forward and backward critical speeds resulting from gyroscopic effects.

More recent investigations (4-10) have made slight extensions of the excellent work of Green and Myklestad-Prohl to include the effects of shear deformation and specialized cases such as the two-bearing machine with an overhung disk. Yamamoto(11) in 1954 presented a major contribution to the study of critical speeds in which he presented both theoretical and experimental observations on the phenomena of forward and backward whirl due to gyroscopic effects. Most current critical speed codes calculate only the synchronous critical speeds of forward precession.

Closely related to the problem of critical speeds is the analysis of unbalance response. A major contribution to steady-state response was the method of Lund (12,13) which uses a modified Myklestad-Prohl technique to solve for unbalance response. A detailed discussion of this approach is presented in Section 2.4. The analysis can include known speed dependent linear fluid-film bearing characteristics and support flexibility and damping. Analysis of multi-mass flexible rotors has also been conducted by Tang and Trumpler (14) and Koenig (15). The effect of support damping is very important from the viewpoint of reducing vibration amplitudes but even more important for the reduction of forces transmitted through the bearing and to the support (16,17,18).

The rotor modeled in Fig. 1.2 has been studied (19) as an extension of the early work of Jeffcott (20) and others (21,22,23) to include support flexibility and damping. The critical speeds of the resultant two-degree of freedom system are shown in Fig. 1.3 where the critical speeds divided by the rigid support critical are plotted versus the ratio of support to shaft stiffness, K, for various values of the ratio

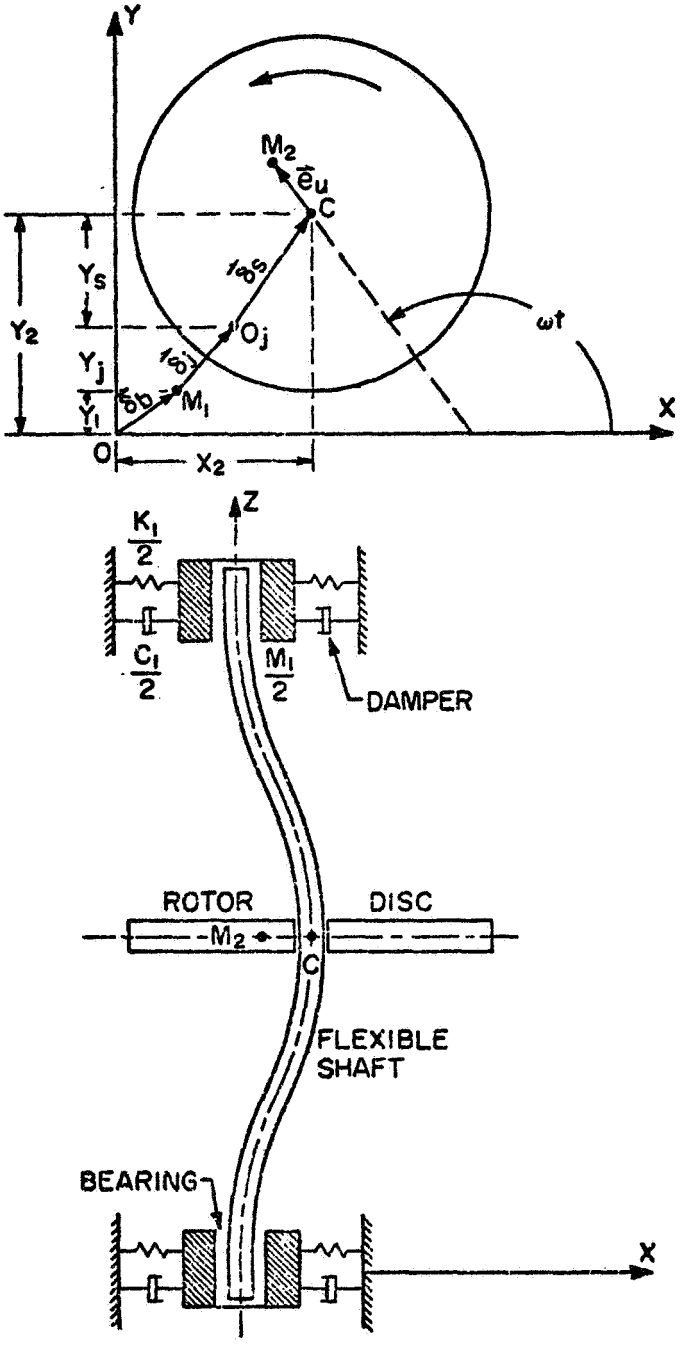

FIG. 1.2 SCHEMATIC DIAGRAM OF A SINGLE MASS ROTOR ON DAMPED ELASTIC SUPPORTS

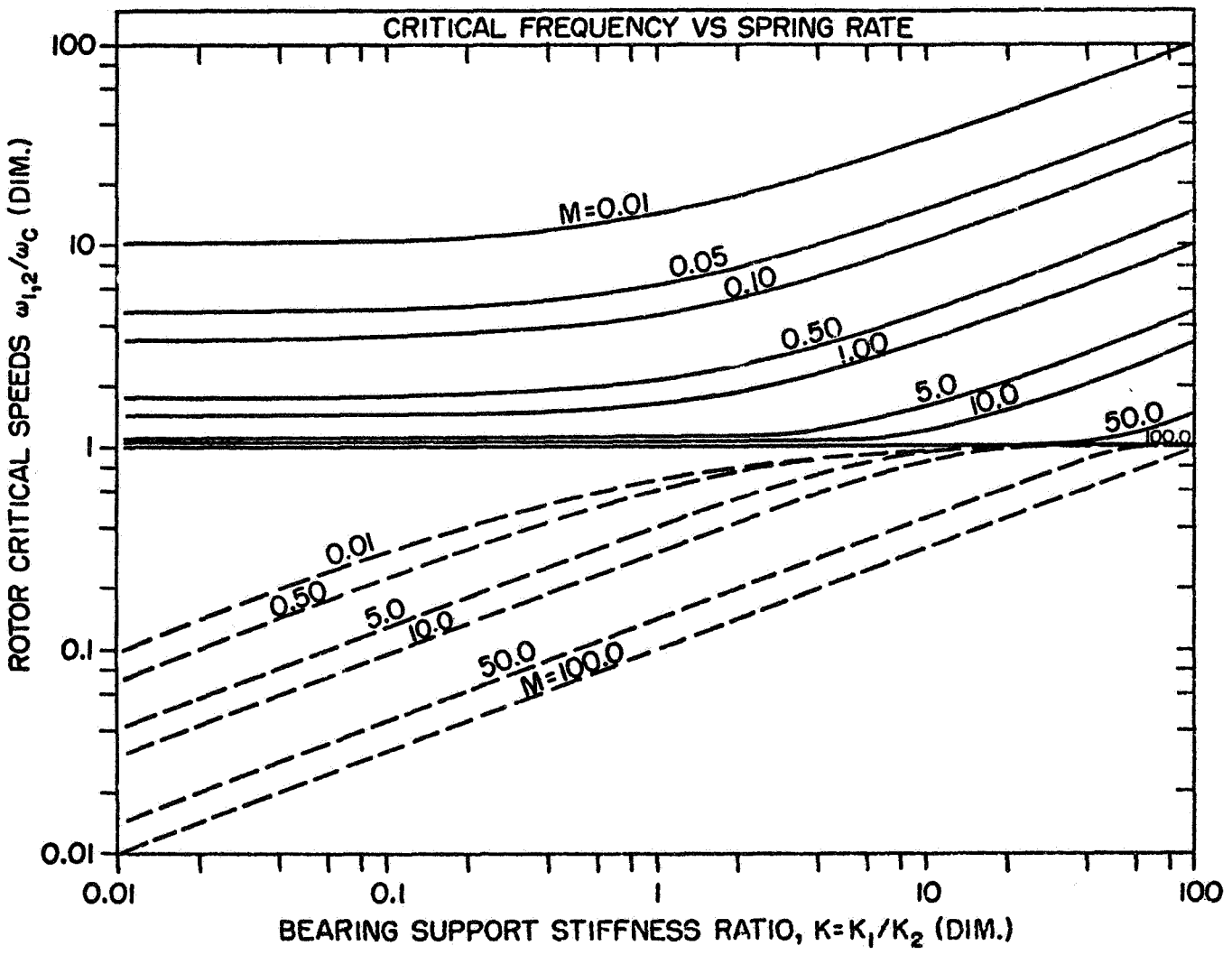

FIG. 1.3 DIMENSIONLESS CRITICAL SPEEDS VS. SUPPORT STIFFNESS RATIO FOR VARIOUS SUPPORT HOUSING MASS RATIOS

of support to rotor mass, M.

The unbalance response of this simple model can be used to illustrate several important aspects of rotor-bearing response characteristics. For example the absolute rotor response is shown in Fig. 1.4 (a) for various values of the ratio of support to rotor damping. A lightly damped support, c = 0.01, produces two distinct resonance zones in the given response range. The accompanying phase shift of the deflection with respect to the unbalance is shown in Fig. 1.4 (b) for the response of 1.4 (a). The lightly damped system is observed to go through a 180° phase shift at the first critical and another phase reversal as the second critical is passed. This phase reversal is suppressed for higher support damping as indicated in Fig. 1.4 (b). The force transmitted to the bearings is shown in Fig. 1.4 (c) where the addition of proper damping clearly would reduce the level of the forces transmitted for the bearing support. The phase shift to 180° and continuing up to 270° at the second critical is a very important concept to note and can be of great importance in the analysis of experimental data. The damped support is clearly advantageous for reduction of the forces transmitted in or near the critical speed regions of operation.

The inverse problem of unbalance response is the ever present problem of balancing of rotating equipment. The method of Thearle (24) is still being used for field balance procedure. Two basic approaches to the problem of balancing flexible rotors have been presented in the literature. The first, modal balancing, consists of balancing at a speed corresponding to the first mode, then successive trials at each of the higher modes to reach the desired speed of operation. The other method known as the

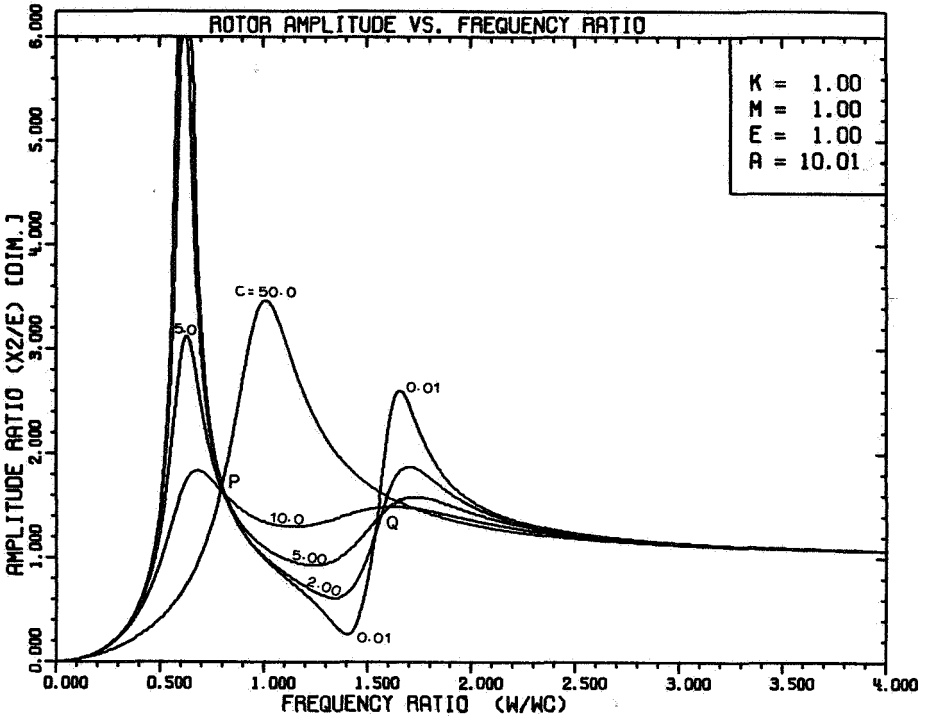

(a) ABSOLUTE ROTOR MOTION WITH A TUNED SUPPORT SYSTEM FOR VARIOUS VALUES OF SUPPORT DAMPING, K = M = 1, A = 10

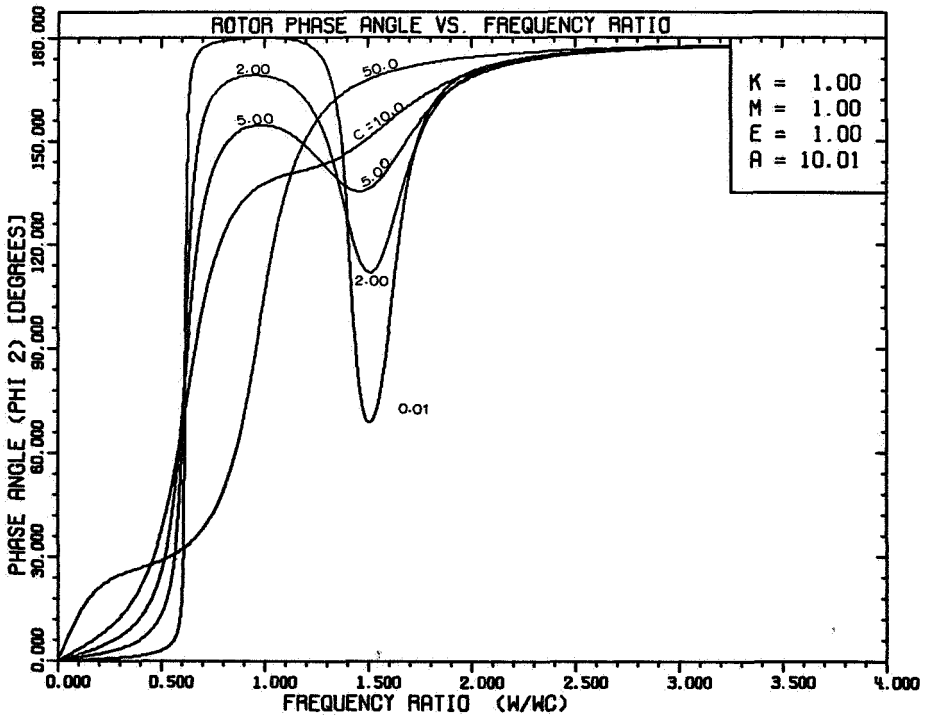

(b) PHASE ANGLE OF ABSOLUTE ROTOR MOTION RELATIVE TO UNBALANCE FOR VARIOUS VALUES OF SUPPORT DAMPING

FIG. 1.4 AMPLITUDE, PHASE, AND FORCES TRANSMITTED FOR A TYPICAL SINGLE MASS FLEXIBLE ROTOR ON DAMPED SUPPORTS

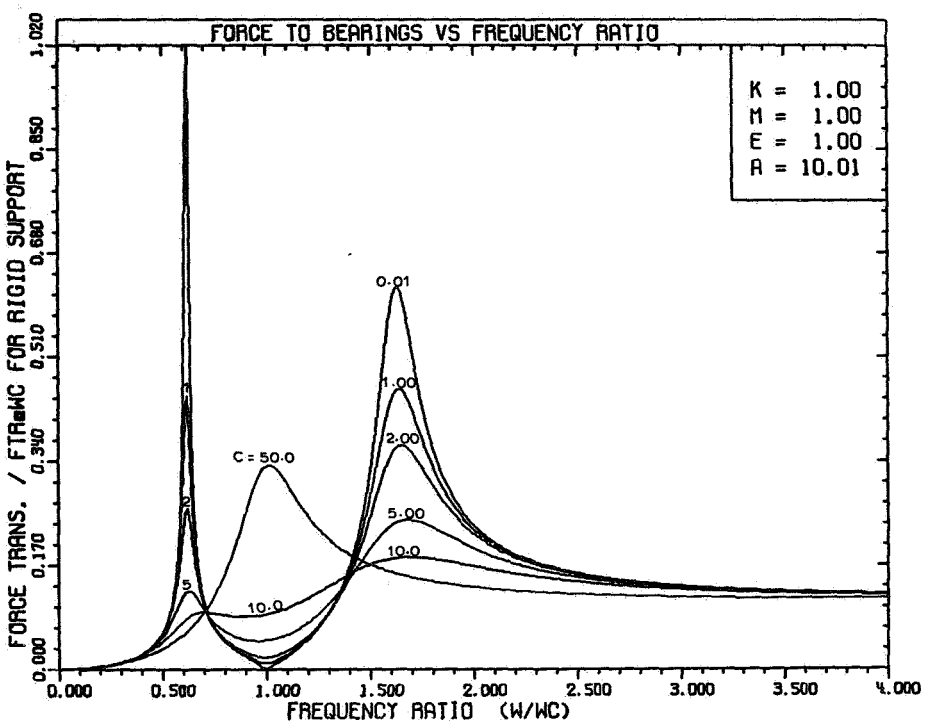

(c) DIMENSIONLESS FORCE TRANSMITTED TO BEARINGS VS SPEED RATIO FOR VARIOUS VALUES OF SUPPORT DAMPING

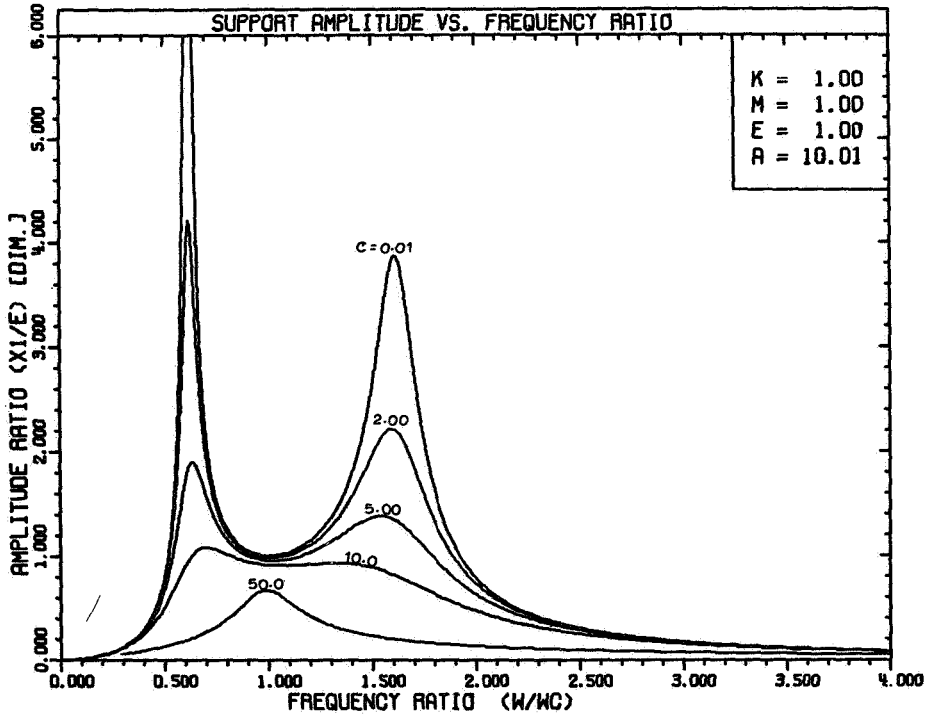

(d) SUPPORT AMPLITUDE VS SPEED FOR VARIOUS VALUES OF SUPPORT DAMPING

FIG. 1.4 CONTINUED

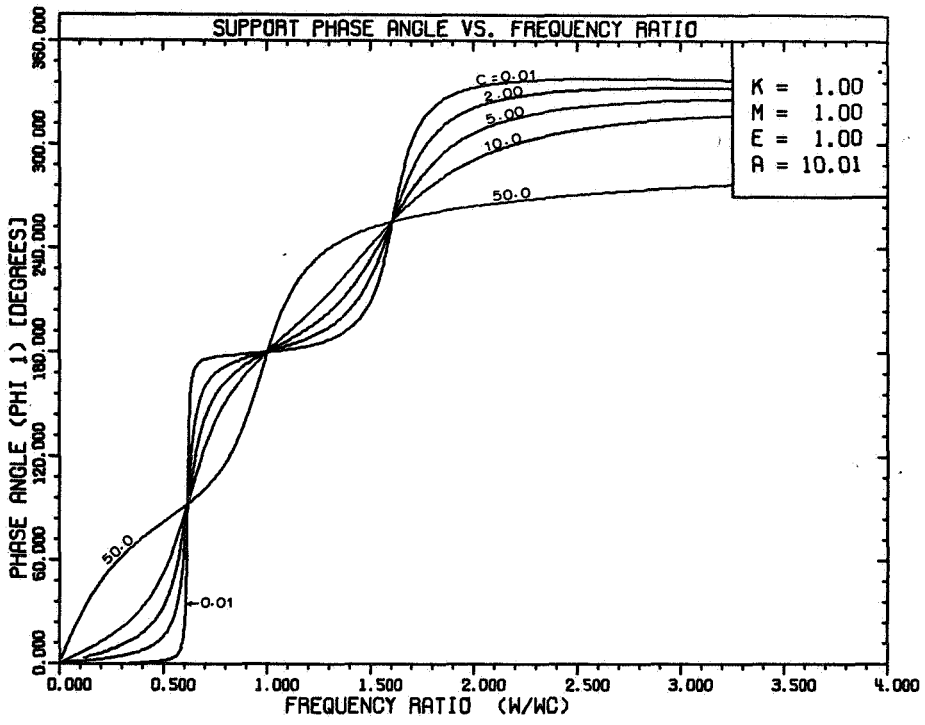

(e) PHASE ANGLE OF SUPPORT MOTION RELATIVE TO ROTOR UNBALANCE FOR VARIOUS VALUES OF SUPPORT DAMPING

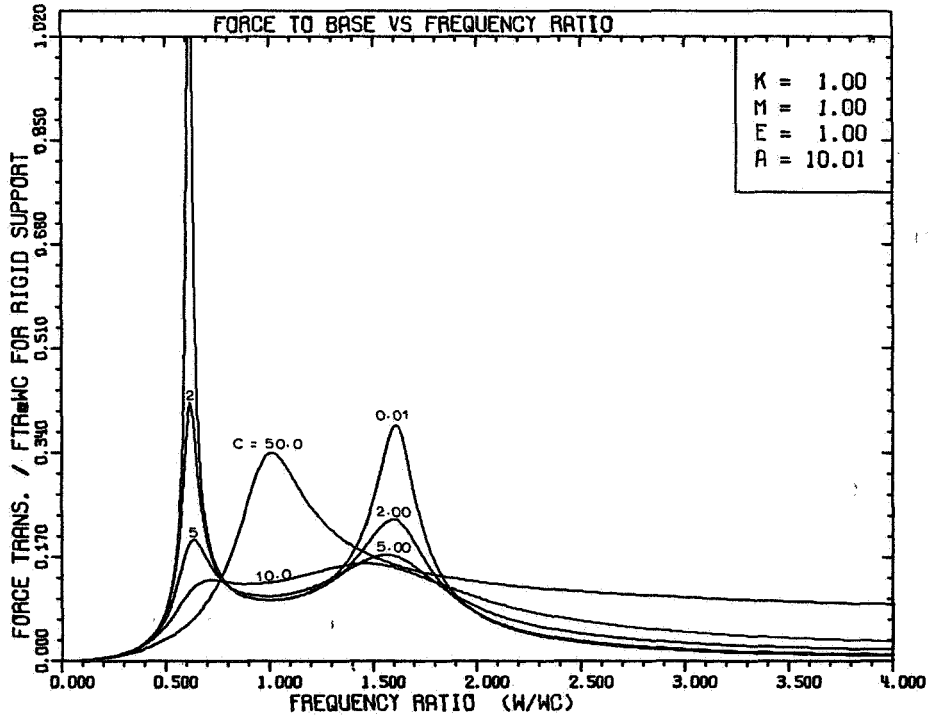

(f) DIMENSIONLESS FORCE TRANSMITTED TO FOUNDATION VS SPEED RATIO FOR VARIOUS VALUES OF SUPPORT DAMPING

FIG. 1.4 CONCLUDED

influence coefficient approach utilizes information obtained from added trial weights and response data at each of several runs to produce a matrix of coefficients which is used to predict the resultant unbalance in the rotor.

A new approach presented by Little (25) uses the influence coefficient technique coupled with the application of linear programming to arrive at the optimum response by proper choice of correction weight size at limited locations along the rotor span. The problems associated with balancing will not be directly treated in this presentation but the literature on this subject is a valuable portion of the theory of rotor dynamics (14, 26-34).

The literature contains many references to the observation and probable cause of self-excited instabilities. The earlier reports by Newkirk (35), Robertson (36), and others (37,38) on internal friction and hydrodynamic bearing instability are well referenced by Gunter (39), Ruhl (40) and also in (41,42,43). A review paper by Newkirk in 1957 (44) points out one distinguishing feature between "cramped-shaft whirl" (ie., internal friction damping) and oil-film whirl. The former may become resonant above the critical speed whereas the later does not become resonant at speeds below twice critical speed. In an earlier presentation (45) Newkirk had distinguished between certain phenomena that may occur as a result of journal bearing instability.

(1) A "half frequency whirl" may occur at any running speed the whirl frequency being slightly less than half the running speed

(2) A "resonant whirl" which occurs when the running speed is equal to or greater than twice the natural frequency of the rotor for transverse vibration at that speed.

the oil film

(4) A subharmonic vibration of an unbalanced rotor, the frequency being a definite fraction of the running speed.

Morrison and Paterson (45) presented an approach to describe the stability threshold of symmetrical two-bearing flexible rotors by one equation and thereby reducing the criterion of other investigators such as Hori (47), Holmes (48) and Pinkus and Sternlicht (49) to the general form

$$\left(\frac{\omega_n}{\omega_g}\right)^2 \leq P \left(\frac{\omega_n}{\omega}\right)^2 - Q \qquad [1.1]$$

where

ω = velocity of rotor

ω_n = natural frequency of simply supported rotor

P,Q = functions of the running condition

and

$$\left(\frac{\omega_n}{\omega_g}\right)^2 = \frac{k}{m}\,\frac{mc}{W} = \frac{c}{\delta}$$

where

c = radial clearance of bearing

δ = static deflection of rotor centerline under gravity loading

Ruhl (50) has recently presented an analysis of the stability of the short journal bearing having shaft flexibility and plots ω/ω_g versus eccentricity for various values of shaft static deflections (δ/c). The introduction of the flexible shaft reduced the stability boundary below the value for rigid rotor analysis. (See Fig. 6.6).

A recent work by Choudhury (43) has examined the effect of linear support flexibility and damping on the plain journal bearing. Numerous stability maps were presented for various ranges of support mass and flexibility. The analysis then investigated the stability of a multi-mass rotor system by producing the characteristic polynomial of the system by numerical methods. The stability study of a particular rotor system was presented which investigated the effect of support flexibility on the system and results verified that an optimum damping exists for a given support stiffness to improve the stability of the rotor system.

Two text books on the subject of rotor dynamics have been published which give detailed derivations of the equations of motion of the fundamental rotor models. Dimentberg, in 1961 published a text (51) which treats flexural vibrations in rotating rotors and considers various aspects of critical speeds, balancing, stability of rotors operating near critical speeds, and the influence of shaft internal friction and shaft asymmetry on stability. Experimental results are reported in the text which add to its importance in the rotor dynamics literature. The text of Tondl (52) investigates instability in rotor systems due to internal friction damping, unequal stiffness, and oil film journal bearings. This extensive treatment is also supplemented by reports of experimental investigations carried out by the author. Tondl has one-fourth of the total volume dealing with the effect of journal bearings on stability. Experimental results for plain cylindrical, elliptical, lobed, grooved, and flexible element bearing are presented and discussed.

Tondl points out one major fact that should be emphasized. For machines of high power rating, measurements made directly on the rotor

are the only reliable guide for the correct assessment of the danger of vibrations. Pedestal mounted pickups are not reliable for determining the level of vibration on the rotor shaft.

Another mechanism creating instabilities in turbomachinery has been reported by Alford (53). Aerodynamic forces arising from labyrinth seals and blade-tip clearance in axial compressors and turbines can cause a resultant driving force component and should not be neglected in simulation studies of real machinery. The analysis of Choudhury discussed earlier in this section had examined this form of instability in the example rotor system presented in that work.

Kerr (54) reported experimental observation of a flexible, damped, air lubricated journal bearing in which a region of whirl could be passed through to a stable operation zone. Gunter (39) had earlier presented a thorough treatment of the effect of internal friction on the flexible support rotor system. Support symmetry and absence of support damping was shown to lower the stability threshold of the rotor system. An added observation pointed out the fact that the stability threshold predicted from linearized theory using for example the method of Routh, did not necessarily represent the limit of safe operation. The growth rate of a given instability may be very low and operation may be possible above theoretical stability boundaries. This fact points out the necessity for the transient solution technique which can examine the nonlinear growth rate of an instability predicted by a linearized stability analysis.

Analog computer simulation of transient whirl for a symmetrical rigid rotor in cavitated short journal bearings was reported by Jennings

and Ocvirk (55) as early as 1962. Steady-state orbits for balanced rotors were presented which had whirl rates of approximately one-half but no orbits which encircled the origin were produced in that analysis resulting from limitations of the analog system. Gunter (39) also presented analog computer produced orbits for both linear bearing characteristics and nonlinear fluid-film bearings. Orbits showing combined effects of synchronous unbalance response and half-frequency whirl instability were presented. The nonlinear case formed finite limit cycles whereas the linear systems were unbounded.

Reddi and Trumpler (56) in 1962 examined the stability of the 360° full journal and the 180° partial-film bearing. End leakage factors were applied to the film force expressions and the resulting equations of motion linearized and examined for stability about the equilibrium position by the Routh criteria. The complete equations of motion were programmed on a digital computer and the resulting orbits presented for the 360° journal. Reddi also demonstrated that if cavitation is not included the bearing will be unstable at all speeds.

Castelli and McCabe (57) presented transient simulation of a rigid rotor supported in tilting pad gas bearings. Results of two case studies are given with experimental verification and excellent agreement.

Elrod, McCabe, and Chu (73) reported an approach to determine stability boundaries of gas-bearing systems by a combination of the transient orbit and linearized equation methods. The system linearized characteristics are calculated using gas-lubrication theory and these linear characteristics are then used in transient simulation to determine stability in the small. Digital computer transient simulation was

also reported by Badgley and Booker (58) who presented stability boundaries for the rigid, balanced rotor system having cavitated journal bearings and several transient whirl orbits illustrating the balanced system response. Kirk and Gunter (18) used the cavitated short bearing theory developed in a fixed coordinate system to study the effect of unbalance and external loading on the stability of the horizontal rotor system. The values of the instantaneous forces transmitted were given for selected cases in addition to absolute whirl rates. The maximum force transmitted was indicated for all whirl orbits in the presentation. The stabilizing effect of certain levels of unbalance on the otherwise unstable vertical journal was also investigated by the time-transient digital computer simulation program.

Akers, Michaelson, and Cameron (60) reported an analysis of finite length journal bearings including friction effects and out of balance loading. Stability boundaries were compared to the work of Badgley and Booker (58) and was found to be in fair agreement. Shapiro and Colsher (61) presented an analysis of a resiliantly mounted hybrid journal bearing and an elastic, gimbal mounted Rayleigh-step thrust bearing. Both time-transient and step-jump dynamic analysis was used for the results on the stability and response of the systems studied. The step-jump approach is used to calculate bearing system characteristics at a given position. Then these linear equations are placed in characteristics to diminish the time that would be required for a complete nonlinear transient solution and is similar to the work of Elrod reported earlier (73).

The development of pseudo-transient techniques (73) for the prediction of journal bearing performance in internal combustion engines has allowed accurate determination of minimum film thickness, bearing loads, and overall system performance. The stability and transient motion of a vertical finite three-lobed bearing with cavitation was investigated by Falkenhagen, Gunter, and Schuller (62) and compared to experimental work and the analytic work of Lund on the three-lobe bearing. Transient orbits for both balanced and unbalanced systems were presented using an approximate finite bearing solution which represented a time saving factor of 100 over the complete numerical finite-difference approach to the solution of the governing Reynolds' equation.

The time-transient approach is not limited to the study of lubrication problems and the power of the approach has been realized in many sciences. The transient analysis of multi-link mechanisms has been implemented (63,64) as well as the transient solution of the dynamic behavior of a closed-cycle gas turbine system (65). The numerical solution to any time dependent system of equations has become a usable tool for the engineer-scientist due to the speed of the present generation of digital computers.

Shen (66) has presented a formulation for the flexible rotor using influence coefficients and the assumptions of small displacements and a torsionally rigid system. Provision was made in the derivation for analytical representation of nonlinear bearings. The derivation also assumed that the bearing mass was negligible at the two major bearing stations and a chord approximation was used to define the gyroscopic torques and thus reduce the number of parameters in the solution.

However, at the same time additional fictitious stations must be specified for the desired accuracy of angular deflections. The procedure outlined by Shen also involves a transformation to rotating coordinates which is not required or thought to be advantageous in the following analysis.

Childs (67) has also presented a formal derivation of the dynamics of flexible rotating system in terms of a spinning reference coordinate system using vector mechanics. These equations are then reduced to the fixed cartesian coordinates by a transformation. This formulation takes into account bearing constraints which may be nonlinear, but no provision has been made for bearing support flexiblity. The approach by Childs requires that the system eigenvalues and eigenvectors first be obtained to allow a modal coordinate transformation and omission of modes higher than running speed if desired.

These formulations for the transient solution of flexible rotor-bearing systems are excellent approaches to a very difficult problem. The following analysis presents a derivation of the equations of motion by yet another approach which readily allows the inclusion of nonlinear time dependent bearing, seal or external shaft forces. Fluid-film bearings with the option of flexible, damped bearing support structures is included in the simulation model. Linearized gyroscopics are included in the derivation and the effects of acceleration on the transient response is included in the analysis and is an option in the computer code developed from the theory. The following analysis investigates steady-state and transient response of both rigid and flexible rotors and stability programs for special rotor systems are also presented and used in connection with the transient analysis.

1.3 Statement of the Problem

The purpose of this analysis is to present the formulation of the time transient solution of a flexible rotor on nonlinear fluid-film bearings that may be used for design studies of real rotor-bearing systems including the determination of bearing support characteristics for optimum system performance.

CHAPTER II

FLEXIBLE ROTOR DYNAMICS

2.1 Description of the Simulation Model

The large class of rotating machinery operating near or above their first bending critical must be analyzed under the general field of study known as flexible rotor dynamics. A typical rotor in general has multiple bearings and the rotor shaft may have disks or impellers located inboard and outboard to the main bearings.

The cross-section of the complex Brayton-cycle turbine-compressor as shown in Fig. 2.1 is typical of the high speed units which can be studied for dynamic behavior by analytical simulation. This particular unit has a six stage axial compressor supported between the main bearings with the single-stage drive turbine located on the right overhang. A thrust pad is located on the front of the compressor as noted in the diagram.

The continuous rotor shaft may be regarded as a series of concentrated mass stations connected by massless elastic shafts. For practical purposes the gyroscopic effects should be included in the analysis of overhung rotor stations but may be neglected in most cases for rotor stations inboard of the main bearings. Although the notation flexible rotor is appropriate, the deflections considered are small in comparison to the dimensions of the rotor and simplified equations for the rotor shaft mechanics may be incorporated into the analysis.

Fig. 2.2 represents an idealized rotor system reduced to the model used for the analytical description. This analysis will consider the

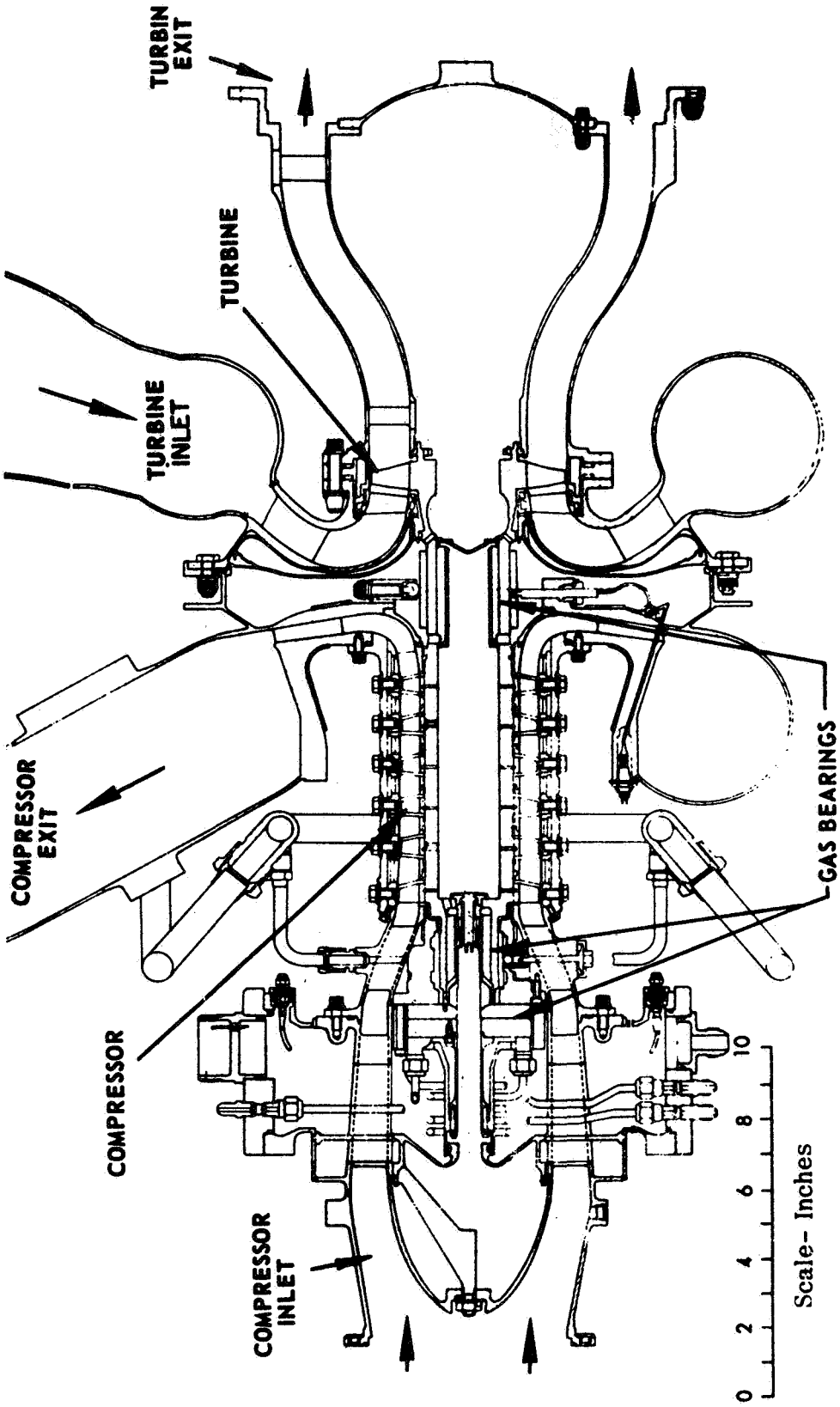

FIG. 2.1 CROSS SECTION OF A TYPICAL COMPRESSOR-TURBINE UNIT

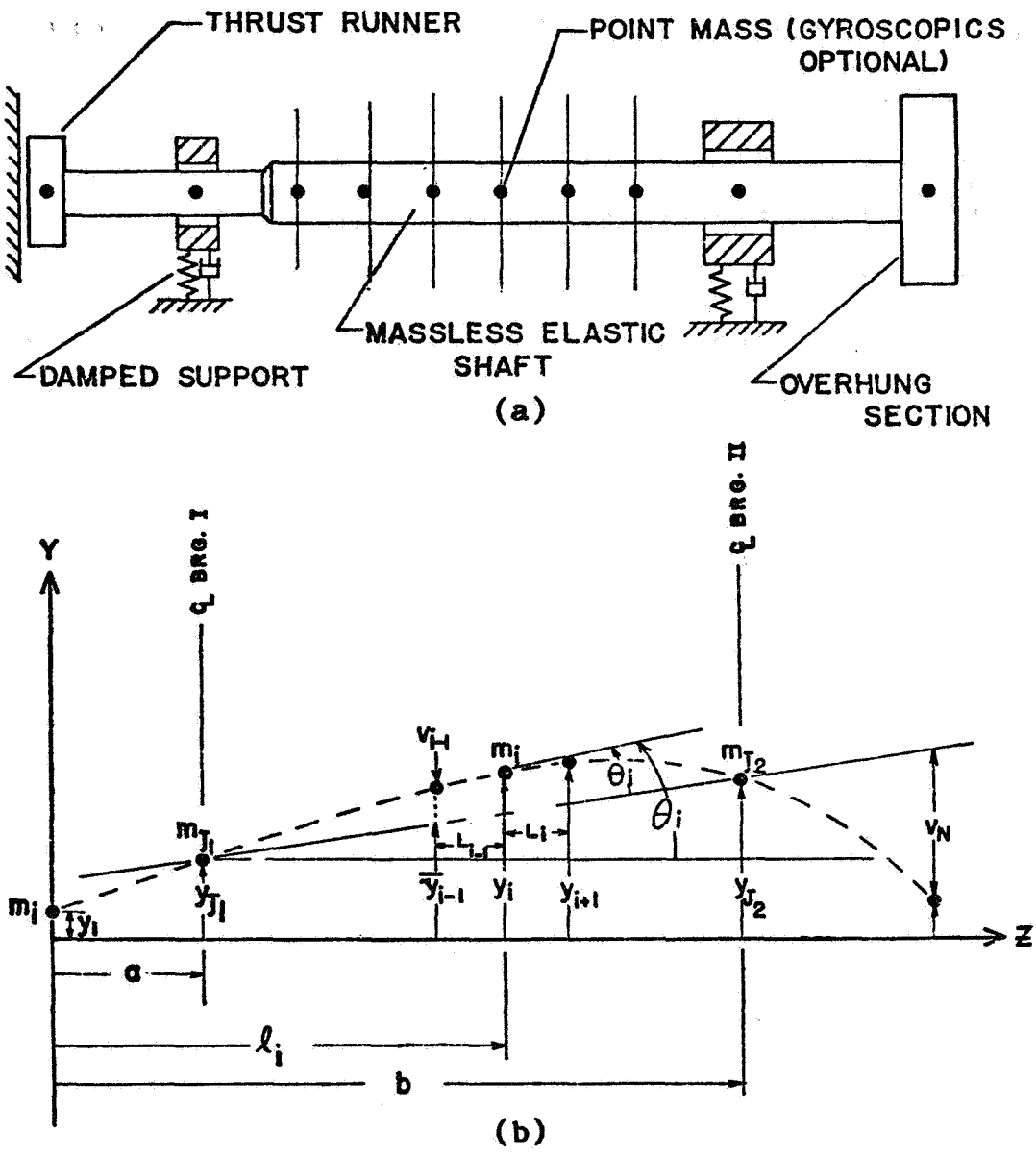

FIG. 2.2(a) MULTI-MASS ROTOR SIMULATION FOR ANALYTIC MODELING
(b) DEFLECTION NOMENCLATURE FOR MULTI-MASS FLEXIBLE ROTOR

rotor to be supported on two main bearings which may in turn be elastically mounted. Any number of additional bearings or seals may be incorporated in a given analysis and is included as an option in the computer code (see Appendix B).

The rotor station deflections will be denoted by the deflections relative to the main bearing centerline (u_i, v_i) and also by the corresponding absolute deflections (x_i, y_i). These are shown in Fig. 2.2 for the y-coordinate deflection in the y-z plane. The relative and absolute angular displacements for the i^{th} rotor station are also shown in Fig. 2.2. Angular displacements of each disk will be denoted by the angles θ_y, which is a rotation in the y-z plane about the negative x-axis and θ_x which is a rotation in the x-z plane about the positive x-axis.

A cross-section of the i^{th} mass station is given in Fig. 2.3 which indicates a possible whirl configuration for the eccentric disk at some instant of time. The absolute and relative deflection nomenclature for the station geometric center, o_g, is illustrated and the displacements of the bearing support and journal are denoted as $(\bar{X}_{s_i}, \bar{Y}_{s_i})$ and $(\bar{X}_i, \bar{Y}_i)$ respectively. These deflections, which represent the rigid rotor centerline and support centerline at this instant in time, are referred from the first bearing location as follows:

$$\bar{X}_i = x_{J_1} + \left(\frac{x_{J_2} - x_{J_1}}{b-a}\right) \times [\ell_i - a] \qquad [2.1]$$

$$\bar{X}_{s_i} = x_{s_1} + \left(\frac{x_{s_2} - x_{s_1}}{b-a}\right) \times [\ell_i - a] \qquad [2.2]$$

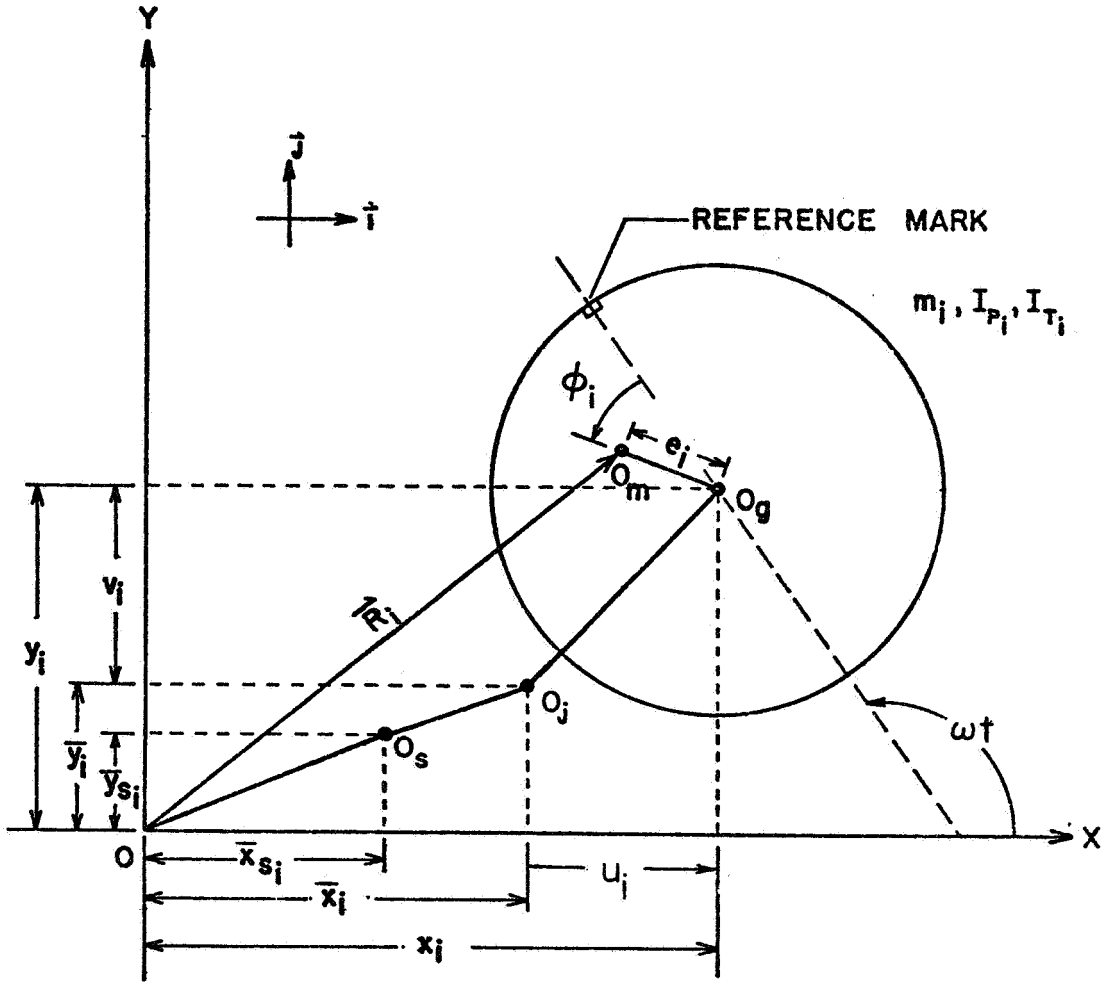

FIG. 2.3 CROSS SECTION OF i^{th} MASS STATION

Similar expressions hold for the y-coordinate deflections referred to the i^{th} station.

2.2 Equations of Motion

The equations of motion of multi-mass flexible rotor are derived in the following sections. The equations are developed in fixed cartesian coordinates and include the effects of gyroscopics and acceleration. The relative deflections of the mass stations are assumed to be small so that linearized gyroscopic moments can be used in the equations. The flexibility influence coefficients for the rotor shaft are assumed to remain constant for the order of approximation being considered.

2.2.1 Gyroscopic Moments

Consider an isolated mass station with symmetry about the z-axis as shown in Fig. 2.4 with the polar and transverse moments of inertia given by I_p and I_T respectively. The standard Eulerian angles are shown in Fig. 2.4 and are denoted as θ the nutation angle of the shaft axis referenced from the fixed Z-axis, ϕ the precession angle as projected in the X-Y plane and referenced from the X-axis, and ψ the local body rotation about the z-axis. Also shown on the figure are the angles (θ_x,θ_y) which are the projections of the nutation angle θ in the fixed X-Z and Y-Z planes respectively.

For a rigid body the angular velocity may be expressed in terms of the Eulerian angles and referred to the body-fixed coordinates (x,y,z). The expression for this relation is readily available in most dynamics texts but a rigorous derivation is usually not included. A derivation of this expression using unit vectors and orthogonal transformations is

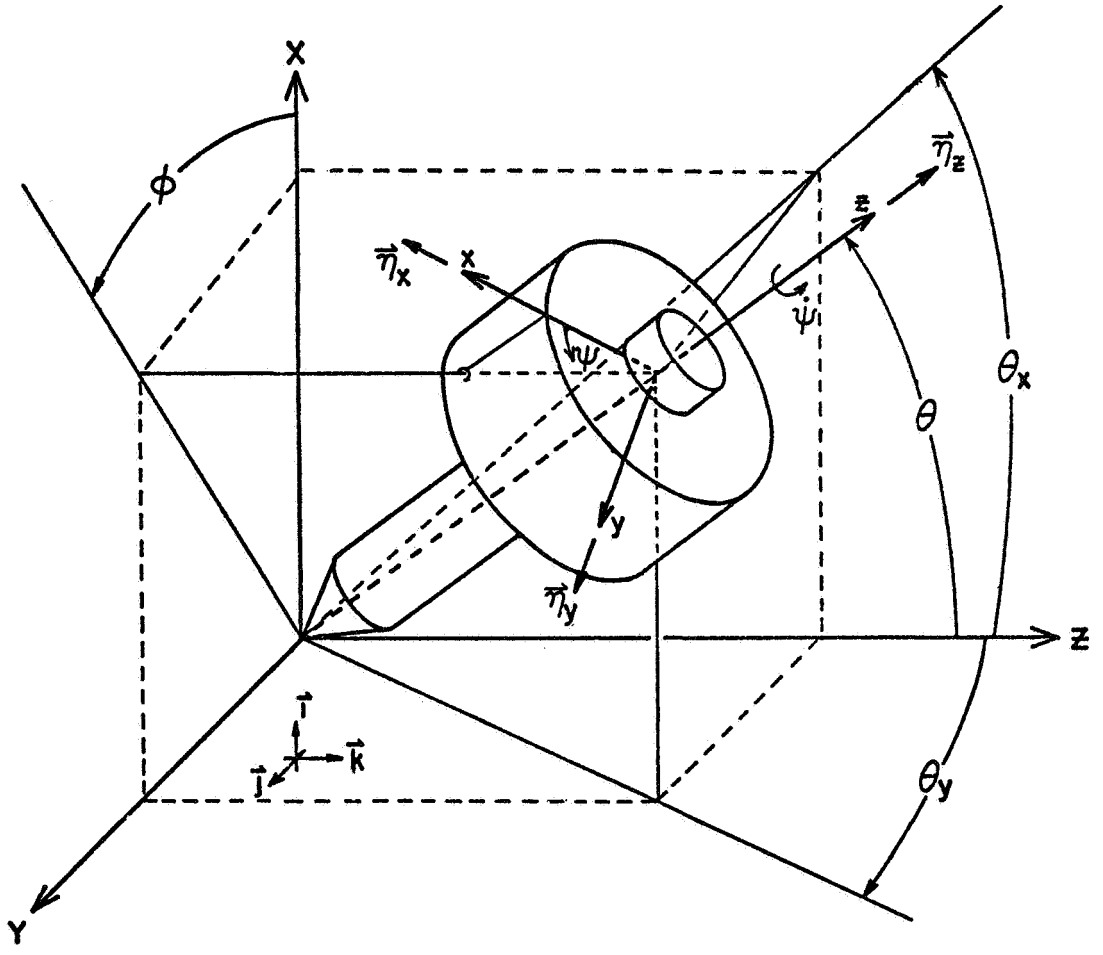

FIG. 2.4 TYPICAL GYROSCOPIC STATION SHOWING EULERIAN ANGLES AND THE ANGULAR DEFLECTIONS θ_x AND θ_y

presented in Appendix A.3. If the unit vectors $\vec{n}_x$, $\vec{n}_y$, and $\vec{n}_z$ lie along the (x,y,z) coordinates, then the angular velocity may be expressed as follows:

$$\vec{\Omega} = (\dot{\theta} \sin \psi - \dot{\phi} \sin \theta \cos \psi)\, \vec{n}_x + (\dot{\theta} \cos \psi + \dot{\phi} \sin \theta \sin \psi)\, \vec{n}_y + (\dot{\phi} \cos \theta + \dot{\psi})\, \vec{n}_z \qquad [2.3]$$

The equations for the inertia torques are most easily derived by energy considerations and the application of the Langrangian.

$$\frac{d}{dt} \left(\frac{\partial L}{\partial \dot{q}_i}\right) - \frac{\partial L}{\partial q_i} = Q_i \qquad [2.4]$$

where

L = $T - V$

T = kinetic energy

V = potential energy

Q = generalized forces

q = generalized coordinates

The kinetic energy is expressed as the sum of the translational kinetic energy and that due to a rigid body rotation of $\vec{\Omega}$. That is

$$T_1 = \tfrac{1}{2}\, m \dot{x}_i\, \dot{x}_j\, \delta_{ij}$$

$$T_2 = \tfrac{1}{2}\, I_{ij}\, \omega_i\, \omega_j\, \delta_{ij} \quad \text{(no cross products of inertia)}$$

Concentrating on the contribution due to rotations it is desired to obtain the equations of motion in terms of the angles θ_x, θ_y and angular velocity ω.

$$T_2 = \tfrac{1}{2} I_T(\vec{\Omega} \cdot \vec{\eta}_x)^2 + \tfrac{1}{2} I_T(\vec{\Omega} \cdot \vec{\eta}_y)^2 + \tfrac{1}{2} I_p(\vec{\Omega} \cdot \vec{\eta}_z)^2$$

or substituting Eq. 2.3 for $\vec{\Omega}$

$$T_2 = \tfrac{1}{2} I_T(\dot{\theta}^2 + \dot{\phi} \sin^2 \theta) + \tfrac{1}{2} I_p (\psi + \dot{\phi} \cos \theta)^2 \qquad [2.5]$$

This expression is in terms of the Eulerian angles and must be transformed to the θ_x, θ_y coordinates. The following relations are valid for small θ (from Eq. 2.3).

$$\omega_z = \dot{\phi} + \dot{\psi} \qquad [2.6a]$$

For infinitesimal rotations the angles may be treated as vectors and the following expressions may be written.

$$\theta_x = \theta \cos \phi \qquad [2.6b]$$

$$\dot{\theta}_x = \dot{\theta} \cos \phi - \theta\dot{\phi} \sin \phi \qquad [2.6c]$$

$$\theta_y = \theta \sin \phi \qquad [2.6d]$$

$$\dot{\theta}_y = \dot{\theta} \text{ sub } \phi + \theta\dot{\phi} \cos \phi \qquad [2.6e]$$

For small θ the kinetic energy T_2 reduces to

$$T_2 = \tfrac{1}{2} I_T(\dot{\theta}^2 + \dot{\phi}\theta^2) + \tfrac{1}{2} I_p(\dot{\psi} + \dot{\phi}(1 - \frac{\theta^2}{2} + \ldots))^2 \qquad [2.7]$$

As shown by Yamamoto (11),

$$\dot{\theta}_x{}^2 + \dot{\theta}_y{}^2 = \dot{\theta}^2 + \theta^2\dot{\phi}^2 \qquad [2.8a]$$

$$\dot{\theta}_y\theta_x - \dot{\theta}_x\theta_y = \theta^2\dot{\phi} \qquad [2.8b]$$

Hence,

$$T_2 = \tfrac{1}{2} I_T(\dot{\theta}_x{}^2 + \dot{\theta}_y{}^2) + \tfrac{1}{2} I_p[\dot{\psi} + \dot{\phi} - \dot{\phi}\theta^2/_2]^2$$

$$T_2 = \tfrac{1}{2} I_T(\dot{\theta}_x{}^2 + \dot{\theta}_y{}^2) + \tfrac{1}{2} I_p[\omega^2 - \omega\dot{\phi}\theta^2 + \dot{\phi}\theta^4/_4]$$

or

$$T_2 = \tfrac{1}{2} I_T(\dot{\theta}_x{}^2 + \dot{\theta}_y{}^2) + \tfrac{1}{2} I_p[\omega^2 + \omega(\dot{\theta}_x\theta_y - \dot{\theta}_y\theta_x)] \qquad [2.9a]$$

For a torsional stiffness K

$$V = \tfrac{1}{2} K(\theta_x{}^2 + \theta_y{}^2) \qquad [2.9b]$$

Application of Eq. 2.3 to 2.9 gives the desired equations for the generalized moments M_x, M_y where the rotations $(-\theta_y, \theta_x)$ correspond to (M_x, M_y).

$$\frac{d}{dt}\left(\frac{\partial T}{\partial \dot{\theta}_y}\right) - \frac{\partial T}{\partial \theta_y} + \frac{\partial V}{\partial \theta_y} = -M_x$$

$$I_T\ddot{\theta}_y - \tfrac{1}{2} I_p\omega\dot{\theta}_x - \tfrac{1}{2} I_p\dot{\omega}\theta_x - \left(\tfrac{1}{2} I_p\omega\dot{\theta}_x\right) + K\theta_y = -M_x \qquad [2.10]$$

Likewise

$$I_T\ddot{\theta}_x + \tfrac{1}{2} I_p\omega\dot{\theta}_y + \tfrac{1}{2} I_p\dot{\omega}\theta_y + \tfrac{1}{2} I_p\omega\dot{\theta}_y + K\theta_x = M_y \qquad [2.11]$$

and

$$I_p\dot{\omega} + \tfrac{1}{2} I_p \frac{d}{dt}(\dot{\theta}_x\theta_y - \dot{\theta}_y\theta_x) = M_z$$

or

$$I_p\dot{\omega} + \tfrac{1}{2} I_p(\ddot{\theta}_x\theta_y - \ddot{\theta}_y\theta_x) = M_z \qquad [2.12]$$

The present analysis is not concerned with the drive torque M_z. The inertia loads due to the gyroscopics and torsional stiffness are given by

$$M_x^{(inertia)} = -M_x = I_T\ddot{\theta}_y - \tfrac{1}{2} I_p\dot{\omega}\theta_x - I_p\omega\dot{\theta}_x + K\theta_y \qquad [2.13]$$

$$M_y^{(inertia)} = -M_y = -I_T\ddot{\theta}_x - \tfrac{1}{2} I_p\dot{\omega}\theta_y - I_p\omega\dot{\theta}_y - K\theta_x \qquad [2.14]$$

2.2.2 Equations of Motion - Rotor Stations

The equations of motion of the flexible rotor may be obtained by application of the flexibility influence coefficients. A discussion of the method of obtaining these coefficients for a stepped round rotor

shaft is presented in Appendix A.1. The influence coefficients are defined as

α_{ij} = the relative deflection at the i^{th} station due to a unit unidirectional load applied at the j^{th} station.

β_{ij} = the relative deflection at the i^{th} station due to a unit torque at the j^{th} station.

ϕ_{ij} = the relative angular rotation at the i^{th} station due to a unit unidirectional load at the j^{th} station.

γ_{ij} = the relative angular rotation at the i^{th} station due to a unit torque at the j^{th} station.

The relative deflection of the i^{th} major mass station can be expressed in terms of the flexibility influence coefficients as follows:

$$u_i = \alpha_{ij} P_{x_j} + \beta_{ij} C_{y_j} \qquad [2.15]$$

$$v_i = \alpha_{ij} P_{y_j} - \beta_{ij} C_{xj} \qquad [2.16]$$

$$\theta_{x_i} = \phi_{ij} P_{x_j} + \gamma_{ij} C_{y_j} \qquad [2.17]$$

$$\theta_{y_i} = \phi_{ij} P_{y_j} - \gamma_{ij} C_{x_j} \qquad [2.18]$$

where the resultant loads $\vec{P}_j$ and couples $\vec{C}_j$ are composed of both inertia loading and effective external loads created by unbalance, internal damping, cross-coupled aerodynamic loading, and any reactions from

fluid-film bearings or seals at the particular station.

The sign convention for the loads and couples is shown in Fig. 2.5 which gives a top view of the i^{th} mass station. Also shown are the absolute and relative translational and angular deflection notations.

The inertia loading acting at the i^{th} mass station is readily derived by differentiating the position vector, $\vec{R}_i$ (see Fig. 2.3).

$$\vec{R}_i = x_i\vec{i} + y_i\vec{j} + e_i \cos(\omega t+\phi_i)\vec{i} + e_i \sin(\omega t+\phi_i)\vec{j} \qquad [2.19]$$

$$\dot{\vec{R}}_i = \frac{d\vec{R}}{dt} = (\dot{x},\dot{y})_i + (-e\omega \sin(\omega t+\phi), e\omega \cos(\omega t+\phi))_i \qquad [2.20]$$

$$\ddot{\vec{R}}_i = (\ddot{x},\ddot{y})_i + (-e\,\omega^2 \cos(\omega t+\phi) - e\,\dot{\omega} \sin(\omega t+\phi),$$

$$-e\omega^2 \sin(\omega t+\phi) + e\dot{\omega} \cos(\omega t+\phi))_i \qquad [2.21]$$

The inertia loading including unbalance is then given by D'Alembert principle as

$$\vec{F}_i^{(inertia)} = -m_i \times (acceleration)_i = (-m\ddot{x}, -m\ddot{y})_i +$$

$$+ (me\omega^2 \cos(\omega t+\phi) + me\dot{\omega} \sin(\omega t+\phi),$$

$$me\omega^2 \sin(\omega t+\phi) - me\dot{\omega} \cos(\omega t+\phi))_i \qquad [2.22]$$

The expressions for the gyroscopic inertia torque and angular stiffness were previously derived (Eqs. 2.13-2.14) and in terms of the absolute angular rotations $(\theta_{x_j},\theta_{y_j})$ these may be written as follows:

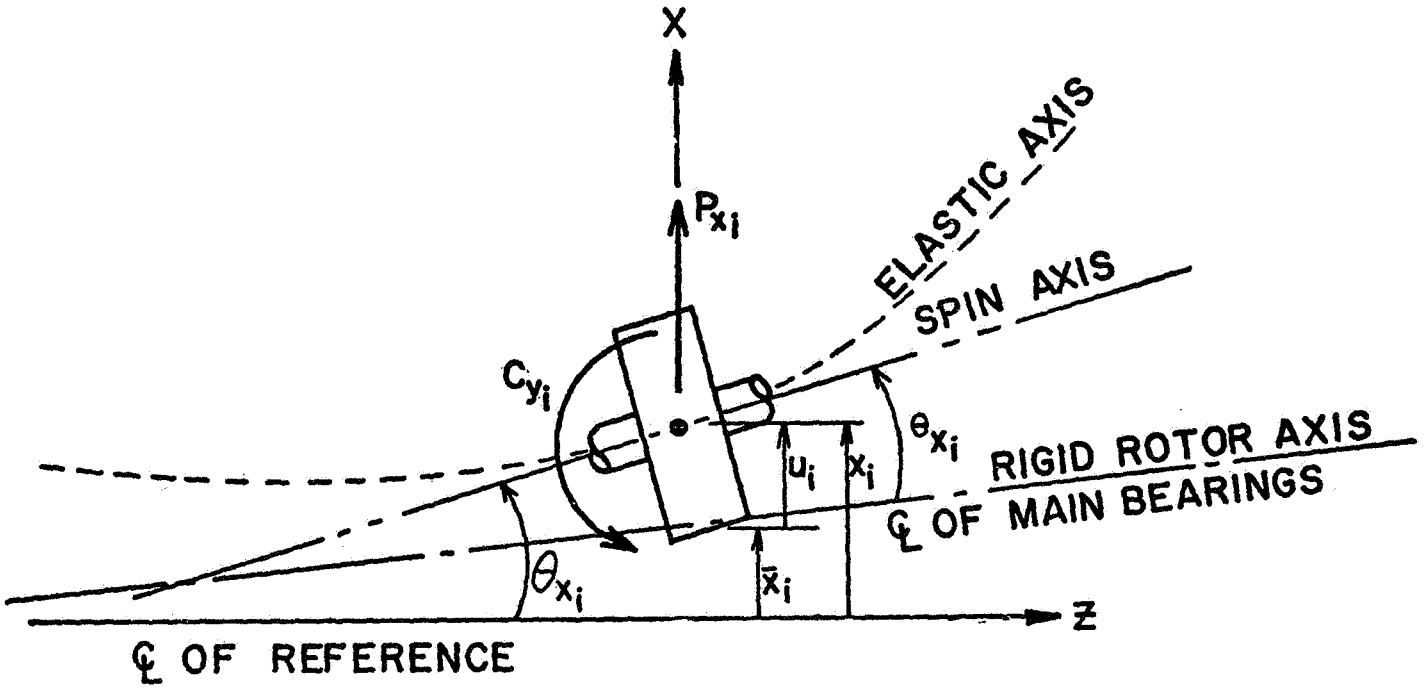

FIG. 2.5 FORCE AND MOMENT SIGN CONVENTION AT i^{th} ROTOR STATION

$$C_{x_j} = M_x^{(inertia)}\Big|_j = (I_T\ddot{\theta}_y - \omega I_p\dot{\theta}_x - \tfrac{1}{2} I_p\dot{\omega}\theta_y + K\theta_y)_j \qquad [2.23]$$

$$C_{y_j} = M_y^{(inertia)}\Big|_j = (-I_T\ddot{\theta}_x - \omega Ip\dot{\theta}_y - \tfrac{1}{2} I_p\dot{\omega}\theta_x - K\theta_x)_j \qquad [2.24]$$

Combining this expression with the representation of internal damping (68), cross-coupling (53,69), and allowing for other nonlinear forces that might occur described in general terms by $\hat{F}_x(x,y,\dot{x},\dot{y})$ and $\hat{F}_y(x,y,\dot{x},\dot{y})$, the components of $\vec{P}_j$ may be expressed as follows:

$$P_{x_j} = (-m\ddot{x} - c\dot{x} - kx + me\omega^2 \cos(\omega t+\phi) + \\ + me\dot{\omega} \sin(\omega t+\phi) - CI\dot{u} - \omega CIv - Qy + \hat{F}_x(x,y,\dot{x},\dot{y}))_j \qquad [2.25]$$

$$P_{y_j} = (-m\ddot{y} - c\dot{y} - ky + me\omega^2 \sin(\omega t+\phi) \\ - me\dot{\omega} \cos(\omega t+\phi) - CI\ \dot{v} + \omega CIu + Qx - W + \hat{F}_y(x,y,\dot{x},\dot{y}))_j \qquad [2.26]$$

Rewritting Eqs. (2.15-2.18) and using the notation

$$P_{x_j} = -m_j\ddot{x}_j + F_{x_j} \qquad [2.27]$$

$$P_{y_j} = -m_j\ddot{y}_j + F_{y_j} \qquad [2.28]$$

$$C_{x_j} = I_{T_j}\ddot{\theta}_{y_j} + H_{x_j} \qquad [2.29]$$

$$C_{y_j} = -I_{T_j}\ddot{\theta}_{x_j} + H_{y_j} \qquad [2.30]$$

then,

$$u_i = \alpha_{ij}(-m\ddot{x} + F_x)_j + \beta_{ij}(-I_T\ddot{\theta}_x + H_y)_j \qquad [2.31]$$

$$v_i = \alpha_{ij}(-m\ddot{y} + F_y)_j - \beta_{ij}(I_T\ddot{\theta}_y + H_x)_j \qquad [2.32]$$

$$\theta_{x_i} = \phi_{ij}(-m\ddot{x} + F_x)_j + \gamma_{ij}(-I_T\ddot{\theta}_x + H_y)_j \qquad [2.33]$$

$$\theta_{y_i} = \phi_{ij}(-m\ddot{y} + F_y)_j - \gamma_{ij}(I_T\ddot{\theta}_y + H_x)_j \qquad [2.34]$$

The equations of motion of the rotor may be expressed in matrix form for convenience. On the following page is the matrix formulation for two major mass stations.

The formulation for larger systems is simplified by defining the following variables.

$$\begin{bmatrix} \alpha_{11}m_1 & \alpha_{12}m_2 & \cdots & \alpha_{1n}m_n \\ \alpha_{21}m_1 & \alpha_{22}m_2 & & \vdots \\ \vdots & & & \\ \alpha_{n1}m_1 & \cdots & & \alpha_{nn}m_n \end{bmatrix} \equiv A^{(n)}$$

$$\begin{bmatrix} \beta_{11}I_{T_1} & \beta_{12}I_{T_2} & \cdots & \beta_{1n}I_{T_n} \\ \beta_{21}I_{T_1} & \cdots & & \vdots \\ \vdots & & & \\ \beta_{n1}I_{T_1} & & & \beta_{nn}I_{T_n} \end{bmatrix} \equiv B^{(n)}$$

$$
\begin{bmatrix}
\alpha_{11}m_1 & \alpha_{12}m_2 & 0 & 0 & 0 & 0 & \beta_{11}I_{T_1} & \beta_{12}I_{T_2} \\
\alpha_{21}m_1 & \alpha_{22}m_2 & 0 & 0 & 0 & 0 & \beta_{21}I_{T_1} & \beta_{22}I_{T_2} \\
0 & 0 & \alpha_{11}m_1 & \alpha_{12}m_2 & \beta_{11}I_{T_1} & \beta_{12}I_{T_2} & 0 & 0 \\
0 & 0 & \alpha_{21}m_1 & \alpha_{22}m_2 & \beta_{21}I_{T_2} & \beta_{22}I_{T_2} & 0 & 0 \\
0 & 0 & \phi_{11}m_1 & \phi_{12}m_2 & \gamma_{11}I_{T_2} & \gamma_{12}I_{T_2} & 0 & 0 \\
0 & 0 & \phi_{21}m_1 & \phi_{22}m_2 & \gamma_{21}I_{T_1} & \gamma_{22}I_{T_2} & 0 & 0 \\
\phi_{11}m_1 & \phi_{12}m_2 & 0 & 0 & 0 & 0 & \gamma_{11}I_{T_1} & \gamma_{12}I_{T_2} \\
\phi_{21}m_1 & \phi_{22}m_2 & 0 & 0 & 0 & 0 & \gamma_{21}I_{T_1} & \gamma_{22}I_{T_2}
\end{bmatrix}
\begin{bmatrix}
\ddot{x}_1 \\ \ddot{x}_2 \\ \ddot{y}_1 \\ \ddot{y}_2 \\ \ddot{\theta}_{y1} \\ \ddot{\theta}_{y2} \\ \ddot{\theta}_{x1} \\ \ddot{\theta}_{x2}
\end{bmatrix}
=
\begin{bmatrix}
-u_1 + \alpha_{1j}F_{x_j} + \beta_{1j}H_{y_j} \\
-u_2 + \alpha_{2j}F_{x_j} + \beta_{2j}H_{y_j} \\
-v_1 + \alpha_{1j}F_{y_j} - \beta_{1j}H_{x_j} \\
-v_2 + \alpha_{2j}F_{y_j} - \beta_{2j}H_{x_j} \\
-\theta_{y1} + \phi_{1j}F_{y_j} - \gamma_{1j}H_{x_j} \\
-\theta_{y2} \quad \phi_{2j}F_{y_j} - \gamma_{2j}H_{x_j} \\
-\theta_{x1} + \phi_{1j}F_{x_j} + \gamma_{1j}H_{y_j} \\
-\theta_{x2} + \phi_{2j}F_{x_j} + \gamma_{2j}H_{y_j}
\end{bmatrix}
$$

$$\begin{bmatrix} \phi_{11}m_1 & \phi_{12}m_2 \cdots & \phi_{1n}m_n \\ \phi_{21}m_1 & & \vdots \\ \vdots & & \\ \phi_{n1}m_1 & \cdots & \phi_{nn}m_n \end{bmatrix} \equiv C^{(n)}$$

$$\begin{bmatrix} \gamma_{11}I_{T_1} & \gamma_{12}I_{T_2} \cdots & \gamma_{1n}I_{T_n} \\ \gamma_{21}I_{T_1} & & \\ \vdots & & \\ \gamma_{n1}I_{T_1} & \cdots & \gamma_{nn}I_{T_n} \end{bmatrix} \equiv D^{(n)}$$

$$\begin{bmatrix} 0 & 0 \cdots & 0 \\ 0 & & \\ \vdots & & \\ 0 \cdots & & 0 \end{bmatrix} \equiv O^{(n)}$$

Also define,

$$\begin{bmatrix} \ddot{x}_1 \\ \ddot{x}_2 \\ \vdots \\ \ddot{x}_n \end{bmatrix} \equiv \ddot{x}^{(n)} \; ; \; \begin{bmatrix} \ddot{y}_1 \\ \ddot{y}_2 \\ \vdots \\ \ddot{y}_n \end{bmatrix} \equiv \ddot{y}^{(n)} \; ; \; \begin{bmatrix} \ddot{\theta}_{x_1} \\ \ddot{\theta}_{x_2} \\ \vdots \\ \ddot{\theta}_{x_n} \end{bmatrix} = \ddot{\theta}_x^{(n)} \; ; \; \begin{bmatrix} \ddot{\theta}_{y_1} \\ \ddot{\theta}_{y_2} \\ \vdots \\ \ddot{\theta}_{y_n} \end{bmatrix} = \ddot{\theta}_y^{(n)}$$

Then the equations may be expressed very simply as

$$\begin{bmatrix} A^{(n)} & 0^{(n)} & 0^{(n)} & B^{(n)} \\ 0^{(n)} & A^{(n)} & B^{(n)} & 0^{(n)} \\ 0^{(n)} & C^{(n)} & D^{(n)} & 0^{(n)} \\ C^{(n)} & 0^{(n)} & 0^{(n)} & D^{(n)} \end{bmatrix} \begin{bmatrix} \ddot{x}^{(n)} \\ \ddot{y}^{(n)} \\ \ddot{\theta}_y^{(n)} \\ \ddot{\theta}_x^{(n)} \end{bmatrix} = \begin{bmatrix} F_x^{(n)} \\ F_y^{(n)} \\ \Theta_y^{(n)} \\ \Theta_x^{(n)} \end{bmatrix} \qquad [2.35]$$

where

$$F_x^{(n)} \equiv \begin{bmatrix} -u_1 + \alpha_{1j} F_{x_j} + \beta_{1j} H_{y_j} \\ \vdots \\ -u_n + \alpha_{nj} F_{x_j} + \beta_{nj} H_{y_j} \end{bmatrix}$$

$$F_y^{(n)} = \begin{bmatrix} -v_1 + \alpha_{1j} F_{y_j} - \beta_{1j} H_{x_j} \\ \vdots \\ -v_n + \alpha_{nj} F_{y_j} - \beta_{nj} H_{x_j} \end{bmatrix}$$

$$\Theta_y^{(n)} = \begin{bmatrix} -\theta_{y_1} + \phi_{1j} F_{y_j} - \gamma_{1j} H_{x_j} \\ \vdots \\ -\theta_{y_n} + \phi_{nj} F_{y_j} - \gamma_{nj} H_{x_j} \end{bmatrix}$$

$$\Theta_x^{(n)} = \begin{bmatrix} -\theta_{x_1} + \phi_{1j} F_{x_j} + \gamma_{1j} H_{y_j} \\ \vdots \\ -\theta_{x_n} + \phi_{nj} F_{x_j} + \gamma_{nj} H_{y_j} \end{bmatrix}$$

This formulation presents the equations of motion which are in the desired form for application of standard integration procedures.

The method of solution employed in the computer code MODELJ will be discussed in Section 2.3.

If the system experiences an acceleration $\dot{\omega}$, then one additional relation must be given to fix the instantaneous angular velocity. That is

$$\dot{\omega} = \frac{d\omega}{dt}$$

Hence

$$d\omega = \dot{\omega} dt$$

or

$$\omega_t = \omega_{t_o} + \int_{t_o}^{t} \dot{\omega} dt$$

For a constant acceleration rate then

$$\omega_t = \omega_{t_o} + \dot{\omega}(t - t_o) \qquad [2.36]$$

The angular velocity can thus be calculated for each time step of the integration process. The external torques necessary to supply this constant acceleration is given by Eq. 2.12.

2.2.3 Equations of Major Bearing Support Stations

The previous equations are all that are necessary when considering a flexible rotor on two rigid bearing supports. If the bearing or supports are allowed to have flexibility, then additional information must be obtained to solve the system. Taking the moments of all external and inertia forces and torques acting on the shaft about the

first bearing station (see Fig. 2.6):

$$\sum M_{y_1} = F_{x_2}(b-a) + \sum_{i=1}^{n} C_{y_i} + \sum_{i=1}^{n} P_{x_i}(\ell_i - a) = 0 \qquad [2.37]$$

Hence, the total resultant force component acting on the shaft at the second major bearing in the x-direction is given by:

$$F_{x_2} = \frac{-\sum_{i=1}^{n} C_{y_i} - \sum_{i=1}^{n} P_{x_i}(\ell_i - a)}{(b - a)} \qquad [2.38]$$

This resultant force is composed of the bearing reaction denoted as (B.F.) and the inertia load at the second major bearing. That is

$$F_{x_2} = -m_{J_2}\ddot{x}_{J_2} + (B.F.)_{x_2} \qquad [2.39]$$

Therefore, solving for the journal acceleration $\ddot{x}_{J_2}$ at the second major bearing station yields

$$\ddot{x}_{J_2} = \frac{1}{m_{J_2}}\{(B.F.)_{x_2} + \frac{1}{(b - a)}\left(\sum_{i=1}^{n} C_{y_i} + \sum_{i=1}^{n} P_{x_i}(\ell_i - a)\right)\} \qquad [2.40]$$

The bearing reactions can also include unbalance excitation acting at the journal. In a similar fashion the acceleration for the first bearing may be expressed as

$$\ddot{x}_{J_1} = \frac{1}{m_{J_1}}\{(B.F.)_{x_1} + \frac{1}{b - a}\left(-\sum_{i=1}^{n} C_{y_i} + \sum_{i=1}^{n} P_{x_i}(b - \ell_i)\right)\} \qquad [2.41]$$

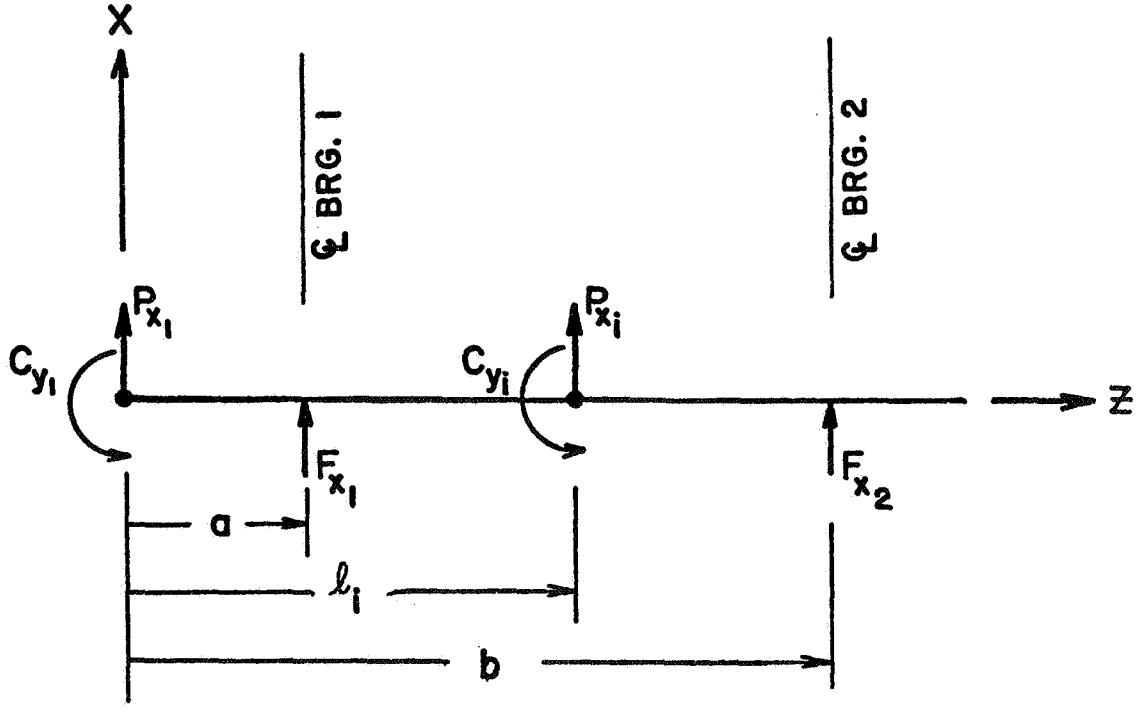

FIG. 2.6 REPRESENTATION FOR BEARING FORCE AND MOMENT BALANCE

The acceleration of the bearings in the y-coordinate are likewise found to be given by the following expressions.

$$\ddot{y}_{J_2} = \frac{1}{m_{J_2}} \{(B.F.)_{y_2} + \frac{1}{b - a}(- \sum_{i=1}^{n} C_{x_i} + \sum_{i=1}^{n} P_{y_i} (\ell_i - a))\} \qquad [2.42]$$

and

$$\ddot{y}_{J_1} = \frac{1}{m_{J_1}} \{(B.F.)_{y_1} + \frac{1}{b - a}(+ \sum_{i=1}^{n} C_{x_i} + \sum_{i=1}^{n} P_{y_i} (b - \ell_i))\} \qquad [2.43]$$

If the bearings are supported by flexibly mounted structures, the equations of the supports are readily deduced using the representation given in Fig. 2.7. A force balance on the support gives

$$\sum F_{support} = m_s a_s = -(B.F.) + (S.F.) \qquad [2.44]$$

where

(S.F.) = support force

a_s = absolute acceleration of the support in any given coordinate direction.

The bearing and support forces have been left in the general terms since the bearing type assumed dictates how the reaction forces are expressed. These forces may be either linear or nonlinear functions of displacement, velocity, and time. For a more detailed analysis of the bearing and support forces refer to Appendix B where the types in the computer code MODELJ are discussed. More detailed discussion of fluid film bearings is presented in Section 4.2 and discussion of the fluid film squeeze damper is presented in Section 6.3.

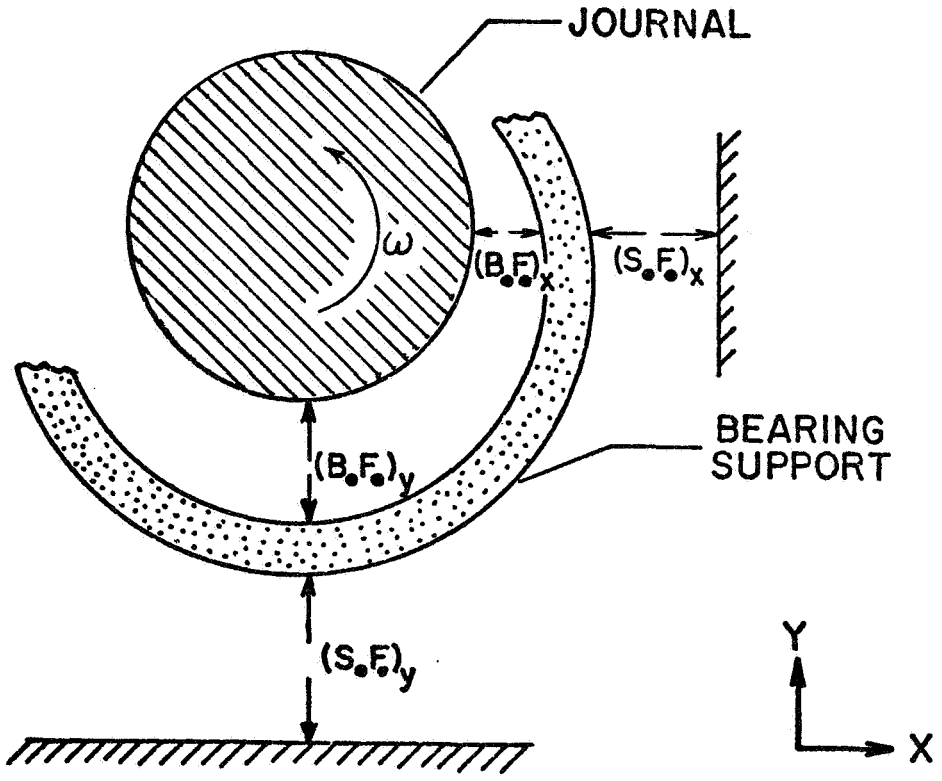

FIG. 2.7 BEARING AND SUPPORT SYSTEM FORCE BALANCE

2.3 Method of Solution

The equations derived in Section 2.2 can be solved for the time transient solution once the inverse of the modified flexibility matrix is obtained. Expressing the equations of motion given in Eq. 2.35 as follows for simplicity:

$$[CXA]\,[\ddot{X}] = [U] \qquad [2.45]$$

where

$[\ddot{X}]$ = column vector of absolute acceleration of the major mass stations.

$[U]$ = column vector of relative displacement as represented in Eq. [2.35]

$[CXA]$ = 4n x 4n matrix given in Eq. [2.35]

Then, premultiplying both sides of Eq. 2.45 by the inverse of the 4n x 4n matrix CXA gives the absolute translational and angular acceleration rates which is expressed as follows:

$$[\ddot{X}] = [CXA]^{-1}[U] \qquad [2.46]$$

With the acceleration values known at time t, the bearing accelerations can be obtained from Eqs. 2.25 and 2.26. As for any time integration of second order equations, the displacements and velocities at time t_o must be specified for all the coordinates being solved. The actual method of solution may be chosen from several available formulations. For the type solutions given by unbalance response the modified Euler method has

been used successfully (57,59,62) and is especially desirable when it is necessary to calculate nonlinear hydrodynamic bearing forces at each step of the solution. A modified Euler method which is equivalent to a second order Runge-Kutta procedure can be utilized at no extra time loss in the integration of the bearing forces. A 4^{th} order Runge-Kutta procedure can be used but becomes time consuming since four calls of the bearing forces are required for each step forward in time of the solution. The numerous predictor-corrector integration schemes such as the Milne, Adams-Bashforth, and Hammings (18) are even more time consuming and have a greater tendency to exhibit numerical instability. The 4^{th} order Runge-Kutta procedure is used in the time transient programs listed in Appendix E and G.

The most important information needed to produce readily recognized trends is the starting conditions. For the linear model the gravity loading can be removed from the solution and any external loading can be investigated from the static equilibrium position. For nonlinear solutions (bearing and support forces) the gravity loading cannot be ignored and the initial conditions given may produce transient motion that the system would never encounter in actual practice. The following section is presented to review work that has been completed on the steady state response of flexible rotors and a computer code modified from (12) is presented in Appendix H that may be used to obtain initial conditions for the transient solution program.

2.4 Steady State Response

The transient solution as proposed in Section 2.3 is indeed very

time consuming and hence very costly to produce even with the tremendous speed of the present generation of digital computers. Poor or misjudged starting conditions for the time transient solution may produce misleading results since the system would have to encounter a transition period to attain the correct phase relation for the many variables being integrated simultaneously.

The equations of motion as presented in Section 2.3 can be solved for the steady-state for the case of assumed linear bearing characteristics. By assuming solutions of the form

$$q_i = A_i \cos(\omega t) + B_i \sin(\omega t) \qquad [2.47]$$

the solution requires that a system of equations be solved. For the assumption of N point-mass rotor stations then a 4N x 4N matrix must be solved. However, if the shaft properties are isotropic then only a 2N x 2N system need be solved. The introduction of support flexibility increases the system of equations to a 8N x 8N matrix representation and increases the solution time per case by approximately a factor of 64 for a simple 2 station rotor. The inclusion of gyroscopic moments at each rotor station in addition to support flexibility increases the system to a 12N x 12N representation and is 216 times as difficult as a two station point-mass rotor with isotropic constraints. Recall that the transient solution requires only a $4(N-2) \times 4(N-2)$ matrix inverse be taken even when gyroscopics are included in the solution. For point-mass assumption the transient solution requires only that an $(N-2) \times (N-2)$ matrix be inverted. The $(N-2)$ expression represents the total

number of shaft stations in the simulation minus the two major bearing stations. A more efficient procedure for obtaining the steady state solution has been reported by Lund (12) which uses a modified Myklestad-Prohl technique to obtain the steady state solution.

Without reproducing the entire analysis of Lund the basic equations for this type analysis will be sumarized in the following discussion. With reference to Fig. 2.8 the moments and deflection relations can be derived by applying simple beam theory for the shaft sections and noting that

$$M_{n+1} = M'_n + L_n V_n \qquad [2.48]$$

By integrating the equation from simple beam theory, $\frac{d^2x}{dz^2} = \frac{M}{EI}$, and using the above expression for the moment

$$\theta_{n+1} = \theta_n + \left[\int_{z=o}^{L_n} \frac{dz}{EI}\right] M'_n + \left[\int_{o}^{L_n} \frac{zdz}{EI}\right] V_n \qquad [2.49]$$

$$X_{n+1} = X_n + L_n\theta_n + L_n\left[\int_{o}^{L_n} \frac{dz}{EI}\right] - \int_{o}^{L_n} \frac{zdz}{EI}$$

$$+ V_n\left\{L_n \int_{o}^{L_n} \frac{zdz}{EI} - \int_{o}^{L_n} \frac{z^2dz}{EI}\right\} \qquad [2.50]$$

For the case of constant shaft properties (EI constant for each different shaft section), then

$$M_{n+1} = M'_n + L_n V_n \qquad [2.51]$$

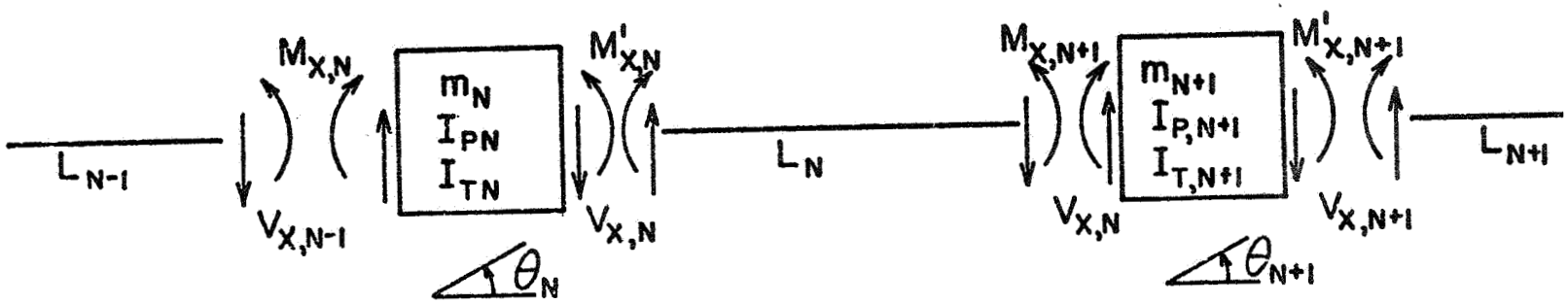

FIG. 2.8 CONVENTION AND NOMENCLATURE FOR STEADY-STATE ROTOR CALCULATION

$$\theta_{n+1} = \theta_n + \frac{L_n}{EI} M'_n + \frac{L_n^2}{2EI} V_n \qquad [2.52]$$

$$x_{n+1} = x_n + L_n\theta_n + \frac{L_n^2}{2EI} M'_n + \frac{L_n^3}{6EI} V_n \qquad [2.53]$$

The moment change across a mass station includes the gyroscopic action and angular spring rates of the bearing. The shear change across a mass station includes the effect of inertia loading, bearing reactions, and unbalance loading. Detailed equations for these contributions are given by Lund (12). Harmonic motion is assumed and the bending moment, shear, angular and lateral deflections may be expressed as

$$M_x = M_{xc} \cos\omega t + M_{xs} \sin\omega t \qquad [2.54]$$

$$V_x = V_{xc} \cos\omega t + V_{xs} \sin\omega t \qquad [2.55]$$

$$\theta = \theta_c \cos\omega t + \theta_s \sin\omega t \qquad [2.56]$$

$$x = x_c \cos\omega t + x_s \sin\omega t \qquad [2.57]$$

and for the y-direction the variables M_y, V_y, ϕ, y are used in similar equations. The resulting equations needed to describe the rotor reactions include the change of moment across a mass station and shaft length (8 equations), change of shear across a mass station (4 equations), and the angular and lateral displacement along a shaft length (8 equations) for a total of 20 equations to step across one mass and shaft section.

For a beam with free ends the bending moment and shear are zero at the extremeties, or they can be calculated for an assumed deflection and

given support characteristics. The unknown quantities are the angular and lateral displacement components at the left or first rotor station. Using the superposition principle, each unknown is given a unit value with all the others set to zero and the twenty equations as mentioned above are used to calculate the bending moment and shear at the right rotor end. An additional calculation is made applying the given unbalance loading with the other unknowns set to zero. The result of the superposition of the applied unit loads produce a set of equations which may be solved for the unknowns at the first rotor station. This procedure is best described as follows:

Let $\theta_{c1} = 1$, set $\theta_{s1} = \phi_{c1} = \phi_{s1} = x_{c1} = x_{s1} = y_{c1} = y_{s1}$

$= u_x = u_y = 0$ (u_{xn} and u_{yn} are unbalance loads)

Calculate the residuals at the right rotor end. Call them

$M'_{xcy,1}$; $M'_{xsy,1}$; $M'_{ycr,1}$; $M'_{ysr,1}$

$V_{xcr,1}$; $V_{xsr,1}$; $V_{ycr,1}$; $V_{ysr,1}$

Let $\theta_{s_1} = 1$ and set the other variables to zero. Calculate the residuals and denote them as

$M'_{xcr,2}$; $M'_{xsr,2}$; $M'_{ycr,2}$; $M'_{ysr,2}$

$V_{xcr,2}$; $V_{xsr,2}$; $V_{ycr,2}$; $V_{ysr,2}$

Repeat the procedure for the eight displacements and then apply the unbalance loading and call the residuals

$M'_{xcr,9}$; $M'_{xsr,9}$; $M'_{ycr,9}$; $M'_{ysr,9}$

$V_{xcr,9}$; $V_{xsr,9}$; $V_{ycr,9}$; $V_{ysr,9}$

This produces a set of influence coefficients which allows the unknowns to be solved. The solution can be expressed as follows:

$$\begin{bmatrix} M'_{xcr,1} & M'_{xcr,2} & \cdots & M'_{xcr,8} \\ M'_{xsr,1} & M'_{xsr,2} & \cdots & \\ M'_{ycr,1} & \vdots & & \\ M'_{ysr,1} & & & \\ V_{xcr,1} & & & \\ V_{xsr,1} & & & \\ V_{ycr,1} & & & \\ V_{ysr,1} & V_{ysr,2} & \cdots & V_{ysr,8} \end{bmatrix} \begin{bmatrix} \theta_{c1} \\ \theta_{s1} \\ \phi_{c1} \\ \phi_{s1} \\ x_{c1} \\ x_{s1} \\ y_{c1} \\ y_{s1} \end{bmatrix} = \begin{bmatrix} -M'_{scr,9} \\ -M'_{xsr,9} \\ -M'_{ycr,9} \\ -M'_{ysr,9} \\ -V_{scr,9} \\ -V_{xsr,9} \\ -V_{ycr,9} \\ -V_{ysr,9} \end{bmatrix} \quad [2.58]$$

The unknowns at the first station can thus be determined and the response all along the rotor can then be calculated for a given speed.

Lund's original analysis included an iterative approach to the solution of the gyroscopic contribution but the linearized gyroscopic equations as presented in Section 2.2.1 have replaced this iterative approach in the computer code given in Appendix H. One additional modification has assumed circular synchronous precession which restricts the bearing and support characteristics to be symmetrical. This allows

a tremendous savings in solution time and rotors having unsymmetrical bearing and support characteristics may be studied by this program if the gyroscopic coupling is small in comparison to the other shaft loads and reactions. The results of this computer program, LUNDJR, may be plotted by a companion program LUNDJRP which is given in Appendix H also. A sample case is given in the following rotor system.

Example 2.1

Total rotor weight	1301 lb.
Center span approximate weight	676.0 lb.
Journal weights (each)	312.5 lb.
Diameter of shaft sections	6.0 in.
Length of each shaft section	34.5 in.
Youngs modulus	30×10^6 lb/in^2
Symmetric bearing stiffness	448,000 lb/in
Bearing damping	501 lb-sec/in
(Rigid bearing support pedestals assumed)	
Unbalance at center station	5.4 oz.-in.

This system may be visualized by letting $K_{xx} = K_{yy} = \infty$ in Fig. 5.1 and $K_{1x} = K_{1y} = 448{,}000$ lb/in while $C_{1x} = C_{1y} = 501$ lb-sec/in. The equivalent shaft stiffness is 280,000 lb/in for this example case study.

Fig. 2.9 represents the undamped critical speed mode plots corresponding to the rotor of example 2.1. It is seen that the rotor first critical speed at 3300 RPM is symmetric with the largest deflection at the rotor midspan. This should be the predominant mode excited by unbalance placed at the rotor mid-span or center. The

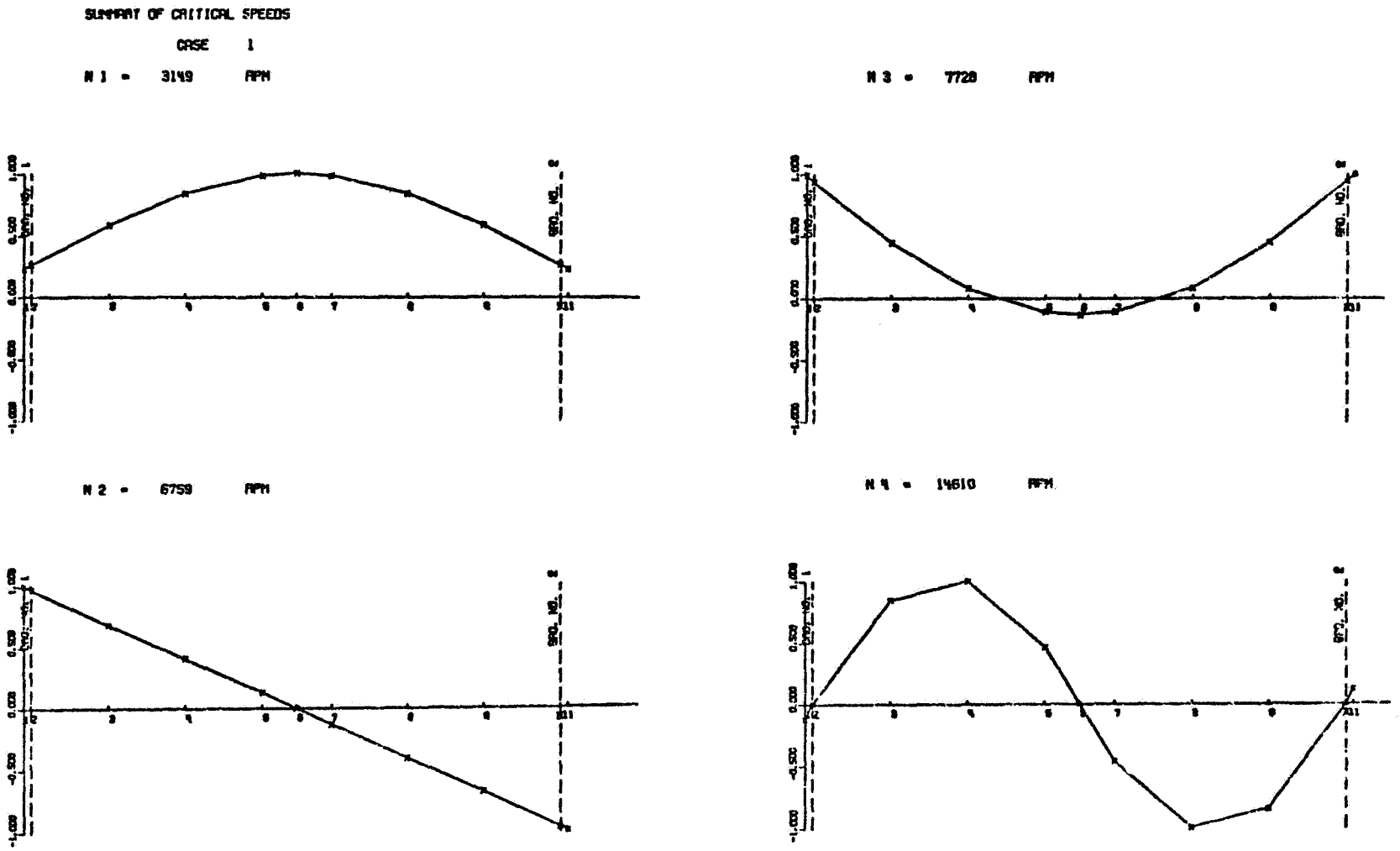

FIG. 2.9 CRITICAL SPEEDS AND MODE SHAPES FOR A THREE-MASS ROTOR INCLUDING GYROSCOPICS (BEARING STIFFNESS= 448,000 LB/IN)

second critical speed is a conical rigid body mode and will not be excited by a centrally located unbalance. The largest amplitude occurs at the bearings and hence should be a highly damped mode for typical bearing damping as given in Ex. 2.1.

The third critical speed shows considerable shaft bending with the largest amplitude occuring at the bearings. Note that the amplitude at the bearings are out of phase to the rotor amplitude at the midspan section. This mode may be excited at the rotor center if the bearing damping is not excessive. The steady state response of the center mass station is shown in Fig. 2.10 and the corresponding phase angle with respect to the unbalance is given in the joining plot. In the speed range shown one critical speed is evident at 3300 RPM and the phase shift through 90° to 180° is shown in the adjoining plot. The bearing amplitude and phase is shown in Fig. 2.11 where the phase angle is observed to climb beyond 180° to more than 300°. The second critical is not excited by the given unbalance and the third critical is completely damped out of the response curves.

It should be quite evident that this computer code alone could be used to optimize a rotor bearing support system over a given speed range. Once a given configuration was decided upon the transient response analysis could be used to determine the sensitivity of the design to shock loading and to determine the stability or instability of the system.

The fourth critical speed shown in Fig. 2.9 is a direct consequence of including the gyroscopics of the lumped rotor mass stations. A point

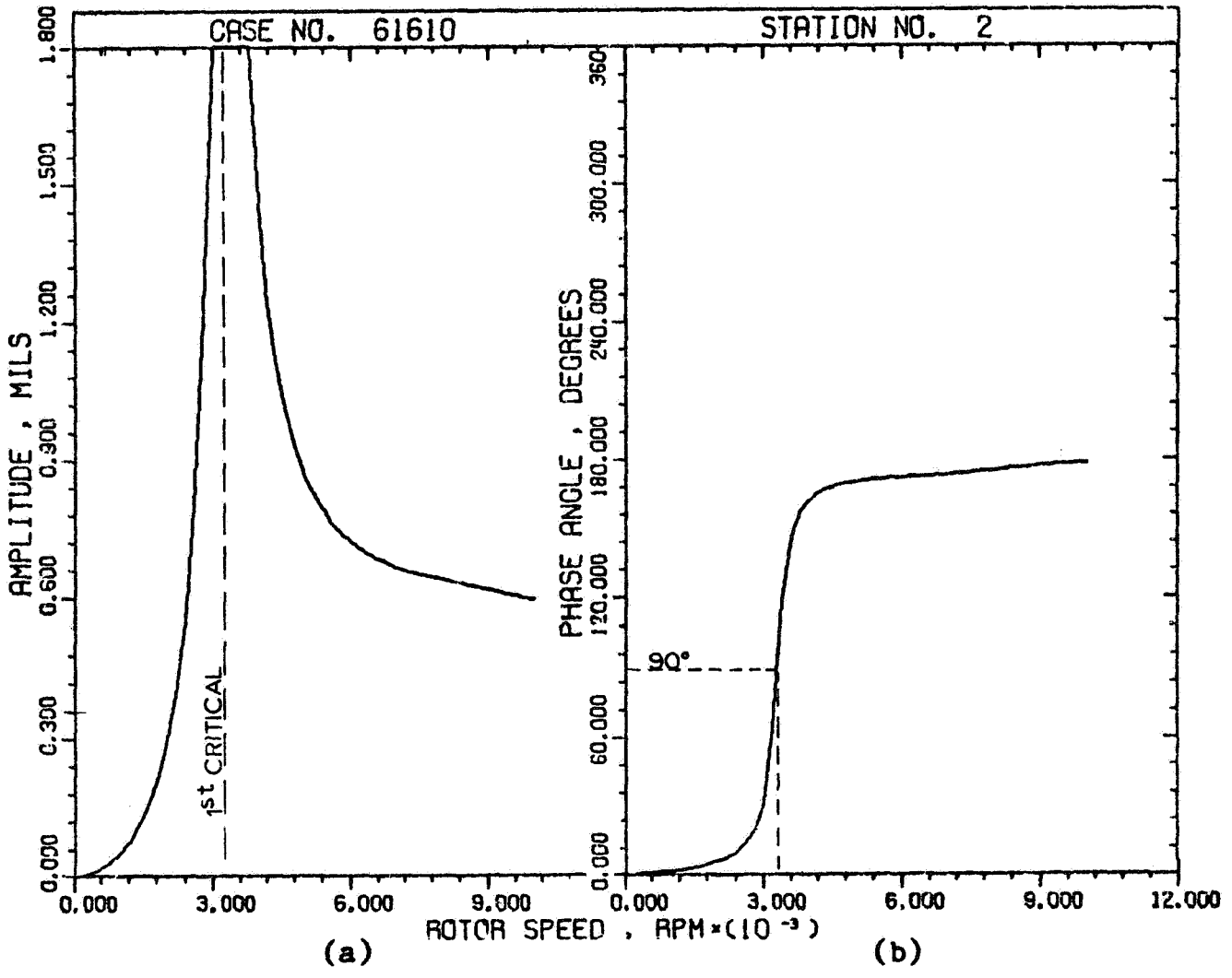

FIG. 2.10(a) ROTOR AMPLITUDE VS. ROTOR SPEED FOR A TYPICAL ROTOR-BEARING SYSTEM
(b) ROTOR PHASE ANGLE VS. SPEED FOR A TYPICAL ROTOR-BEARING SYSTEM

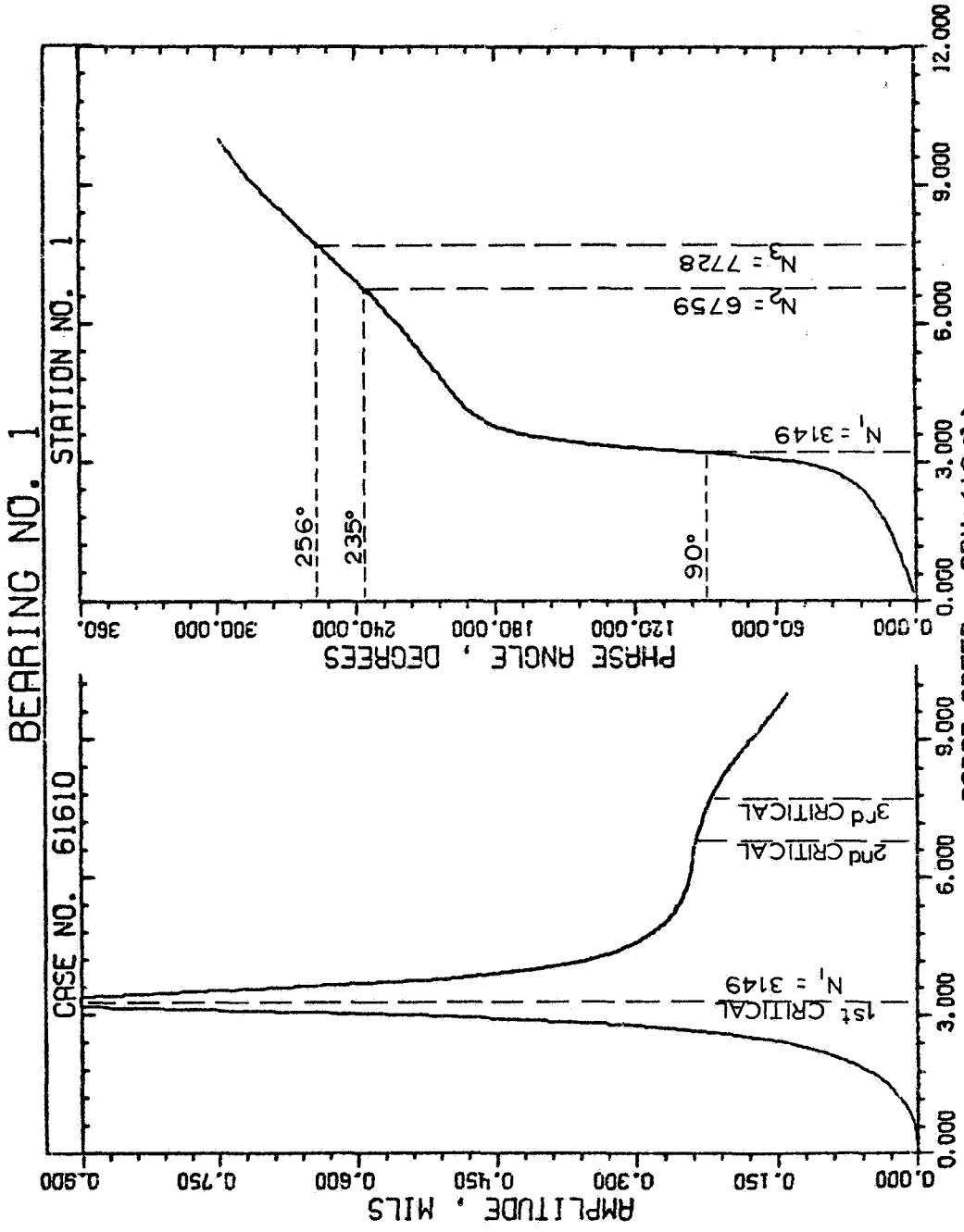

FIG. 2.11(a) BEARING AMPLITUDE VS. ROTOR SPEED FOR A TYPICAL ROTOR-BEARING SYSTEM
(b) BEARING PHASE ANGLE VS. ROTOR SPEED FOR A TYPICAL ROTOR-BEARING SYSTEM

mass model calculation would only have produced the first three criticals shown in Fig. 2.9. The steady-state response given in Figs. 2.10 and 2.11 did not cover the speed range of the fourth critical speed and unbalance at the center station would not have excited the mode even if the range was extended to beyond 14,600 RPM. This mode could be excited by an unbalance moment such as that caused by a skewed disk. The inclusion of gyroscopics in general will lower the critical speeds if the transverse moment of inertia is larger than the polar moment of inertia. However, in most applications to compressor and turbine disk locations the polar moment of inertia is larger and the inclusion of gyroscopics will tend to stiffen the shaft and hence raise the critical speeds.

CHAPTER III

DYNAMICS OF A TWO STATION ROTOR HAVING ONE SECTION OVERHUNG

3.1 Description of the Simulation Model

One class of industrial rotors may be represented by a model as suggested in Fig. 3.1.(a). This class of machines has a massive midspan section and an overhung section supported in fluid film or rolling element bearings. If the effect of the bearings can be neglected and gyroscopics are neglected on the midspan, then the model is reduced to the system as shown in Fig. 3.1.(b). This representation has a point mass at the midspan station and a massive disk at the overhung section.

3.2 Equations of Motion

The system being analyzed must be represented by six equations of motion. The midspan characteristics are denoted by the subscript 1 while the overhung station will be denoted by the subscript 2. The equations for the deflections are given in Chapter II and may be written as follows:

$$x_1 = u_1 = \alpha_{11}P_{x_1} + \alpha_{12}P_{x_2} + \beta_{12}C_{y_2} \qquad [3.1]$$

$$y_1 = v_1 = \alpha_{11}P_{y_1} + \alpha_{12}P_{y_2} - \beta_{12}C_{x_2} \qquad [3.2]$$

$$x_2 = u_2 = \alpha_{21}P_{x_1} + \alpha_{22}P_{x_2} + \beta_{22}C_{y_2} \qquad [3.3]$$

$$y_2 = v_2 = \alpha_{21}P_{y_1} + \alpha_{22}P_{y_2} - \beta_{22}C_{x_2} \qquad [3.4]$$

$$\theta_{x_2} = \theta_{x_2} = \phi_{21}P_{x_1} + \phi_{22}P_{x_2} + \gamma_{22}C_{y_2} \qquad [3.5]$$

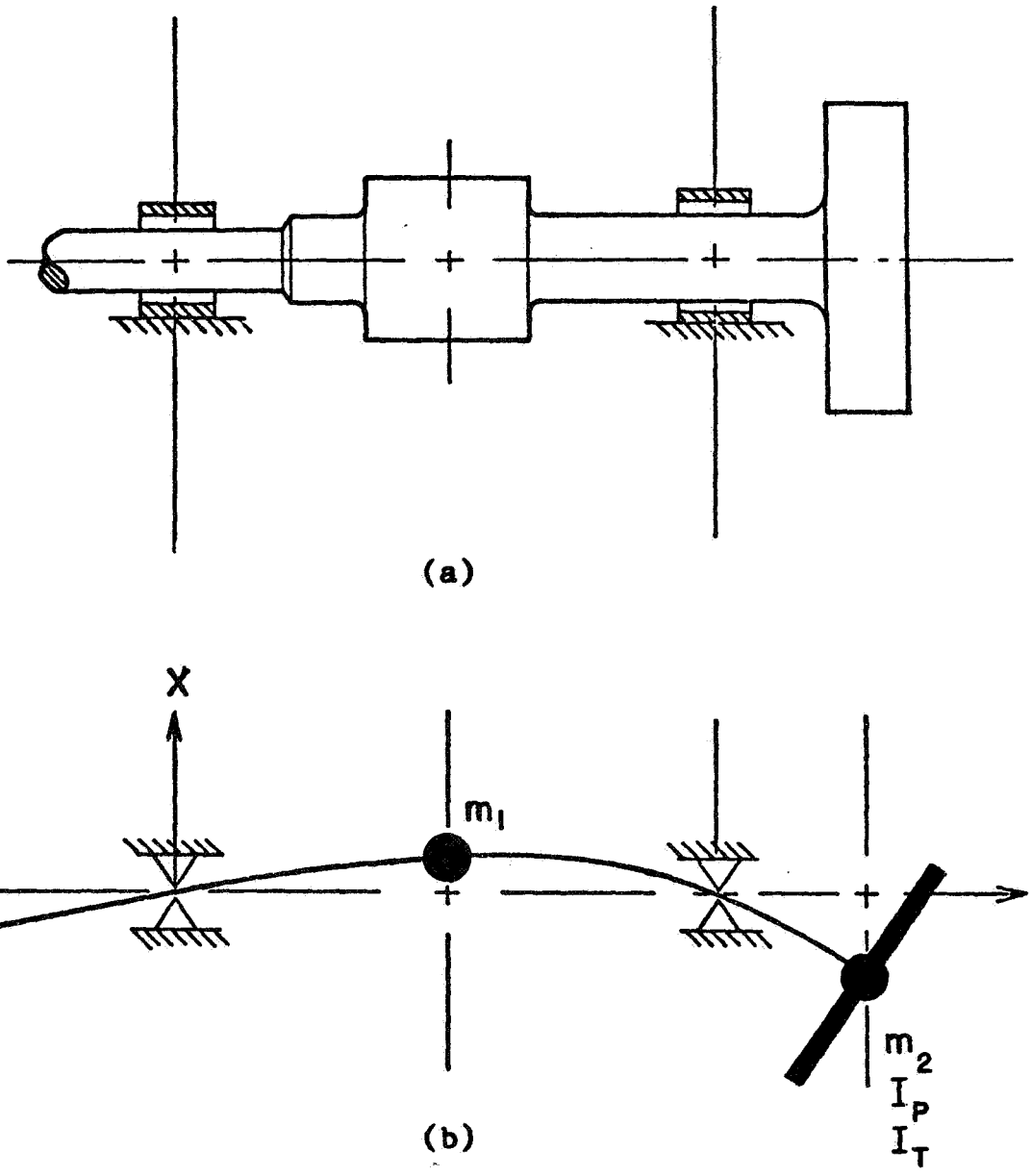

FIG. 3.1(a) TYPICAL TWO MASS ROTOR WITH MASSIVE MIDSECTION AND AN OVERHUNG STATION
(b) ASSUMED SYSTEM FOR ANALYTIC FIRST APPROXIMATION SIMULATION

$$\theta_{y_2} = \theta_{y_2} = \phi_{21}P_{y_1} + \phi_{22}P_{x_2} - \gamma_{22}C_{x_2} \qquad [3.6]$$

where

$$P_{x_1} = -m_1\ddot{x}_1 - c_1\dot{x}_1 - k_1x_1 - CI_1\dot{x}_1 - \omega CI_1y_1 - Q_1y_1$$
$$- k_{xx}x_1 - k_{xy}y_1 - c_{xx}\dot{x}_1 - c_{xy}\dot{y}_1 \qquad [3.7]$$

$$P_{y_1} = -m_1\ddot{y}_1 - c_1\dot{y}_1 - k_1y_1 - CI_1\dot{y}_1 + \omega CI_1x_1 + Q_1x_1$$
$$- k_{yy}y_1 - k_{yx}x_1 - c_{yy}\dot{y}_1 - c_{yx}\dot{x}_1 \qquad [3.8]$$

$$P_{x_2} = -m_2\ddot{x}_2 - c_2\dot{x}_2 - k_2x_2 - CI_2\dot{x}_2 - \omega CI_2y_2 - Q_2y_2 \qquad [3.9]$$

$$P_{y_2} = -m_2\ddot{y}_2 - c_2\dot{y}_2 - k_2y_2 - CI_2\dot{y}_2 + \omega CI_2\dot{x}_2 + Q_2x_2 \qquad [3.10]$$

$$C_{x_2} = I_T\ddot{\theta}_{y_2} - \omega I_P\dot{\theta}_{x_2} + K_2\theta_{y_2} \qquad [3.11]$$

$$C_{y_2} = -I_T\ddot{\theta}_{x_2} - \omega I_P\dot{\theta}_{y_2} - K_2\theta_{x_2} \qquad [3.12]$$

This formulation requires that the flexibility influence coefficients be known and the resulting equations are coupled in the acceleration terms as were the equations in Chapter II. The method and computer code used to investigate the stability of these equations will be explained in the following section and the results of the time transient solution is presented in Section 3.4.

3.3 Stability Analysis

The equations of motion given by Eqs. 3.1-3.6 may be examined for stability by applying the Routh criterion (69). This procedure requires

that the system characteristic equation be known. If solutions of the following form are assumed:

$$x_1 = A_1 e^{\lambda t}$$

$$y_1 = A_2 e^{\lambda t}$$

$$x_2 = A_3 e^{\lambda t}$$

$$y_2 = A_4 e^{\lambda t}$$

$$\theta_{x_2} = A_5 e^{\lambda t}$$

$$\theta_{y_2} = A_6 e^{\lambda t}$$

the equations of motion may be readily written as a six by six matrix formulation. Substituting the above expressions into Eqs. 3.1-3.6 and collecting terms produces the matrix formulation presented on the following page.

A computer program, OCSTB, was written to expand this matrix which has elements quadratic in λ to obtain the characteristic equation, examine the resulting characteristic equation for stability by the Routh criterion, and to find all the roots of the resulting twelth order polynomial (69). The real part of the roots indicate the stability of the system (positive for instability) and the imaginary part gives the natural frequencies of the system. A listing and explanation of the input required for OCSTB are presented in Appendix C.

The stability analysis produces the natural frequencies of the system. As an example consider the following rotor system.

$$
\begin{array}{c}
\\
x_1: \\
\\
y_1: \\
\\
x_2: \\
\\
y_2: \\
\\
\theta_{x_2}: \\
\\
\theta_{y_2}:
\end{array}
\begin{bmatrix}
1+\alpha_{11}[\lambda^2 m_1 & \alpha_{11}[\lambda c_{xy} & \alpha_{12}[\lambda^2 m_2 & \alpha_{12}(\omega CI_2+Q_2) & \beta_{12}[\lambda^2 I_T+K_2] & \beta_{12}[\lambda\omega I_p] \\
+\lambda(c_1+CI_1+c_{xx}) & +\omega CI_1+Q_1+k_{xy} & +\lambda(c_2+CI_2) & & & \\
+k_1+k_{xx}] & & +k_2] & & & \\
\alpha_{11}[\lambda c_{yx} & 1+\alpha_{11}[\lambda^2 m_1 & \alpha_{12}(-\omega CI_2-Q_2) & \alpha_{12}[\lambda^2 m_2 & \beta_{12}[-\omega I_p\lambda] & \beta_{12}[\lambda^2 I_T \\
+k_{yx}-\omega CI_1-Q_1] & +\lambda(c_1+CI_1+c_{yy}) & & +\lambda(c_2+CI_2) & & +K_2] \\
& +k_1+k_{yy} & & +k_2] & & \\
\alpha_{21}[\lambda^2 m_1 & \alpha_{21}[\lambda c_{xy} & +\alpha_{22}[\lambda^2 m_2 & \alpha_{22}(\omega CI_2+Q_2) & \beta_{22}[\lambda^2 I_T+K_2] & \beta_{22}[\lambda\omega I_p] \\
+\lambda(c_1+CI_1+c_{xx} & +\omega CI_1+Q_1+k_{xy}] & +\lambda(c_2+CI_2) & & & \\
+k_1+k_{xx}] & & +k_2] & & & \\
\alpha_{21}[\lambda c_{yx} & \alpha_{21}[\lambda^2 m_1+ & \alpha_{22}(-\omega CI_2-Q_2) & 1+\alpha_{22}[\lambda^2 m_2 & \beta_{22}[-\lambda\omega I_p] & \beta_{22}[\lambda^2 I_T \\
+k_{yx}-\omega CI_1-Q_1] & \lambda c_1+CI_1+c_{yy} & & +\lambda(c_2+CI_2) & & +K_2] \\
& +k_1+k_{yy}] & & +k_2] & & \\
\phi_{21}[\lambda^2 m_1 & \phi_{21}[\lambda c_{xy} & \phi_{22}[\lambda^2 m_2 & \phi_{22}[\omega CI_2+Q_2] & 1+\gamma_{22}[\lambda^2 I_T+K_2] & \gamma_{22}[\lambda\omega I_p] \\
+\gamma(c_1+CI_1+c_{xx} & +k_{xy}+\omega CI_1+Q_1] & +\lambda(c_2+CI_2 & & & \\
+k_1+k_{xx}] & & +k_2] & & & \\
\phi_{21}[\lambda c_{yx} & \phi_{21}[\lambda^2 m_1 & \phi_{22}(-\omega CI_2-Q_2) & \phi_{22}[\lambda^2 m_2 & \gamma_{22}[-\lambda\omega I_p] & 1+\gamma_{22}[\lambda^2 I_T \\
+k_{yx}-\omega CI_1-Q_1] & +\lambda(c_1+CI_1+c_{yy} & & +\lambda(c_2+CI_2) & & +K_2] \\
& +k_1+k_{yy}] & & +k_2] & &
\end{bmatrix}
\begin{bmatrix} A_1 \\ A_2 \\ A_3 \\ A_4 \\ A_5 \\ A_6 \end{bmatrix}
=
\begin{bmatrix} 0 \\ 0 \\ 0 \\ 0 \\ 0 \\ 0 \end{bmatrix}
$$

Example 3.1

W_1 = 1.86 lb.

W_2 = 1.86 lb.

I_P = 0.00542 lb.-in.-sec.^{2}

I_T = 0.00274 lb.-in.-sec.^{2}

overhung span = 3 in.

bearing span = 12.75 in.

shaft diameter = 0.375 in.

$E = 30 \times 10^6$ lb./in.^{2}

The influence coefficients were calculated from the procedure described in Appendix A. The results are as follows:

$\alpha_{11} = 1.483 \times 10^{-3}$ $\alpha_{12} = -1.047 \times 10^{-3}$ $\beta_{12} = 3.489 \times 10^{-4}$

$\alpha_{21} = -1.047 \times 10^{-3}$ $\alpha_{22} = 1.622 \times 10^{-3}$ $\beta_{22} = -5.923 \times 10^{-4}$

$\phi_{21} = 3.489 \times 10^{-4}$ $\phi_{22} = -5.923 \times 10^{-4}$ $\gamma_{22} = 2.49 \times 10^{-4}$

The natural frequencies were calculated and are given in Fig. 3.2. The solid lines are the forward critical speeds and the dashed lines give the backward criticals (3,43). Note that the scale on the ordinate is broken and the gyroscopic critical is very high indeed. The gyroscopics increase the two lower forward criticals as the speed increases. The synchronous forward critical speeds are approximately 2750 RPM and 6250 RPM as taken from Fig. 3.2 The critical speeds and mode shapes of synchronous forward precession were also obtained by a program (70) using the Myklestad-Prohl technique. These results are given in Fig. 3.3-4 where it is noted that the bearing characteristics

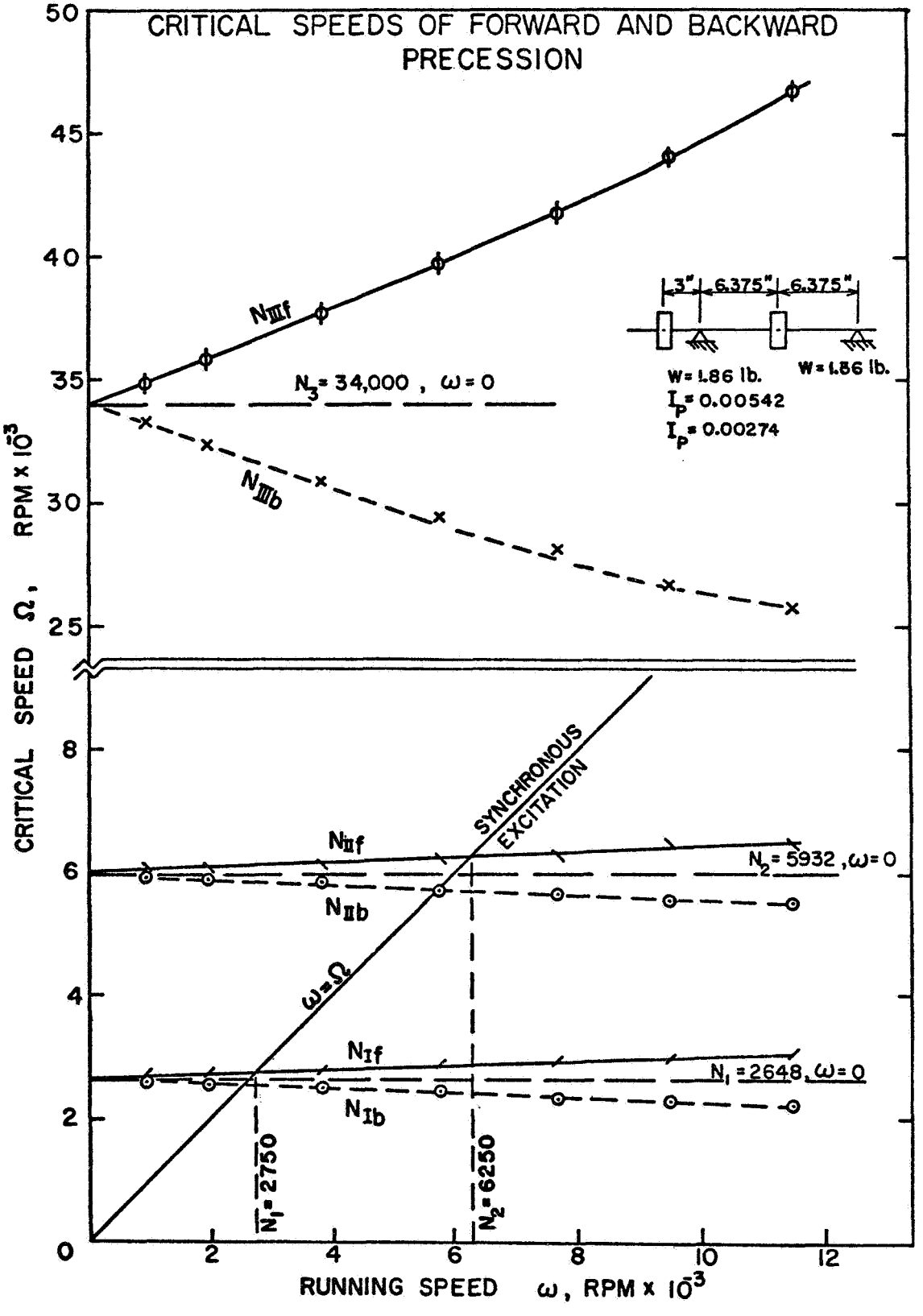

FIG. 3.2 CRITICAL SPEEDS OF FORWARD AND BACKWARD PRECESSION FOR A TWO MASS ROTOR SYSTEM

N 1 = 2745 RPM

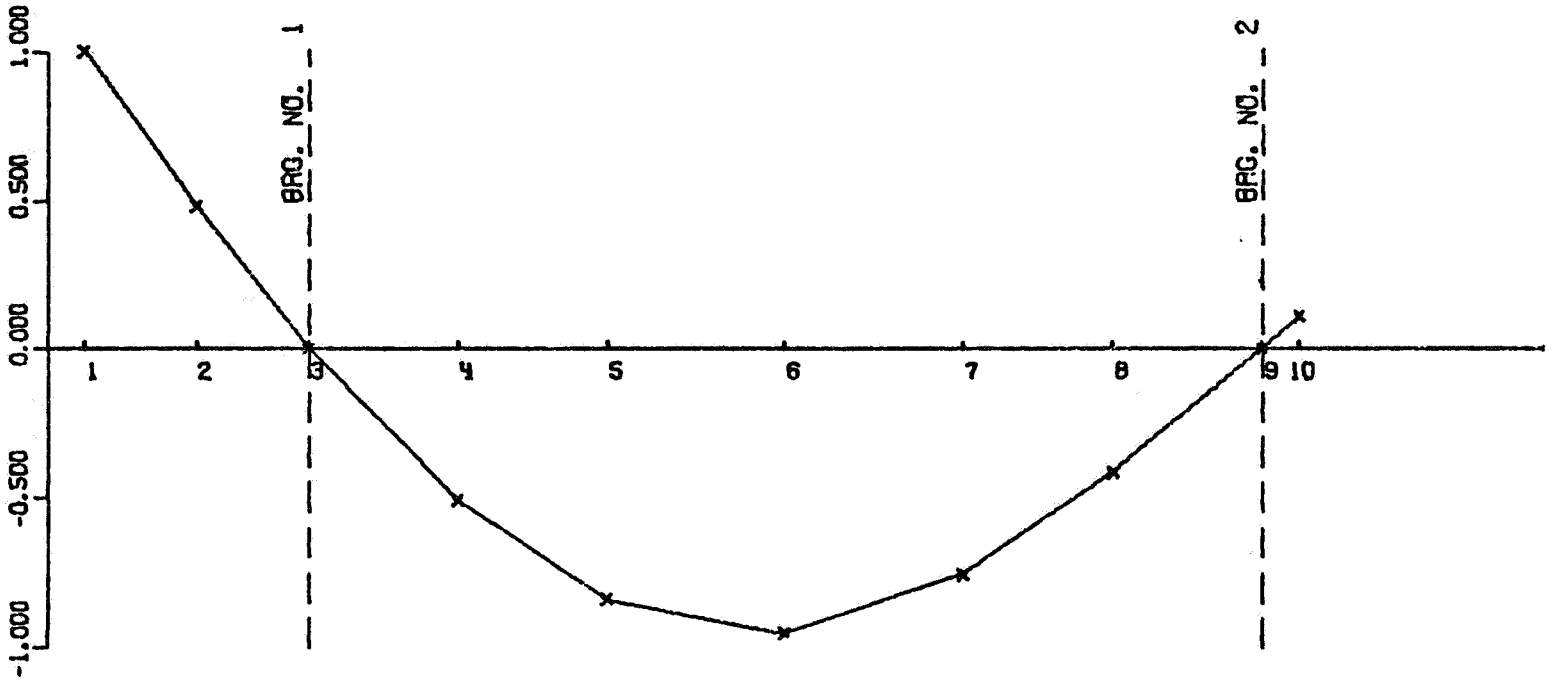

SUMMARY OF BEARING STIFFNESS VALUES

K * 10 $^{-3}$ LB/IN

10000.00000

10000.00000

FIG. 3.3 MODE SHAPE OF AN OVERHUNG ROTOR AT THE FIRST FORWARD CRITICAL (OVERHANG = 3IN.)

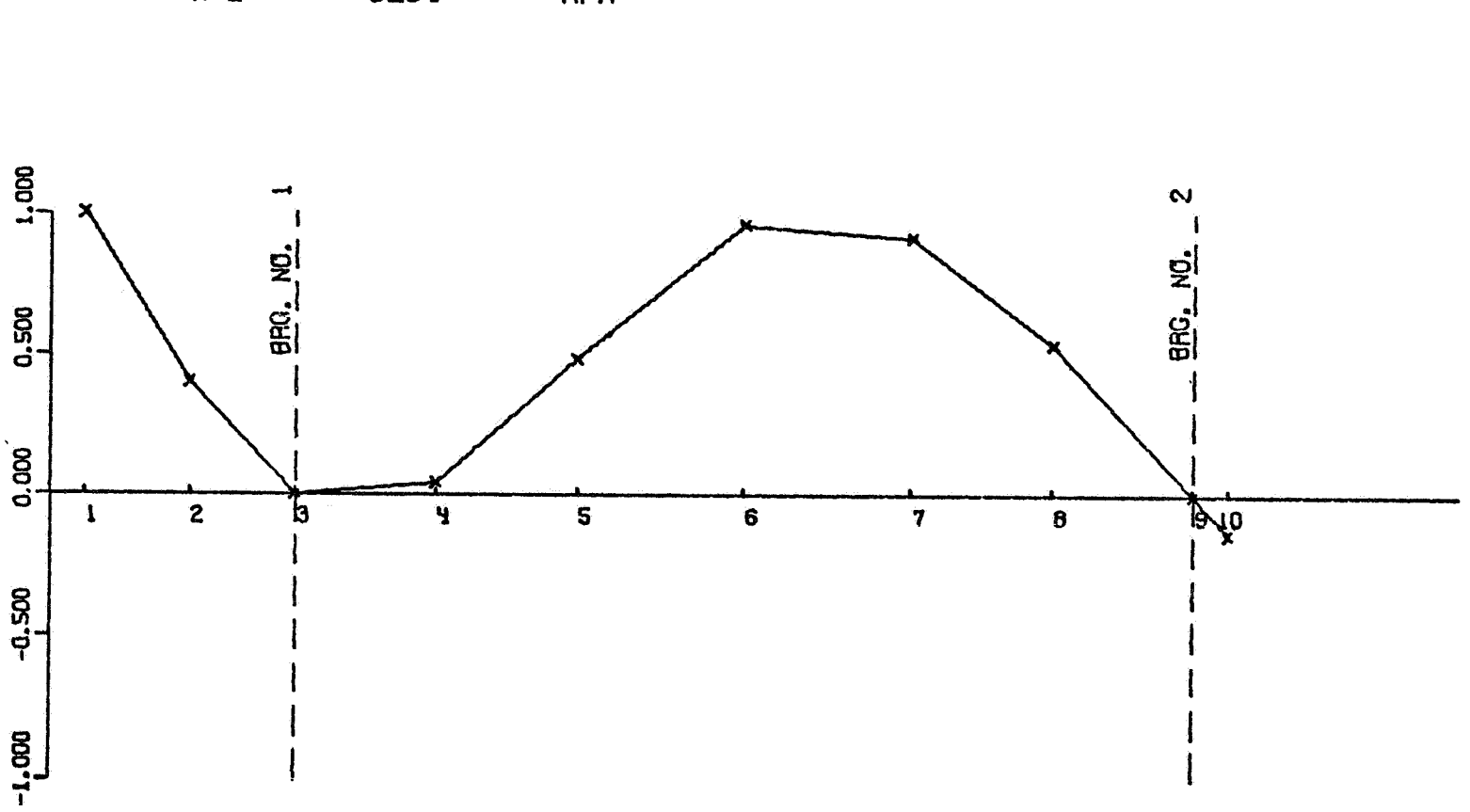

FIG. 3.4 MODE SHAPE OF AN OVERHUNG ROTOR AT THE SECOND FORWARD CRITICAL (OVERHANG = 3IN.)

were chosen to approximate rigid supports. The critical speeds were given as 2745 RPM and 6284 RPM by this computer code and it was concluded that the two programs were in agreement. The mode shapes given could be made smoother by simply taking more points along the rotor shaft. The rotor of Example 3.1 was modified slightly and will be the basis for the analysis of the remainder of this chapter.

Example 3.2

This rotor is the same as the rotor of Example 3.1 with the following exception:

overhung station = 5 in.

The influence coefficients for the rotor are:

$\alpha_{11} = 1.483 \times 10^{-3}$ $\alpha_{12} = -1.744 \times 10^{-3}$ $\beta_{12} = 3.489 \times 10^{-3}$

$\alpha_{21} = -1.744 \times 10^{-3}$ $\alpha_{22} = 5.079 \times 10^{-3}$ $\beta_{22} = -1.159 \times 10^{-3}$

$\phi_{21} = 3.489 \times 10^{-4}$ $\phi_{22} = -1.159 \times 10^{-3}$ $\gamma_{22} = 3.176 \times 10^{-4}$

The resulting critical speed plot is given in Fig. 3.5 where it is observed that the extended overhung section has lowered the two forward bending criticals N_{I_f}, N_{II_f} to 1825 RPM and 4960 RPM respectively. The corresponding mode shapes are given in Figs. 3.6 and 3.7 Also indicated on Fig. 3.5 is the effect of internal friction damping acting at station one and at station two. With a value for internal damping of 0.2 lb.-sec./in. acting at the rotor midspan, the system threshold occurs at a shaft speed of 2500 RPM and whirls at 75% of running speed which is observed to be the lowest critical N_{I_f} at this operating speed. For the same internal damping at the overhung station the system threshold occurs at 1890 RPM and whirls at 95% of running speed which

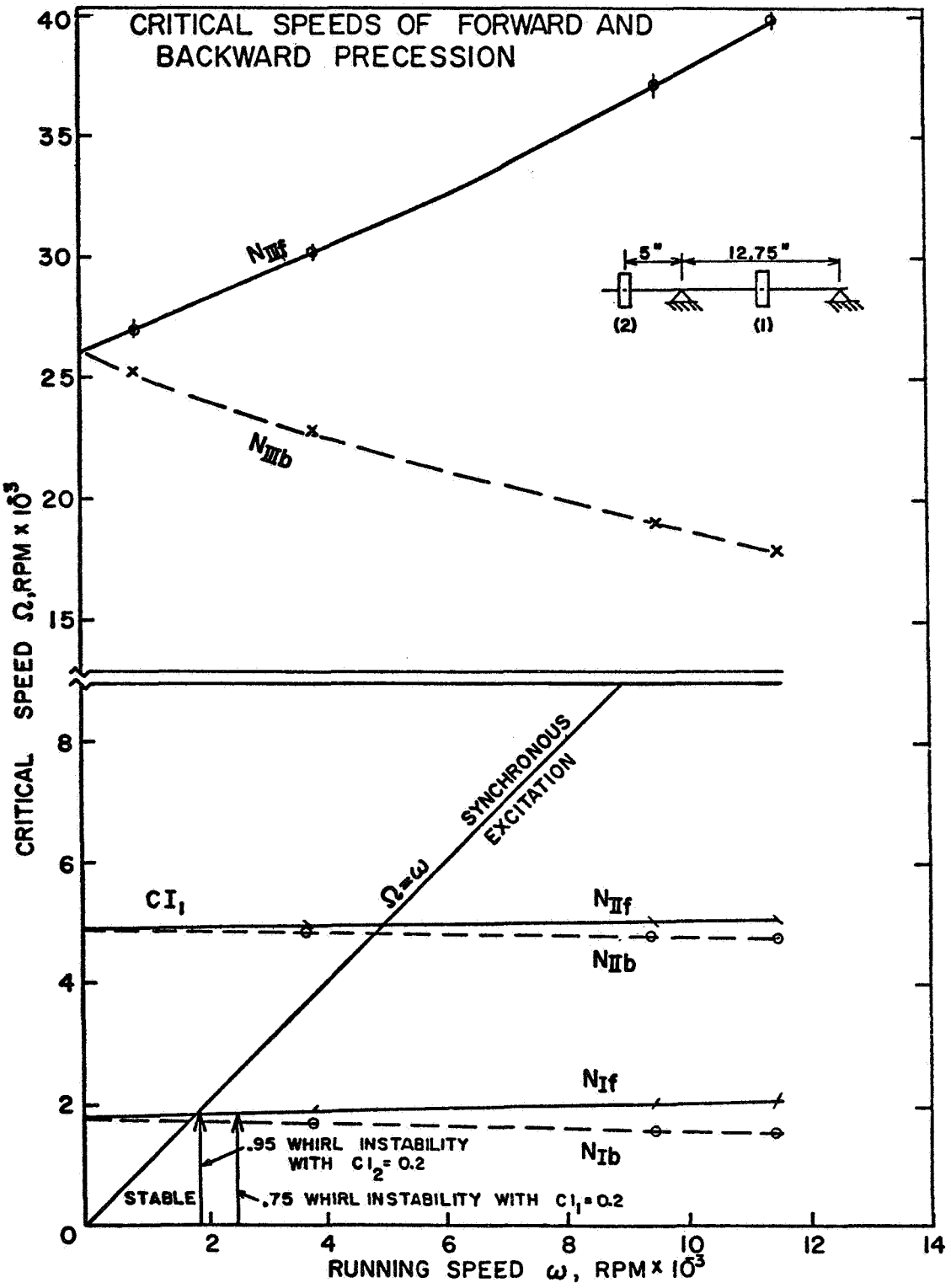

FIG. 3.5 CRITICAL SPEEDS OF FORWARD AND BACKWARD PRECESSION SHOWING INFLUENCE OF INTERNAL DAMPING ON WHIRL RATIO

N 1 = 1827 RPM

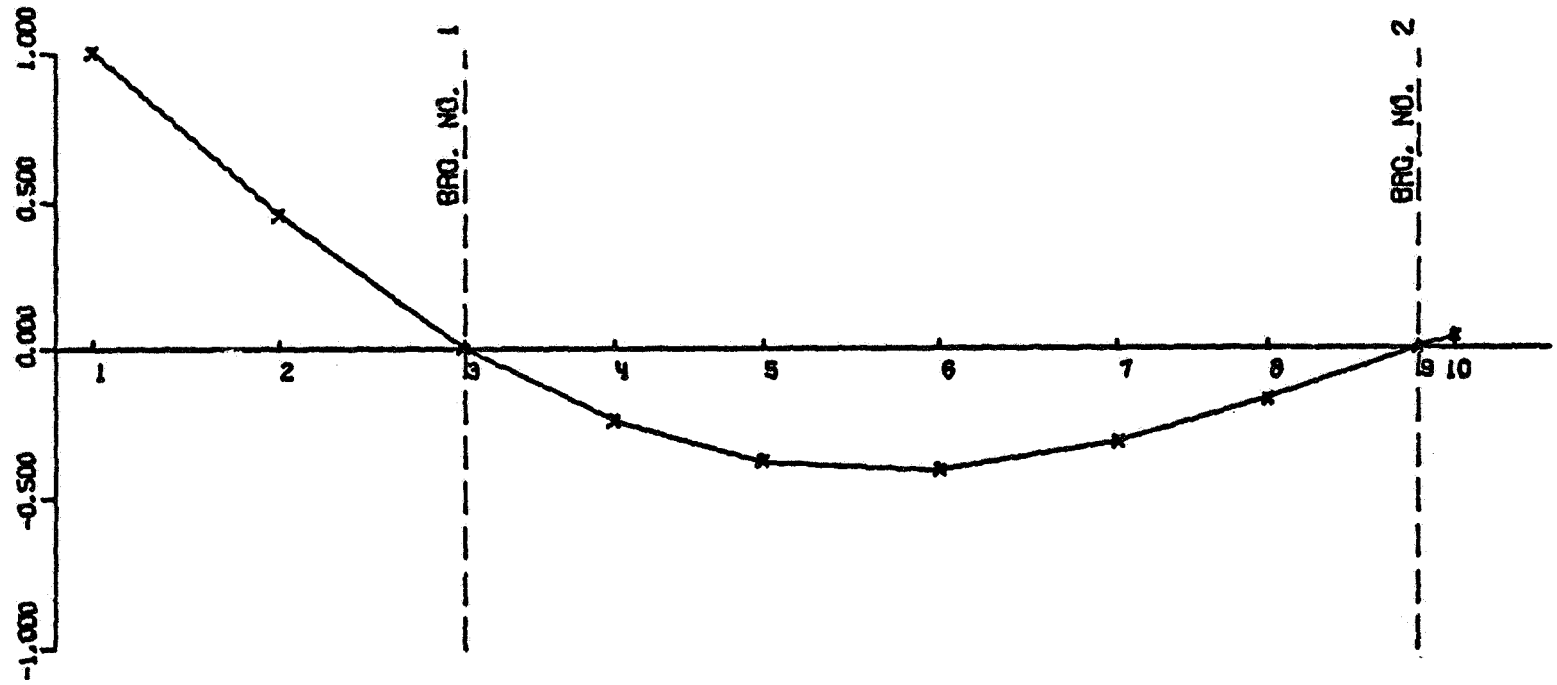

SUMMARY OF BEARING STIFFNESS VALUES

K x 10 $^{-3}$ LB/IN

1000.00000

1000.00000

FIG. 3.6 MODE SHAPE OF AN OVERHUNG ROTOR AT THE FIRST FORWARD CRITICAL (OVERHANG = 5IN.)

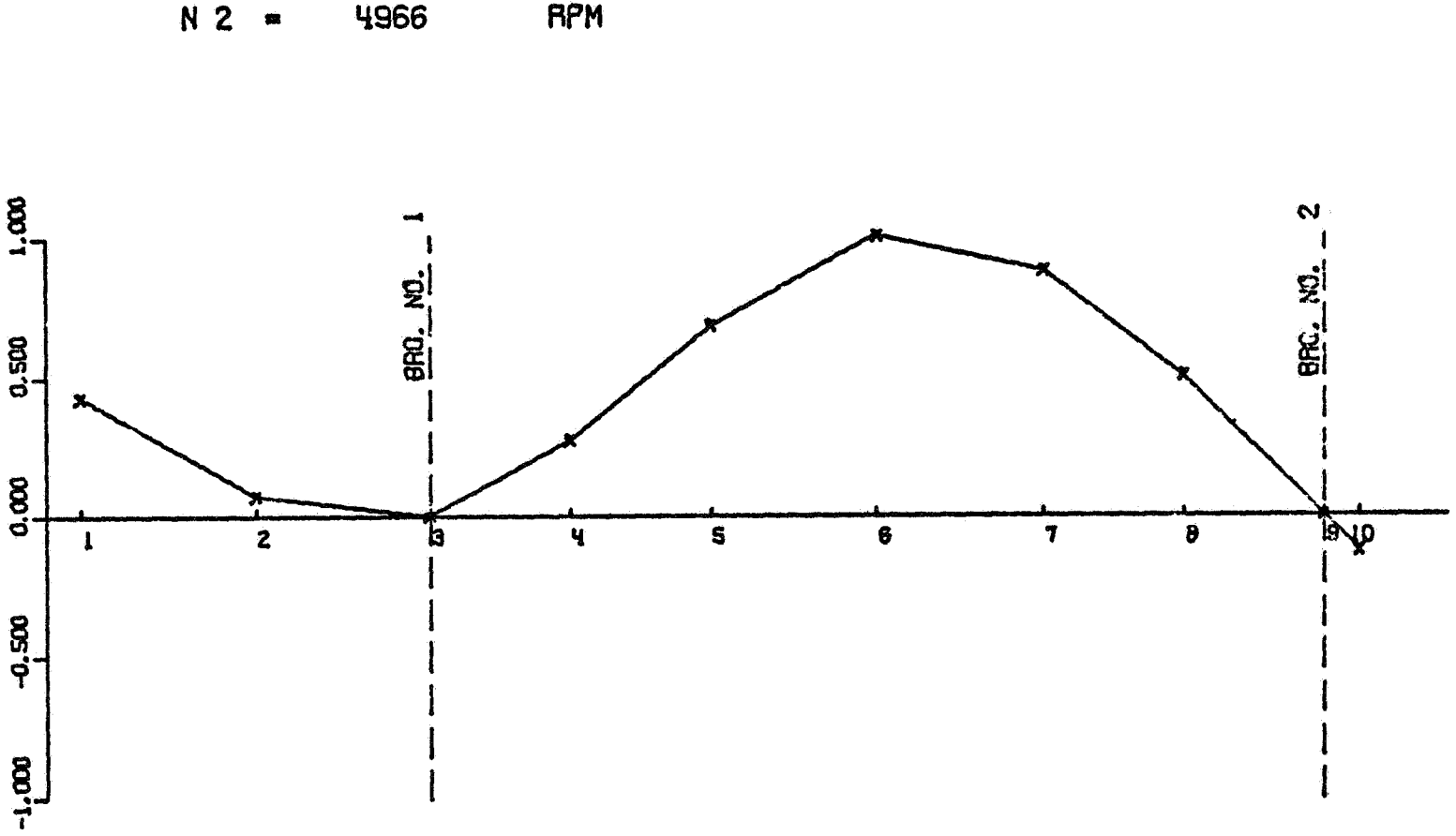

FIG. 3.7 MODE SHAPE OF AN OVERHUNG ROTOR AT THE SECOND FORWARD CRITICAL (OVERHANG = 5IN.)

corresponds once again to the lowest forward critical of the system. At higher speeds the whirl remains at that frequency corresponding to the lowest critical speed. The results for a rotor speed of 3000 RPM produces a whirl which is 62% of the running speed as shown in the computer results given in Table 3.1.

The rotor specifications are printed at the top of the table with the corresponding influence coefficients. The matrix for the system is shown and corresponds to the elements of the system as shown on page 60. Each element of the 6 x 6 matrix has three coefficients with the first one being the coefficient of the quadratic term, λ^2, the second the coefficient of λ and finally the constant term. The roots to the resulting characteristic equation are also shown with the real and imaginary parts, then the imaginary part in RPM and finally the fraction of running speed for each solution.

3.4 Transient Whirl Analysis

The simple model of Example 3.2 was chosen to test the transient program which was formulated in Chapter 2. Of particular interest is the effect of the inclusion of gyroscopics on the results of the time-transient analysis. The rotor shaft specifications used in the analysis are presented in Table 3.2 along with the approximated rotor specifications which correspond to the rotor of Example 3.2. A gyroscopic station on the overhang and a dummy seal (bearing) location are also specified in Table 3.2. For the purpose of simplifying the initial conditions required a zero gravity field is assumed.

For a rotor speed of 3000 RPM the results of the stability program with no internal friction damping are as given in Table 3.3. These

```
OVERHUNG ROTOR SIMULATION - RIGID BEARINGS
    (UNITS ARE INCH-POUND-SECOND)

ROTOR MID SPAN SPECIFICATIONS
M1 =        1.66    CS1 =        .01
KS1 =       0.00    CI1 =       0.00
Q1 =        0.00    CXX =       0.00
KXX =       0.00    CXY =       0.00
KXY =       0.00    CYX =       0.00
KYX =       0.00    CYY =       0.00
KYY =       0.00

ROTOR OVERHUNG SPECS
M2 =        1.66
IP =     .005420    CS2 =        .01
IT =     .002740    CI2 =        .28
KS2 =       0.00
Q2 =        0.00

INFLUENCE COEFFICIENTS
A11 =  1.4830-03   A12 = -1.7440-03   B12 =  3.4890-04
A21 = -1.7440-03   A22 =  5.0790-03   B22 = -1.1590-03
B21 =  3.4840-04   B22 = -1.1590-03   G22 =  3.1780-04

MATRIX FOR OVERHUNG COMPR
 7.145100-06 |  0.          | -8.403730-06 |  0.          |  9.559860-07 |  0.          |
 1.482800-05 |  0.          | -3.662400-04 |  0.          |  0.          |  5.940880-04 |
 1.000000+00 |  0.          |  0.          | -1.095790-01 |  0.          |  0.          |
 0.          |  7.145100-06 |  0.          | -8.403730-06 |  0.          |  9.559860-07 |
 0.          |  1.482800-05 |  0.          | -3.662400-04 |  0.          |  0.          |
 0.          |  1.000000+00 |  1.095790-01 |  0.          |  0.          |  0.          |
-8.403730-06 |  0.          |  2.447390-05 |  0.          | -3.175660-06 |  0.          |
-1.744000-05 |  0.          |  1.066590-03 |  0.          |  0.          | -1.973480-03 |
 0.          |  0.          |  1.000000+00 |  3.191240-01 |  0.          |  0.          |
 0.          | -8.403730-06 |  0.          |  2.447390-05 |  0.          | -3.175660-06 |
 0.          | -1.744000-05 |  0.          |  1.066590-03 |  1.973480-03 |  0.          |
 0.          |  0.          | -3.191240-01 |  1.000000+00 |  0.          |  0.          |
 1.681230-06 |  0.          | -5.584820-06 |  0.          |  8.702240-07 |  0.          |
 3.489000-06 |  0.          | -2.433900-04 |  0.          |  0.          |  5.407930-04 |
 0.          |  0.          |  0.          | -7.282230-02 |  1.000000+00 |  0.          |
 0.          |  1.681230-06 |  0.          | -5.584820-06 |  0.          |  8.702240-07 |
 0.          |  3.489000-06 |  0.          | -2.433900-04 |  0.          |  5.407930-04 |
 0.          |  0.          |  7.282230-02 |  0.          |  0.          |  1.000000+00 |

CHARACTERISTIC EQUATION
GIVEN IN FORM A0 + A1*L + A2*L**2 + ... A13*L**12)

 1.181840+00   2.452060-03   6.736290-05   8.291000-08   1.299290-09   5.721320-13   7.397590-15
 1.187010-16   1.367150-20   2.966560-25   3.317160-27   1.892260-32   2.072310-34

COEFFICIENTS IN REVERSE NORMALIZED FORM

 1.000000+00   9.131180+01   1.660710+02   1.432490+04   6.597260+13   5.727960+15   3.569730+19
 2.760850+21   6.269770+24   4.000850+26   3.250620+29   1.183250+31   5.316970+33
SRPM =   5000.01   KONTRI =  0   KOUNT =  0
CI1 =    0.00   CI2 =    .28

THE ROOTS OF THE CHAR. EQ. ARE AS FOLLOWS

-4.696737700+01   -1.8117360+02    -1730.1 RPM.    -.5767
-4.696737700+01    1.8117360+02     1730.1 RPM.     .5767
 9.802611100+00   -1.9586960+02    -1870.6 RPM.    -.6235
 9.802611100+00    1.9586960+02     1870.6 RPM.     .6235
-4.631400160+00   -5.0992670+02    -4869.4 RPM.   -1.6231
-4.631400160+00    5.0992670+02     4869.4 RPM.    1.6231
-2.139246200+00   -5.1771430+02    -4943.8 RPM.   -1.6479
-2.139246200+00    5.1771430+02     4943.8 RPM.    1.6479
-1.160274900+00   -2.4997530+03   -23868.9 RPM.   -7.8296
-1.160274900+00    2.4997530+03    23868.9 RPM.    7.8296
-4.838251600-01   -3.0566960+03   -29208.4 RPM.   -9.7361
-4.838251600-01    3.0566960+03    29208.4 RPM.    9.7361
```

TABLE 3.1 SYSTEM CHARACTERISTICS OF A TWO MASS ROTOR CONFIGURATION HAVING INTERNAL DAMPING AT THE OVERHANG

FLEXIBLE ROTOR TRANSIENT RESPONSE --BY R. GORDON KIRK-#

(UNITS ARE IN.-LB.-SEC. UNLESS OTHERWISE SPECIFIED)
THIS IS AN EXPERIMENTAL ROTOR TEST CASE
RIGID BEARINGS AND GYROSCOPICS ARE ASSUMED

CASE NUMBER = 1206.7101

ROTOR SHAFT SPECIFICATIONS

ROTOR ACCEL = 0.0 RPM/SEC

SECTION	LENGTH	DIAMETER	YOUNGS MODULUS	PRODUCT OF E.I	INSIDE DIAMETER
1	2.00	0.375	3.000E 07	1.092E 04	0.000
2	2.00	0.375	3.000E 07	1.092E 04	0.000
3	5.00	0.375	3.000E 07	1.092E 04	0.000
4	6.38	0.375	3.000E 07	1.092E 04	0.000
5	6.38	0.375	3.000E 07	1.092E 04	0.000

BEARING NO. 1 IS 9.00 INCHES FROM THE LEFT END, STATION NO. 4

BEARING NO. 2 IS 21.75 INCHES FROM THE LEFT END, STATION NO. 6

BEARING SPAN IS 12.75 INCHES

APPROXIMATED ROTOR SPECIFICATIONS

STATION	LENGTH FROM END	WEIGHT	MASS	STIFFNESS	DAMPING	INT. DAMP	STIFF-Q	EXT. WT	EMU	PHI
3	4.00	1.860	0.0048	0.0	0.000	0.000	0.0	1.75	0.00	0.0
5	15.38	1.860	0.0048	0.0	8.000	0.200	0.0	1.66	0.00	0.0

(EMU GIVEN IN OZ-IN UNITS)

(ALL OTHER STATIONS EXCEPT THE BEARINGS HAVE ZERO MASS)

TOTAL LENGTH OF ROTOR = 21.750 IN.
ACTUAL WEIGHT OF ROTOR = 4.092 LBS.
TOTAL WEIGHT OF APPROXIMATE ROTOR = 3.998 LBS.

GYROSCOPIC SPECIFICATIONS

STATION	LENGTH FROM END	POLAR MOM. OF INER.	TRANSVERSE MOM. OF INER.	KTRST (IN-LB/RAD)
3	4.00	0.0054	0.0027	0.0000

MAJOR MASS STATION SEAL SPECS

STATION NUMBER	KXX (LB/MIL)	KYY (LB/MIL)	KXY (LB/MIL)	KYX (LB/MIL)	CXX (LB-SEC/IN)	CYY (LB-SEC/IN)	CXY (LB-SEC/IN)	CYX (LB-SEC/IN)
5	0.001	0.001	0.000	0.000	0.000	0.000	0.000	0.000

TABLE 3.2 SPECIFICATIONS FOR THE ROTOR OF EXAMPLE 3.2 FOR TRANSIENT RESPONSE (MODELJ)

```
OVERHUNG ROTOR SIMULATION - RIGID BEARINGS
   (UNITS ARE INCH-POUND-SECOND)

ROTOR MID SPAN SPECIFICATIONS
M1 =      1.46    CS1 =      .01
KS1 =     0.00    CI1 =     0.00
G1 =      0.00    CYX =     0.00
KXX =     0.00    CXY =     0.00
KXY =     0.00    CYX =     0.00
KYX =     0.00    CYY =     0.00
KYY =     0.00

ROTOR OVERHUNG SPECS
M2 =      1.06
IP =    .005420   CS2 =      .01
IY =    .002740   CI2 =     0.00
KS2 =     0.00
G2 =      0.00

INFLUENCE COEFFICIENTS
A11 =  1.4830-03  A12 = -1.7440-03  B12 =  3.4890-04
A21 = -1.7440-03  A22 =  5.0790-03  B22 = -1.1590-03
P21 =  3.4890-04  P22 = -1.1590-03  G22 =  3.1760-04
```

```
MATRIX FOR OVERHUNG COMPR
I  7.145100-06 I     0.      I -8.403730-06 I     0.      I  9.559486-07 I     0.      I
I  1.482800-05 I     0.      I -1.744000-05 I     0.      I     0.      I  5.941080-04 I
I  1.000000+00 I     0.      I     0.       I     0.      I     0.      I     0.      I

I     0.       I  7.145100-06 I     0.      I -8.403730-06 I     0.      I  9.559486-07 I
I     0.       I  1.482800-05 I     0.      I -1.744000-05 I -5.941080-04 I     0.      I
I     0.       I  1.000000+00 I     0.      I     0.       I     0.      I     0.      I

I -8.403730-06 I     0.      I  2.447390-05 I     0.      I -3.175660-06 I     0.      I
I -1.744000-05 I     0.      I  5.079000-05 I     0.      I     0.      I -1.973460-03 I
I     0.       I     0.      I  1.000000+00 I     0.      I     0.      I     0.      I

I     0.       I -8.403730-06 I     0.      I  2.447390-05 I     0.      I -3.175660-06 I
I     0.       I -1.744000-05 I     0.      I  5.079000-05 I  1.973460-03 I     0.      I
I     0.       I     0.       I     0.      I  1.000000+00 I     0.      I     0.      I

I  1.681230-06 I     0.      I -5.564620-06 I     0.      I  8.702240-07 I     0.      I
I  3.489000-06 I     0.      I -1.159000-05 I     0.      I     0.      I  5.407930-04 I
I     0.       I     0.      I     0.       I     0.      I  1.000000+00 I     0.      I

I     0.       I  1.681230-06 I     0.      I -5.564620-06 I     0.      I  8.702240-07 I
I     0.       I  3.489000-06 I     0.      I -1.159000-05 I -5.407930-04 I     0.      I
I     0.       I     0.       I     0.      I     0.      I     0.      I  1.000000+00 I
```

```
CHARACTERISTIC EQUATION
GIVEN IN FORM A0 + A1*L + A2*L**2 + ... A13*L**12)

  1.000000D+00   1.312360-04   6.527620-05   5.174500-09   1.265970-09   4.423740-14   7.369480-15
  1.074330-19   1.366440-20   2.704370-26   3.316890-27   1.720240-33   2.072310-34

COEFFICIENTS IN REVERSE NORMALIZED FORM

  1.000000+00   8.301080+00   1.600480+07   1.305010+08   6.593080+13   5.184230+14   3.556130+19
  2.134690+20   6.205510+24   2.496970+25   3.149930+29   8.332850+29   4.829540+33
SRPM =  3000.01   KONTBI =  0   KOUNT =  0
CI1 =  0.00   CI2 =  0.00

THE ROOTS OF THE CHAR. EQ. ARE AS FOLLOWS

-9.68687670-01   -1.79502600+02   -1714.1 RPM.   -.5714
-9.68687670-01    1.79502600+02    1714.1 RPM.    .5714
-1.05264550+00   -1.94640170+02   -1858.7 RPM.   -.6196
-1.05264550+00    1.94640170+02    1858.7 RPM.    .6196
-1.01763520+00   -5.10379650+02   -4873.8 RPM.  -1.6246
-1.01763520+00    5.10379650+02    4873.8 RPM.   1.6246
-1.03275990+00   -5.17761780+02   -4944.3 RPM.  -1.6481
-1.03275990+00    5.17761780+02    4944.3 RPM.   1.6481
-5.20800610-02   -2.45977600+03   -23489.2 RPM.  -7.8297
-5.20800610-02    2.45977600+03    23489.2 RPM.   7.8297
-2.67292950-02   -3.05869690+03   -29208.4 RPM.  -9.7361
-2.67292950-02    3.05869690+03    29208.4 RPM.   9.7361
```

TABLE 3.3 SYSTEM CHARACTERISTICS OF A TWO MASS ROTOR CONFIGURATION SHOWING STABLE RESPONSE FOR THE CASE OF NO INTERNAL DAMPING

results predict a stable operating condition. Since the gyroscopics are not predominant at this low speed a point mass rotor simulation was run using the code MODELJ. The rotor specifications for this assumption are given in Table 3.5 (see page 76).

The initial conditions were given to excite the first mode response with a synchronous initial whirl rate. Fig. 3.8(a) represents the transient response of the overhung disk for five cycles of running speed. The motion has an average whirl of nearly 60% and is stable as predicted by the stability analysis. The midsection response given in Fig. 3.8(b) indicates the presence of a higher mode developed in the x-direction. The running speed is between the first and second criticals and a combination of the modes is to be expected for free response of the system.

If internal damping is introduced at the midsection the stability analysis indicates an unstable whirl of 62% as given in Table 3.4. The rate of growth of the instability should not be too great due to the relatively small real part of the root. The specifications for the transient simulation are given in Table 3.5. The transient orbits for synchronous first mode excitation are given in Fig. 3.9. The first five cycles for the overhung and midsection are given in Fig. 3.9(a) and 3.9(b) respectively. The orbits indicate an approximate whirl of 60% with definite indication that the motion is orbiting out into an unstable pattern. The continuation for cycles six through ten are shown in Figs. 3.9(c) and 3.9(d) with definite indication of an unstable system. The 60% whirl has predominated the response at the midsection as indicated in Fig. 3.9(d).

SEGMENT	N-INIT. (RPM)	N-FINAL (RPM)	T-FINAL (RAD)
1	3000.0	3000.0	6.3
2	3000.0	3000.0	12.6
3	3000.0	3000.0	18.8
4	3000.0	3000.0	25.1
5	3000.0	3000.0	31.4

TRANSIENT RESPONSE OF ROTOR STATION NO. 3

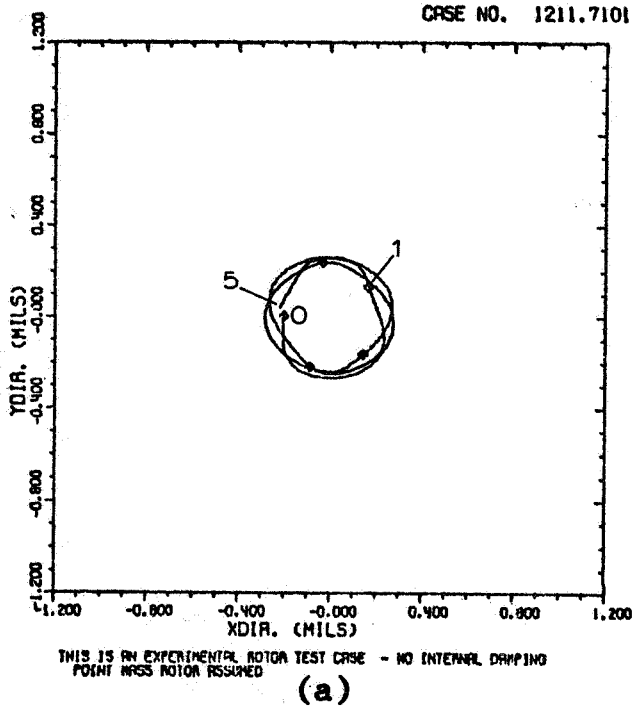

(a)

TRANSIENT RESPONSE OF ROTOR STATION NO. 5

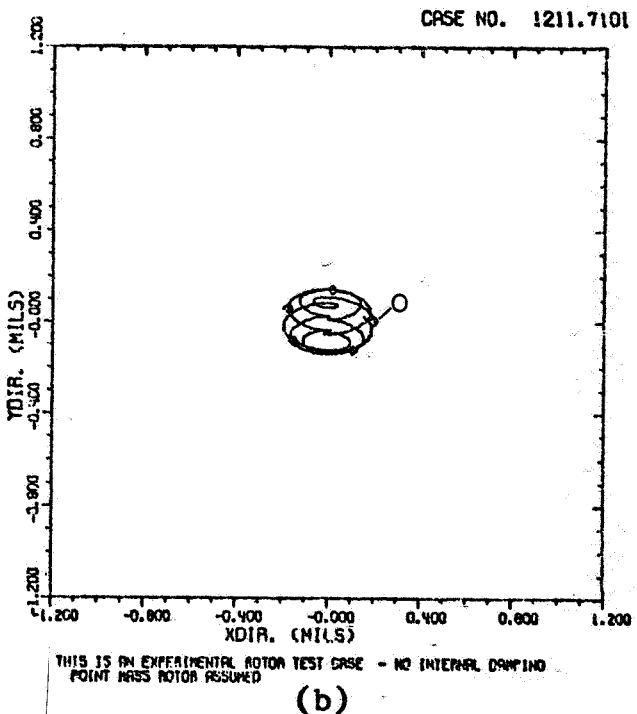

(b)

FIG. 3.8(a) TRANSIENT MOTION AT OVERHUNG STATION - NO GYROSCOPIC MOMENTS (H=0.05)
(b) TRANSIENT MOTION AT MIDSPAN STATION - NO GYROSCOPIC MOMENTS (H=0.05)

```
OVERHUNG ROTOR SIMULATION - RIGID BEARINGS
   (UNITS ARE INCH-POUND-SECOND)

ROTOR MID SPAN SPECIFICATIONS
M1 =      1.86    CS1 =      .01
KS1 =     0.00    CI1 =      .28
Q1 =      0.00    CYX =      0.00
KXX =     0.00    CXY =      0.00
KXY =     0.00    CYX =      0.00
KYX =     0.00    CYY =      0.00
KYY =     0.00

ROTOR OVERHUNG SPECS
M2 =      1.86
IP =      .005420   CS2 =      .01
IT =      .002740   CI2 =      0.00
KS2 =     0.00
Q2 =      0.00

INFLUENCE COEFFICIENTS
A11 =  1.4830-03   A12 = -1.7440-03   A12 =  3.4890-04
A21 = -1.7440-03   A22 =  5.0790-03   A22 = -1.1590-03
A21 =  3.4890-04   A22 = -1.1590-03   A22 =  1.1760-04

MATRIX FOR OVERHUNG COMPR
 7.145100-06 |  0.          | -8.403730-06 |  0.          |  9.559860-07 |  0.
 3.113860-04 |  0.          | -1.744080-05 |  0.          |  0.          |  5.946860-04
 1.000000+00 | -9.316730-02 |  0.          |  0.          |  0.          |  0.
-------------+--------------+--------------+--------------+--------------+-------------
 0.          |  7.145100-06 |  0.          | -8.403730-06 |  0.          |  9.559860-07
 0.          |  3.113860-04 |  0.          | -1.744080-05 | -5.946860-04 |  0.
-9.316730-02 |  1.000000+00 |  0.          |  0.          |  0.          |  0.
-------------+--------------+--------------+--------------+--------------+-------------
-8.403730-06 |  0.          |  2.447190-05 |  0.          | -3.175660-06 |  0.
-5.862480-04 |  0.          |  5.379000-05 |  0.          |  0.          | -1.973480-03
 0.          | -1.095790-01 |  1.000000+00 |  0.          |  0.          |  0.
-------------+--------------+--------------+--------------+--------------+-------------
 0.          | -8.403730-06 |  0.          |  2.447390-05 |  0.          | -3.175660-06
 0.          | -3.862480-04 |  0.          |  5.079000-05 |  1.973480-03 |  0.
 1.095790-01 |  0.          |  0.          |  1.000000+00 |  0.          |  0.
-------------+--------------+--------------+--------------+--------------+-------------
 1.681230-06 |  0.          | -5.584820-06 |  0.          |  8.702240-07 |  0.
 7.326980-05 |  0.          | +1.159080-05 |  0.          |  0.          |  5.407930-04
 0.          |  2.192210-02 |  0.          |  0.          |  1.000000+00 |  0.
-------------+--------------+--------------+--------------+--------------+-------------
 0.          |  1.681230-06 |  0.          | -5.584820-06 |  0.          |  8.702240-07
 0.          |  7.326980-05 |  0.          | -1.159080-05 | -5.407930-04 |  0.
-2.192210-02 |  0.          |  0.          |  0.          |  0.          |  1.000000+00

CHARACTERISTIC EQUATION
GIVEN IN FORM A0 + A1*L + A2*L**2 + ... A13*L**13

 1.000000+00   7.505290-04   6.568650-05   3.344500-08   1.292170-09   4.077070-13   7.397100-15
 1.176570-18   1.367160-20   2.981090-25   3.317160-27   1.892200-32   2.872310-34

COEFFICIENTS IN REVERSE NORMALIZED FORM

 1.000000+00   9.131180+01   1.600710+07   1.438540+09   6.597280+13   5.677580+15   3.569500+19
 1.907410+21   6.235440+24   1.013900+26   3.169730+29   3.623640+30   4.867430+33
SRPM =   3000.01   KONTRI =  0   KOUNT =  0
CI1 =     .20   CI2 =    0.00

THE ROOTS OF THE CHAR. EQ. ARE AS FOLLOWS

-8.058612D+00   -1.800828D+02      -1719.7 RPM.      -.5732
-8.058612D+00    1.800828D+02       1719.7 RPM.       .5732
 8.240249D-01   -1.946965D+02      -1859.2 RPM.      -.6197
 8.240249D-01    1.946965D+02       1859.2 RPM.       .6197
-7.979293D+00   -5.174962D+02      -4941.7 RPM.     -1.6472
-7.979293D+00    5.174962D+02       4941.7 RPM.      1.6472
-3.027173D+01   -5.095932D+02      -4866.3 RPM.     -1.6221
-3.027173D+01    5.095932D+02       4866.3 RPM.      1.6221
-5.223016D-02   -3.065965D+03     -29268.4 RPM.     -9.7361
-5.223016D-02    3.065965D+03      29268.4 RPM.      9.7361
-1.168729D-01   -2.453774D+03     -23489.1 RPM.     -7.8297
-1.168729D-01    2.453774D+03      23489.1 RPM.      7.8297
```

TABLE 3.4 CHARACTERISTICS OF TWO MASS ROTOR SYSTEM WITH LIGHT INTERNAL DAMPING AT MIDSPAN (CI1= 0.2LB-SEC/IN)

FLEXIBLE ROTOR TRANSIENT RESPONSE --BY R. GORDON KIRK--

(UNITS ARE IN.-LB.-SEC. UNLESS OTHERWISE SPECIFIED)
POINT MASS ROTOR IS ASSUMED - INTERNAL DAMPING AT STATION 5
INITIAL CONDITIONS GIVEN TO EXCITE 1ST MODE

CASE NUMBER = 1216.7101

ROTOR SHAFT SPECIFICATIONS

ROTOR ACCEL = 0.0 RPM/SEC

SECTION	LENGTH	DIAMETER	YOUNGS MODULUS	PRODUCT OF E*I	INSIDE DIAMETER
1	2.00	0.375	3.000E 07	1.092E 04	0.000
2	2.00	0.375	3.000E 07	1.092E 04	0.000
3	5.00	0.375	3.000E 07	1.092E 04	0.000
4	6.38	0.375	3.000E 07	1.092E 04	0.000
5	6.38	0.375	3.000E 07	1.092E 04	0.000

BEARING NO. 1 IS 9.00 INCHES FROM THE LEFT END, STATION NO. 4

BEARING NO. 2 IS 21.75 INCHES FROM THE LEFT END, STATION NO. 6

BEARING SPAN IS 12.75 INCHES

APPROXIMATED ROTOR SPECIFICATIONS

STATION	LENGTH FROM END	WEIGHT	MASS	STIFFNESS	DAMPING	INT. DAMP	STIFF-D	EXT. WT	EMU	PHI
3	4.00	1.860	0.0048	0.0	0.010	0.000	0.0	1.75	0.0000	180.0
5	15.38	1.860	0.0048	0.0	0.010	0.200	0.0	1.66	0.0000	0.0

(EMU GIVEN IN OZ-IN UNITS)

(ALL OTHER STATIONS EXCEPT THE BEARINGS HAVE ZERO MASS)

TOTAL LENGTH OF ROTOR = 21.750 IN.
ACTUAL WEIGHT OF ROTOR = 4.092 LBS.
TOTAL WEIGHT OF APPROXIMATE ROTOR = 3.998 LBS.

CASE NUMBER = 1216.7101

BEARING STATION SPECIFICATIONS

RIGID BEARING SUPPORT SYSTEM

TABLE 3.5 SPECIFICATIONS OF ROTOR FOR POINT MASS STATIONS AND INTERNAL DAMPING AT MIDSPAN

SEGMENT	N-INIT. (RPM)	N-FINAL (RPM)	T-FINAL (RAD)
1	3000.0	3000.0	6.3
2	3000.0	3000.0	12.6
3	3000.0	3000.0	18.8
4	3000.0	3000.0	25.1
5	3000.0	3000.0	31.4

TRANSIENT RESPONSE OF ROTOR STATION NO. 3

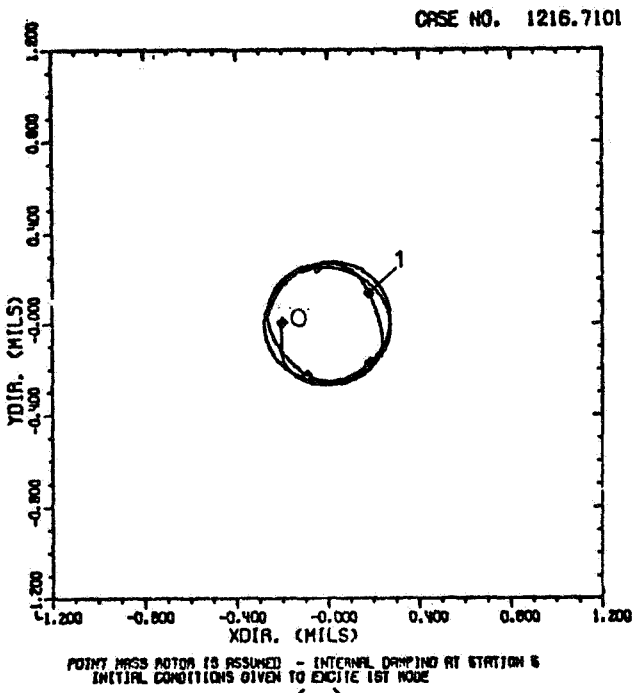

(a)

TRANSIENT RESPONSE OF ROTOR STATION NO. 5

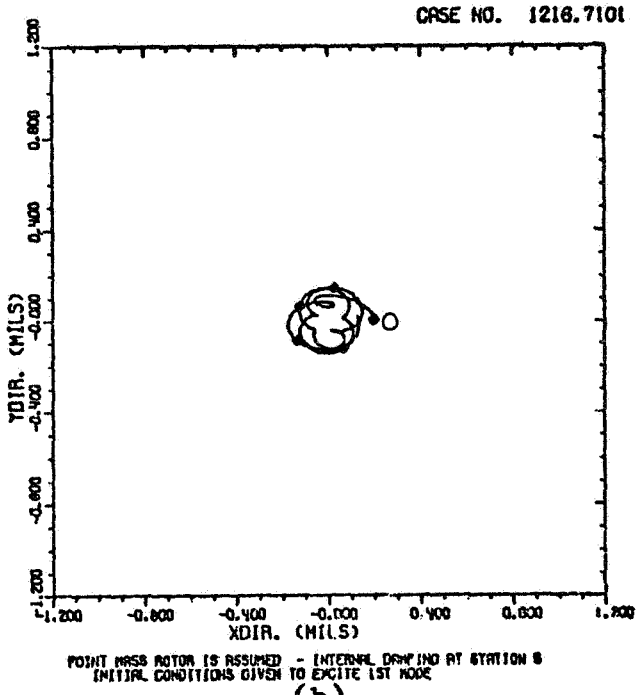

(b)

FIG. 3.9(a) TRANSIENT MOTION OF OVERHUNG STATION WITH INTERNAL DAMPING AT MIDSPAN STATION
(b) TRANSIENT MOTION OF MIDSPAN STATION FOR FIVE CYCLES OF MOTION

SEGMENT	N-INIT. (RPM)	N-FINAL (RPM)	T-FINAL (RAD)
1	3000.0	3000.0	37.6
2	3000.0	3000.0	43.9
3	3000.0	3000.0	50.2
4	3000.0	3000.0	56.5
5	3000.0	3000.0	62.7

TRANSIENT RESPONSE OF ROTOR STATION NO. 3

CASE NO. 1216.7101

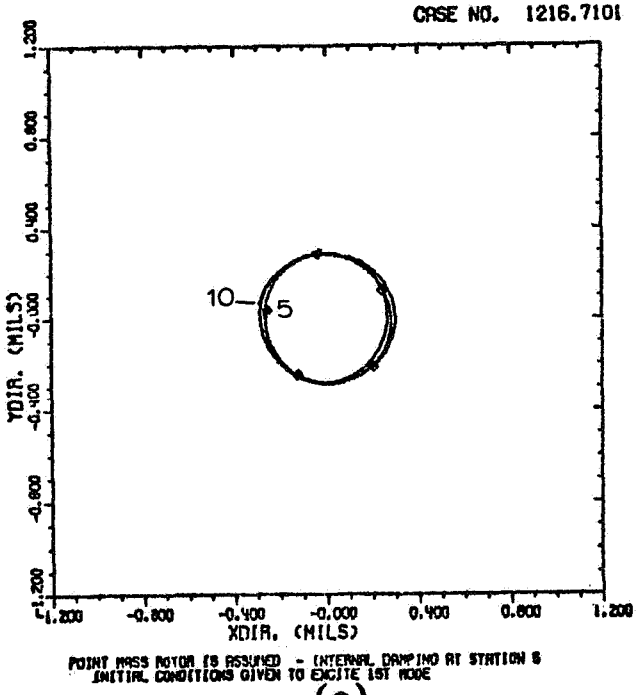

POINT MASS ROTOR IS ASSUMED - INTERNAL DAMPING AT STATION 6
INITIAL CONDITIONS GIVEN TO EXCITE 1ST MODE

(c)

TRANSIENT RESPONSE OF ROTOR STATION NO. 5

CASE NO. 1216.7101

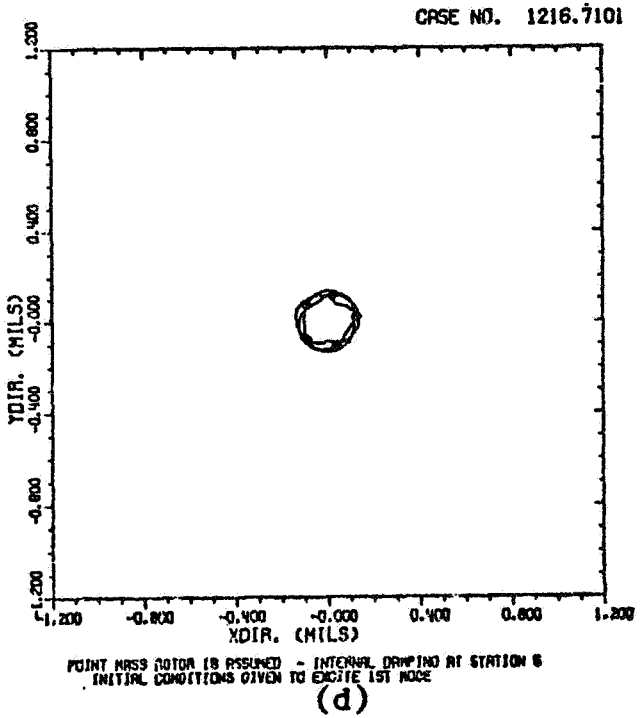

POINT MASS ROTOR IS ASSUMED - INTERNAL DAMPING AT STATION 6
INITIAL CONDITIONS GIVEN TO EXCITE 1ST MODE

(d)

FIG. 3.9(c) TRANSIENT MOTION OF OVERHANG STATION FOR CYCLES FIVE THROUGH TEN (CI1 = 0.2)
(d) TRANSIENT RESPONSE OF MIDSPAN FOR CYCLES FIVE THROUGH TEN (CI1 = 0.2)

The inclusion of the gyroscopic properties of the overhung section should not drastically alter the transient response from that obtained for the point mass simulation. With the same time step as for the previous solution but including the gyroscopics at the overhang the transient response indicated from the program is shown in Fig. 3.10. The initial response is smooth but small cusps are developed which grow into inner loops and finally the response is dominated by an approximate 10/1 whirl rate. The cusps and inner loops are actual solutions of a simple gyro (71) but the large jumps in the later portion of the solution are clearly inaccurate. There are no energy producing mechanisms in the system and hence the physical considerations do not allow this type response (72).

The system has been excited by a frequency ten times running speed and Fig. 3.5 shows that the gyroscopic critical is very nearly ten times running speed for the case of N = 3000 RPM. The initial conditions on the angular displacements of the overhung were specified as zero and hence induced small excitations of the order of 10/1 of running speed. The time step of the solution was not small enough to accurately track these excitations and they eventually became dominant due to numerical difficulties. The solution at the end of the third cycle of running speed was used for initial conditions with the step size reduced to H = 0.01 (radians). This gives 628 steps per cycle or for a 10/1 whirl there would be 63 steps per whirl revolution. A sustained whirl of 10/1 should result from such starting conditions and the solution should be bounded. The results for one cycle of running speed is shown in Fig. 3.11 where the expected sustained 10/1 whirl is evident.

FLEXIBLE ROTOR TRANSIENT RESPONSE --BY R. GORDON KIRK--

(UNITS ARE IN.-LB.-SEC. UNLESS OTHERWISE SPECIFIED)
THIS IS AN EXPERIMENTAL ROTOR TEST CASE - NO INTERNAL DAMPING
RIGID BEARINGS AND GYROSCOPICS ARE ASSUMED

CASE NUMBER = 1210.7101

ROTOR SHAFT SPECIFICATIONS

ROTOR ACCEL = 0.0 RPM/SEC

SECTION	LENGTH	DIAMETER	YOUNGS MODULUS	PRODUCT OF E*I	INSIDE DIAMETER
1	2.00	0.375	3.000E 07	1.092E 04	0.000
2	2.00	0.375	3.000E 07	1.092E 04	0.000
3	5.00	0.375	3.000E 07	1.092E 04	0.000
4	6.38	0.375	3.000E 07	1.092E 04	0.000
5	6.38	0.375	3.000E 07	1.092E 04	0.000

BEARING NO. 1 IS 9.00 INCHES FROM THE LEFT END, STATION NO. 4

BEARING NO. 2 IS 21.75 INCHES FROM THE LEFT END, STATION NO. 6

BEARING SPAN IS 12.75 INCHES

APPROXIMATED ROTOR SPECIFICATIONS

STATION	LENGTH FROM END	WEIGHT	MASS	STIFFNESS	DAMPING	INT. DAMP	STIFF-Q	EXT. WT	EMU	PHI
3	4.00	1.860	0.0048	0.0	0.000	0.000	0.0	1.75	0.00	0.0
5	15.38	1.860	0.0048	0.0	0.000	0.000	0.0	1.66	0.00	0.0

(EMU GIVEN IN 07-IN UNITS)

(ALL OTHER STATIONS EXCEPT THE BEARINGS HAVE ZERO MASS)

CASE NUMBER = 1210.7101

TOTAL LENGTH OF ROTOR = 21.750 IN.
ACTUAL WEIGHT OF ROTOR = 4.092 LBS.
TOTAL WEIGHT OF APPROXIMATE ROTOR = 3.998 LBS.

BEARING STATION SPECIFICATIONS

RIGID BEARING SUPPORT SYSTEM

GYROSCOPIC SPECIFICATIONS

STATION	LENGTH FROM END	POLAR MOM. OF INER.	TRANSVERSE MOM. OF INER.	RTHST (IN-LB/RAD)
3	4.00	0.0058	0.0027	0.0000

MAJOR MASS STATION SEAL SPECS

STATION NUMBER	KXX (LB/MIL)	KYY (LB/MIL)	KXY (LB/MIL)	KYX (LB/MIL)	CXX (LB-SEC/IN)	CYY (LB-SEC/IN)	CXY (LB-SEC/IN)	CYX (LB-SEC/IN)
5	0.001	0.001	0.000	0.000	0.000	0.000	0.000	0.000

TABLE 3.6 SPECIFICATIONS FOR ROTOR WITH INCLUSION OF GYROSCOPIC MOMENTS AND SEAL SPECIFICATIONS

SEGMENT	N-INIT. (RPM)	N-FINAL (RPM)	T-FINAL (RAD)
1	3000.0	3000.0	0.3
2	3000.0	3000.0	12.6
3	3000.0	3000.0	18.8
4	3000.0	3000.0	25.1
5	3000.0	3000.0	31.4

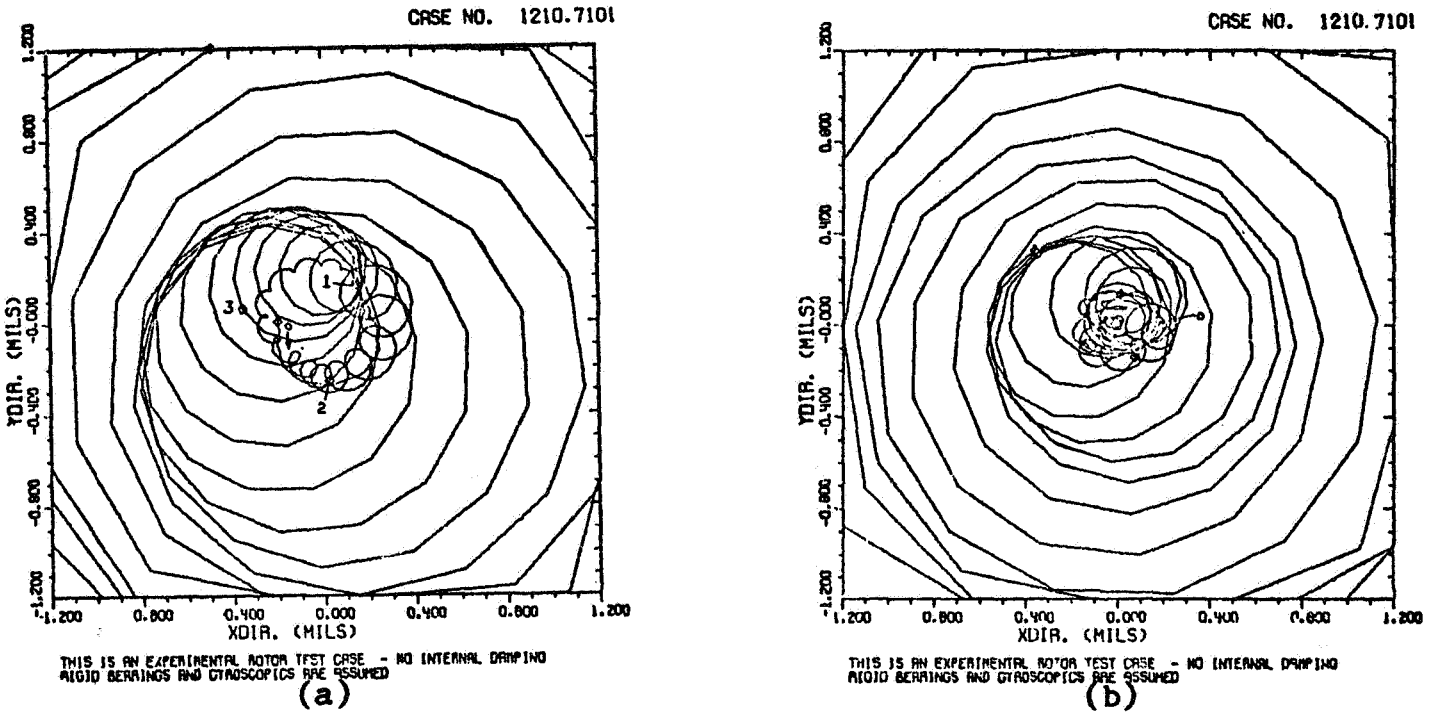

FIG. 3.10(a) TRANSIENT RESPONSE OF OVERHANG INCLUDING GYROSCOPICS SHOWING INSTABILITY DUE TO RELATIVELY LARGE TIME STEP (H = 0.05)
(b) MIDSPAN RESPONSE SHOWING EFFECT OF NUMERICAL INSTABILITY AT OVERHANG DUE TO GYROSCOPIC NUMERICAL INSTABILITY

FLEXIBLE ROTOR TRANSIENT RESPONSE --BY R. GORDON KIRK--

(UNITS ARE IN.-LB.-SEC. UNLESS OTHERWISE SPECIFIED)
RIGID BEARINGS AND GYROSCOPICS ARE ASSUMED = OVERHUNG CASE
STEP SIZE H = 0.01

CASE NUMBER = 112.7201

ROTOR SHAFT SPECIFICATIONS

ROTOR ACCEL = 0.0 RPM/SEC

SECTION	LENGTH	DIAMETER	YOUNGS MODULUS	PRODUCT OF E*I	INSIDE DIAMETER
1	2.00	0.375	3.000E 07	1.092E 04	0.000
2	2.00	0.375	3.000E 07	1.092E 04	0.000
3	5.00	0.375	3.000E 07	1.092E 04	0.000
4	6.38	0.375	3.000E 07	1.092E 04	0.000
5	6.38	0.375	3.000E 07	1.092E 04	0.000

BEARING NO. 1 IS 9.00 INCHES FROM THE LEFT END, STATION NO. 4

BEARING NO. 2 IS 21.75 INCHES FROM THE LEFT END, STATION NO. 6

BEARING SPAN IS 12.75 INCHES

APPROXIMATED ROTOR SPECIFICATIONS

STATION	LENGTH FROM END	WEIGHT	MASS	STIFFNESS	DAMPING	INT. DAMP	STIFF-R	EXT. WT	EMU	PHI
3	4.00	1.860	0.0048	0.0	0.000	0.000	0.0	1.75	0.0000	180.0
5	15.38	1.860	0.0048	0.0	0.000	0.000	0.0	1.66	0.0000	0.0

(EMU GIVEN IN OZ-IN UNITS)

(ALL OTHER STATIONS EXCEPT THE BEARINGS HAVE ZERO MASS)

TOTAL LENGTH OF ROTOR = 21.750 IN.
ACTUAL WEIGHT OF ROTOR = 4.092 LBS.
TOTAL WEIGHT OF APPROXIMATE ROTOR = 3.998 LBS.

GYROSCOPIC SPECIFICATIONS

STATION	LENGTH FROM END	POLAR MOM. OF INER.	TRANSVERSE MOM. OF INER.	KTRST (IN-LB/RAD)
3	4.00	0.0058	0.0027	0.0000

CASE NUMBER = 112.7201

BEARING STATION SPECIFICATIONS

RIGID BEARING SUPPORT SYSTEM

TABLE 3.7 SPECIFICATIONS FOR ROTOR OF CASE NO. 112.7201 (GYROSCOPICS INCLUDED)

SEGMENT	N-INIT. (RPM)	N-FINAL (RPM)	T-FINAL (RAD)
1	3000.0	3000.0	20.1
2	3000.0	3000.0	21.3
3	3000.0	3000.0	22.6
4	3000.0	3000.0	23.8
5	3000.0	3000.0	25.1

TRANSIENT RESPONSE OF ROTOR STATION NO. 3

TRANSIENT RESPONSE OF ROTOR STATION NO. 5

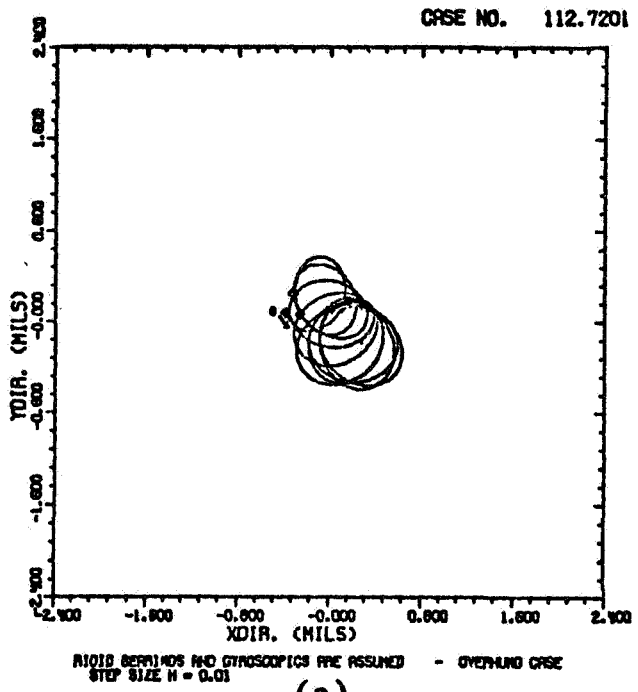

(a)

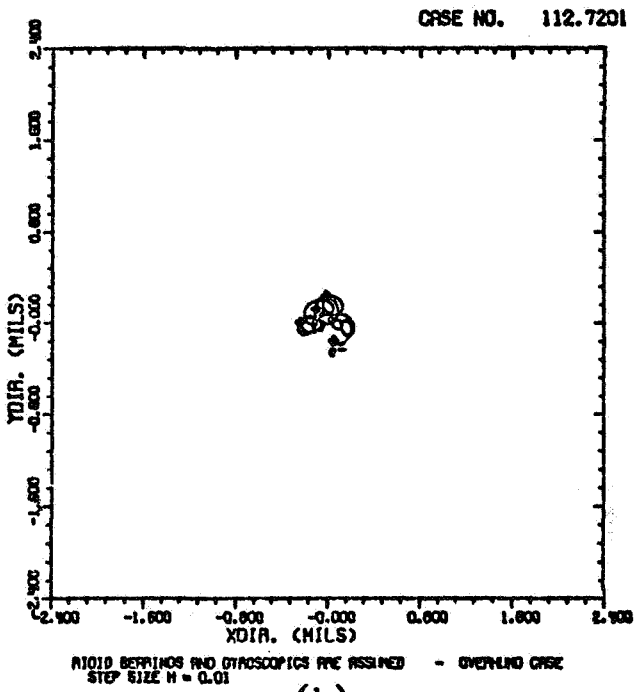

(b)

FIG. 3.11(a) OVERHANG RESPONSE CONTINUE FROM CYCLE THREE OF CASE 112.7201 WITH TIME STEP REDUCED TO H=0.01
(b) MIDSPAN RESPONSE WITH H=0.01 FROM CYCLE THREE OF CASE 112.7201 SHOWING STABILITY OF NUMERICAL SOLUTION

The next case considered was to start the solution with the initial conditions as in Fig. 3.10 but using a reduced time step of H = 0.01. The rotor specifications are indicated in Table 3.8 and the results for two cycles are shown in Fig. 3.12. The overhung station is observed to have a slight excitation of approximately 10/1 as indicated by the whirl path from cycle 1 to the end of this solution orbit. The reduced time step has not allowed the excitation to grow as it had in the previous case with the larger time step.

The next example case considers the influence of unbalance on the resulting transient including gyroscopics. The unbalance specifications are as given in Table 3.9 which indicates 0.002 oz-in. unbalance at each of the two major mass station and 180° out of phase. The response for five cycles is given in Fig. 3.13 where the gyroscopics are observed to once again excite the solution and alter the orbits much the same as before. The step size in this case was the larger value of H = 0.05. A smooth orbit is obtained up to the end of the third cycle of motion. Additional translational damping at both stations was introduced as indicated in Table 3.10 with the results obtained shown in Fig. 3.14. The initial response is suppressed but the gyroscopic influence persists to enter the solution in the fourth revolution. The point mass model as indicated in Table 3.11 produces the response shown in Fig. 3.15. The overhung station has a very regular symmetric pattern and would approximately repeat itself for the next five cycles as would the mid-section.

The next consideration was to again reduce the time step and start the solution at the end of cycle three for the case of Fig. 3.13.

FLEXIBLE ROTOR TRANSIENT RESPONSE --BY R. GORDON KIRK--

(UNITS ARE IN.-LB.-SEC. UNLESS OTHERWISE SPECIFIED)
RIGID BEARINGS AND GYROSCOPICS ARE ASSUMED - OVERHUNG CASE
STEP SIZE H = 0.01

CASE NUMBER = 1217.7101

ROTOR SHAFT SPECIFICATIONS

ROTOR ACCEL = 0.0 RPM/SEC

SECTION	LENGTH	DIAMETER	YOUNGS MODULUS	PRODUCT OF E*I	INSIDE DIAMETER
1	2.00	0.375	3.000E 07	1.092E 04	0.000
2	2.00	0.375	3.000E 07	1.092E 04	0.000
3	5.00	0.375	3.000E 07	1.092E 04	0.000
4	6.38	0.375	3.000E 07	1.092E 04	0.000
5	6.38	0.375	3.000E 07	1.092E 04	0.000

BEARING NO. 1 IS 9.00 INCHES FROM THE LEFT END, STATION NO. 4

BEARING NO. 2 IS 21.75 INCHES FROM THE LEFT END, STATION NO. 6

BEARING SPAN IS 12.75 INCHES

APPROXIMATED ROTOR SPECIFICATIONS

STATION	LENGTH FROM END	WEIGHT	MASS	STIFFNESS	DAMPING	INT. DAMP	STIFF-Q	EXT. WT	EMU	PHI
3	4.00	1.860	0.0048	0.0	0.010	0.000	0.0	1.75	0.0000	180.0
5	15.38	1.860	0.0048	0.0	0.010	0.000	0.0	1.66	0.0000	0.0

(EMU GIVEN IN OZ-IN UNITS)

(ALL OTHER STATIONS EXCEPT THE BEARINGS HAVE ZERO MASS)

TOTAL LENGTH OF ROTOR = 21.750 IN.
ACTUAL WEIGHT OF ROTOR = 4.092 LBS.
TOTAL WEIGHT OF APPROXIMATE ROTOR = 3.998 LBS.

CASE NUMBER = 1217.7101

BEARING STATION SPECIFICATIONS

RIGID BEARING SUPPORT SYSTEM

GYROSCOPIC SPECIFICATIONS

STATION	LENGTH FROM END	POLAR MOM. OF INER.	TRANSVERSE MOM. OF INER.	KTRST (IN-LB/RAD)
3	4.00	0.0054	0.0027	0.0000

TABLE 3.8 ROTOR SPECIFICATIONS (CASE NO. 1217.7101)

SEGMENT	N-INIT. (RPM)	N-FINAL (RPM)	T-FINAL (RAD)
1	3000.0	3000.0	1.3
2	3000.0	3000.0	2.5
3	3000.0	3000.0	3.8
4	3000.0	3000.0	5.0
5	3000.0	3000.0	6.3
6	3000.0	3000.0	7.6
7	3000.0	3000.0	8.8
8	3000.0	3000.0	10.1
9	3000.0	3000.0	11.3
10	3000.0	3000.0	12.6

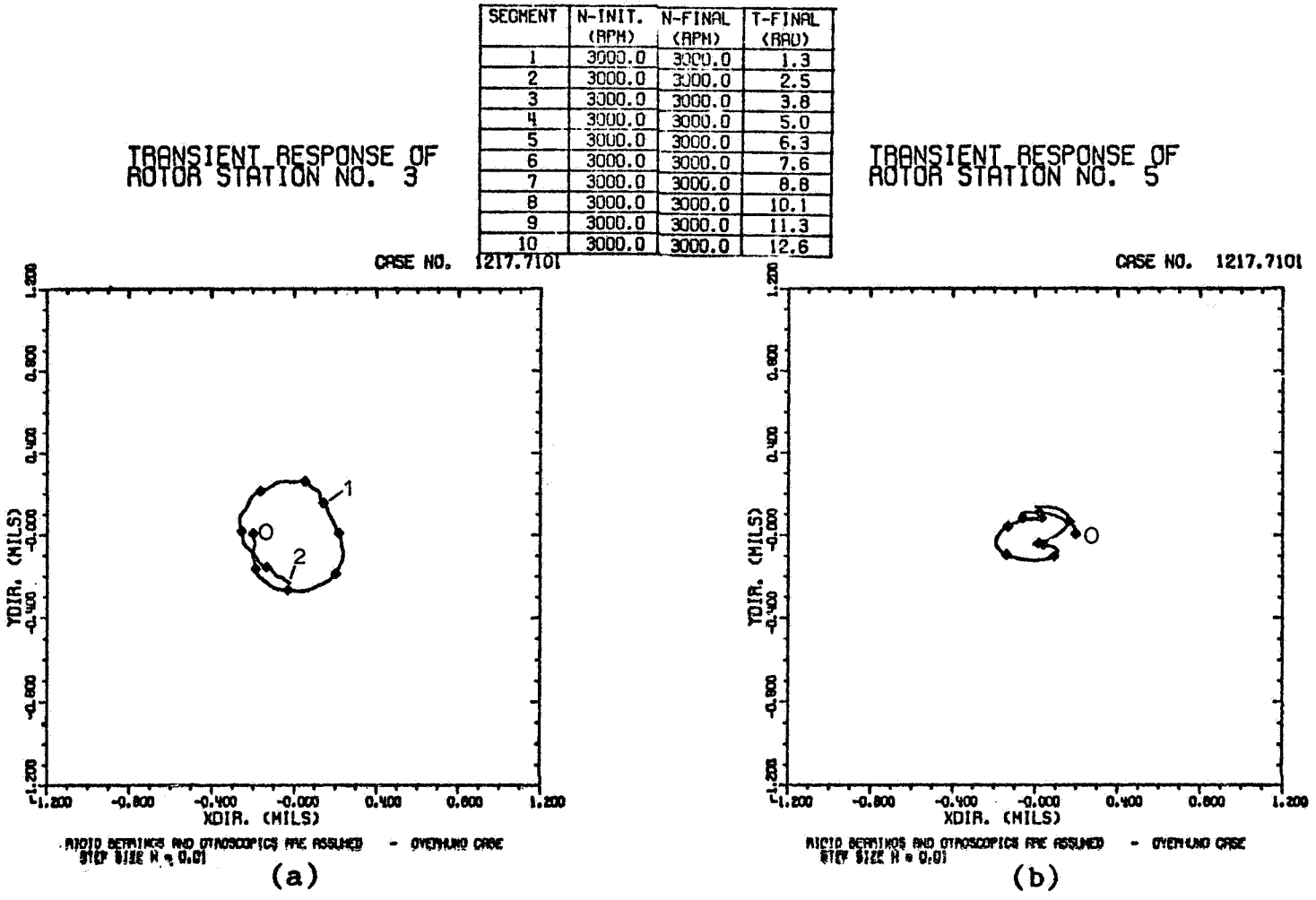

FIG. 3.12(a) RESPONSE OF OVERHUNG STATION SHOWING NUMERICALLY STABLE SOLUTION INCLUDING GYROSCOPICS (H=0.01)
(b) RESPONSE OF MIDSPAN STATION (H=0.01)

FLEXIBLE ROTOR TRANSIENT RESPONSE --BY R. GORDON KIRK--

(UNITS ARE IN.-LB.-SEC. UNLESS OTHERWISE SPECIFIED)
THIS IS AN EXPERIMENTAL ROTOR TEST CASE - NO INTERNAL DAMPING
RIGID BEARINGS AND GYROSCOPICS ARE ASSUMED- UNBALANCE TO EXCITE 2ND MOD

CASE NUMBER = 1215.7101

ROTOR SHAFT SPECIFICATIONS

ROTOR ACCEL = 0.0 RPM/SEC

SECTION	LENGTH	DIAMETER	YOUNGS MODULUS	PRODUCT OF E*I	INSIDE DIAMETER
1	2.00	0.375	3.000E 07	1.092E 04	0.000
2	2.00	0.375	3.000E 07	1.092E 04	0.000
3	5.00	0.375	3.000E 07	1.092E 04	0.000
4	6.38	0.375	3.000E 07	1.092E 04	0.000
5	6.38	0.375	3.000E 07	1.092E 04	0.000

BEARING NO. 1 IS 9.00 INCHES FROM THE LEFT END, STATION NO. 4

BEARING NO. 2 IS 21.75 INCHES FROM THE LEFT END, STATION NO. 6

BEARING SPAN IS 12.75 INCHES

APPROXIMATED ROTOR SPECIFICATIONS

STATION	LENGTH FROM END	WEIGHT	MASS	STIFFNESS	DAMPING	INT. DAMP	STIFF-Q	EXT. WT	EMU	PHI
3	4.00	1.860	0.0048	0.0	0.010	0.000	0.0	1.75	0.0020	180.0
5	15.38	1.860	0.0048	0.0	0.010	0.000	0.0	1.66	0.0020	0.0

(EMU GIVEN IN OZ-IN UNITS)

(ALL OTHER STATIONS EXCEPT THE BEARINGS HAVE ZERO MASS)

CASE NUMBER = 1215.7101

TOTAL LENGTH OF ROTOR = 21.750 IN.
ACTUAL WEIGHT OF ROTOR = 4.092 LBS.
TOTAL WEIGHT OF APPROXIMATE ROTOR = 3.998 LBS.

BEARING STATION SPECIFICATIONS

RIGID BEARING SUPPORT SYSTEM

GYROSCOPIC SPECIFICATIONS

STATION	LENGTH FROM END	POLAR MOM. OF INER.	TRANSVERSE MOM. OF INER.	KTRST (IN-LB/RAD)
3	4.00	0.0054	0.0027	0.0000

TABLE 3.9 ROTOR SPECIFICATIONS FOR UNBALANCE RESPONSE AND LIGHT DAMPING

SEGMENT	N-INIT. (RPM)	N-FINAL (RPM)	T-FINAL (RAD)
1	3000.0	3000.0	6.3
2	3000.0	3000.0	12.6
3	3000.0	3000.0	18.8
4	3000.0	3000.0	25.1
5	3000.0	3000.0	31.4

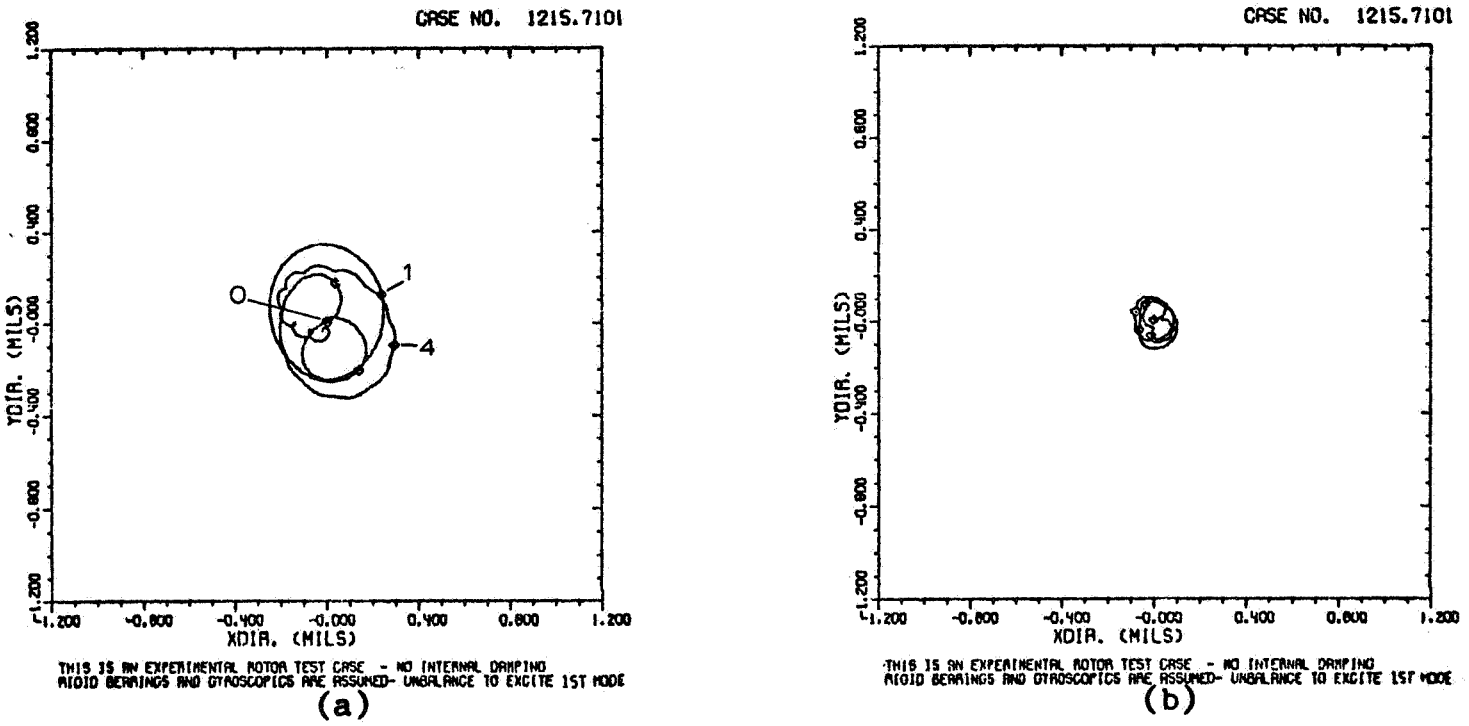

FIG. 3.13(a) TRANSIENT UNBALANCE RESPONSE OF OVERHANG SHOWING DEVELOPMENT OF NUMERICAL INSTABILITY IN GYROSCOPIC CALCULATIONS
(b) MIDSPAN RESPONSE

FLEXIBLE ROTOR TRANSIENT RESPONSE --BY R. GORDON KIRK--

(UNITS ARE IN-LB.-SEC. UNLESS OTHERWISE SPECIFIED)
THIS IS AN EXPERIMENTAL ROTOR TEST CASE - NO INTERNAL DAMPING
RIGID BEARINGS AND GYROSCOPICS ARE ASSUMED- UNBALANCE TO EXCITE 2ND MOD

CASE NUMBER = 1215.7102

ROTOR SHAFT SPECIFICATIONS

ROTOR ACCEL = 0.0 RPM/SEC

SECTION	LENGTH	DIAMETER	YOUNGS MODULUS	PRODUCT OF E*I	INSIDE DIAMETER
1	2.00	0.375	3.000E 07	1.092E 04	0.000
2	2.00	0.375	3.000E 07	1.092E 04	0.000
3	5.00	0.375	3.000E 07	1.092E 04	0.000
4	6.38	0.375	3.000E 07	1.092E 04	0.000
5	6.38	0.375	3.000E 07	1.092E 04	0.000

BEARING NO. 1 IS 9.00 INCHES FROM THE LEFT END, STATION NO. 4

BEARING NO. 2 IS 21.75 INCHES FROM THE LEFT END, STATION NO. 6

BEARING SPAN IS 12.75 INCHES

APPROXIMATED ROTOR SPECIFICATIONS

STATION	LENGTH FROM END	WEIGHT	MASS	STIFFNESS	DAMPING	INT. DAMP	STIFF-0	EXT. WT	EMU	PHI
3	4.00	1.860	0.0048	0.0	0.100	0.000	0.0	1.75	0.0020	180.0
5	15.38	1.860	0.0048	0.0	0.100	0.000	0.0	1.66	0.0020	0.0

(EMU GIVEN IN OZ-IN UNITS)

(ALL OTHER STATIONS EXCEPT THE BEARINGS HAVE ZERO MASS)

CASE NUMBER = 1215.7102

TOTAL LENGTH OF ROTOR = 21.750 IN.
ACTUAL WEIGHT OF ROTOR = 4.092 LBS.
TOTAL WEIGHT OF APPROXIMATE ROTOR = 3.998 LBS.

BEARING STATION SPECIFICATIONS

RIGID BEARING SUPPORT SYSTEM

GYROSCOPIC SPECIFICATIONS

STATION	LENGTH FROM END	POLAR MOM. OF INER.	TRANSVERSE MOM. OF INER.	KTRST (IN-LB/RAD)
3	4.00	0.0054	0.0027	0.0000

TABLE 3.10 UNBALANCED ROTOR SPECIFICATIONS WITH INCREASED TRANSLATIONAL DAMPING

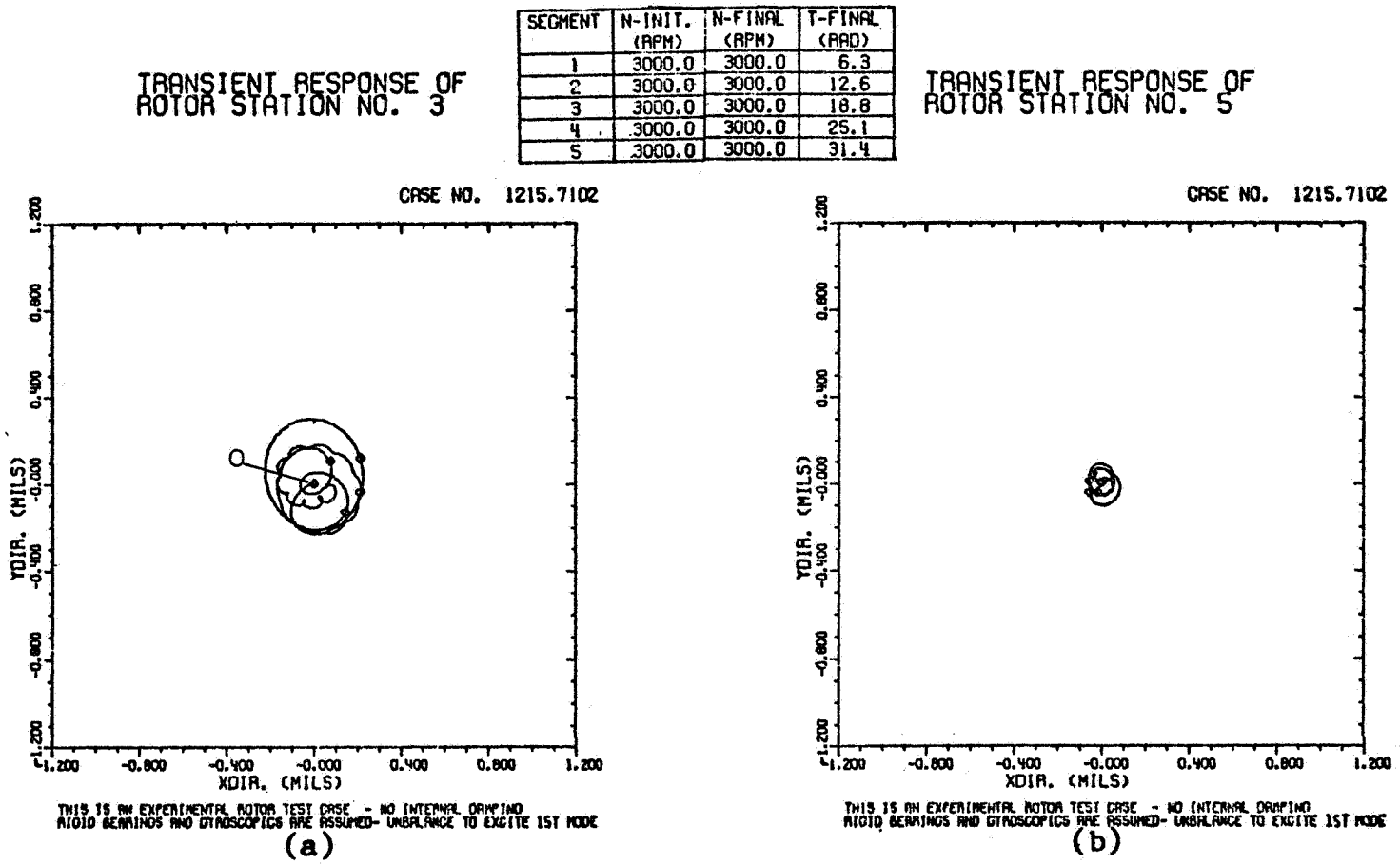

FIG. 3.14(a) UNBALANCE RESPONSE WITH INCREASED TRANSLATIONAL DAMPING
(b) MIDSPAN RESPONSE (H=0.05)

FLEXIBLE ROTOR TRANSIENT RESPONSE --BY R. GORDON KIRK--

(UNITS ARE IN.-LB.-SEC. UNLESS OTHERWISE SPECIFIED)
POINT MASS ROTOR ASSUMPTION - NO INTERNAL DAMPING
UNBALANCE GIVEN TO EXCITE 1ST MODE - LIGHT DAMPING

CASE NUMBER = 1216.7102

ROTOR SHAFT SPECIFICATIONS

ROTOR ACCEL = 0.0 RPM/SEC

SECTION	LENGTH	DIAMETER	YOUNGS MODULUS	PRODUCT OF E*I	INSIDE DIAMETER
1	2.00	0.375	3.000E 07	1.092E 04	0.000
2	2.00	0.375	3.000E 07	1.092E 04	0.000
3	5.00	0.375	3.000E 07	1.092E 04	0.000
4	6.38	0.375	3.000E 07	1.092E 04	0.000
5	6.38	0.375	3.000E 07	1.092E 04	0.000

BEARING NO. 1 IS 9.00 INCHES FROM THE LEFT END, STATION NO. 4

BEARING NO. 2 IS 21.75 INCHES FROM THE LEFT END, STATION NO. 6

BEARING SPAN IS 12.75 INCHES

APPROXIMATED ROTOR SPECIFICATIONS

STATION	LENGTH FROM END	WEIGHT	MASS	STIFFNESS	DAMPING	INT. DAMP	STIFF-Q	EXT. WT	EMU	PHI
3	8.00	1.860	0.0048	0.0	0.010	0.000	0.0	1.75	0.0020	180.0
5	15.38	1.860	0.0048	0.0	0.010	0.000	0.0	1.66	0.0020	0.0

(EMU GIVEN IN 07-IN UNITS)

(ALL OTHER STATIONS EXCEPT THE BEARINGS HAVE ZERO MASS)

TOTAL LENGTH OF ROTOR = 21.750 IN.
ACTUAL WEIGHT OF ROTOR = 4.092 LBS.
TOTAL WEIGHT OF APPROXIMATE ROTOR = 3.998 LBS.

CASE NUMBER = 1216.7102

BEARING STATION SPECIFICATIONS

RIGID BEARING SUPPORT SYSTEM

TABLE 3.11 ROTOR SPECIFICATIONS FOR UNBALANCED POINT MASS RESPONSE (CASE NO. 1216.7102)

SEGMENT	N-INIT. (RPM)	N-FINAL (RPM)	T-FINAL (RAD)
1	3000.0	3000.0	6.3
2	3000.0	3000.0	12.6
3	3000.0	3000.0	18.8
4	3000.0	3000.0	25.1
5	3000.0	3000.0	31.4

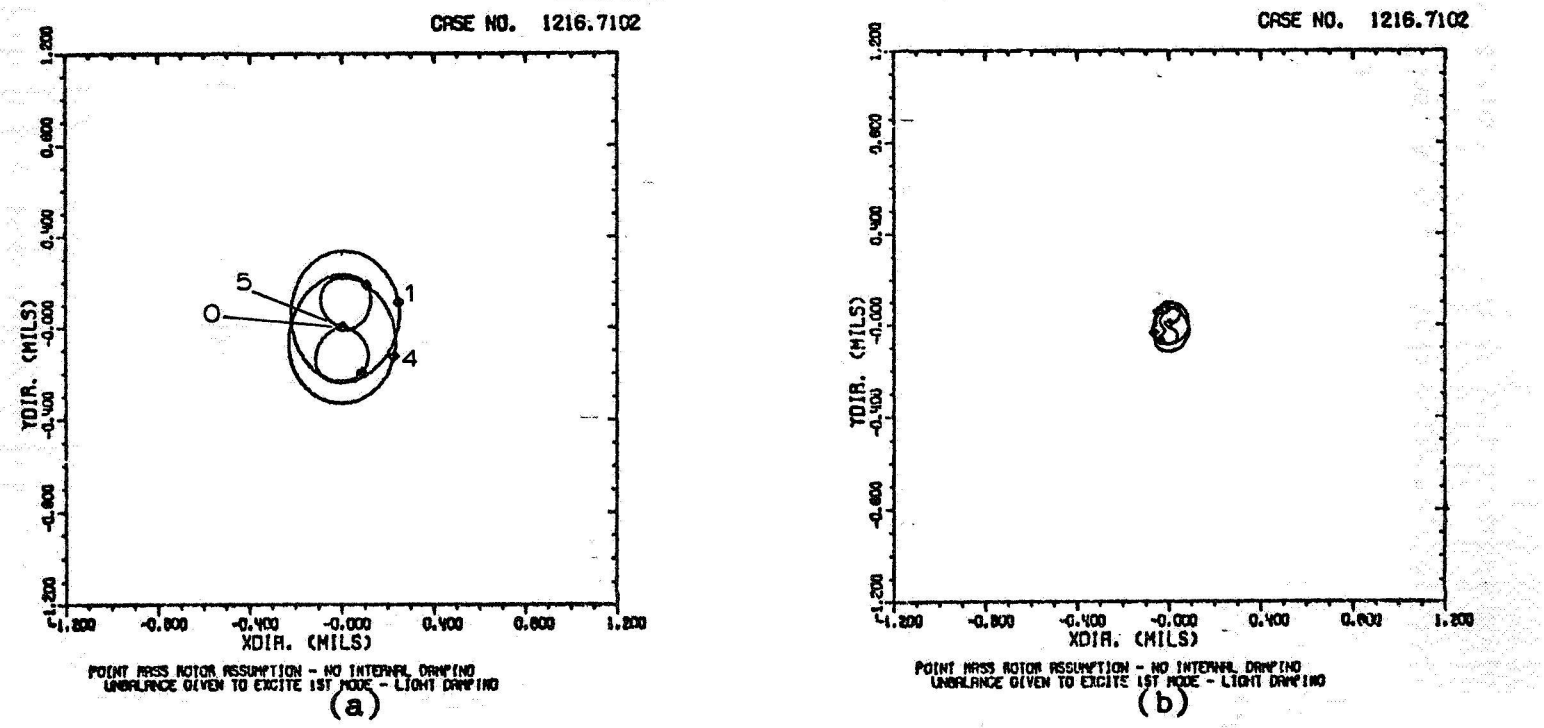

FIG. 3.15(a) RESPONSE OF UNBALANCED OVERHANG FOR POINT MASS SIMULATION
(b) MIDSECTION RESPONSE (H=0.05)

Fig. 3.16 shows cycles four and five and no indication that numerical instability is present in this solution. A small amount of angular damping was next considered to control the gyroscopic harmonics and prevent them from producing inaccurate results. Five cycles at the larger step of 0.05 is shown in Fig. 3.17 and indicates that the instabilities have been suppressed.

For the same initial conditions as the previous orbit the response for ten cycles with an initial step in speed to 10,000 RPM is shown in Fig. 3.18. Fig. 3.19 indicates the effect of an acceleration rate of 50,000 RPM/sec. on this same motion for ten cycles.

These results indicate that the proposed transient solution can produce whirl orbits that may be used to study the performance of rotating machines. The predicted unstable whirl from the stability analysis program was verified with good agreements. The inclusion of gyroscopics in a multi-mass system must be handled with extreme care so as to avoid numerical instabilities in the solutions and it is suggested that a point mass model simulation precede any run including gyroscopics.

Additional results for flexible supports using this computer code are presented in Chapter V.

SEGMENT	N-INIT. (RPM)	N-FINAL (RPM)	T-FINAL (RAD)
1	3000.0	3000.0	20.1
2	3000.0	3000.0	21.3
3	3000.0	3000.0	22.6
4	3000.0	3000.0	23.8
5	3000.0	3000.0	25.1
6	3000.0	3000.0	26.4
7	3000.0	3000.0	27.6
8	3000.0	3000.0	28.9
9	3000.0	3000.0	30.1
10	3000.0	3000.0	31.4

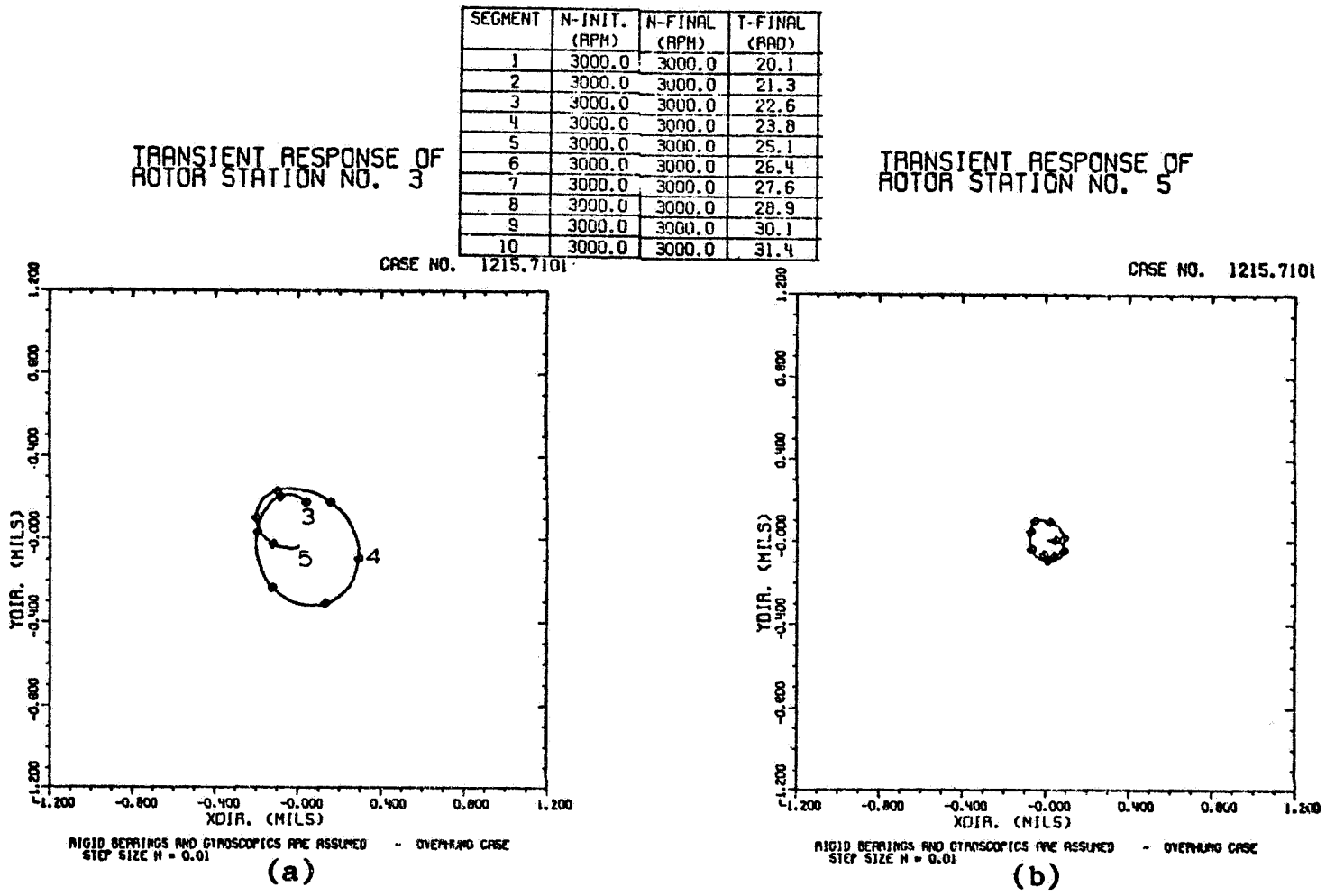

FIG. 3.16(a) UNBALANCE RESPONSE OF OVERHANG FROM THIRD CYCLE OF CASE NO. 1215.7101
(b) MIDSECTION RESPONSE (H=0.01, CYCLES 4-5)

SEGMENT	N-INIT. (RPM)	N-FINAL (RPM)	T-FINAL (RAD)
1	3000.0	3000.0	25.1
2	3000.0	3000.0	31.4
3	3000.0	3000.0	37.6
4	3000.0	3000.0	43.9
5	3000.0	3000.0	50.2

TRANSIENT RESPONSE OF ROTOR STATION NO. 3

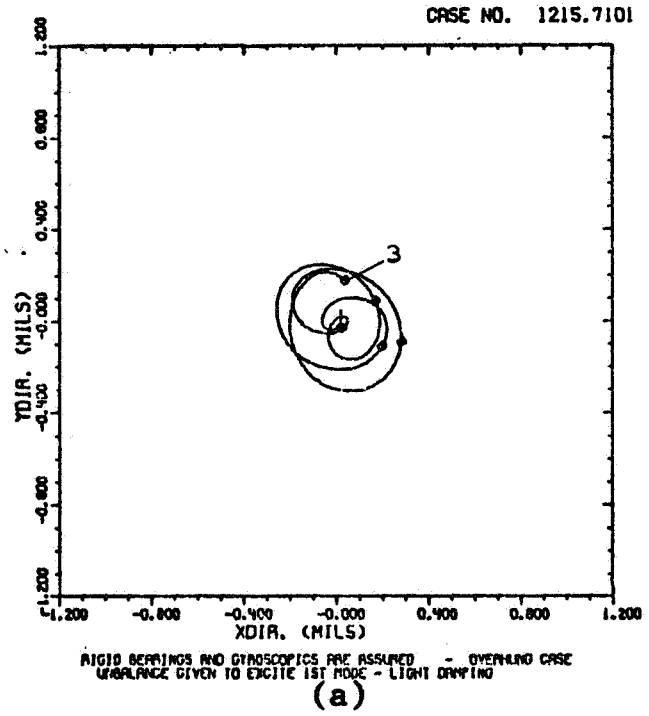

(a)

TRANSIENT RESPONSE OF ROTOR STATION NO. 5

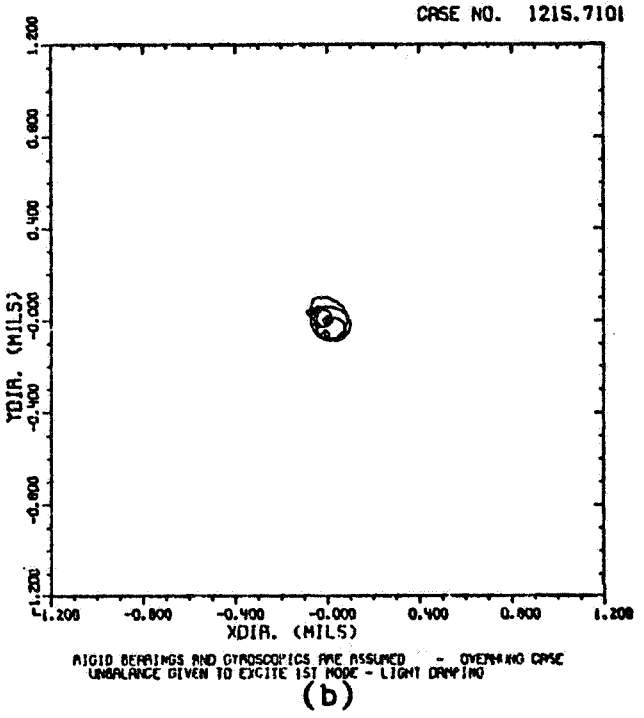

(b)

FIG. 3.17(a) OVERHUNG RESPONSE (GYROSCOPIC DAMPING = 1IN.-LB.-SEC.)
(b) MIDSECTION RESPONSE (H=0.05, CYCLES 4-8)

SEGMENT	N-INIT. (RPM)	N-FINAL (RPM)	T-FINAL (RAD)
1	10000.0	10000.0	25.1
2	10000.0	10000.0	31.4
3	10000.0	10000.0	37.6
4	10000.0	10000.0	43.9
5	10000.0	10000.0	50.2
6	10000.0	10000.0	56.5
7	10000.0	10000.0	62.8
8	10000.0	10000.0	69.0
9	10000.0	10000.0	75.3
10	10000.0	10000.0	81.6

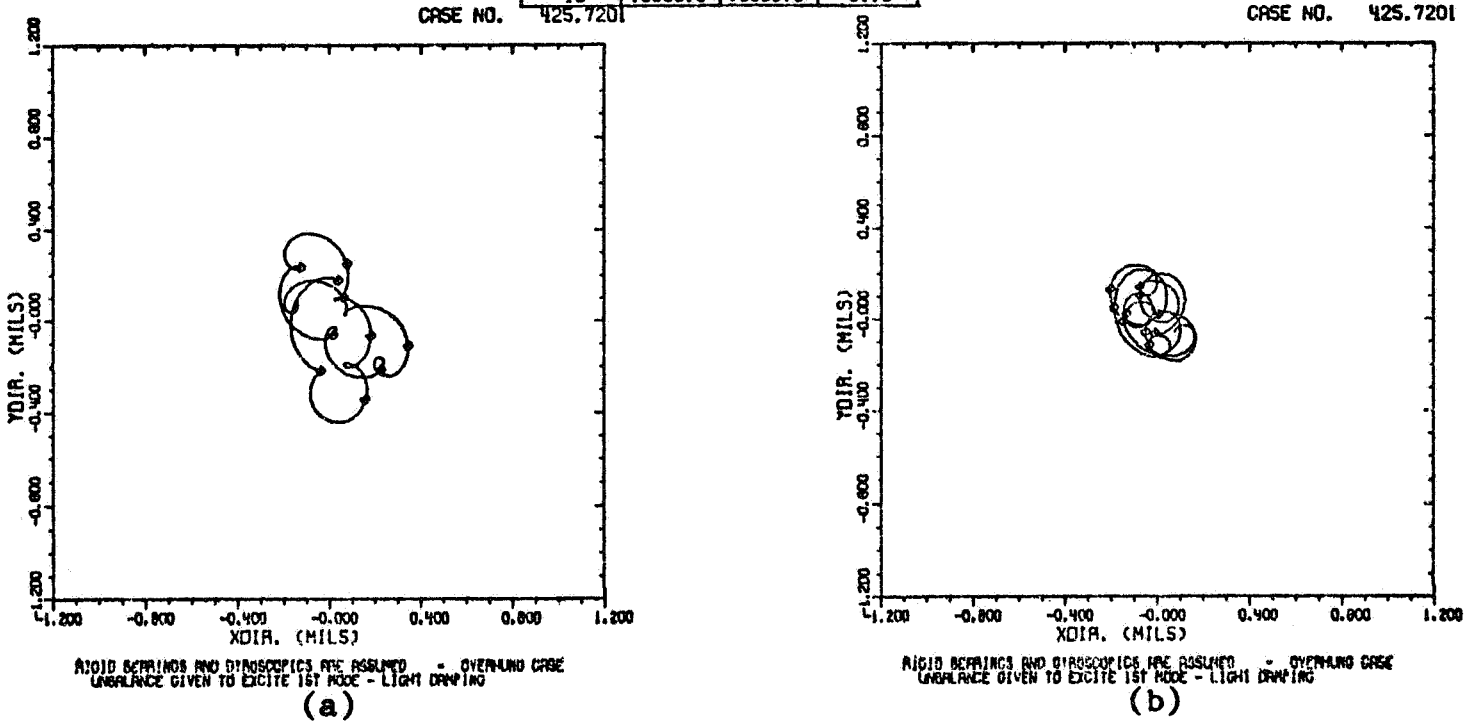

FIG. 3.18(a) OVERHUNG RESPONSE WITH STEP INCREMENT OF SPEED TO 10,000 RPM (GYROSCOPIC DAMPING = 1IN-LB-SEC)
(b) MIDSECTION RESPONSE (CYCLES 4-13, H=0.05)

SEGMENT	N-INIT. (RPM)	ACCEL. (RPM/SEC)	N-FINAL (RPM)	T-FINAL (RAD)
1	10000.0	50000.0	10291.8	25.1
2	10291.8	50000.0	10577.8	31.4
3	10577.8	50000.0	10854.1	37.6
4	10854.1	50000.0	11125.7	43.9
5	11125.7	50000.0	11388.7	50.2
6	11388.7	50000.0	11647.8	56.5
7	11647.8	50000.0	11901.3	62.8
8	11901.3	50000.0	12147.5	69.0
9	12147.5	50000.0	12390.7	75.3
10	12390.7	50000.0	12627.4	81.6

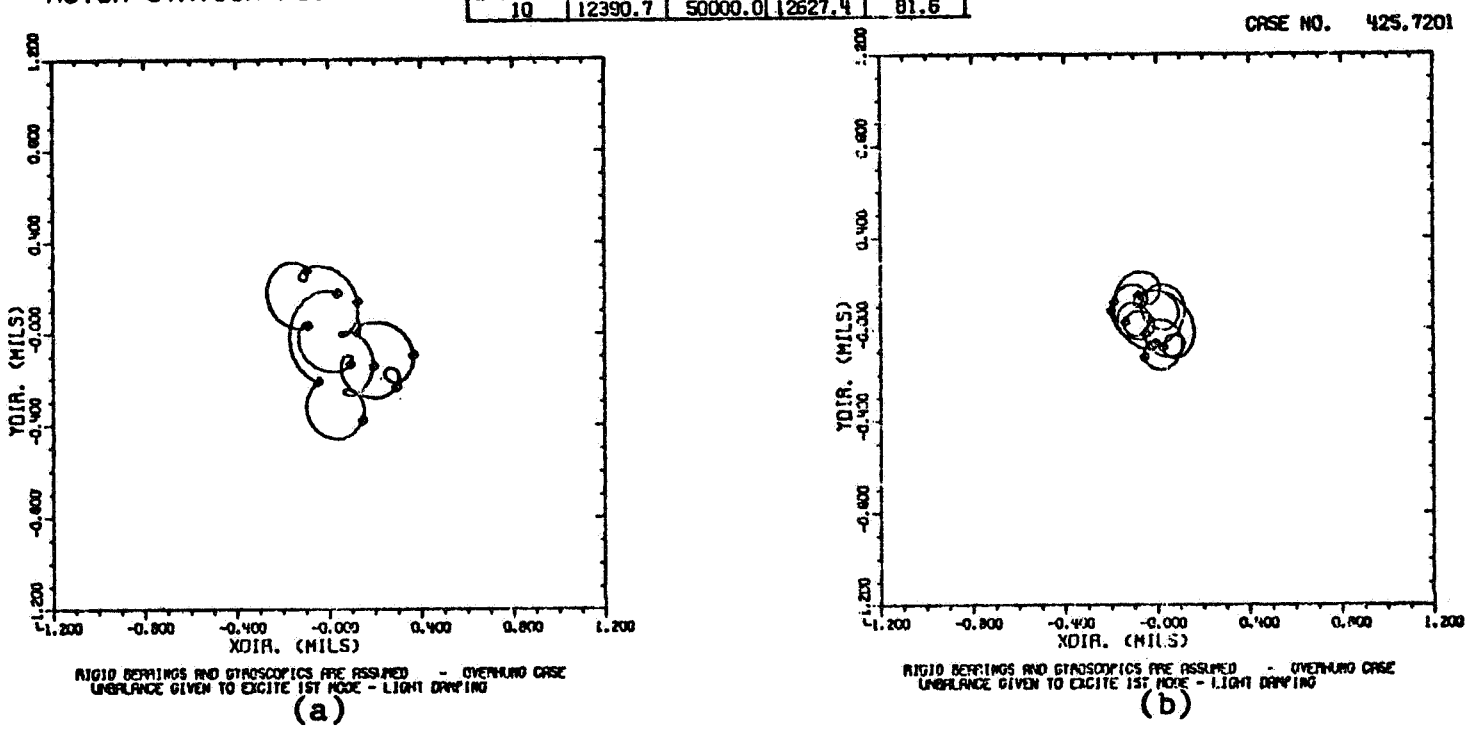

FIG. 3.19(a) TRANSIENT RESPONSE OF OVERHANG WITH ACCELERATION FOR TEN CYCLES
(b) MIDSECTION RESPONSE (H=0.05, CYCLES 4-13)

CHAPTER IV

STABILITY OF SOFT MOUNTED JOURNAL BEARINGS

The favorable increase of stable operating speed range as a result of support flexibility and damping has been reported in the literature (16,74,75,76). A recent analysis by Choudhury (43) has examined the effect of simple soft mounts on the stability of the plain cylindrical short journal bearing. The present analysis will present the equations necessary for the time-transient solution. The resulting computer code results are then compared with the stability boundaries presented by Choudhury. The influence of unbalance on the horizontal and vertical bearing system is also discussed and several transient orbits are presented in connection with that discussion.

4.1 Description of the System

An idealized rigid symmetric rotor supported by identical bearings on elastic supports is shown in Fig. 4.1. If the rigid rotor is excited only in the cylindrical mode then the equivalent system shown in Fig. 4.2 may be used to examine the resulting response. A fluid-film bearing is shown in Fig. 4.2 with a region of cavitation which must be included in the solution to simulate the behavior of actual fluid-film bearings.

The journal motion may be represented by the coordinates as shown in Fig. 4.3. The absolute support motion and the relative journal motion will be used to formulate the equations of motion. Unbalance response may be expressed as a small eccentricity, e_μ, of the mass center from the geometric center of the journal. The journal orbits will be

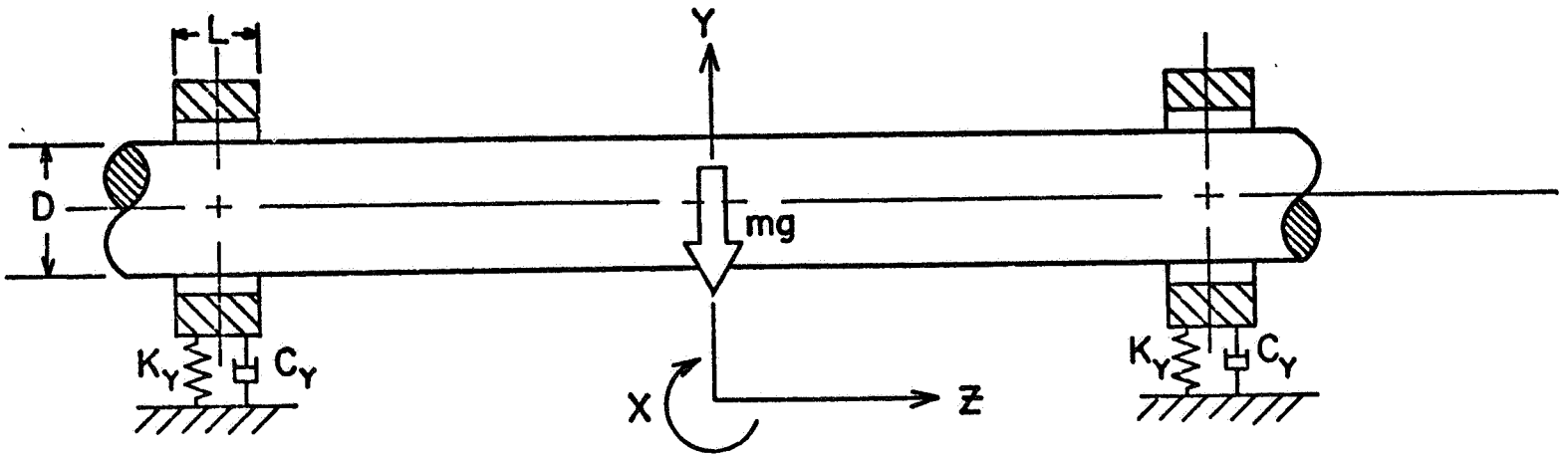

FIG. 4.1 SYMMETRIC RIGID ROTOR SUPPORTED BY SIMILAR FLUID-FILM JOURNAL BEARINGS ON ELASTIC SUPPORTS

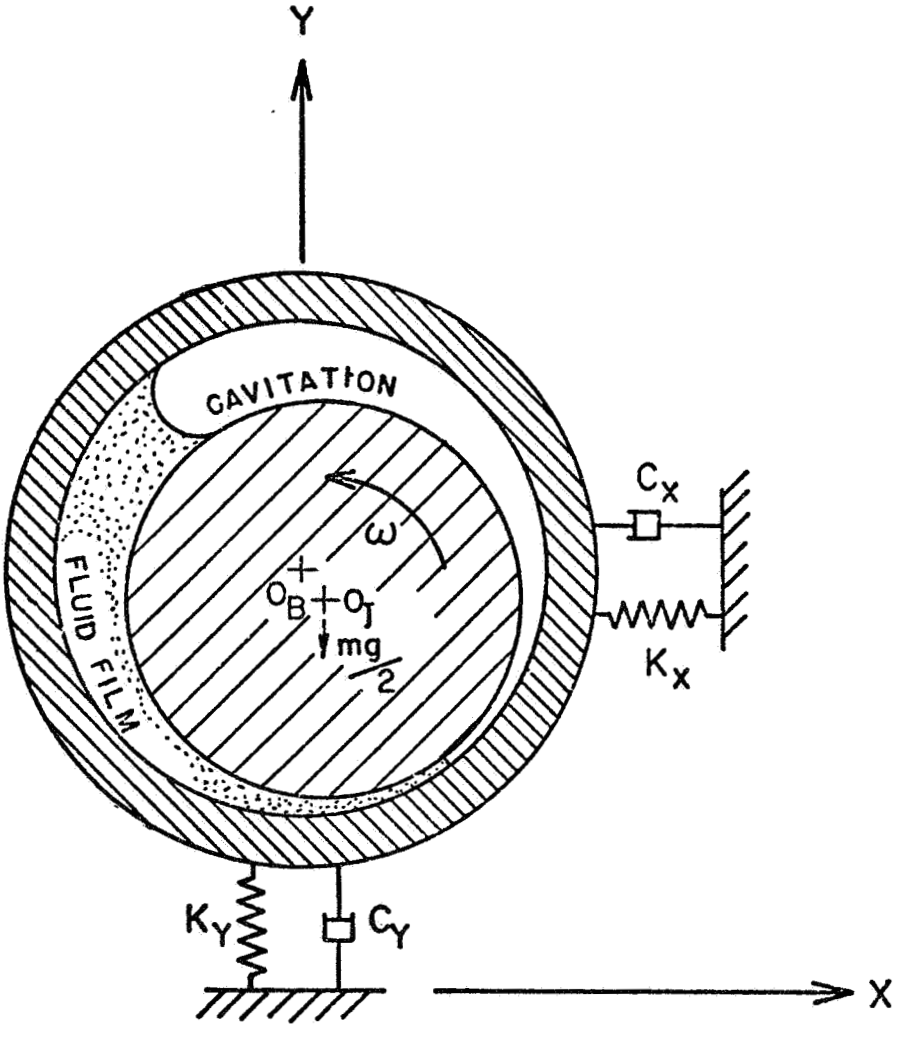

FIG. 4.2 CROSS-SECTION OF EQUIVALENT RIGID ROTOR SYSTEM SHOWING REGION OF FLUID CAVITATION

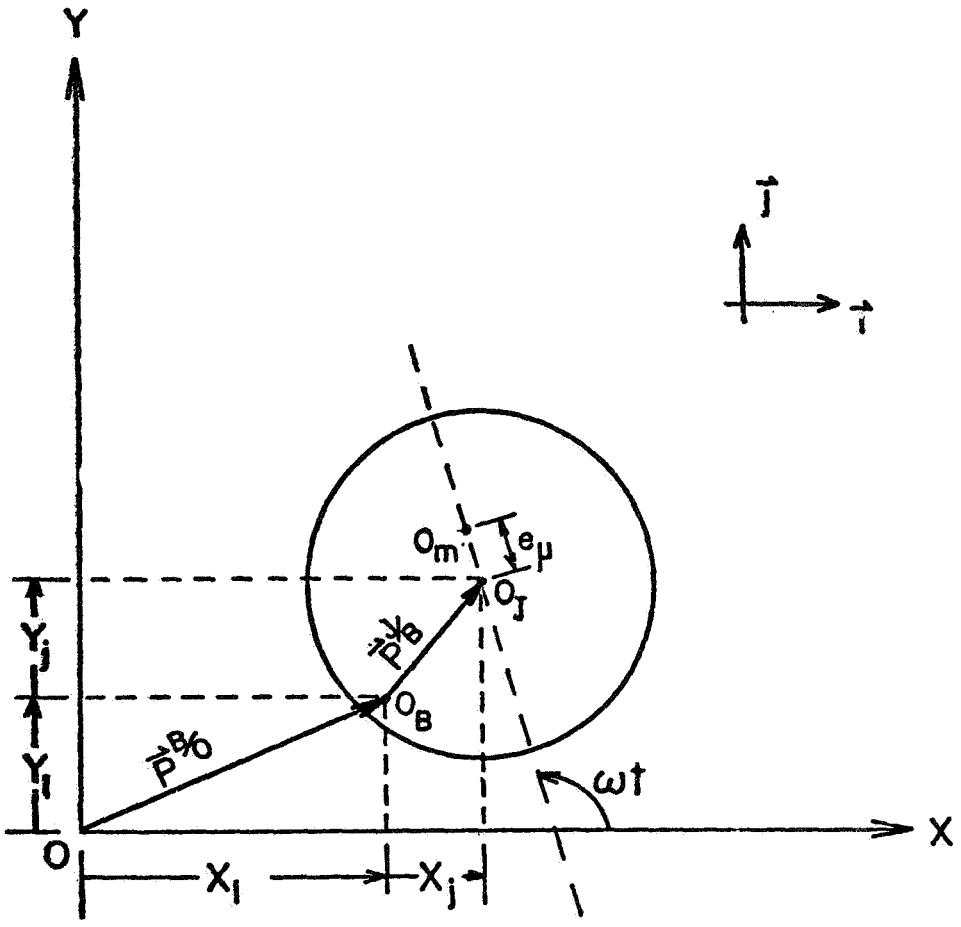

FIG. 4.3 CROSS-SECTION INDICATING NOMENCLATURE FOR JOURNAL DISPLACEMENT SHOWING UNBALANCE OF ROTOR MASS

presented as the trajectories of the journal center inside of the clearance circle as has been the practice in journal bearing transient studies (18,41,60).

4.2 Equations of Motion for the Transient Solution

The equations of motion of a rigid rotor supported by journal bearings can be written if the expressions for the fluid-film bearing forces are known or can be calculated. One approach has been to assume that the short-bearing theory is applicable when L/D < 1. Booker (77) has reported that the short bearing equations compare favorably with finite difference solutions. The expressions for the forces can be written as (18)

$$\begin{Bmatrix} \hat{F}_x \\ \hat{F}_y \end{Bmatrix} = \frac{\mu R L^3}{2} \int_{\theta=0}^{2\pi} \frac{(\omega_b + \omega_j)(x \sin\theta - y \cos\theta) - 2(\dot{x} \cos\theta + \dot{y} \sin\theta)}{(c - x \cos\theta - y \sin\theta)^3} \begin{Bmatrix} \cos\theta \\ \sin\theta \end{Bmatrix} d\theta \qquad [4.1]$$

where the integral is to be calculated numerically and negative pressures set to ambient to model cavitation.

The coordinate system is shown in Fig. 4.3 where the absolute bearing and relative journal displacements have been chosen to describe the system behavior. The position vectors are given as:

$$\vec{P}^{b/o} = x_1 \vec{i} + y_1 \vec{j} \qquad [4.2]$$

$$\vec{P}^{j/o} = \vec{P}^{b/o} + \vec{P}^{j/n} \qquad [4.3]$$

where

$$P^{j/b} = x_j \vec{i} + y_j \vec{j} \qquad [4.4]$$

The position vector of the mass center of the journal is given as

$$\vec{p}^{\,j_{g/o}} = (x_1 + x_j + e_\mu \cos(\omega_j t))\,\vec{i} + (y_1 + y_j + e_\mu \sin(\omega_j t))\,\vec{j} \qquad [4.5]$$

The acceleration of the journal mass center is found by direct differentiation of the above expression.

$$v^{j/o} = (\dot{x}_1 + \dot{x}_j - e_\mu \omega_j \sin(\omega_j t))\,\vec{i} + (\dot{y}_1 + \dot{y}_j + e_\mu \omega_j \cos(\omega_j t))\,\vec{j} \qquad [4.6]$$

$$\vec{a}^{j/o} = (\ddot{x}_1 + \ddot{x}_j - e_\mu \dot{\omega}_j \sin(\omega_j t) - e_\mu \omega_j^2 \cos(\omega_j t))\,\vec{i} + (\ddot{y}_1 + \ddot{y}_j + e_\mu \dot{\omega}_j \cos(\omega_j t) - e_\mu \omega_j^2 \sin(\omega_j t))\,\vec{j} \qquad [4.7]$$

Once the bearing force expression and acceleration components are known the equations of motion are easily written by applying Newton's Second Law:

$$\sum \vec{F}_i = m_i \vec{a}_i, \quad i = 1,2 \qquad [4.8]$$

where

i = 1 refers to the bearing motion

i = 2 refers to the journal absolute motion

Hence for the journal equation:

$$m_2(\ddot{x}_2\vec{i} + \ddot{y}_2\vec{j}) = \sum F_{j_x}\,\vec{i} + \sum F_{j_y}\,\vec{j} \qquad [4.9]$$

x-component:

$$m_2(\ddot{x}_1 + \ddot{x}_j - e_\mu \dot{\omega}_j \sin(\omega_j t) - e_\mu \omega_j^2 \cos(\omega_j t)$$

$$= F_o \cos(\eta\omega_j t) + (\text{Film Force})\Big|_{x\text{-dir.}} \qquad [4.10a]$$

y-component:

$$m_2(\ddot{y}_1 + \ddot{y}_j + e_\mu \dot{\omega}_j \cos(\omega_j t) - e_\mu \omega_j^2 \sin(\omega_j t))$$

$$= F_o \sin(\eta\omega_j t) + (\text{Film Force})\Big|_{y\text{-dir.}} - W_2 \qquad [4.10b]$$

The bearing equations of motion are as follows:

x-component:

$$m_1\ddot{x}_1 = \sum F_{b_x} = -k_x x_1 - c_x \dot{x}_1 - (\text{Film Force})\Big|_{x\text{-dir.}} \qquad [4.11a]$$

y-component:

$$m_1\ddot{y}_1 = \sum F_{b_y} = -k_y y_1 - c_y \dot{y}_1 - (\text{Film Force})\Big|_{y\text{-dir.}} - W_1 \qquad [4.11b]$$

The expressions for the film forces can be expressed as equivalent linear stiffness and damping at any given instant. That is,

$$\hat{F}_x = (\text{Film Force})\Big|_x = -[k_{xx}x_j + k_{xy}y_j + c_{xx}\dot{x}_j + c_{xy}\dot{y}_j] \qquad [4.12a]$$

$$\hat{F}_y = (\text{Film Force})\Big|_y = -[k_{yy}y_j + k_{yx}x_j + c_{yy}\dot{y}_j + c_{yx}\dot{x}_j] \qquad [4.12b]$$

where

$$k_{xx} = -\frac{\partial \hat{F}_x}{\partial x_j} \qquad [4.13]$$

$$k_{xy} = -\frac{\partial \hat{F}_x}{\partial y_j} \qquad [4.14]$$

$$k_{yx} = - \frac{\partial F_y}{\partial x_j} \qquad [4.15]$$

$$k_{yy} = - \frac{\partial \hat{F}_y}{\partial y_j}, \qquad [4.16]$$

and

$$c_{xx} = - \frac{\partial \hat{F}_x}{\partial \dot{x}_j} \qquad [4.17]$$

$$c_{xy} = - \frac{\partial \hat{F}_x}{\partial \dot{y}_j} \qquad [4.18]$$

$$c_{yx} = - \frac{\partial \hat{F}_y}{\partial \dot{x}_j} \qquad [4.19]$$

$$c_{yy} = - \frac{\partial \hat{F}_y}{\partial \dot{y}_j} \qquad [4.20]$$

The limits of integration and the force components are determined by the steady state equilibrium position (42,43). The equations of motion may be made dimensionless by defining the following variables:

$$X_1 = \frac{x_1}{c}, \quad \dot{X}_1 = \frac{\dot{x}_1}{c\omega_j}, \quad \ddot{X}_1 = \frac{\ddot{x}_1}{c\omega_j^2}, \quad E_\mu = \frac{e_\mu}{c}$$

$$X_j = \frac{x_j}{c}, \quad \dot{X}_j = \frac{\dot{x}_j}{c\omega_j}, \quad \ddot{X}_j = \frac{\ddot{x}_j}{c\omega_j^2}, \quad T = \omega_j t$$

where c = radial clearance of the journal bearing.

Rewritting the equations of motion and solving for the acceleration terms results in

$$\ddot{X}_1 = \frac{m_2}{m_1} \left[- \frac{k_x}{m_2\omega_j^2} X_1 - \frac{c_x}{m_2\omega^2} \dot{X}_1 - \frac{\hat{F}_x}{m_2 c\omega_j^2} \right] \qquad [4.21]$$

$$\ddot{Y}_1 = \frac{m_2}{m_1}\left[-\frac{k_y}{m_2\omega_j^2} Y_1 - \frac{c_y}{m_2\omega_j} \dot{Y}_1 - \frac{F_y}{m_2 c\omega_j^2} - \frac{W_1}{m_2 c\omega_j^2}\right] \qquad [4.22]$$

$$\ddot{X}_j = -\ddot{X}_1 + E_\mu \cos(T) + \frac{F_o}{m_2 c\omega_j^2} \cos(\eta T) + \frac{\hat{F}_x}{m_2 c\omega_j^2} \qquad [4.23]$$

$$\ddot{Y}_j = -\ddot{Y}_1 + E_\mu \sin(T) + \frac{F_o}{m_2 c\omega_j^2} \sin(\eta T) + \frac{\hat{F}_y}{m_2 c\omega_j^2} - \frac{W_2}{m_2 c\omega_j^2} \qquad [4.24]$$

These equations may be integrated forward in time by any one of several methods of integrating first-order differential equations (42). This means that to solve the above equations, eight first order equations must be integrated. The fluid-film forces can be solved at each time step and the solution tracked for a given rotor system. This method of solution is essential for determining the dynamic loading under different transient motion caused by shock or unbalance forcing functions. This approach is not the appropriate method to determine the threshold of instability. The characteristic equation can be examined for instability by solving for the roots and noting when a positive real part of the root, λ, exists. Moreover, the method of Routh does not require the roots to be solved for but only that an array derived from the coefficients of the characteristic equation be formed and examined. The results of this type analysis (43) produces stability plots that will be discussed in the following section.

4.3 Horizontal Journal Bearing Stability

The plain cylindrical bearing has received much attention in the literature (78-85). Recent investigations (18,41,69) have presented

stability maps that have agreed that the stability boundary is approximated at $\omega/\omega_g = 2.5$ for short journal bearings loaded up to an eccentricity of 0.80. At higher eccentricities the bearing is stable at all speeds. The whirl orbit in Fig. 4.4 represents the motion of the journal in the clearance circle for five cycles of motion. The journal was released with all initial conditions zero and operating at an angular speed of 6500 RPM which is very near but below the stability threshold (ω/ω_g = WS = 2.45). The journal is spiraling in toward the equilibrium eccentricity ε_o = ES = 0.211.

If a step increase of speed to 10,500 RPM occurs at the end condition of Fig. 4.4 the resulting motion is shown in Fig. 4.5(a). The journal whirls out in an orbit that has an average whirl rate of close to one-half journal speed as indicated by the small timing marks on the orbit path. The maximum force has doubled to 145.6 lb. and occurs at 8.96 cycles as indicated by the asterisk on the orbit. The motion is continued for another five cycles in Fig. 4.5(b) showing the orbit forming a limit cycle and whirling at slightly less than 1/2 running speed. The maximum force occurs at the end of the 15^{th} cycle of motion and has increased to almost four times the static loading.

The equations in Section 4.2 for the soft mounted journal bearing have been examined by Choudhury (43) for stability. If solutions of the form $X_i = A_i\, e^{\lambda t}$ are assumed the equations of motion produces a determinant given by:

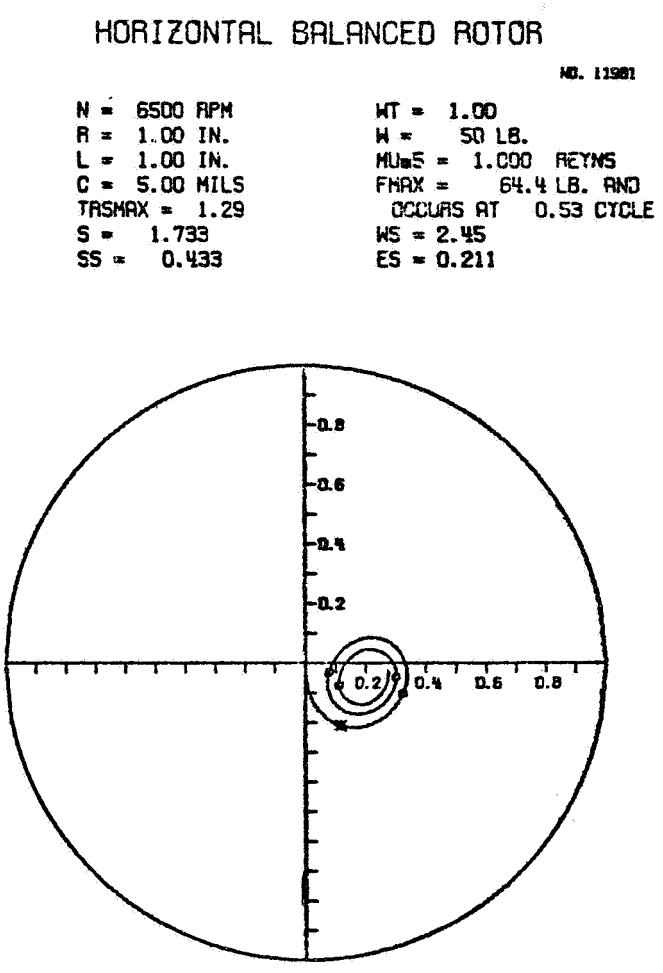

FIG. 4.4 JOURNAL ORBIT OF A BALANCED HORIZONTAL ROTOR ON RIGID SUPPORTS (N=6500, W=50, C=0.005, L/D=½)

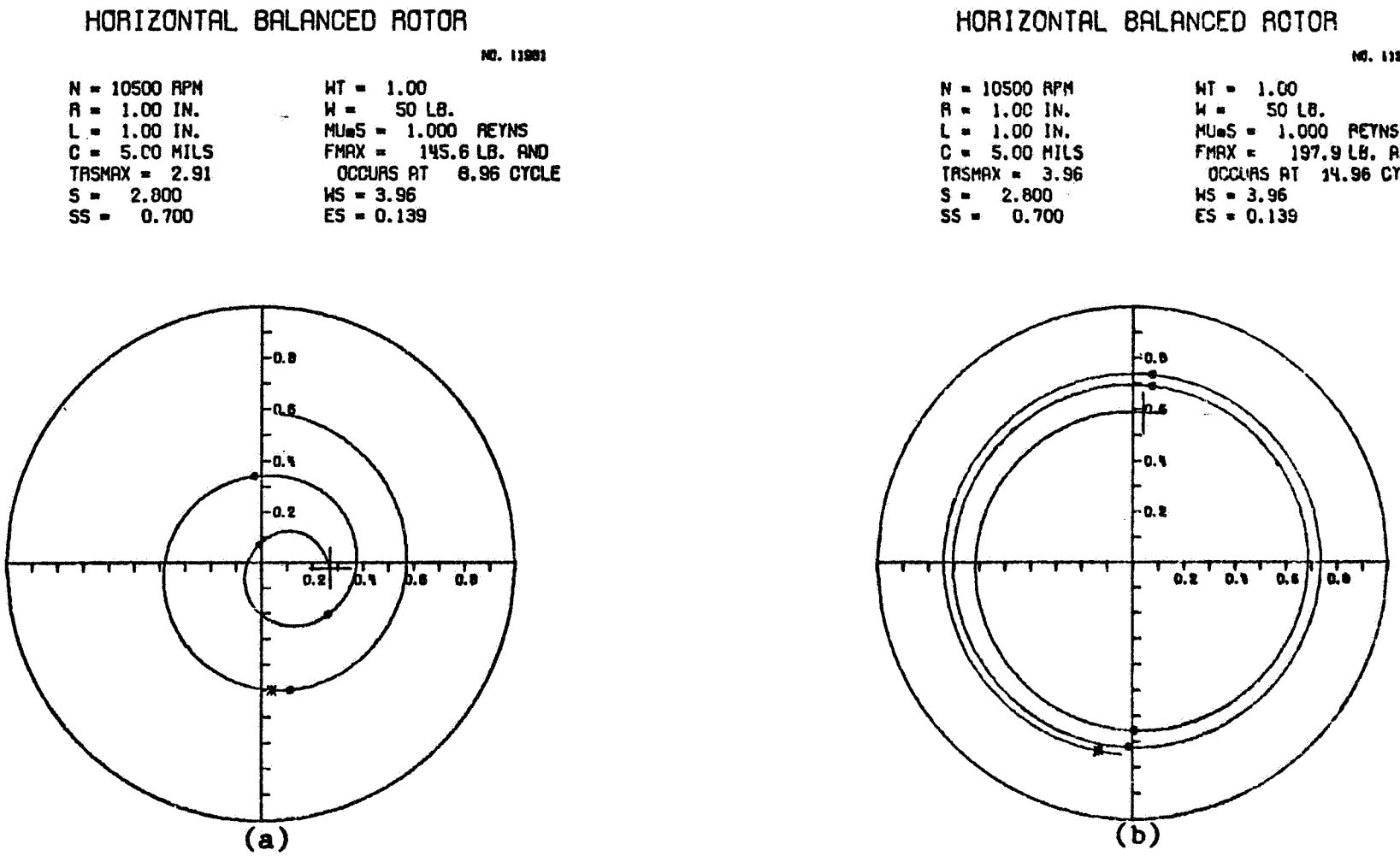

FIG. 4.5(a) JOURNAL ORBIT OF A BALANCED HORIZONTAL ROTOR FOR CYCLES 6-10 (N=10,500, W=50, C=0.005, L/D=½)
(b) JOURNAL ORBIT OF A BALANCED HORIZONTAL ROTOR FOR CYCLES 11-15 (N=10,500)

$$
\begin{vmatrix}
m_2\lambda^2 + c_{xx}\lambda + k_{xx} & c_{xy}\lambda + k_{xy} & m_2\lambda^2 & 0 \\
c_{yx}\lambda + k_{yx} & m_2\lambda^2 + c_{yy}\lambda + k_{yy} & 0 & m_2\lambda^2 \\
0 & 0 & m_1\lambda^2 + (c_x - c_{xx})\lambda + k_x - k_{xx} & -c_{xy}\lambda - k_{xy} \\
0 & 0 & -c_{yx}\lambda - k_{yx} & m_1\lambda^2 + (c_y - c_{yy})\lambda + k_y - k_{yy}
\end{vmatrix} = 0
$$

The bearing characteristics are calculated at a given equilibrium eccentricity and the resulting characteristic polynomial which is eighth order in λ was examined by Choudhury using the Routh criterion (86). Many stability maps were produced by the analysis and one series is given in Fig. 4.6-4.8. The series of curves is for a support to journal mass ratio of 0.1 and stiffness ratio $\overline{K}_B$ of 0.01, 0.1, and 1.0. The effect of support damping is shown by the family of curves for the damping ratio C_B. The length to diameter ratio, L/D, was chosen as 0.5 for this series of plots. The rigid support stability boundary is shown by the dash-dot curve and is as described earlier in this discussion. The constant load lines given by the dashed curves represents the eccentricity that a particular journal would have as the journal speed is varied.

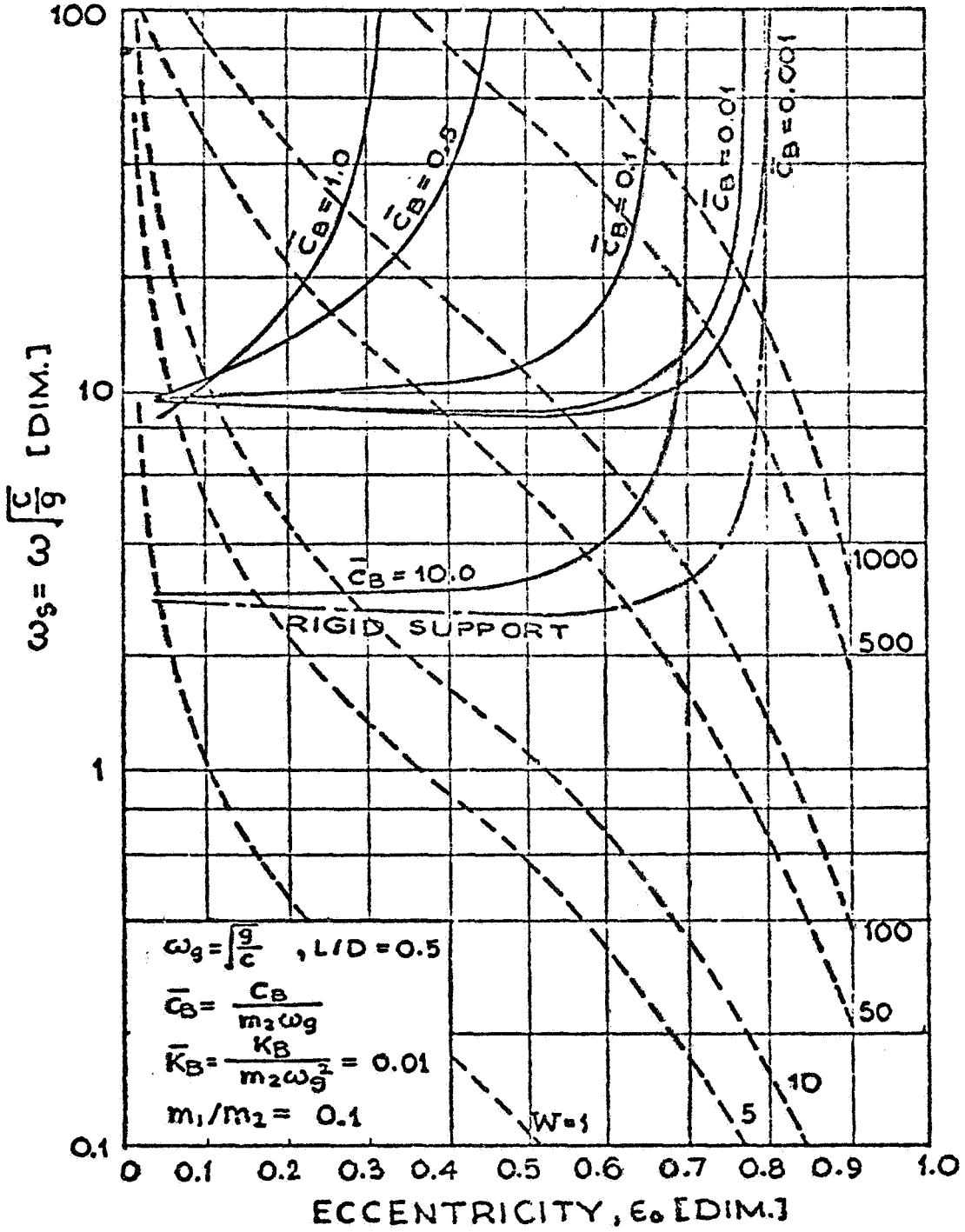

FIG. 4.6 STABILITY MAP FOR JOURNAL ON ELASTIC DAMPED SUPPORTS ($L/D=\frac{1}{2}$, $K_B=0.01$, $M_1/M_2=0.1$)

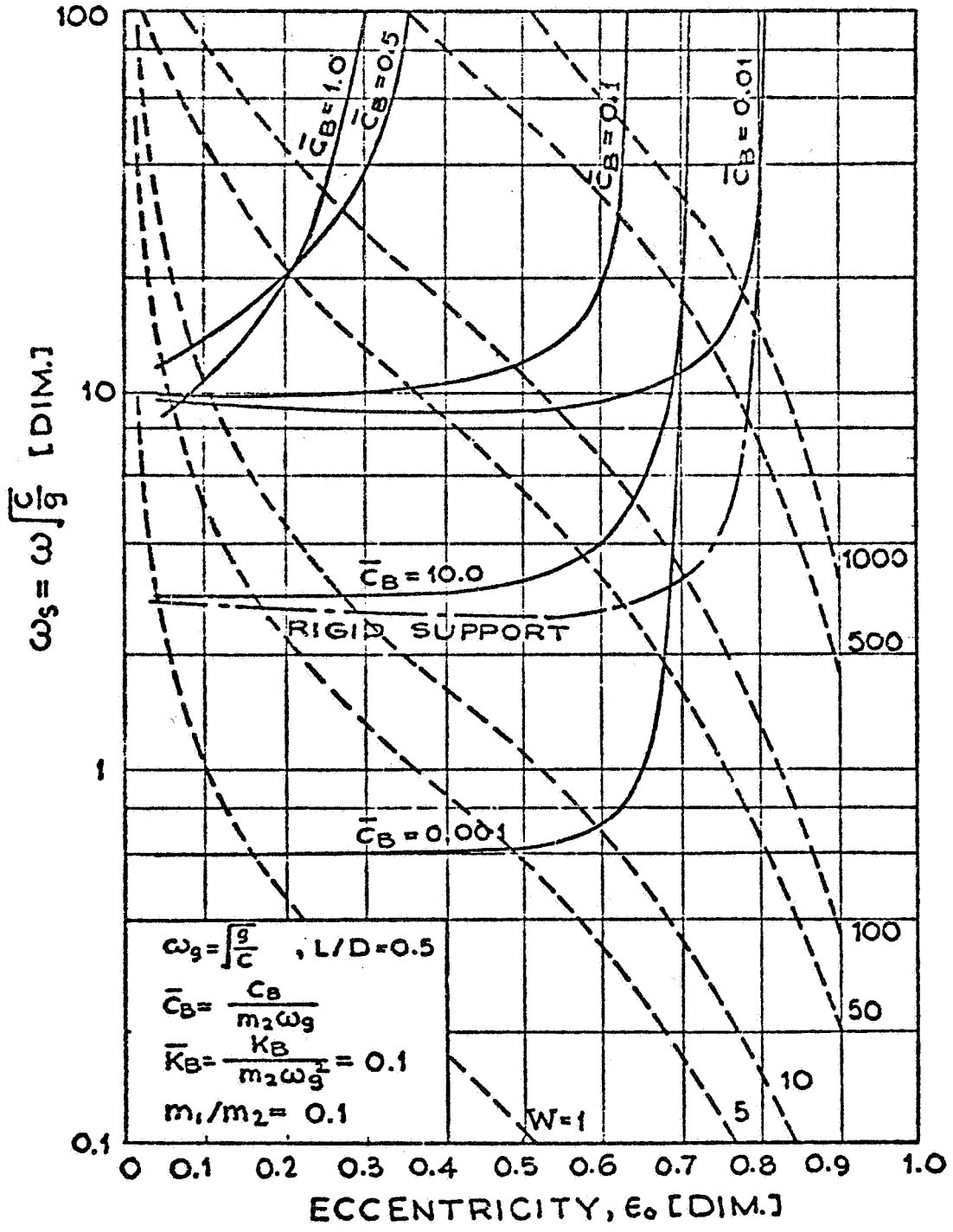

FIG. 4.7 STABILITY MAP FOR JOURNAL ON ELASTIC DAMPED SUPPORTS ($L/D=\frac{1}{2}$, $\bar{K}_B=0.1$, $M_1/M_2=0.1$)

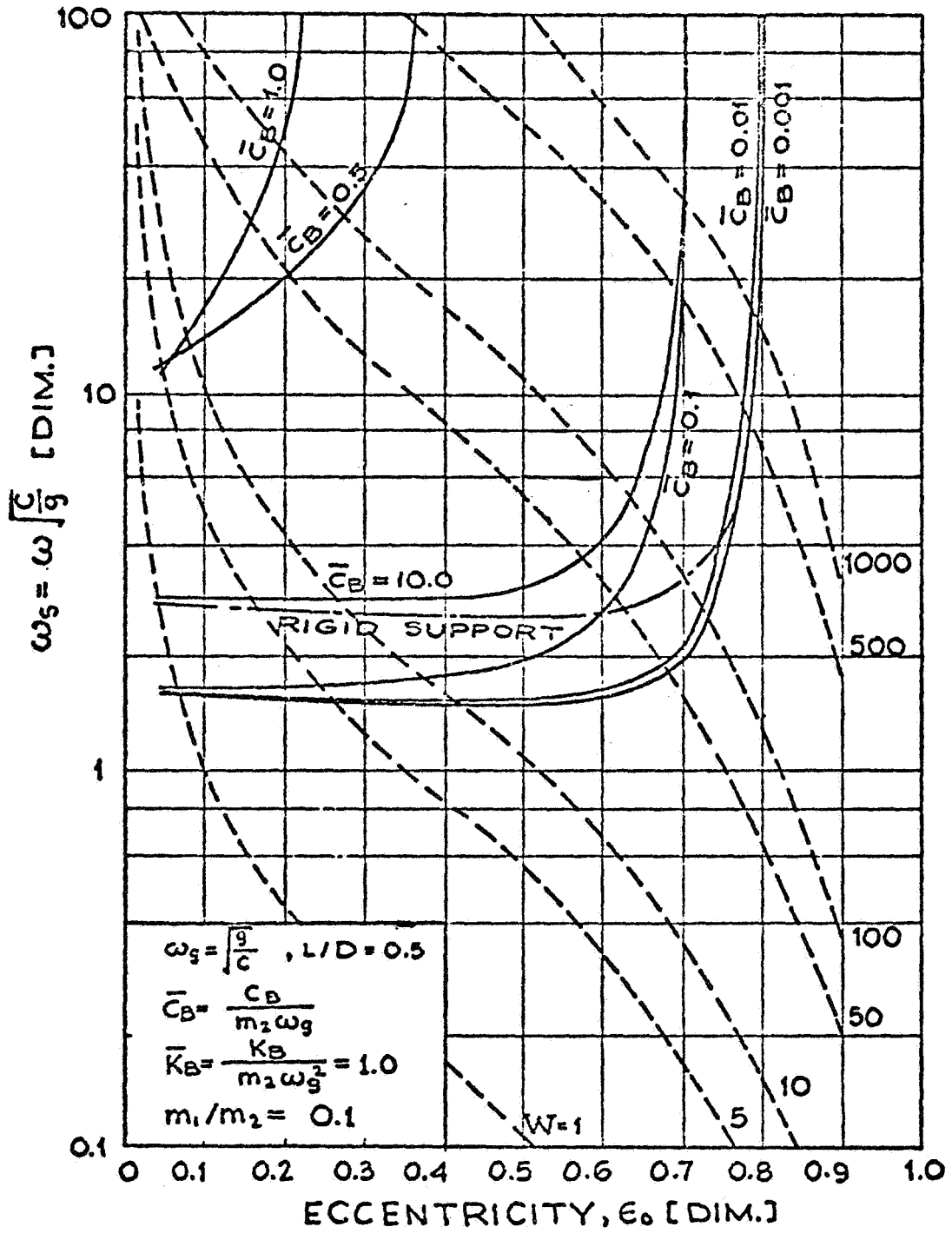

FIG. 4.8 STABILITY MAP FOR JOURNAL ON ELASTIC DAMPED SUPPORTS ($L/D=\frac{1}{2}$, $K_B=1.0$, $M_1/M_2=0.1$)

Examination of this series of plots reveals that there is an optimum support stiffness and damping that will produce the greatest stable operating range. The lightest stiffness ratio ($\overline{K}_B = 0.01$) appears to produce a great increase of ω_s even if the support damping is very light. Consider the effect of a support stiffness of $K_B = 1000.0$ lb/in, damping $C_B = 20.0$ lb-sec/in., and weight of 5 lb. Considering these values for the example of Fig. 4.4:

$$\omega_g = \sqrt{g/c} = 278 \text{ rad/sec}$$

$$m_1/m_2 = 0.1$$

$$\overline{K}_B = \frac{1000}{50/386\ \frac{g}{c}} = 0.1$$

$$\overline{C}_B = \frac{20}{\frac{50}{386}(278)} = 0.556$$

The stability boundary should occur at $\omega_s = 12$ as indicated by the stability maps of Fig. 4.6 for $\overline{K}_B = 0.1$. For the case of journal speed, N = 10,500 RPM, WS = ω_s = 3.96 and should be stable for this support system. Fig. 4.9(a) shows four cycles of the time transient of the journal on the support system and it is apparent that the journal has been stabilized. The support motion is given in Fig. 4.9(b) and has no instability apparent in the motion. The high bearing force is completely damped out by the support system. The force to the support is only 6.1 lb. over the static loading of the system.

For a rotor speed of 31,500 RPM the stability parameter $\omega_s = 11.86$ and is at the threshold. The orbit shown in Fig. 4.10(a) indicates that

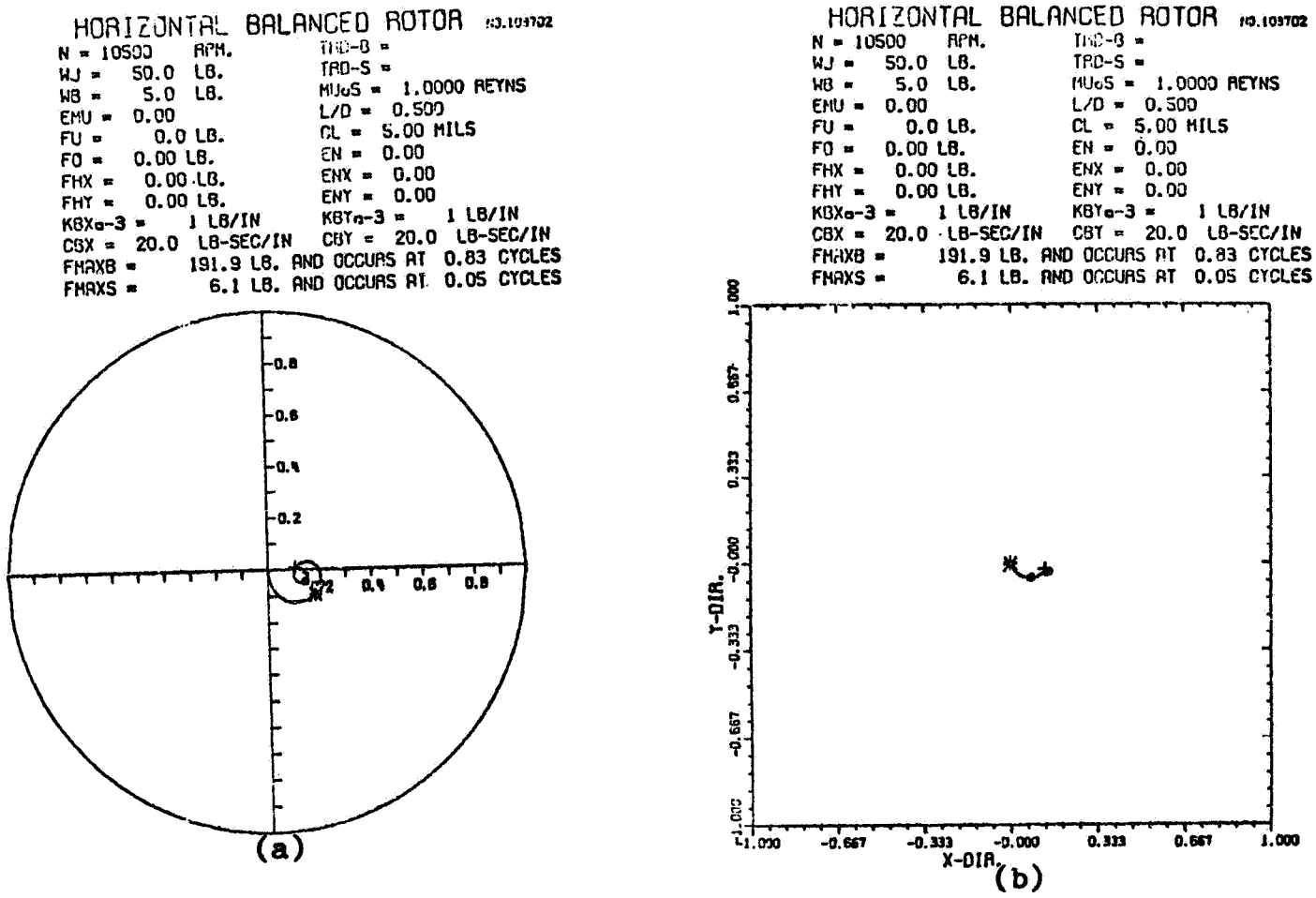

FIG. 4.9(a) JOURNAL RELATIVE MOTION SHOWING STABILIZED RESPONSE (N=10,000, WS=3.96)
(b) SUPPORT SYSTEM RESPONSE

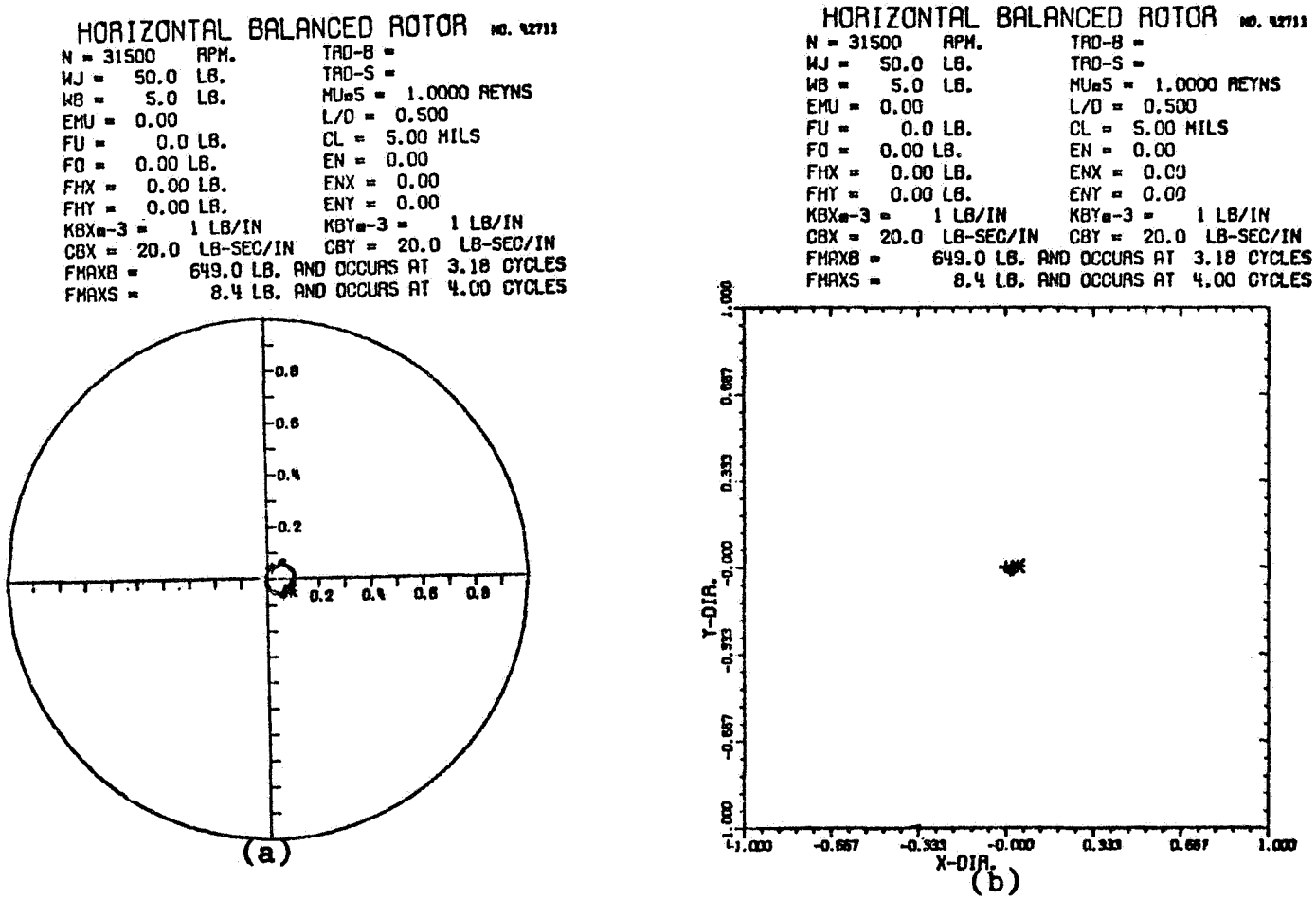

FIG. 4.10(a) ROTOR RELATIVE MOTION AT THRESHOLD OF STABILITY (N=31,500, WS=11.9)
(b) SUPPORT RESPONSE AT THRESHOLD FOR FIVE CYCLES

the journal is indeed unstable and growing at a very slow rate. The support motion is neglibible and is absorbing the large journal forces very well but is no doubt increasing at the end of the fourth cycle.

For a journal speed of 45,000 RPM the system is well above the threshold and as indicated in Fig. 4.11(a) the rate of growth is greatly increased. The bearing force is 20 times the static loading with the support force at the fifth cycle given by 21.9 lb. over the static loading. The support motion given in Fig. 4.11(b) is, even in this case, still negligible after five cycles of motion.

Stability analyses such as that conducted by Choudhury must treat balanced rotor systems and do not give any indication of the behavior under external loading or the degree of stability. Some indication of the rate of growth can be obtained if the roots of the characteristic equation are solved for in addition to applying the Routh criterion. The time transient technique is capable of giving this type information and is the reason this type solution is so important to practical design theory. Unbalance or any other timewise describable force is easily included in the solution. Considerable attention has been given to the rigid mount short journal bearing time transient behavior (18,41). The following discussion will extend this rigid mount journal to include the effect of support flexibility on the unbalance response.

Fig. 4.12 represents five cycles of motion of an unbalanced rotor running at 6500 RPM. This is the same rotor that was examined earlier in this section. The journal mass center is eccentric by 0.20 of the clearance (ie. EMU = E_{μ} = 0.20). The orbit indicates that the motion is a combination of synchronous and fractional frequency whirl. The timing

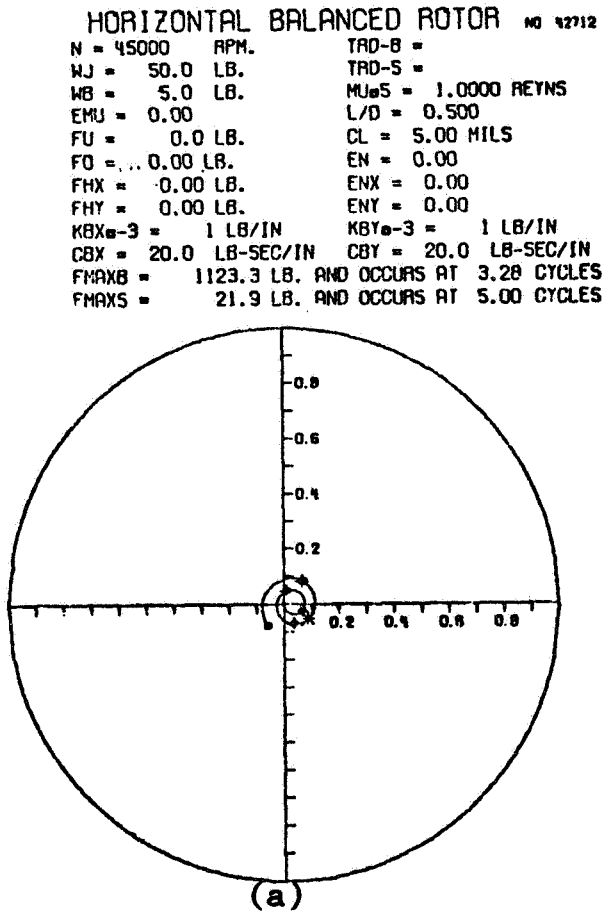

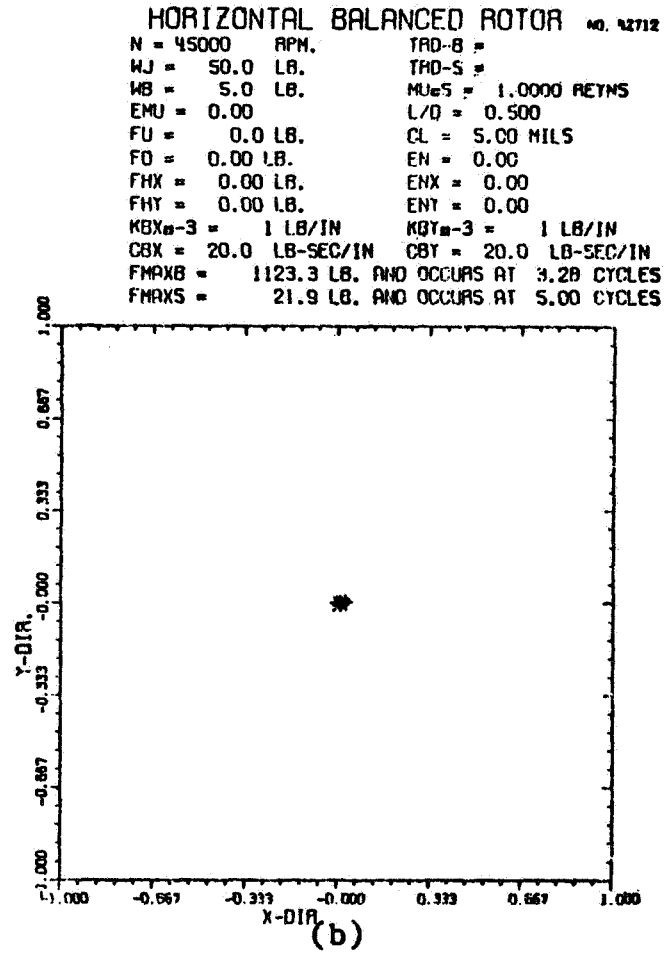

FIG. 4.11(a) ROTOR RELATIVE MOTION FOR FIVE CYCLES SHOWING JOURNAL INSTABILITY (N=45,000, WS=17)
(b) SUPPORT TRANSIENT FOR FIVE CYCLES (N=45,000)

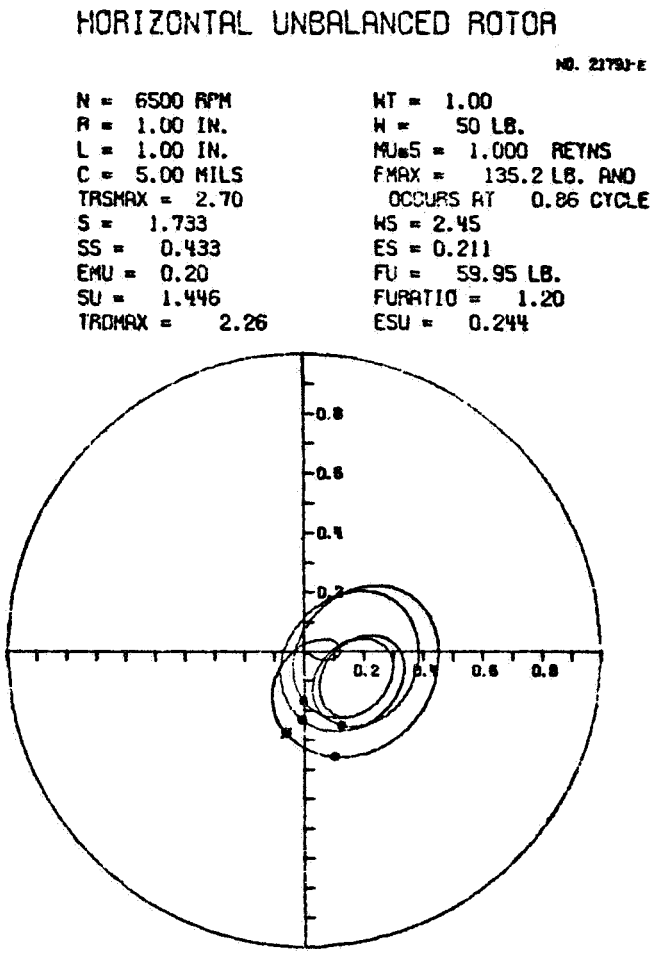

FIG. 4.12 JOURNAL ORBIT OF AN UNBALANCED ROTOR ON RIGID SUPPORTS FOR FIVE CYCLES (N=6,500, W=50, C=0.005, L/D=½, EMU=0.2)

marks indicate that the average whirl is somewhat less than synchronous and the inner loops indicate the presence of a fractional whirl component. As the rotor speed is increased to 10,500 RPM Fig. 4.13 indicates that the fractional whirl dominates the motion as the inner loops disappear and the timing marks begin to fall two per whirl cycle. Consider the following support system for this example.

Let

mass of bearing = 5.0 lb.; $m_1/m_2 = 0.1$

stiffness of support = 10,000 lb/in; $\overline{K}_B = 1.0$

damping of support = 200 lb-sec/in; $\overline{C}_B = 5.56$

From the stability map of Fig. 4.8 the system should be stable at 6500 RPM ($\omega_s = 2.45$) and possibly close the threshold at 10,500 RPM. Figure 4.14(a)shows the elliptical steady state orbit for the case of 6500 RPM. The next figure, 4.14(b) indicates the corresponding motion of the support system (ie., bearing housing mass).

When orbits are calculated by any type integration scheme there is always the possibility that the results are meaningless. To illustrate this fact, the case just considered was run with a larger time step and produced the orbit of Fig. 4.14(c). It is quite obvious that the orbit is not correct due to the oscillations starting near the end of the first cycle of motion. The next figure, 4.14(d) is not nearly as obvious that the solution is incorrect. The support motion is very nearly the same as the orbit of Fig. 4.14(b). Extreme caution must be exercised by the researcher when producing the time-transient solution for just these reasons.

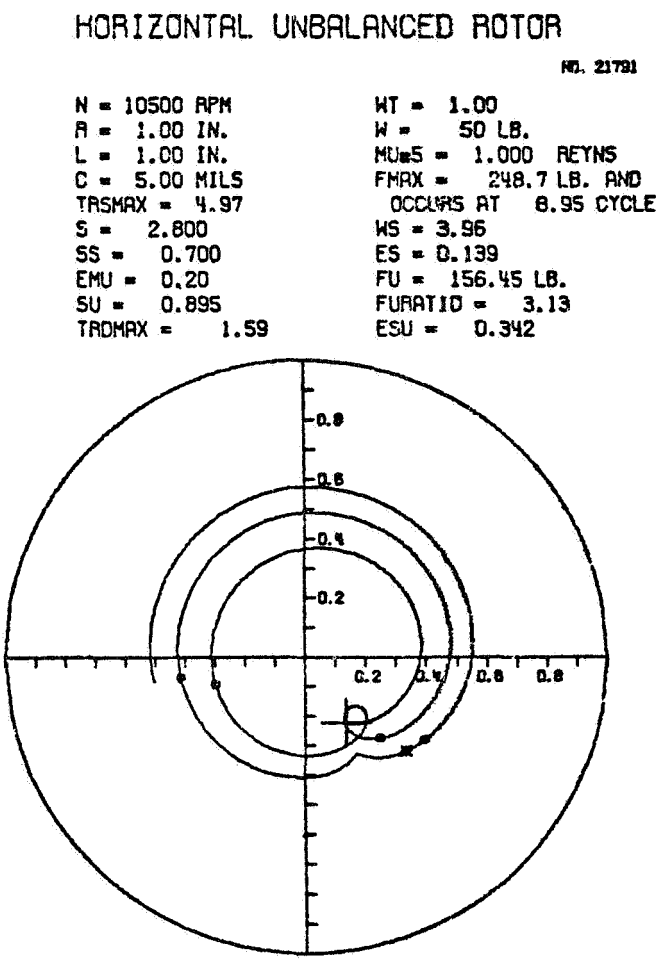

FIG. 4.13 JOURNAL ORBIT OF AN UNBALANCED ROTOR ABOVE THE STABILITY THRESHOLD FOR CYCLES 6-10(N=10,500)

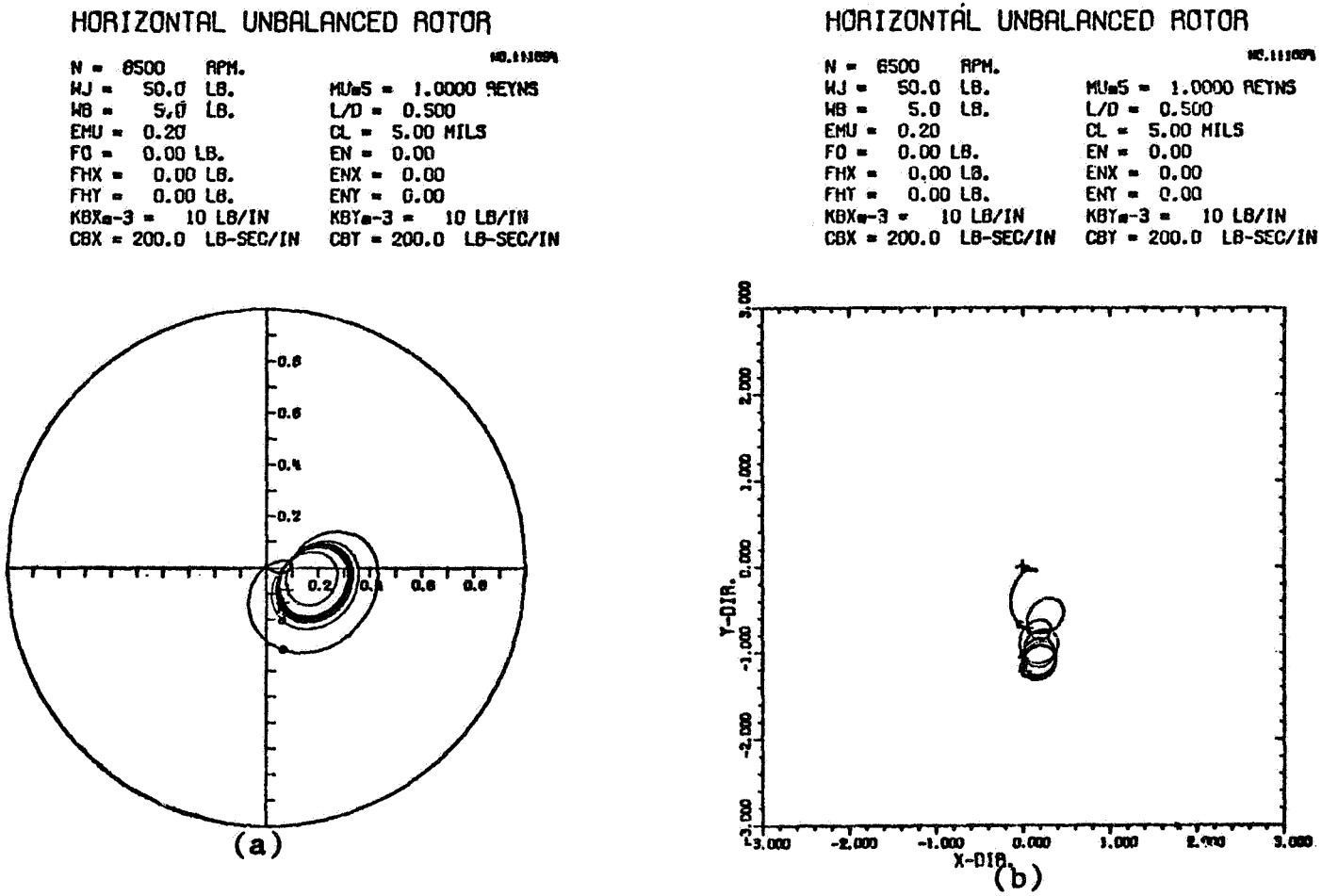

FIG. 4.14(a) JOURNAL RELATIVE MOTION OF UNBALANCED ROTOR ON ELASTIC SUPPORTS SHOWING STEADY-STATE ELLIPTIC ORBIT
(b) SUPPORT TRANSIENT MOTION (N=6,500)

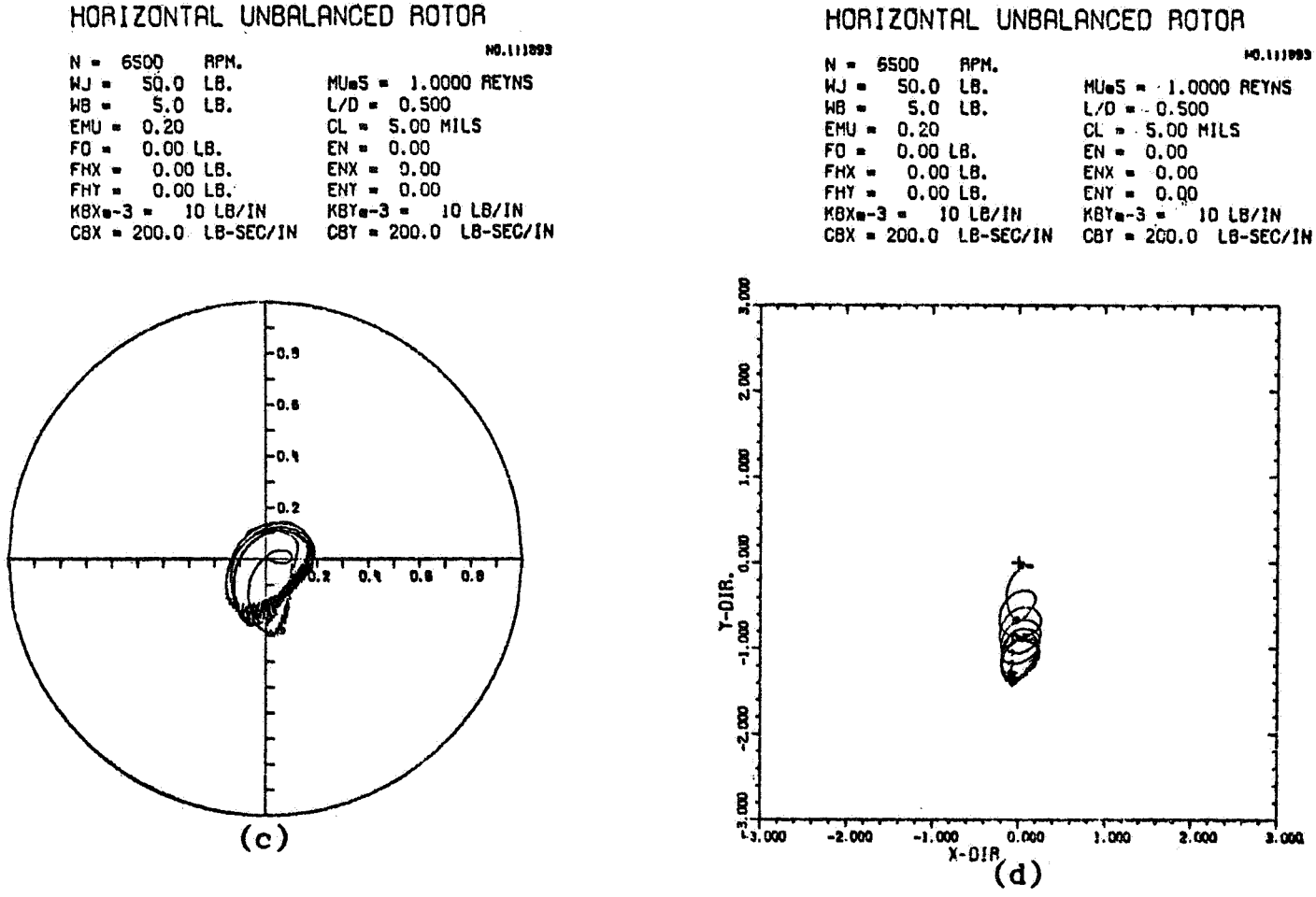

FIG. 4.14(c) JOURNAL RELATIVE MOTION SHOWING NUMERICAL INSTABILITY FOR SOLUTION TIME STEP TOO LARGE
(d) SUPPORT RESPONSE FOR NUMERICALLY UNSTABLE SOLUTION

For the support system being considered and journal speed of 10,500 RPM, Fig. 4.15(a) indicates that the whirl is dominated by a fractional whirl and is indeed beyond the threshold speed. The corresponding support motion is shown in Fig. 4.15(b).

Figure 4.16 was an orbit run as a check case while the computer code was being developed. The support system was frozen (K_s = 1 million, C_s = 100) and the resulting orbit can be compared to the orbit of Fig. 4.12 which was presented in (18).

A lighter support system has been indicated (19) to give better steady-state response attenuation. Reducing the stiffness to K_s = 1000 lb/in and damping to 20 lb-sec/in, the unbalance response is given by Fig. 4.17 a for an unbalance eccentricity of E_μ = 0.20. The improved response attenuation is readily apparent and the forces transmitted are moderate since the unbalance load is 156.6 lb. for this example. The support motion and forces are referenced from static conditions and Fig. 4.17(b) indicates the bearing housing motion for this particular case. The support experiences a maximum force of 33.5 lb. over the static loading (55 lb.).

An increase of the unbalance eccentricity to 0.80 produces an unbalance load of 626.4 lb. Fig. 4.18(a) gives the transient and resulting synchronous orbit and a maximum force to the bearing of only 474.7 lb., less than the unbalance load. The corresponding bearing motion is given in Fig. 4.18(b) and the maximum force transmitted is only 136.7 lb. above the static loading.

This type unbalance attenuation of both amplitude and transmitted forces is very desirable when considering the extended life of a machine.

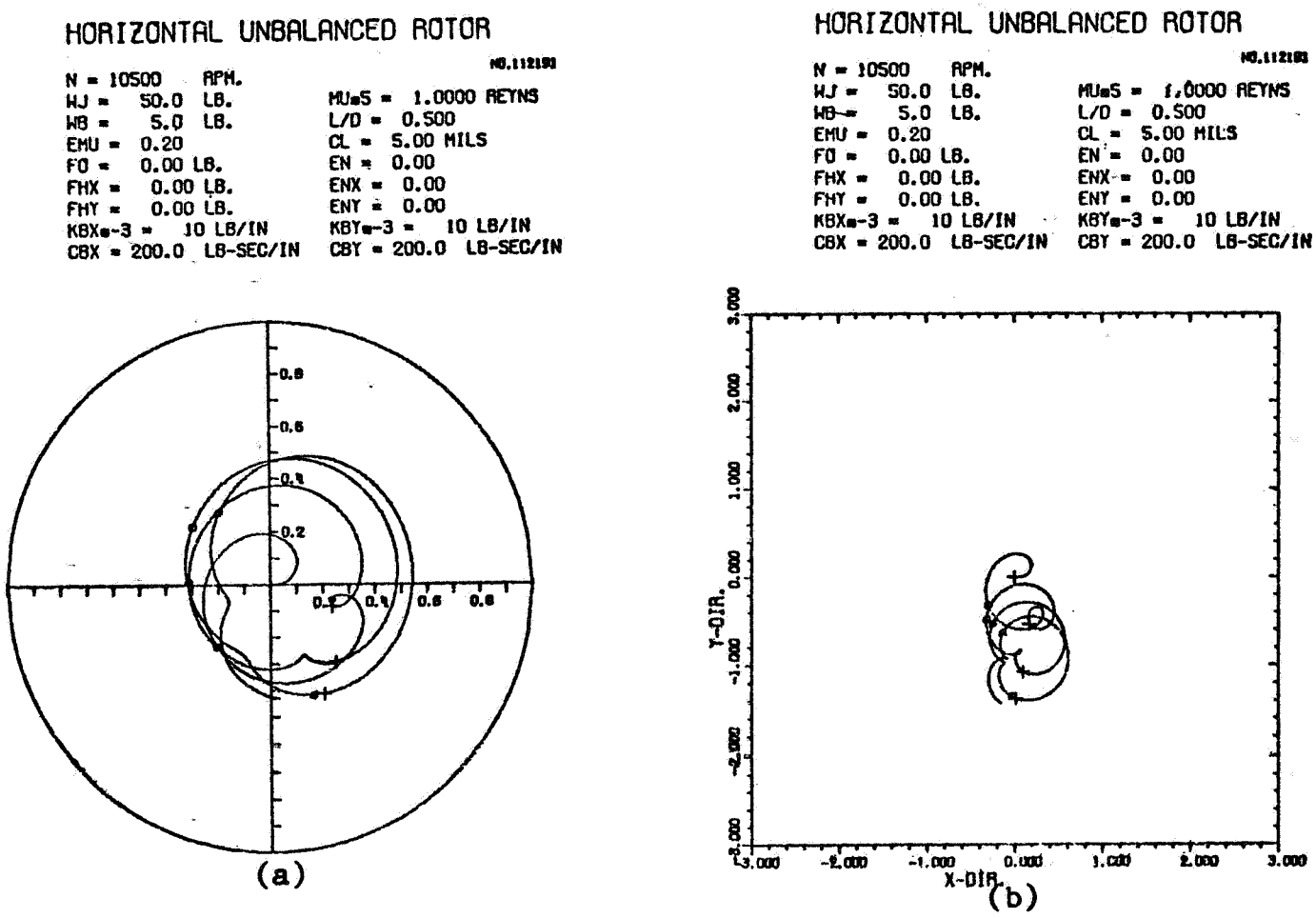

FIG. 4.15(a) JOURNAL TRANSIENT RESPONSE FOR OVERDAMPED SUPPORT (N=10,500, EMU=0.2)
(b) SUPPORT RESPONSE (KBX=KBP=10,000, CBX= CBY=200)

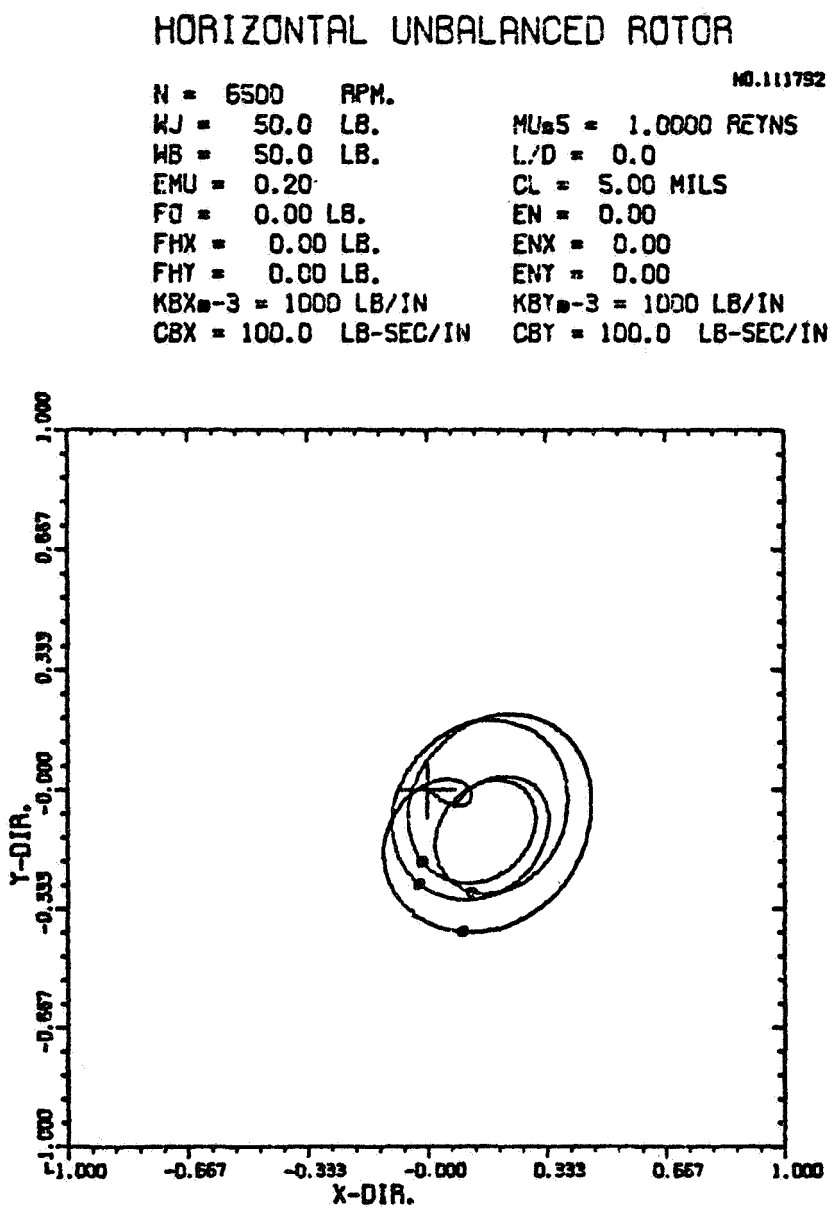

FIG. 4.16 JOURNAL TRANSIENT UNBALANCE RESPONSE FOR FROZEN SUPPORT SYSTEM (N=6,500, EMU=0.2)

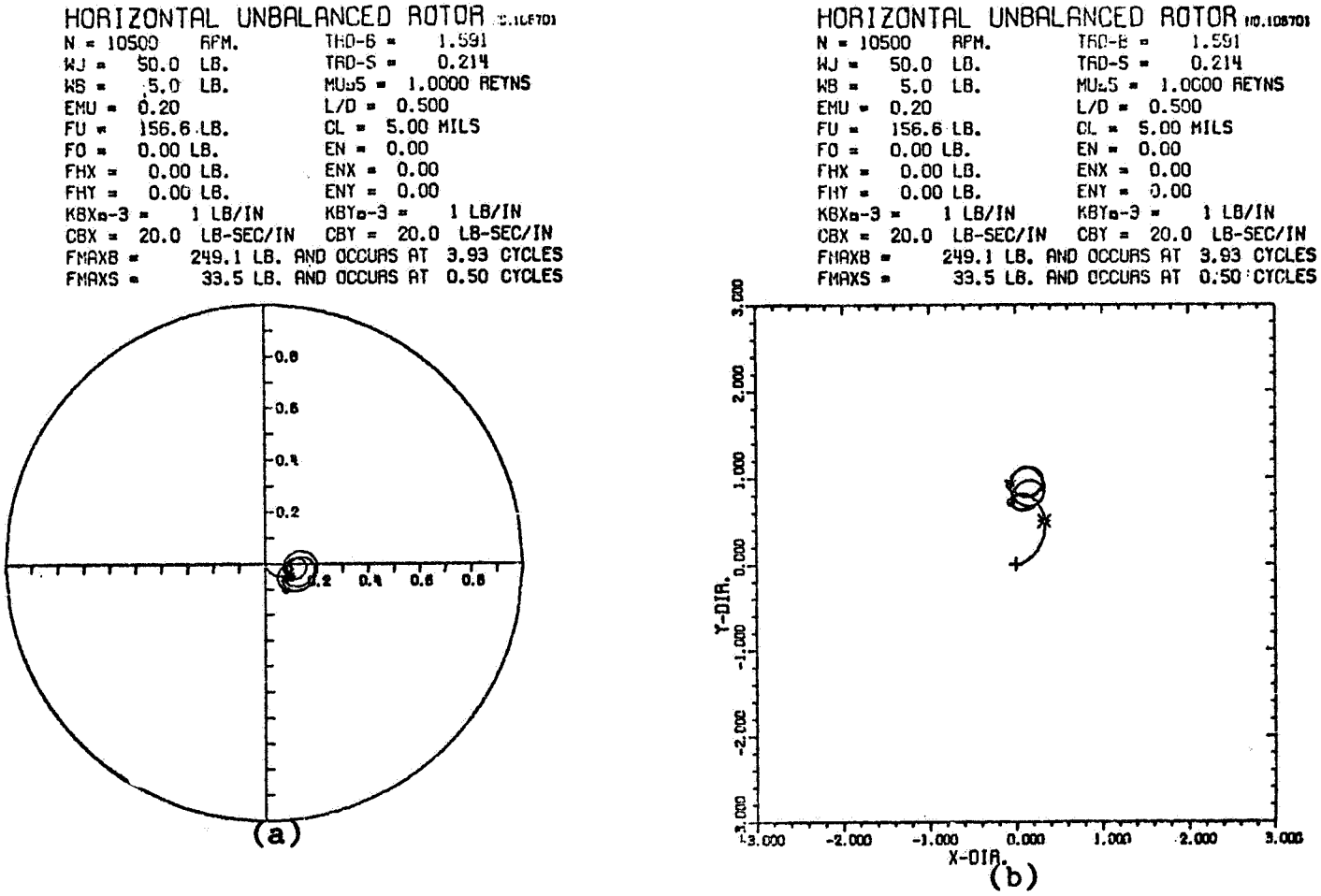

FIG. 4.17(a) JOURNAL UNBALANCE RESPONSE FOR IMPROVED SUPPORT SYSTEM (N=10,500, EMU=0.2)
(b) SUPPORT SYSTEM TRANASIENT RESPONSE FOR FIVE CYCLES (KBX=KBY=1,000, CBX=CBY=20)

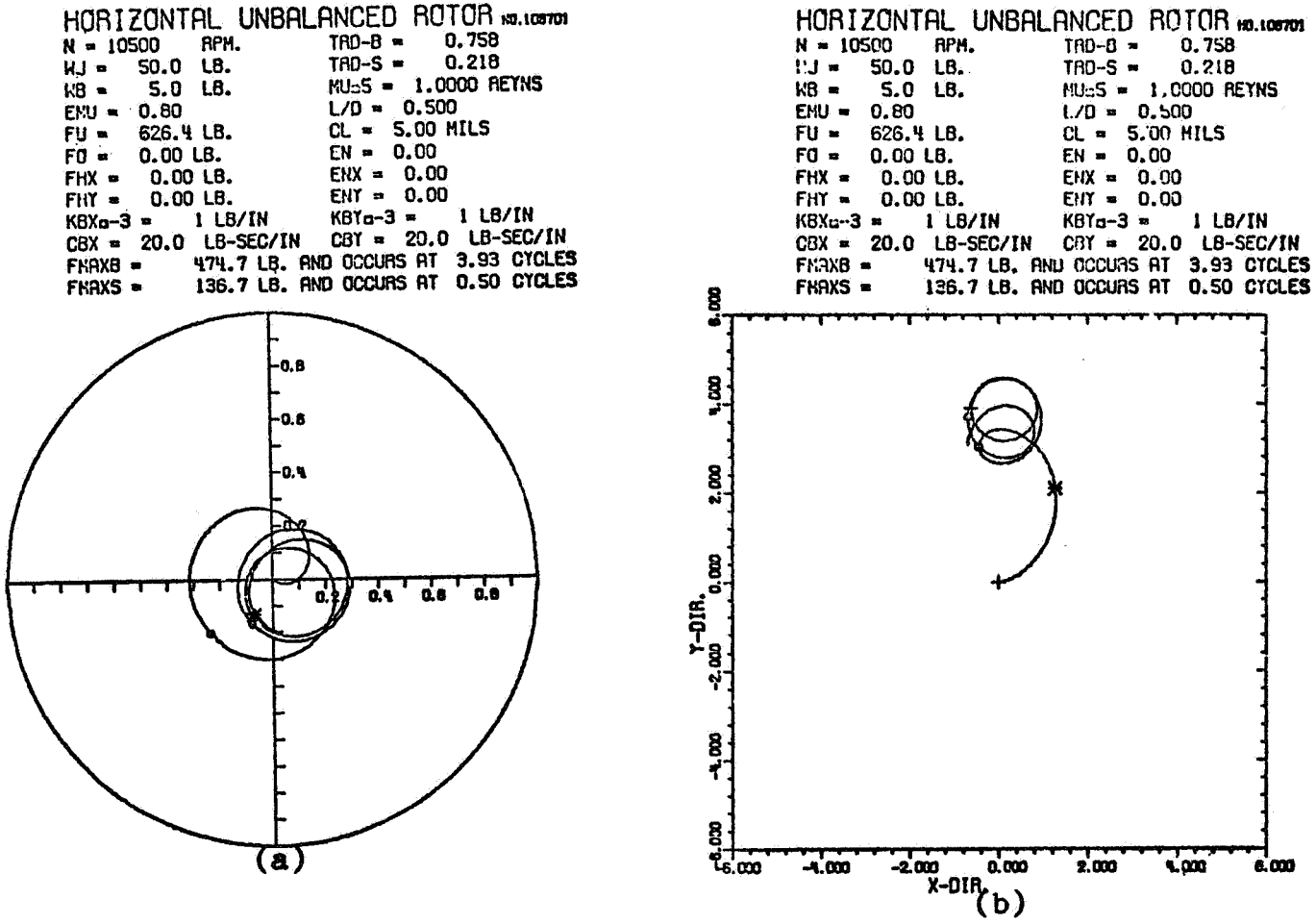

FIG. 4.18(a) JOURNAL UNBALANCE RESPONSE FOR FOUR CYCLES (N=10,500, EMU=0.8)
(b) SUPPORT SYSTEM RESPONSE (KBX=KBY=1,000, CBX=CBY=20)

In many cases the forces transmitted increase when the amplitudes are reduced but this case demonstrates that damping can be designed into nonlinear fluid film bearings to reduce the transmissibility to the bearing surface as well as to the support housing.

4.4 Vertical Bearing Whirl

The balanced vertical journal bearing is unstable at all speeds. Yet there are machines running in the vertical mode that exhibit reasonable response. It has been shown (18) that net external unidirectional loading can improve the stability of rigidly mounted journal bearings. The addition of a damped support system does not improve the stability of the vertical balanced journal bearing. The system that was stable in the horizontal mode is shown to be unstable in Fig. 4.20(a). The journal was given initial conditions

$$\dot{X} = Y = 0.0$$

$$X = -\dot{Y} = 0.15$$

where

$$X = x/c, \quad Y = y/c$$

$$\dot{X} = \dot{x}/(c\omega), \quad \dot{Y} = \dot{y}/(c\omega)$$

The transient response indicates that these initial conditions were compatible with the natural response. Although the system is unstable the rate of growth is considerably less than that of the rigid case, Fig. 4.19. Although the support does not stabilize the journal, it does effect the degree of instability. The corresponding support response is given in Fig. 4.20(b). It was shown in (18) that an unbalance eccentricity greater than 0.16 was required to cancel the nonsynchronous

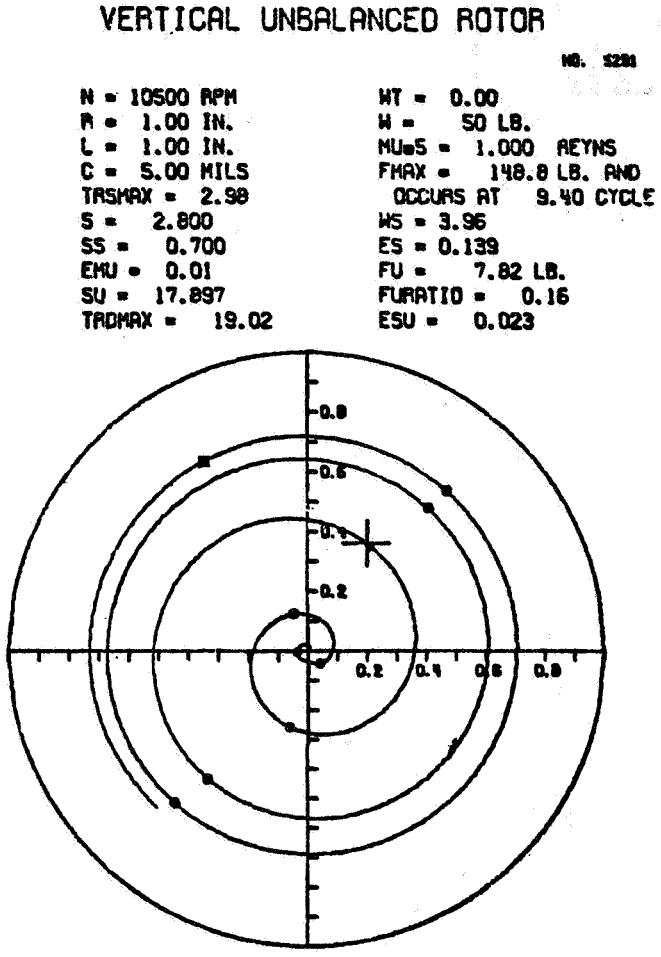

FIG. 4.19 JOURNAL ORBIT OF A SLIGHTLY UNBALANCED VERTICAL ROTOR FOR 10 CYCLES (N=10,500, EMU=0.01)

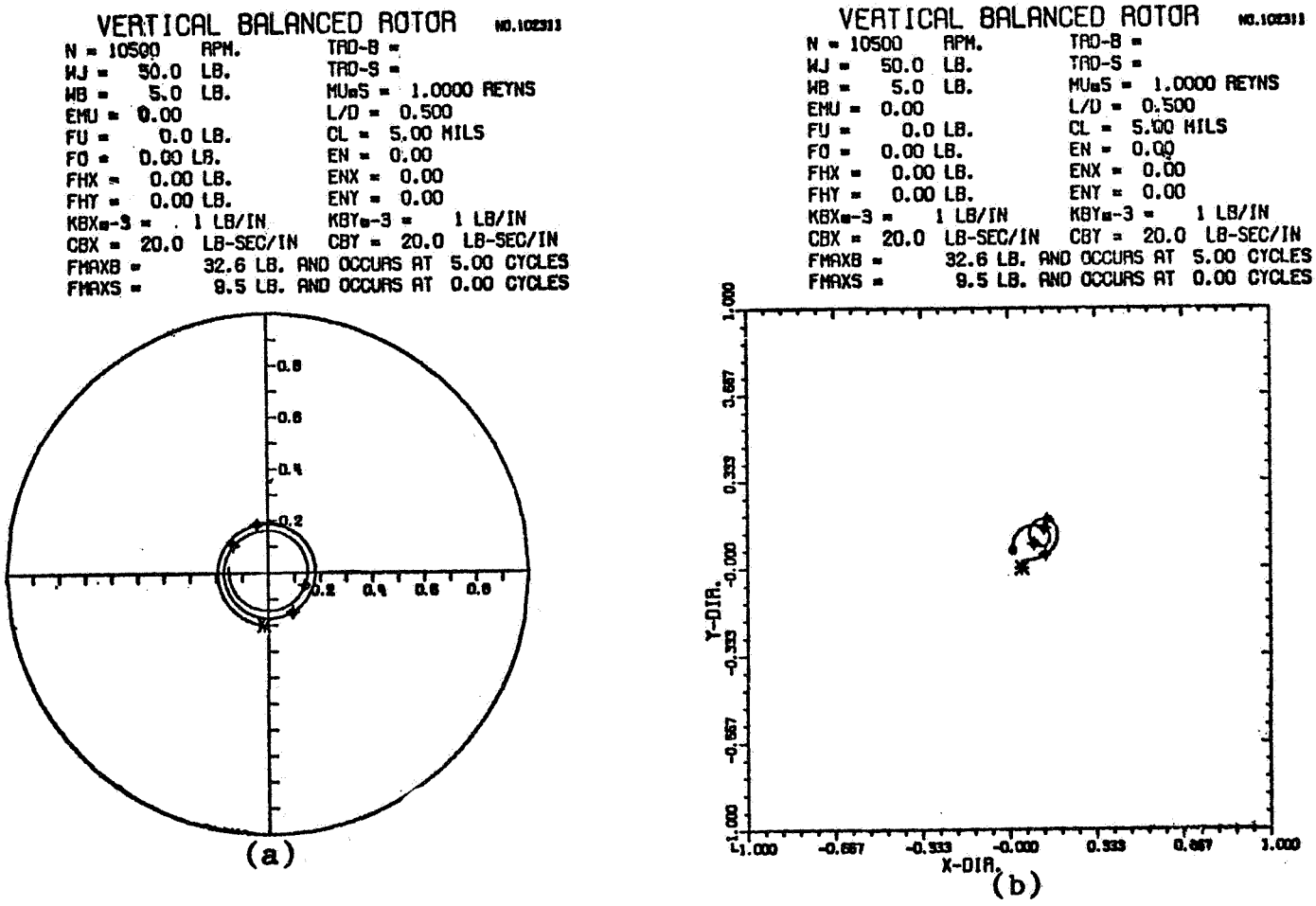

FIG. 4.20(a) JOURNAL RELATIVE MOTION FOR FIVE CYCLES OF A BALANCED VERTICAL ROTOR (N=10,500)
(b) SUPPORT SYSTEM RESPONSE (KBX=KBY=1,000, CBX=CBY=20)

instability whirl and produce a synchronous limit cycle. It was also demonstrated that even the unbalance did not alter the fractional whirl above the corresponding horizontal stability threshold. The following series of curves will have an unbalance eccentricity of 0.2. A support stiffness of 10,000 lb/in and damping of 20 lb-sec/in. results in the transient orbit shown in Fig. 4.21(a) for a speed of 6500 RPM. The support motion is double that of the journal relative motion as indicated in Fig. 4.21(b). If the journal were on rigid supports the motion would be stable synchronous as indicated in Fig. 4.22 with the maximum force less than the unbalance load. This example illustrates that an improperly designed damped support can give undesirable response. If the damping is increased to 200 lb-sec/in the journal relative motion is shown in Fig. 4.23(a) and indicates that the amplitude has been reduced by the increased support damping. The support motion is also suppressed as indicated in Fig. 4.23(b).

The preceding analysis of horizontal journal bearings indicated that a lighter support stiffness would give improved response. Figure 4.24(a) shows the transient of the improved support system operating at 10,500 RPM. This lighter support stiffness of 1000 lb/in gives a highly attenuated relative journal response. The support system motion given in Fig. 4.24(b) has an initial transient that is damping out to a reasonably small whirl orbit. The forces to the support is noted to be about one-fifth of the unbalance load. The bearing force is also less than the unbalance loading. The rigid support journal is shown in Fig. 4.25 with a substantially larger response and also a larger maximum force transmitted to the bearing support than that of Fig. 4.24(a).

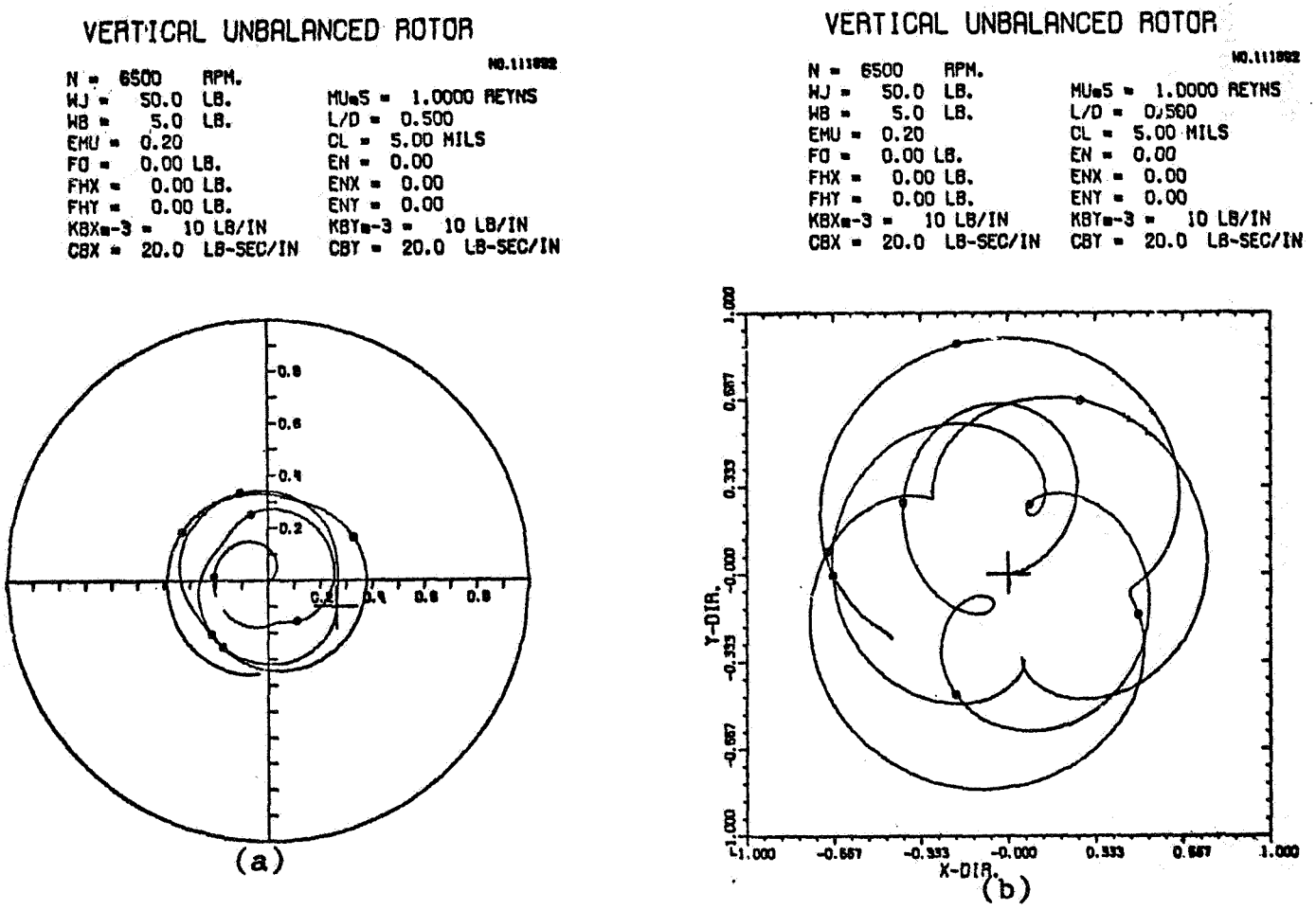

FIG. 4.21(a) VERTICAL UNBALANCED ROTOR RESPONSE FOR TEN CYCLES (N=6,500, EMU=0.2)
(b) SUPPORT SYSTEM RESPONSE (KBX=KBY=10,000, CBX=CBY=20)

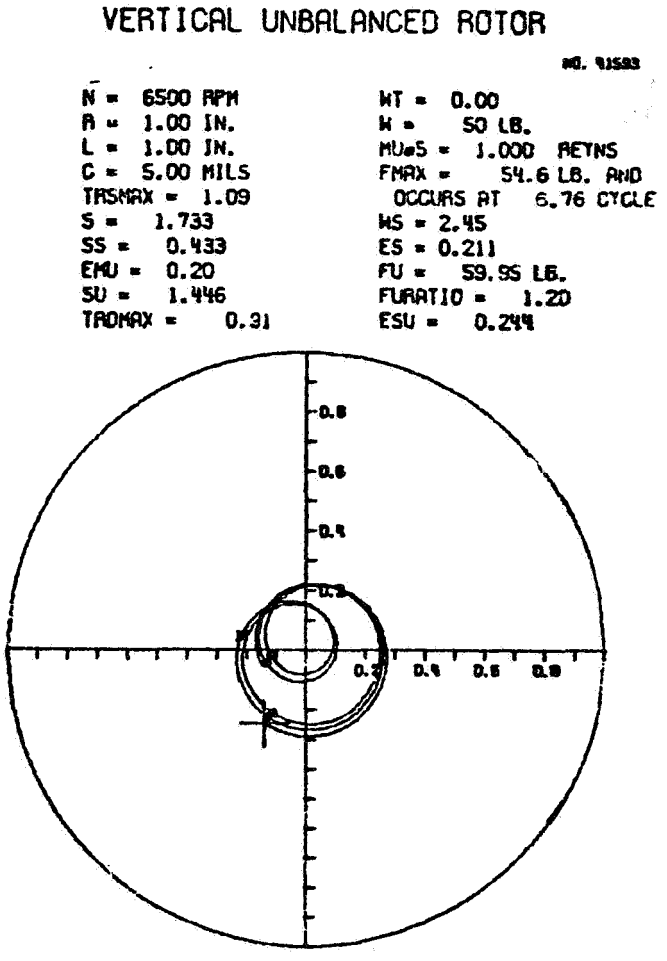

FIG. 4.22 JOURNAL ORBIT OF AN UNBALANCED VERTICAL ROTOR FOR CYCLES 6-10 SHOWING MOTION APPROACHING SYNCHRONOUS (N=6,500, EMU=0.2)

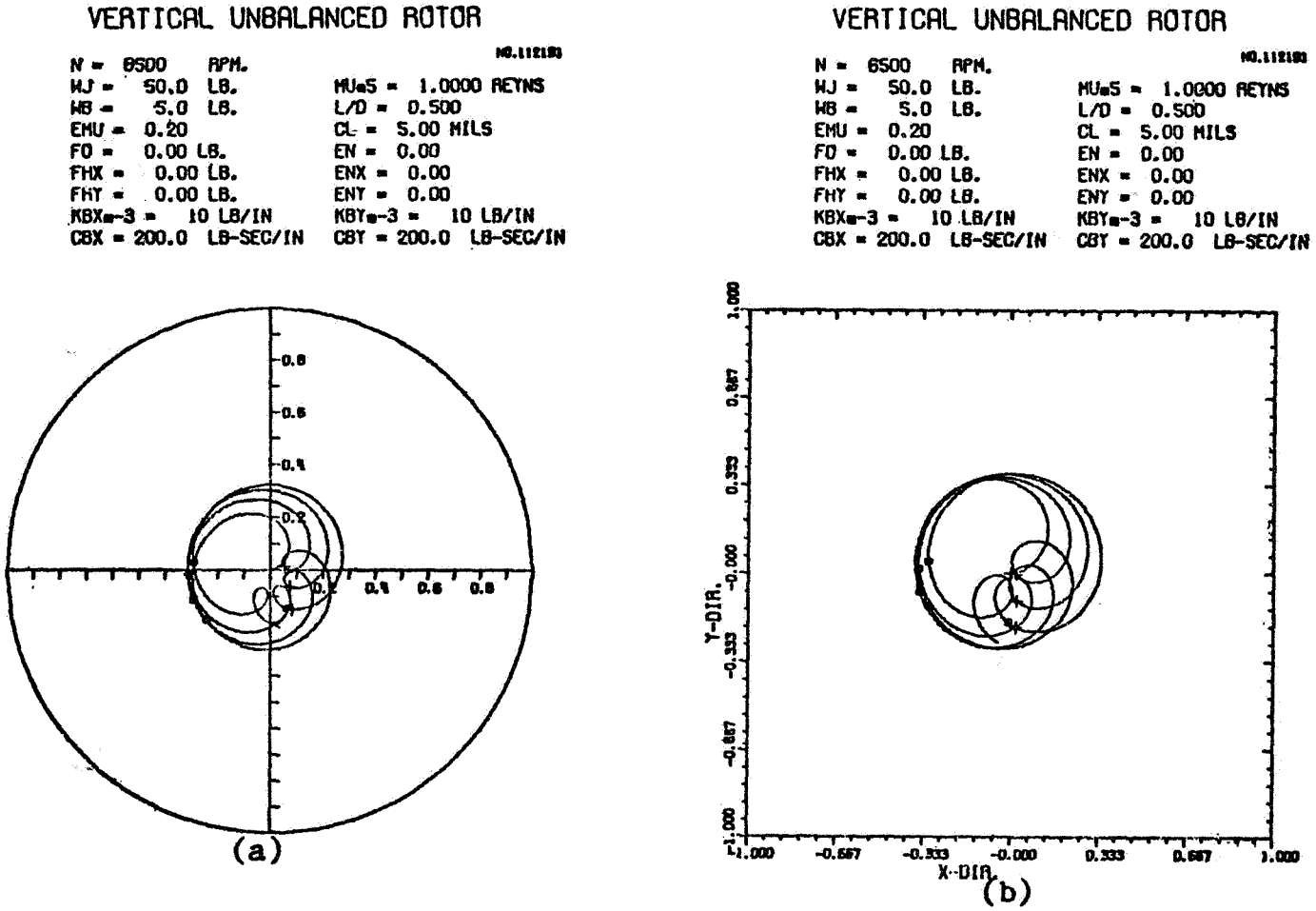

FIG. 4.23(a) VERTICAL JOURNAL UNBALANCE RESPONSE FOR OVERDAMPED SUPPORT SYSTEM (N=6,500, EMU=0.2)
(b) SUPPORT SYSTEM RESPONSE (KBX=KBY=10,000, CBX=CBY=200)

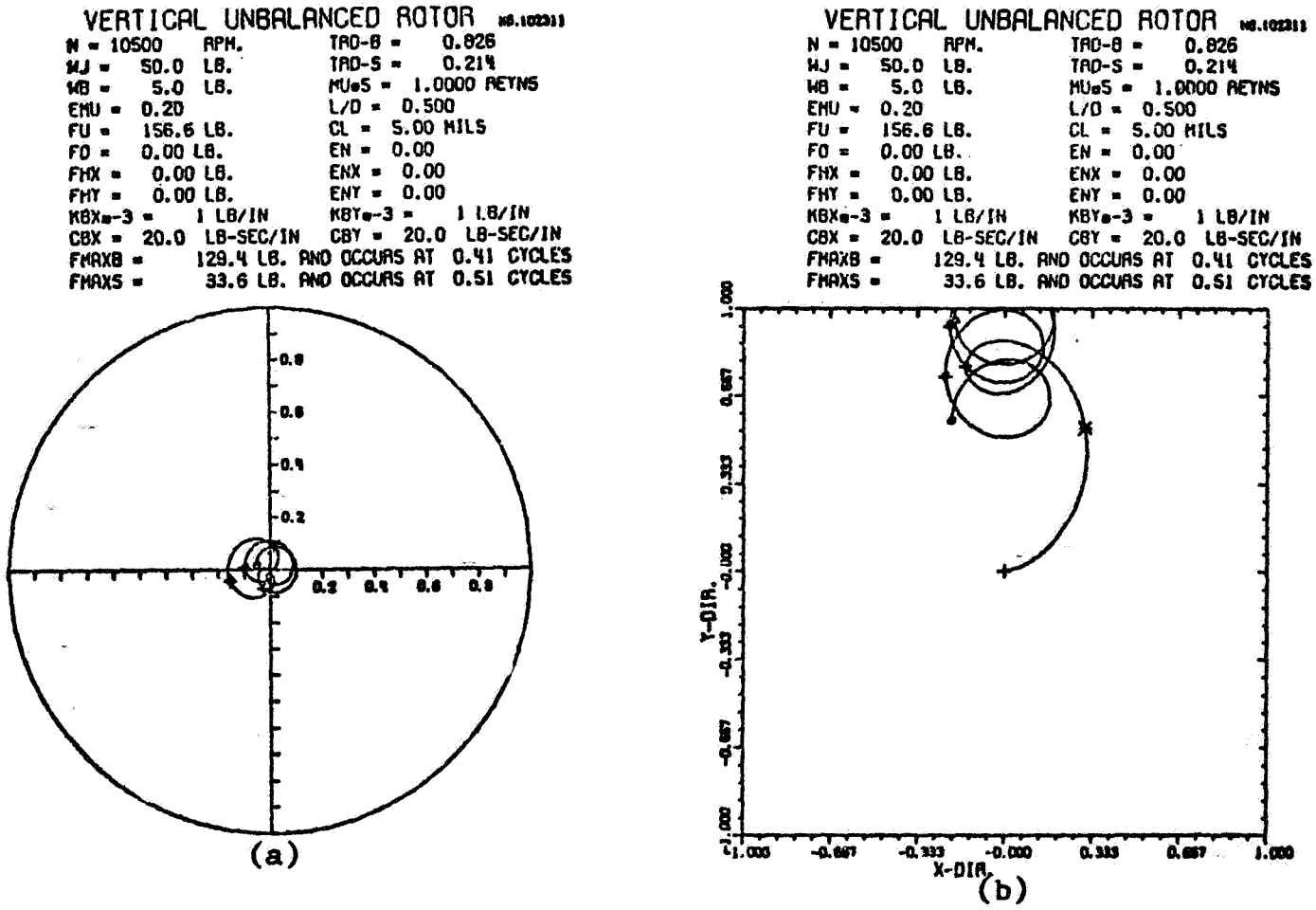

FIG. 4.24(a) VERTICAL JOURNAL UNBALANCE RESPONSE FOR IMPROVED SUPPORT SYSTEM (N=10,500, EMU=0.2) (b) SUPPORT SYSTEM RESPONSE (KBX=KBY=1,000, CBX=CBY=20)

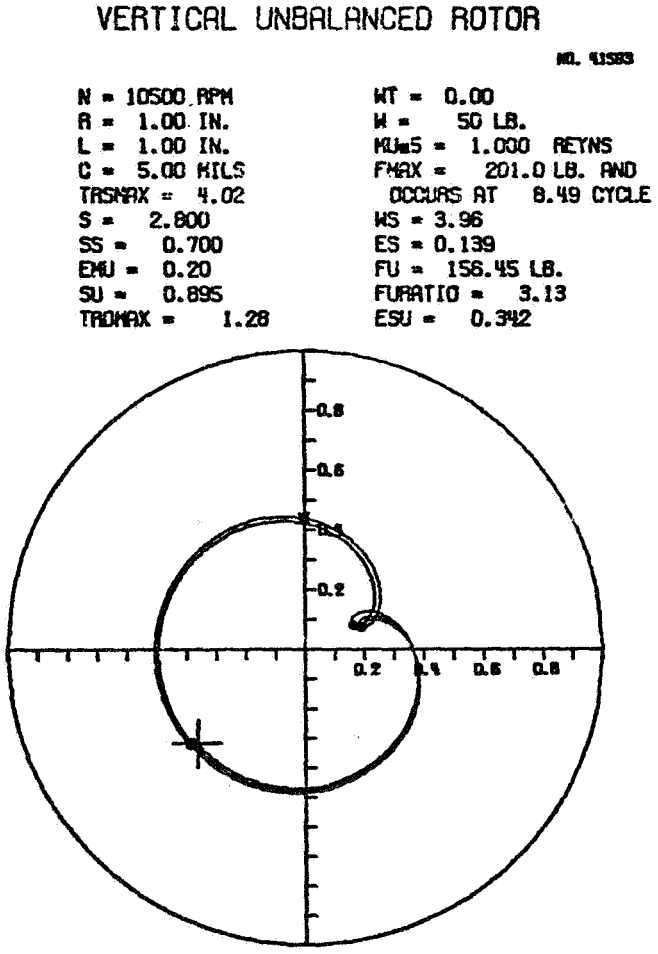

FIG. 4.25 JOURNAL ORBIT OF AN UNBALANCED VERTICAL ROTOR FOR CYCLES 5-10 (N=10,500, EMU=0.2)

An increase of unbalance eccentricity to 0.80 produces an unbalance loading of 626 lb. The resulting response is given in Fig. 4.26(a) and has a maximum force of 538 lb., less than the unbalance loading. The support transient is shown in Fig. 4.26(b) where the maximum force to the support housing is only 139 lb.

The influence of unbalance on vertical bearings has recently been found to be effective in producing stable operation of vertical water pumps for use in nuclear power plants. This design procedure is just the opposite of what is desirable for horizontal machines where unbalance induces a synchronous whirling motion. This particular case of vertical bearings is another example of the power of the time-transient solution in real bearing design.

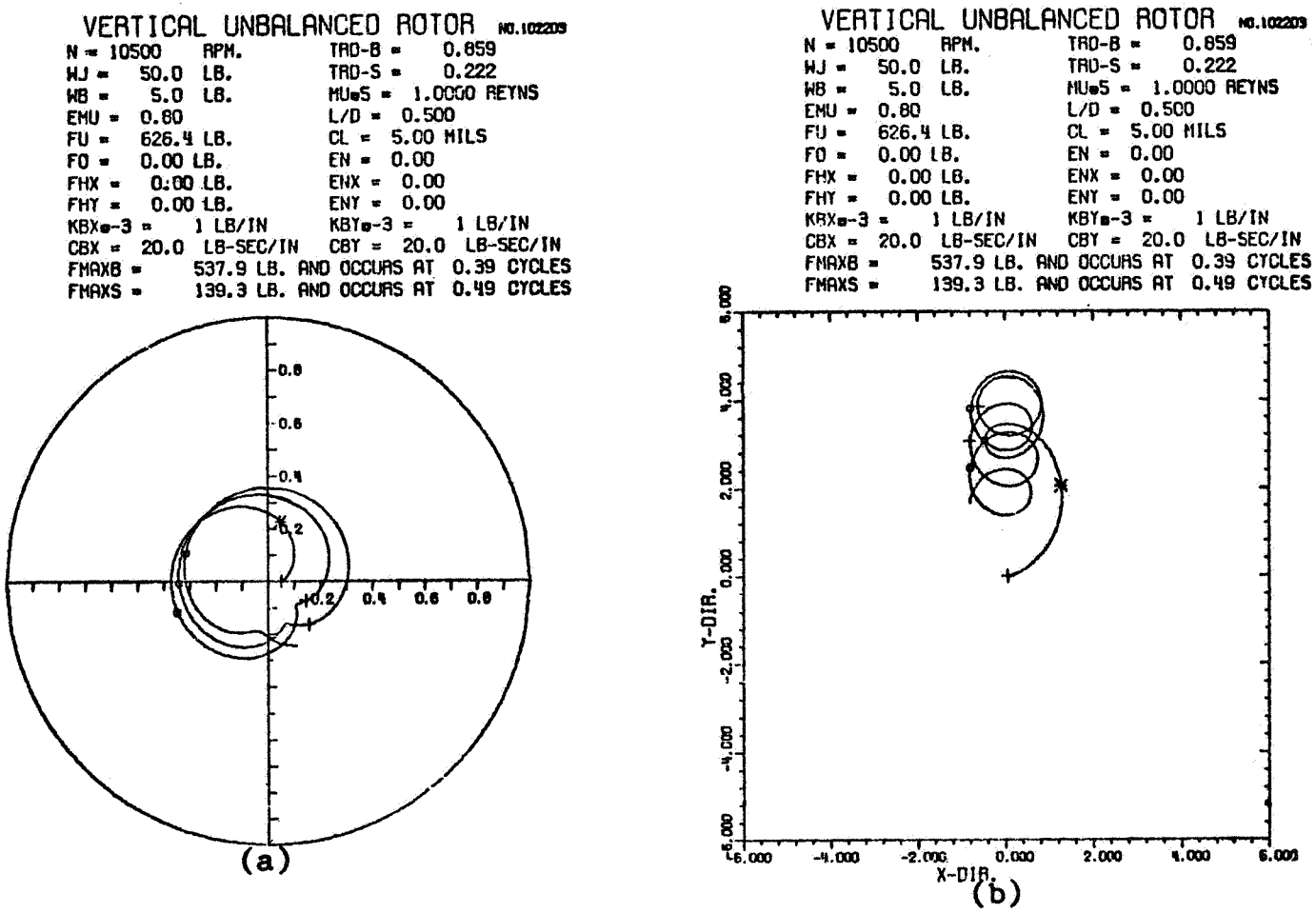

FIG. 4.26(a) VERTICAL JOURNAL UNBALANCE RESPONSE FOR INCREASED UNBALANCE EXCITATION (N=10,500, EMU=0.8)
(b) SUPPORT SYSTEM RESPONSE FOR SIX CYCLES
(KBX=KBY=1,000, CBX=CBY=20)

CHAPTER V

MULTI-MASS FLEXIBLE ROTOR WITH LINEAR SOFT MOUNTED BEARINGS

5.1 Description of the Rotor Model

A rotor shaft supported by two similar bearings can be reduced to the study of motion in a plane if the excitation to the system is symmetrical about the rotor midsection. The continuous rotor mass may be lumped at the shaft center and journal locations as illustrated in Fig. 5.1. This model then allows the effects of cross coupling Q, internal damping C_i, unbalance, and bearing housing flexibility to be studied from a relatively simple mathematical model. The coordinates used to study the response are given in Fig. 5.2. The bearing housing motion is noted as (x_1, y_1), the journal relative motion as (x_j, y_j), and the rotor absolute motion as (x_2, y_2).

The influence of the support flexibility and damping with the journal mass neglected was discussed in Section 1.2 and gives a good basis for understanding the results to be obtained from this analysis.

5.2 Equations of Motion

The system represented in Fig. 5.1 is best described in terms of the shaft stiffness and equivalent mass, k_s and m_2 respectively. If each journal has an equivalent mass m_j and each support has mass m_1, then the equations of motion are easily derived (59) and result in the following equations:

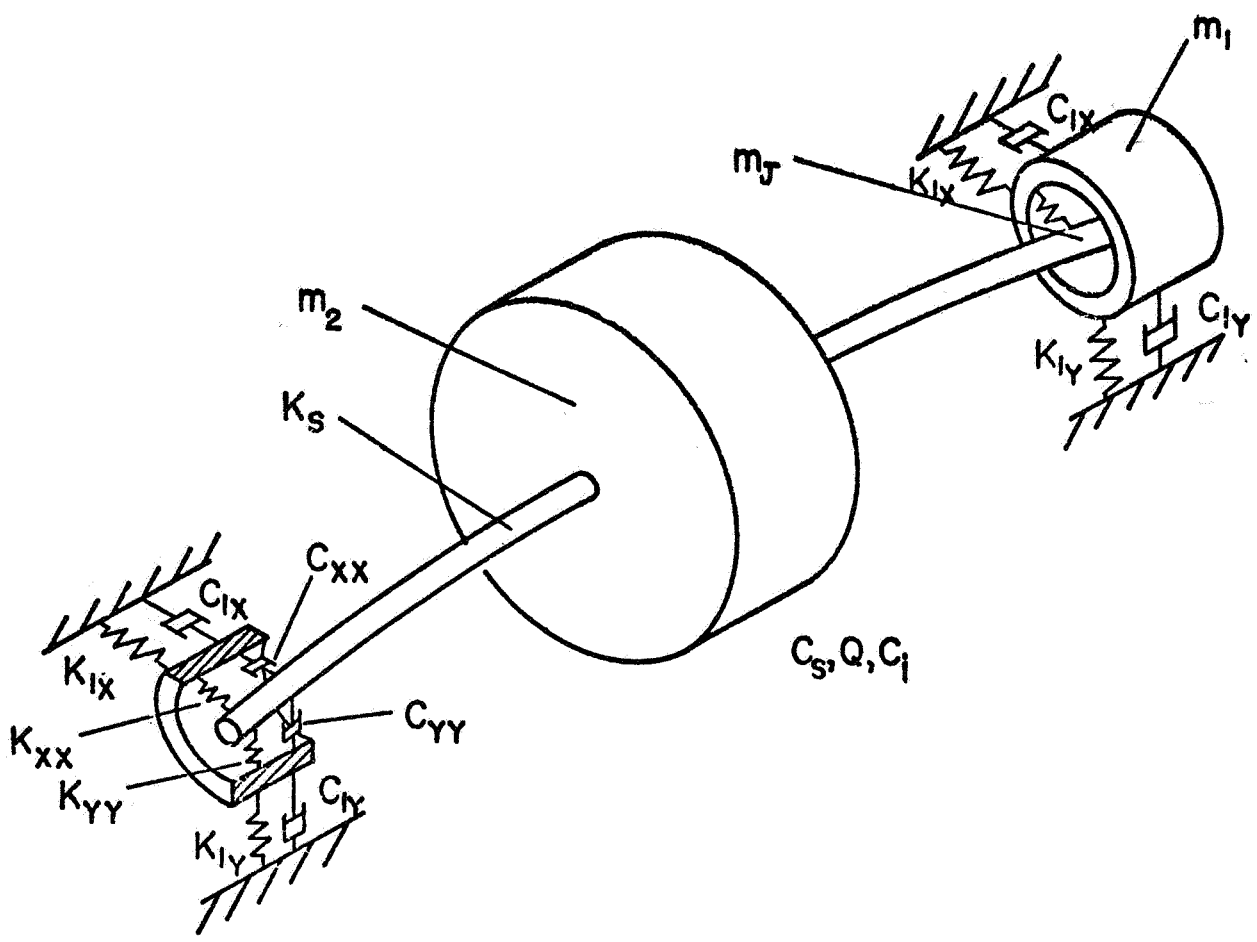

FIG. 5.1 THREE-MASS FLEXIBLE ROTOR HAVING LINEAR DAMPED ELASTIC SUPPORTS

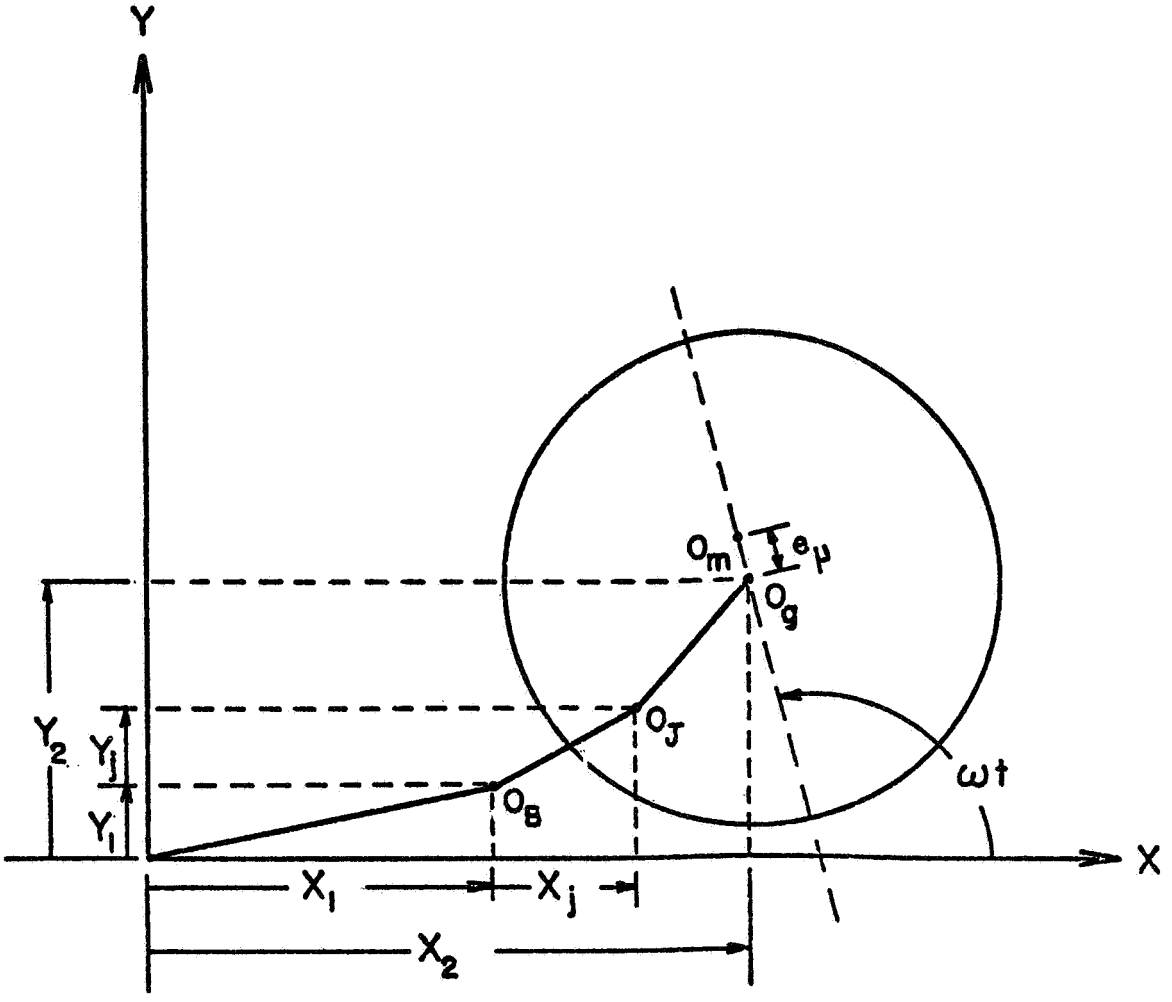

FIG. 5.2 CROSS SECTION OF ROTOR MIDSPAN INDICATING DEFLECTION NOMENCLATURE

Rotor Equations:

$$m_2\ddot{x}_2 + c_s\dot{x}_2 + c_i(\dot{x}_2 - \dot{x}_1 - \dot{x}_j) + k_s(x_2 - x_1 - x_j) + Qy_2 + \omega c_i(y_2 - y_1 - y_j) = m_2 e_\mu \omega^2 \cos(\omega t) \quad [5.1]$$

$$m_2\ddot{y}_2 + c_s\dot{y}_2 + c_i(\dot{y}_2 - \dot{y}_1 - \dot{y}_j) + k_s(y_2 - y_1 - y_j) - Qx_2 - \omega c_i(x_2 - x_1 - x_j) = m_2 e_\mu \omega^2 \sin(\omega t) \quad [5.2]$$

Journal Equations:

$$2m_j(\ddot{x}_1 + \ddot{x}_j) + (c_i + 2c_{xx})\dot{x}_j - c_i(\dot{x}_2 - \dot{x}_1) + (2k_{xx} + k_s)x_j - k_s(x_2 - x_1) - c_i\omega(y_2 - y_1 - y_j) + 2(k_{xy}y_j + c_{xy}\dot{y}_j) = 0 \quad [5.3]$$

$$2m_j(\ddot{y}_1 + \ddot{y}_j) + (c_i + 2c_{yy})\dot{y}_j - c_i(\dot{y}_2 - \dot{y}_j) + (2k_{yy} + k_s)y_j - k_s(y_2 - y_1) + c_i\omega(x_2 - x_1 - x_j) + 2(k_{yx}x_j + c_{yx}\dot{x}_j) = 0 \quad [5.4]$$

Support Equations:

$$2m_1\ddot{x}_1 + 2m_j(\ddot{x}_1 + \ddot{x}_j) + (2c_{1x} + c_i)\dot{x}_1 - c_i(\dot{x}_2 - \dot{x}_j) + (2k_{1x} + k_s)x_1 - k_s(x_2 - x_j) - c_i\omega(y_2 - y_1 - y_j) = 0 \quad [5.5]$$

$$2m_1\ddot{y}_1 + 2m_j(\ddot{y}_1 + \ddot{y}_j) + (2c_{1y} + c_l)\dot{y}_1 - c_l(\dot{y}_2 - \dot{y}_j)$$

$$+ (2k_{1y} + k_s)y_1 - k_s(y_2 - y_j) + c_l\omega(x_2 - x_1 - x_j) = 0 \quad [5.6]$$

The support equations can be reduced to the following form by using Eqs. 5.4-5.5.

$$m_1\ddot{x}_1 + c_{1x}\dot{x}_1 + k_{1x}x_1 - c_{xx}\dot{x}_j - k_{xx}x_j - c_{xy}\dot{y}_j - k_{xy}y_j = 0 \quad [5.7]$$

$$m_1\ddot{y}_1 + c_{1y}\dot{y}_1 + k_{1y}y_1 - c_{yy}\dot{y}_j - k_{yy}y_j - c_{yx}\dot{x}_j - k_{yx}x_j = 0 \quad [5.8]$$

5.3 Steady State Solution

5.3.1 Amplitudes of Motion

The equations of motion of the symmetric three-mass rotor may be solved for the steady-state solution by standard procedures available in the literature (87). If solutions of the following form are assumed,

$$x_2 = A\cos(\omega t) + B\sin(\omega t) \quad [5.9]$$

$$y_2 = C\cos(\omega t) + D\sin(\omega t) \quad [5.10]$$

$$x_j = E\cos(\omega t) + F\sin(\omega t) \quad [5.11]$$

$$y_j = G\cos(\omega t) + H\sin(\omega t) \quad [5.12]$$

$$x_1 = K\cos(\omega t) + L\sin(\omega t) \quad [5.13]$$

$$y_1 = N\cos(\omega t) + P\sin(\omega t) \quad [5.14]$$

the resulting equations will be a 12 x 12 system of equations which may

be represented in matrix notation as shown on the following page.

If the following variables are defined,

$ZZ = m_2\omega$

$ZZ2 = m_2\omega^2$

$Z1 = c_s/ZZ$, $Z2 = c_j/ZZ$, $Z3 = k_s/ZZ2$, $F4 = Q/ZZ2$

$Z5 = m_2/m_j$, $Z6 = (c_j + 2c_{xx})/(2 \times Z2)$, $Z22 = Z2/2$

$Z7 = (2k_{xx} + k_s)/(2 \times ZZ2)$, $Z32 = Z3/2$

$Z8 = (c_j + 2c_{yy})/(2 \times Z2)$, $Z9 = (2k_{yy} + k_s)/(2 \times ZZ2)$

$Z19 = k_{xy}/ZZ2$, $Z20 = c_{xy}/ZZ$, $Z21 = k_{yx}/ZZ2$, $Z23 = c_{yx}/ZZ$

$Z10 = m_2/m_1$, $Z11 = k_{1x}/ZZ2$, $Z12 = c_{1x}/ZZ$, $Z13 = k_{xx}/ZZ2$

$Z14 = c_{xx}/ZZ$, $Z15 = k_{1y}/ZZ2$, $Z16 = c_{1y}/ZZ$

$Z17 = k_{yy}/ZZ2$, $Z18 = c_{yy}/ZZ$

then the elements of the matrix may be obtained from the listing of the computer program SSFROLS in Appendix E as the array A[I,J]. The maximum amplitudes in the x and y coordinate directions are then given by

$$|x_2| = X_2 = \sqrt{A^2 + B^2} \qquad [5.15]$$

$$|y_2| = Y_2 = \sqrt{C^2 + D^2} \qquad [5.16]$$

with similar equations for the journal and support equations.

5.3.2 Phase Angles for Elliptic Orbits

If a particular motion is described by the equations:

$$x = A\cos(\omega t) + B\sin(\omega t) \qquad [5.17]$$

$$y = C\cos(\omega t) + D\sin(\omega t) \qquad [5.18]$$

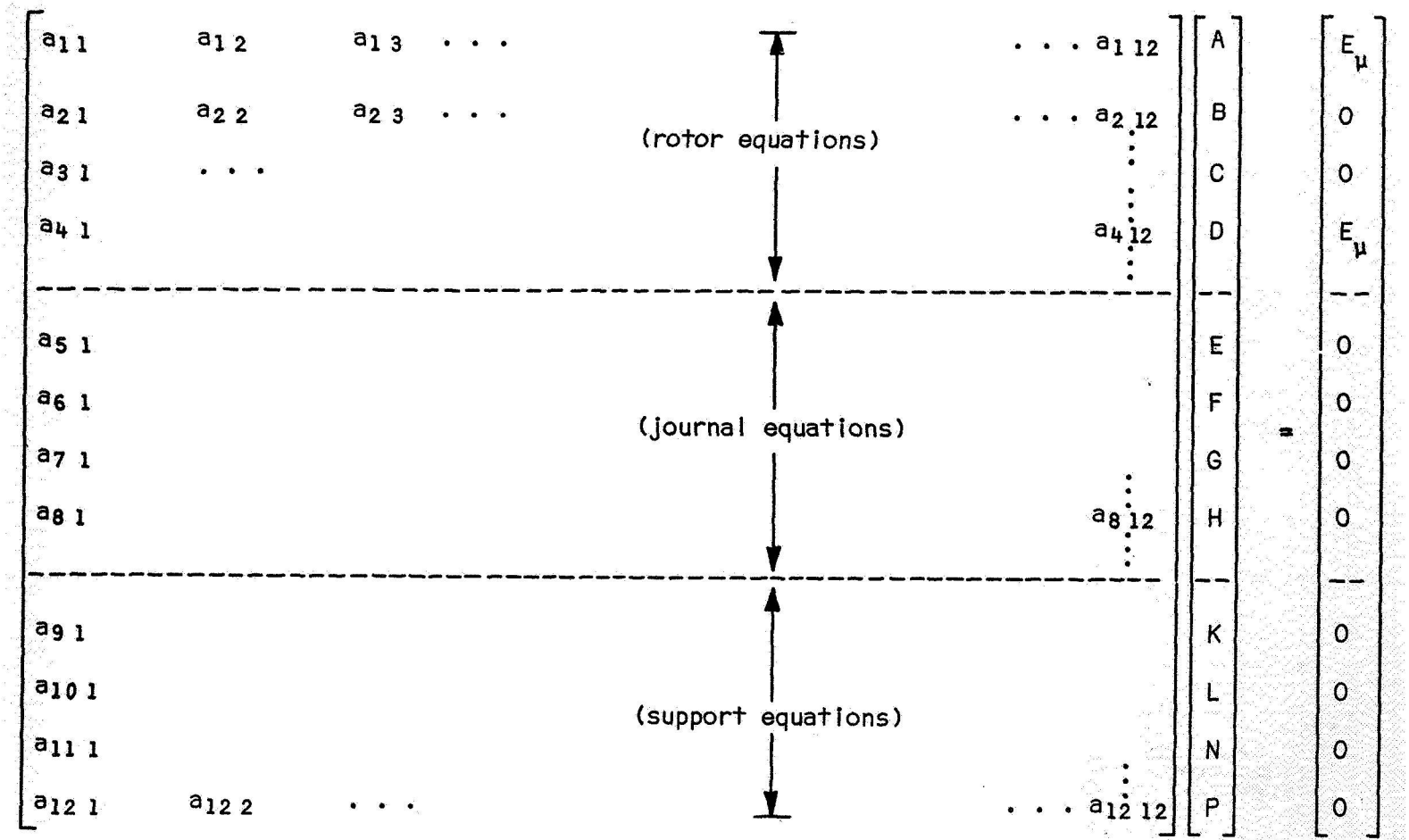
(rotor equations)
(journal equations)
(support equations)

then the resulting motion is given (87) by the major and minor ellipse semi-axis, a and b, and angle of inclination, θ, as shown in Fig. 5.3, where

$$a = \sqrt{\tfrac{1}{2}\eta + \tfrac{1}{2}\sqrt{\eta^2 - 4\beta^2}} \qquad [5.19]$$

$$b = \sqrt{\tfrac{1}{2}\eta - \tfrac{1}{2}\sqrt{\eta^2 - 4\beta^2}} \qquad [5.20]$$

with

$$\eta = A^2 + B^2 + C^2 + D^2$$

$$\beta = AD - BC$$

and

$$\theta = \tfrac{1}{2}\arctan(2\xi/\gamma) \qquad [5.21]$$

where

$$\gamma = A^2 + B^2 - C^2 - D^2$$

$$\xi = AC + BD$$

These equations may be applied to the rotor, journal, and support displacements to describe the motion. An alternate representation is to write the x,y components of motion as

$$x = X\cos(\omega t - \beta_x) \qquad [5.22]$$

$$y = Y\sin(\omega t - \beta_y') = Y\cos(\omega t - \beta_y) \qquad [5.23]$$

These amplitudes and phase angles can be obtained from experimental results as indicated in Fig. 5.4 if the direction of whirl can be determined. The phase angles are dependent on whether the whirl is

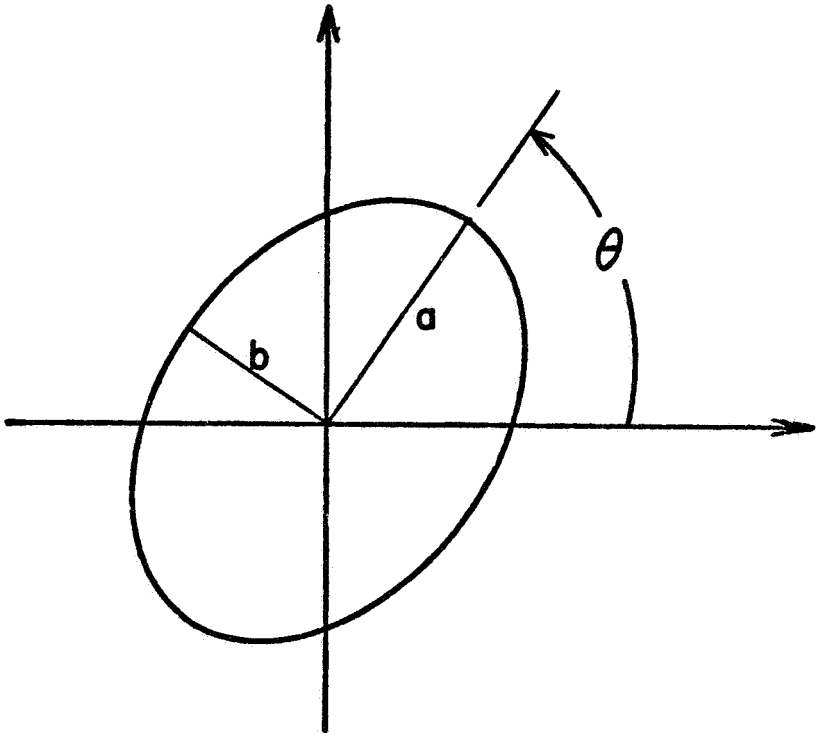

FIG. 5.3 ELLIPTIC ORBIT SHOWING ELLIPSE ANGLE Θ, MAJOR SEMI-AXIS a, AND MINOR SEMI-AXIS b

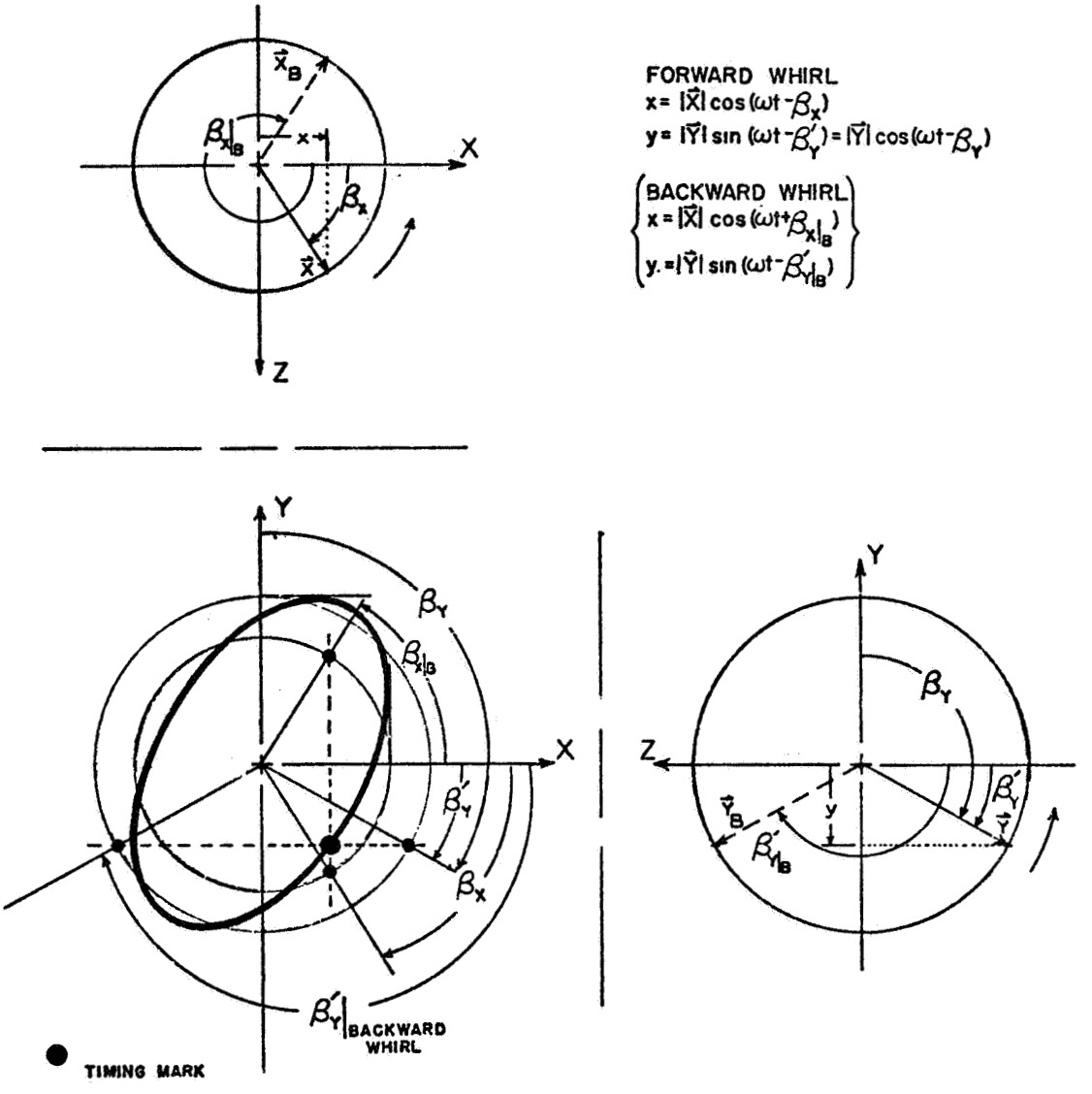

FIG. 5.4 CONSTRUCTION FOR OBTAINING CIRCULAR PHASE ANGLES FROM ELLIPTIC WHIRL ORBITS

forward or backward. If whirl direction is known, then the amplitudes and phase angles are easily measured with a compass, straight edge, and protractor as shown in Fig. 5.4. The inverse problem of trying to determine the unbalance level using an orbit trace from an oscilloscope requires that these phase angles be determined for an orbit that is usually noncircular. Computer codes have been developed (88) which will calculate unbalance correction if given amplitudes and phase angles for a coordinate direction in two planes.

5.3.3 Forces Transmitted

The forces to the bearings and support system can be found with ease once the bearing and support amplitudes are computed. The force to the bearing is expressed as:

$$\vec{F}_{Bearing} = (k_{xx}x_j + c_{xx}\dot{x}_j + k_{xy}y_j + c_{xy}\dot{y}_j)\vec{i} + (k_{yy}y_j + c_{yy}\dot{y}_j + k_{yx}x + c_{yx}\dot{x})\vec{j} \qquad [5.24]$$

If the following variables are defined (corresponding to computer code):

$$Z19 = k_{xy}/(m_2\omega^2)$$
$$Z20 = c_{xy}/(m_2\omega)$$
$$Z21 = k_{yx}/(m_2\omega^2)$$
$$Z23 = c_{yx}/(m_2\omega)$$

then the dimensionless force expression is

$$\vec{F}_B = \vec{F}_{Bearing}/m_2\omega^2 = (Z13 \cdot x_j + Z14 \cdot \dot{x}_j + Z19 \cdot y_j + Z20 \cdot \dot{y}_j)\vec{i} + (Z17 \cdot y_j + Z18 \cdot \dot{y}_j + Z21 \cdot x_j + Z23 \cdot \dot{x}_j)\vec{j} \qquad [5.25]$$

This can also be expressed by the component forces in terms of the amplitudes of the formulation of page 147/

$$F_{BX} = (Z13 \cdot E + Z14 \cdot F + Z19 \cdot G + Z20 \cdot H)\cos(\omega t) + (Z13 \cdot F - Z14 \cdot E + Z19 \cdot H - Z20 \cdot G)\sin(\omega t) \quad [5.26]$$

$$F_{BY} = (Z17 \cdot G + Z18 \cdot H + Z21 \cdot E + Z23 \cdot F)\cos(\omega t) + (Z17 \cdot H - Z18 \cdot G + Z21 \cdot F - Z23 \cdot E)\sin(\omega t) \quad [5.27]$$

or

$$F_{BX} = F_{BA}\cos(T) + F_{BB}\sin(T) \quad [5.28]$$

$$F_{BY} = F_{BC}\cos(T) + F_{BD}\sin(T) \quad [5.29]$$

where

$$|F_{BX}| = \sqrt{F_{BA}^2 + F_{BB}^2} \quad [5.30]$$

$$|F_{BY}| = \sqrt{F_{BC}^2 + F_{BD}^2} \quad [5.31]$$

Hence,

$$\eta_B = F_{BA}^2 + F_{BB}^2 + F_{BC}^2 + F_{BD}^2 \; ; \quad \beta_B = F_{BA}F_{BD} - F_{BB}F_{BC}$$

$$\gamma_B = F_{BA}^2 + F_{BB}^2 - (F_{BC}^2 + F_{BD}^2) \; ; \quad \xi_B = F_{BA}F_{BC} + F_{BB}F_{BD}$$

and the major and minor semi-axis can be found by equations similar to the equations for amplitudes of motion.

The support forces may be found by defining the following variables.

$$\frac{k_{1x}}{m_2\omega^2} = Z11, \quad \frac{c_{1x}}{m_2\omega} = Z12, \quad \frac{k_{1y}}{m_2\omega^2} = Z15, \quad \frac{c_{1y}}{m_2\omega} = Z16$$

$$\vec{F}_S = (Z11 \cdot x_1 + Z12 \cdot \dot{x}_1)\vec{i} + (Z15 \cdot y_1 + Z16 \cdot \dot{y}_1)\vec{j} \qquad [5.32]$$

$$F_{SX} = (Z11 \cdot K + Z12 \cdot L)\cos\omega t + (Z11 \cdot L - Z12 \cdot K)\sin(\omega t)$$

$$= F_{SA}\cos\omega t + F_{SB}\sin\omega t \qquad [5.33]$$

$$F_{SY} = (Z15 \cdot N + Z16 \cdot P)\cos\omega t + (Z15 \cdot P - Z16 \cdot N)\sin(\omega t)$$

$$= F_{SC}\cos\omega t + F_{SD}\sin\omega t \qquad [5.34]$$

Hence,

$$\eta_S = F_{SA}^2 + F_{SB}^2 + F_{SC}^2 + F_{SD}^2; \quad \beta_S = F_{SA}F_{SD} - F_{SB}F_{SC}$$

$$\gamma_S = F_{SA}^2 + F_{SB}^2 - (F_{SC}^2 + F_{SD}^2); \quad \xi_S = F_{SA}F_{SC} + F_{SB}F_{SD}$$

and the solution may be obtained in terms of the elliptic characteristics as before.

The previous equations for forces give expressions which have units of length. A transmissibility may be defined as the force divided by the unbalance loading for a rigid rotor. Then

$$TRB = a_{FB} \times 2/E_\mu = \frac{\text{maximum force to bearing}}{\frac{1}{2}\text{ unbalance load}} \qquad [5.35]$$

where

a_{FB} = major semi-axis for the force expression.

Likewise

$$TRS = a_{FS} \times 2/E_{\mu} \qquad [5.36]$$

For a linear system the dead weight component may be removed from the solutions without effecting the resulting transmissibility solutions. It must be remembered that the system weight must be added to the above forces to give the true loading values.

5.4 Transient Analysis

5.4.1 Equations for Transient Solution

The equations of motion as presented in Section 5.3.1 are easily solved in terms of acceleration. The linear equations may then be solved for the time-transient solution by integration using any of several standard procedures available for digital computer simulation. The program SMFROLS developed for the transient solution is given in Appendix E. Since the equations are linear the solution is obtained very quickly as compared to an analysis including nonlinear fluid-film bearings.

The solution may be obtained in terms of mils and dimensionless time (ωt) by the following transformation. Let

$$X = x \times 1000 \; ; \; \dot{X} = \dot{x} \times 1000/\omega \quad \text{where} \quad \dot{X} = \frac{d(1000x)}{dT}, \; T = \omega t$$

$$\ddot{X} = \frac{1}{\omega^2} \times \ddot{x} \times 1000 \text{ or } \ddot{X} = \frac{d^2(1000x)}{dT^2}$$

with similar expressions for the y-coordinate variables. Then the equations are:

$$\ddot{X}_2 = (e_\mu \times 10^3)\cos(T) - \left(\frac{C_s}{m_2\omega}\right)\dot{X}_2 - \left(\frac{C_i}{m_2\omega}\right)(\dot{X}_2 - \dot{X}_1 - \dot{X}_j)$$

$$- \left(\frac{K_s}{m_2\omega^2}\right)(X_2 - X_1 - X_j) - \left(\frac{Q}{m_2\omega^2}\right)Y_2 - \left(\frac{C_i}{m_2\omega}\right)(Y_2 - Y_1 - Y_j) \quad [5.37]$$

$$\ddot{Y}_2 = (e_\mu \times 10^3)\sin(T) - \left(\frac{C_s}{m_2\omega}\right)\dot{Y}_2 - \left(\frac{C_i}{m_2\omega}\right)(\dot{Y}_2 - \dot{Y}_1 - \dot{Y}_j)$$

$$- \left(\frac{K_s}{m_2\omega^2}\right)(Y_2 - Y_1 - Y_j) + \left(\frac{Q}{m_2\omega^2}\right)(X_2) + \left(\frac{C_i}{m_2\omega}\right)(X_2 - X_1 - X_j) \quad [5.38]$$

$$\ddot{X}_j = -\ddot{X}_1 - \left(\frac{m_2}{m_j}\right)\left\{\left(\frac{C_i + 2C_{xx}}{2m_2\omega}\right)\dot{X}_j - \left(\frac{C_i}{2m_2\omega}\right)(\dot{X}_2 - \dot{X}_1)\right.$$

$$+ \left(\frac{2K_{xx} + K_s}{2m_2\omega^2}\right)X_j - \left(\frac{K_s}{2m_2\omega^2}\right)(X_2 - X_1) - \left(\frac{C_i}{2m_2\omega}\right)(Y_2 - Y_1 - Y_j)$$

$$\left. + \left(\frac{K_{xy}}{m_2\omega^2}\right)Y_j + \left(\frac{C_{xy}}{m_2\omega}\right)\dot{Y}_j\right\} \quad [5.39]$$

$$\ddot{Y}_j = -\ddot{Y}_1 - \left(\frac{m_2}{m_j}\right)\left\{\left(\frac{C_i + 2C_{yy}}{2m_2\omega}\right)\dot{Y}_j - \left(\frac{C_i}{2m_2\omega}\right)(\dot{Y}_2 - \dot{Y}_1)\right.$$

$$+ \left(\frac{2K_{yy} + K_s}{2m_2\omega^2}\right)Y_j - \left(\frac{K_s}{2m_2\omega^2}\right)(Y_2 - Y_1) + \left(\frac{C_i}{2m_2\omega}\right)(X_2 - X_1 - X_j)$$

$$\left. + \left(\frac{K_{yx}}{m_2\omega^2}\right)X_j + \left(\frac{C_{yx}}{m_2\omega}\right)\dot{X}_j\right\} \quad [5.40]$$

$$\ddot{X}_1 = -\left(\frac{m_2}{m_1}\right)\left\{\left(\frac{K_{1x}}{m_2\omega^2}\right)X_1 + \left(\frac{C_{1x}}{m_2\omega}\right)\dot{X}_1 - \left(\frac{K_{xx}}{m_2\omega^2}\right)X_j - \left(\frac{C_{xx}}{m_2\omega}\right)\dot{X}_j\right.$$

$$\left. - \left(\frac{K_{xy}}{m_2\omega^2}\right)\dot{Y}_j - \left(\frac{C_{xy}}{m_2\omega}\right)\dot{Y}_j\right\} \quad [5.41]$$

$$\ddot{Y}_1 = -\left(\frac{m_2}{m_1}\right)\left\{\left(\frac{K_{1y}}{m_2\omega^2}\right)Y_1 + \left(\frac{C_{1y}}{m_2\omega}\right)\dot{Y}_1 - \left(\frac{K_{yy}}{m_2\omega^2}\right)Y_j - \left(\frac{C_{yy}}{m_2\omega}\right)\dot{Y}_j - \left(\frac{K_{yx}}{m_2\omega^2}\right)\dot{X}_j - \left(\frac{C_{yx}}{m_2\omega}\right)\dot{X}_j\right\} \qquad [5.42]$$

5.4.2 Time Transient Whirl Orbits

Consider the following example rotor system.

Example 5.1

Rotor Weight = W_2 = 675 lb.

Journal Weight = W_j = 312 lb.

Support Weight = W_1 = 50 lb.

Bearing Characteristics:

K_{xx} = 1,287,000 lb/in.

K_{yy} = 1,428,000 lb/in.

C_{xx} = 1,200 lb.-sec./in.

C_{yy} = 1,290 lb.-sec./in.

Support Characteristics:

$K_{1x} = K_{1y}$ = 130,000 lb./in.

$C_{1x} = C_{1y}$ = 150 lb.-sec./in.

The shaft stiffness is 280,000 lb./in. for this example. The anti-symmetrical bearing characteristics given are typical for a rotor of this weight. The critical speeds for rigid support housings are 3630 RPM and 3647 RPM for the x and y coordinate directions respectively. A series of orbits representing steady-state solutions were calculated using the transient solution computer code and the steady-state

starting conditions as calculated by the program SSFROLS. The mark on the orbits represent a timing mark such as that produced by a keyphasor probe detecting a mark on the rotor shaft. Examination of the three orbits (ie., rotor, journal, and support motion) indicate phase angles of approximately 30° at the speed of 1800 RPM (Fig. 5.5). The next series of orbits at 3600 RPM indicate phase shifts of nearly 180° which indicate that the rotor system including the support has passed through its first critical speed (see Fig. 5.6(a),(b),(c)). The last series of steady-state orbits (Fig. 5.7) at 18000 RPM indicate that the absolute rotor motion phase remains at 180°. The journal relative motion phase is approximately 280° while the absolute motion phase is close to 350°. The support motion has a phase shift of 360° at this speed of 18,000 RPM. It is noted that the rotor amplitude is approximately equal to the unbalance eccentricity, EU = e_μ = 5 mils.

The maximum force encountered during the corresponding cycles of motion has been indicated on the previous series of figures. The absolute rotor motion orbit has the unbalance force, FU indicated. The force transmitted to the bearing is indicated on the journal motion orbits as TRDB. The time of the maximum force is indicated in parentheses following the value of TRDB. The maximum force transmitted to the support is likewise indicated on the support motion plots. For reference the TRDB values for 1800, 3600, and 18,000 RPM are 2.88, 0.920, and 0.007 while the TRDS values are 2.984, 1.043, and 0.005 respectively.

If the support system is rigid then the rotor motion for EU = 0.5 mils, CI = 20 lb-sec/in, and N = 16000 RPM is shown in Fig. 5.8(a) for ten cycles of motion and continued for cycles 10 - 20 in Fig. 5.8(b).

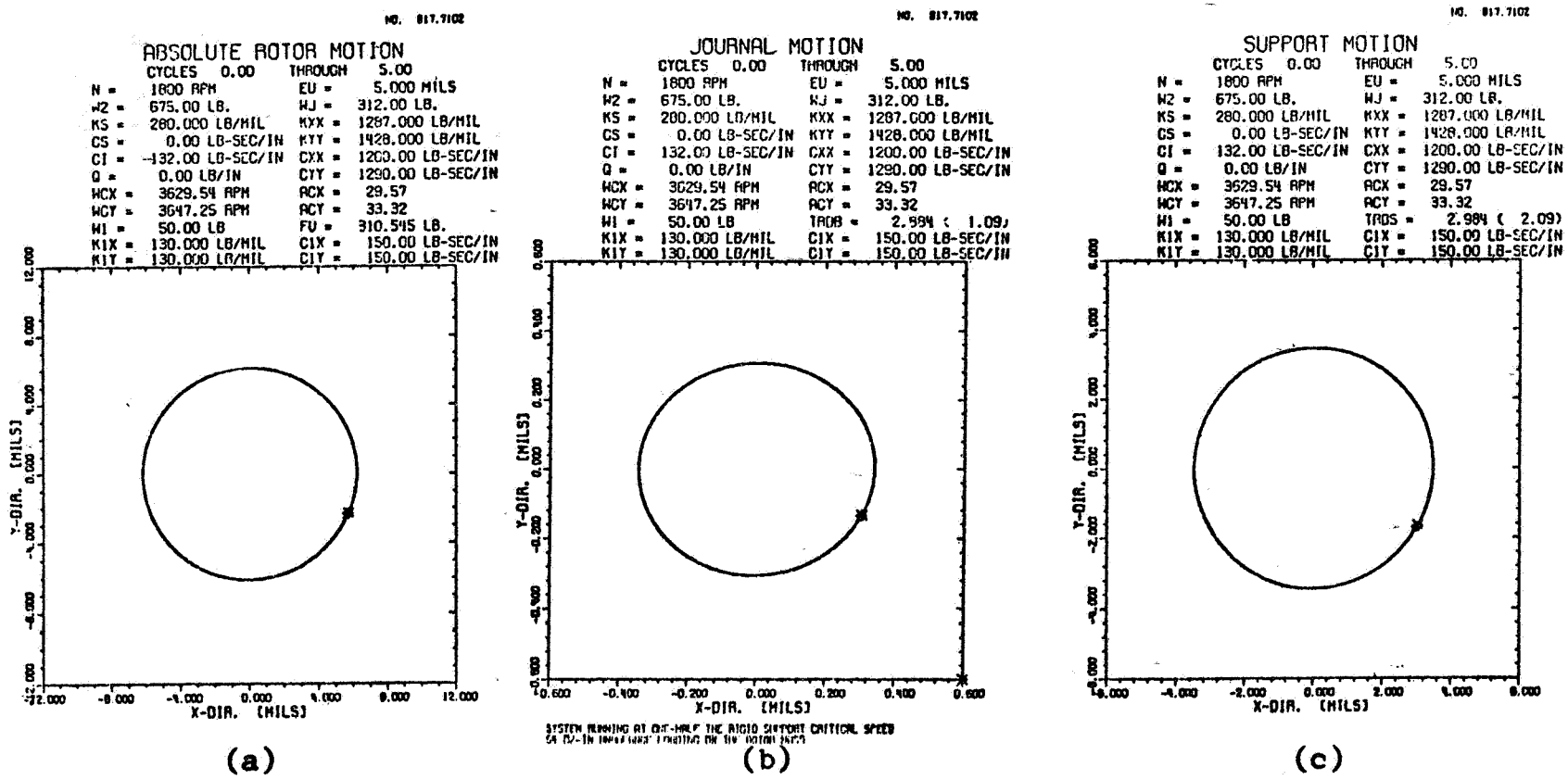

FIG. 5.5(a) STEADY-STATE ORBIT FOR ROTOR OPERATING AT ONE-HALF THE RIGID SUPPORT CRITICAL SPEED
(b) JOURNAL MOTION FOR FIVE CYCLES
(c) SUPPORT MOTION INDICATING A PHASE OF 30°

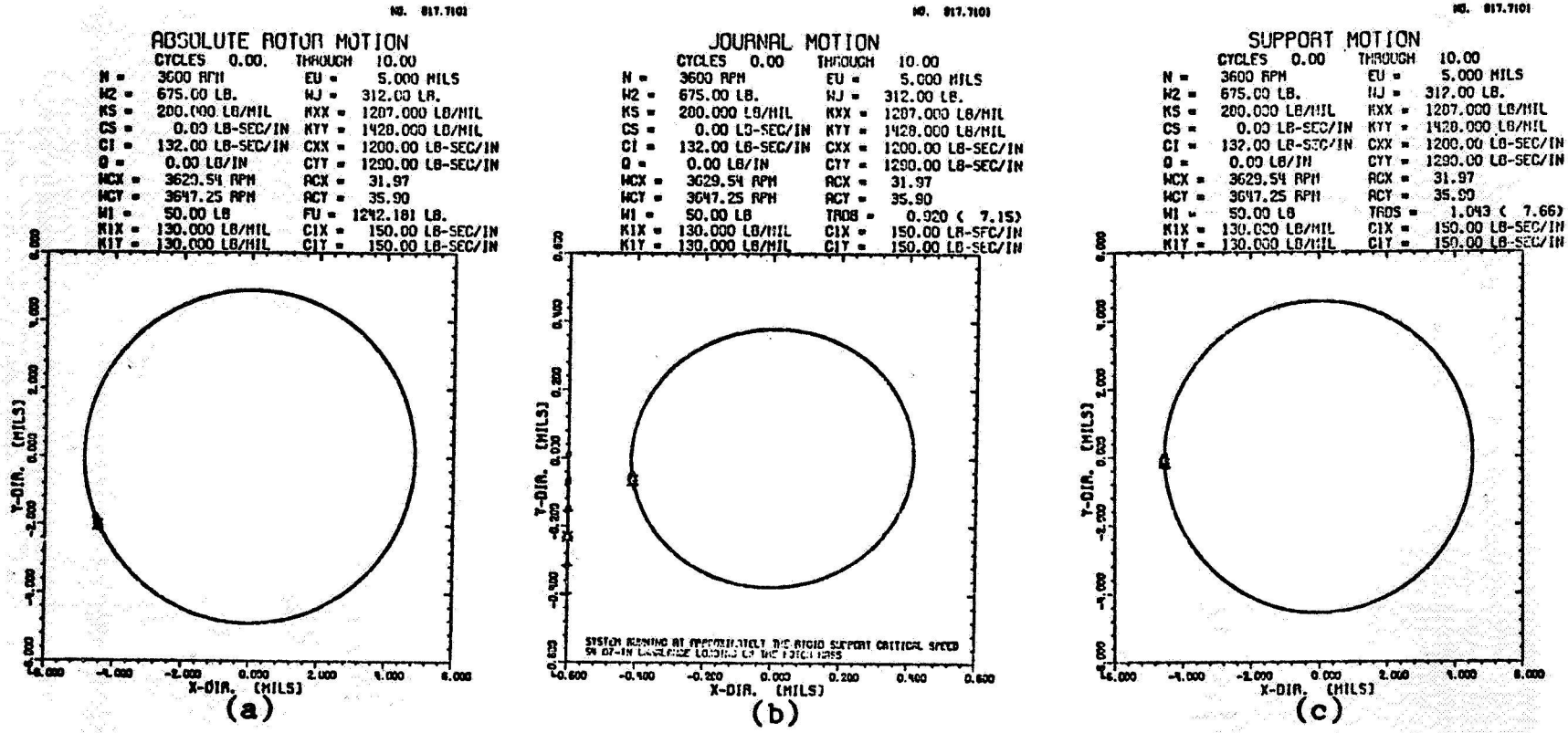

FIG. 5.6(a) STEADY-STATE ORBIT FOR ROTOR OPERATING AT APPROXIMATELY THE RIGID SUPPORT CRITICAL SPEED
(b) JOURNAL STEADY-STATE ORBIT SHOWING PHASE ANGLE APPROACHING 180°
(c) SUPPORT MOTION SHOWING PHASE OF 180°

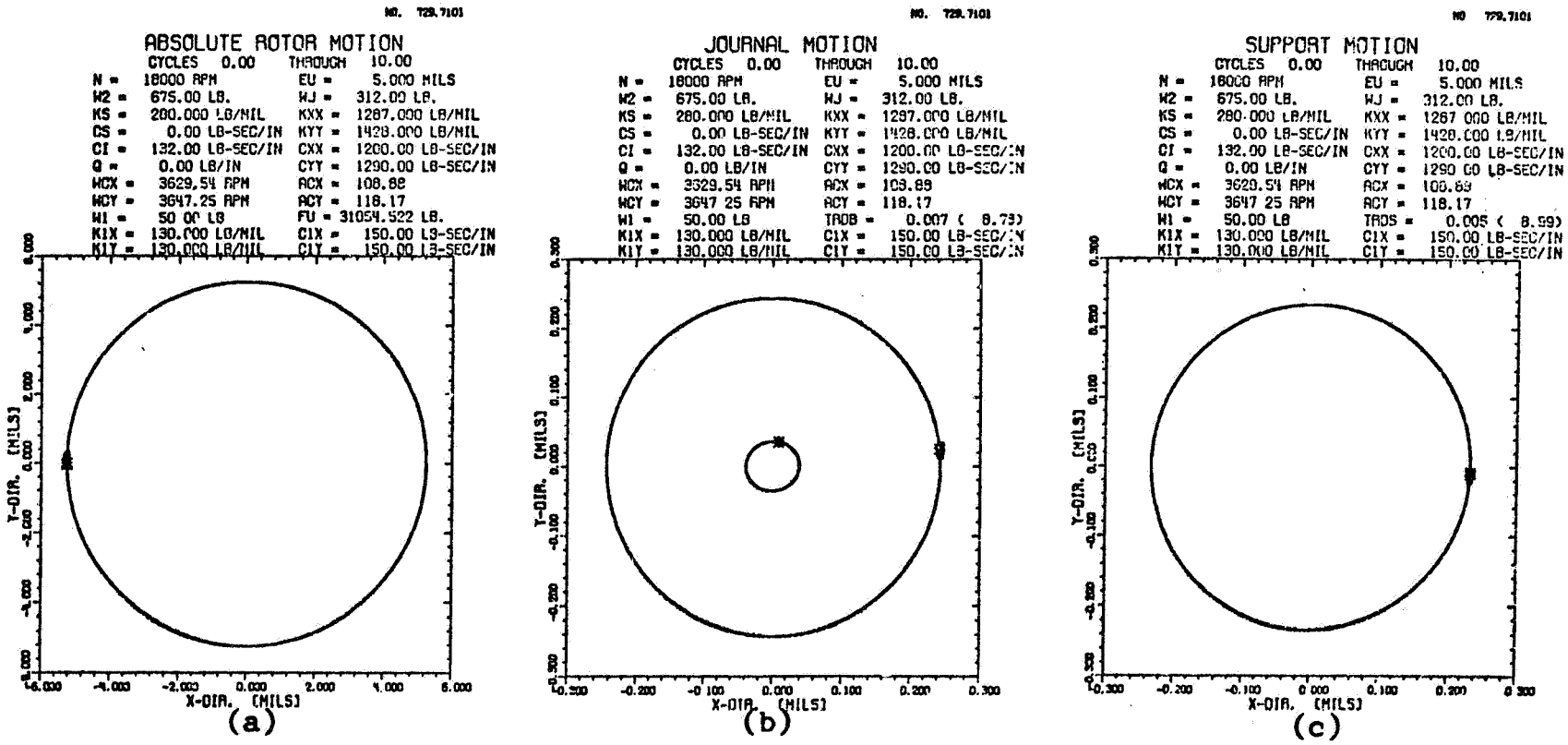

FIG. 5.7(a) STEADY-STATE ORBIT FOR ROTOR OPERATING WELL ABOVE RIGID SUPPORT CRITICAL SPEED (PHASE=180°)
(b) JOURNAL RELATIVE MOTION (PHASE=275°) AND ABSOLUTE MOTION (PHASE=355°)
(c) SUPPORT MOTION SHOWING PHASE OF 360°

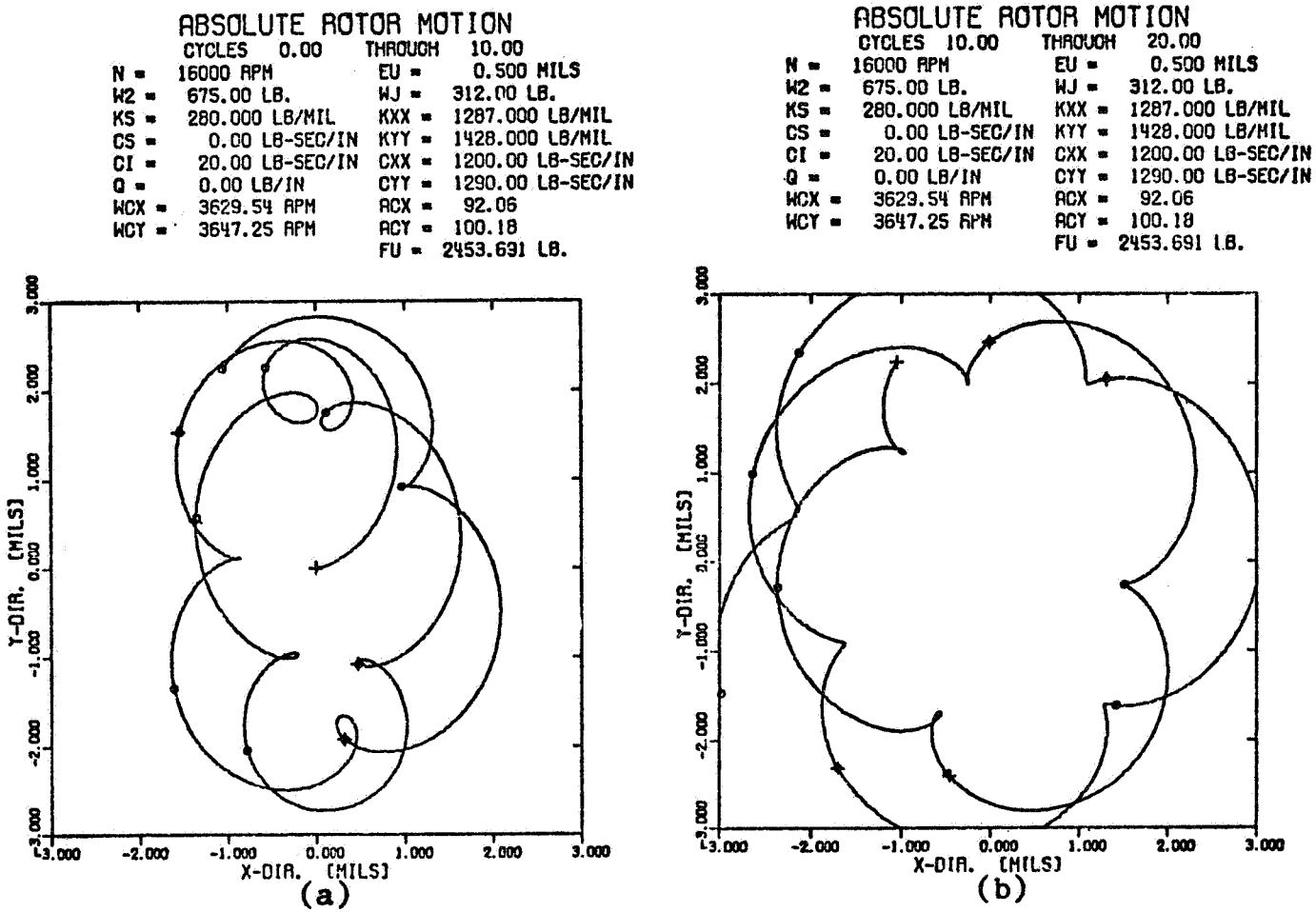

FIG. 5.8(a) RIGID SUPPORT ROTOR MOTION SHOWING UNBALANCE RESPONSE WITH LIGHT INTERNAL DAMPING (CYCLES 0-10)
(b) RIGID SUPPORT ROTOR MOTION CONTINUED FOR AN ADDITIONAL TEN CYCLES

The system is highly unstable under these conditions. The journal motion given in Fig. 5.9(a) and 5.9(b) indicate the same instability. The maximum force for the motion is given as 0.33 of the unbalance loading to the bearing.

If the rotor system in the previous rigid support orbits has a damped flexible support of stiffness 130,000 lb/in and damping of 300.0 lb-sec/in the results are shown in Fig. 5.10. The motion indicates that the support has absorbed the instability and would reduce to circular synchronous motion after the initial transients have decayed.

Fig. 5.11 represent the system motion for a reduced support damping and increased internal damping CI = 132 lb-sec/in. The unbalance level was reduced and the motion was started from steady-state conditions by an initial velocity perturbation on the rotor. The instability is observed to begin in the support system and would eventually drive the absolute rotor motion to an unstable whirl orbit.

The computer code SMFROLS can be used as an additional check on the program MODELJ developed in Chapter II. The same rotor system as Example 5.1 will be used to compare the results of the two programs.

For a rotor speed of 10,000 RPM and an unbalance of 0.500 mils the rotor absolute motion is shown in Fig. 5.12(a) for ten cycles of motion. The unbalance load in 958.73 lb. as indicated on the figure heading. The corresponding journal motion is given in Fig. 5.12(b) where the maximum force transmitted to the bearing support is indicated to be 314 lb. This is calculated from the dynamic transmissibility factor as follows:

$$F_{max} = TRDB \times FU/2 = 0.656 \times 958.473/2.0 = 314 \text{ lb.}$$

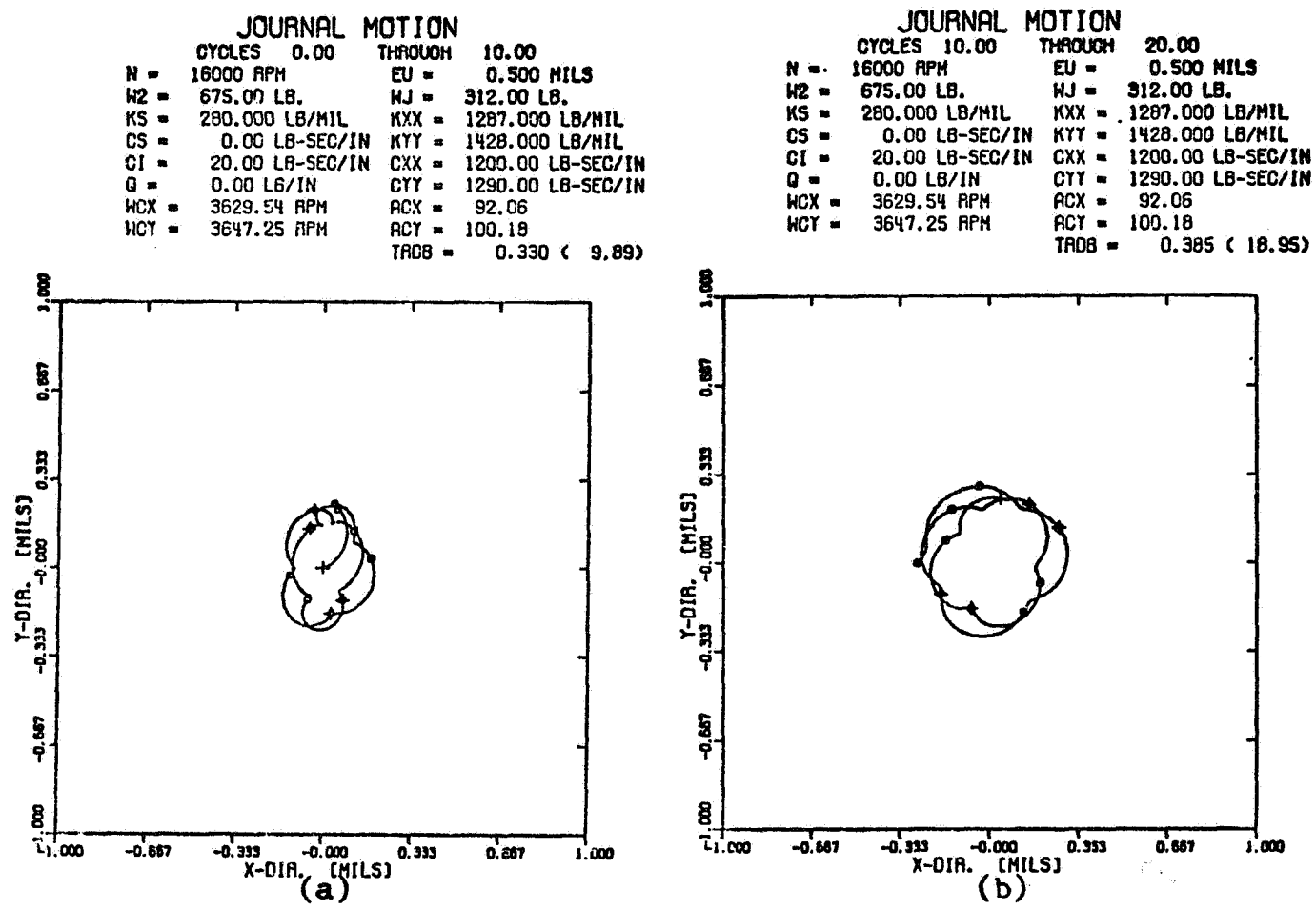

FIG. 5.9(a) JOURNAL MOTION FOR UNBALANCE RESPONSE WITH LIGHT DAMPING AND RIGID SUPPORT SYSTEM
(b) JOURNAL MOTION CONTINUED FOR AN ADDITIONAL TEN CYCLES

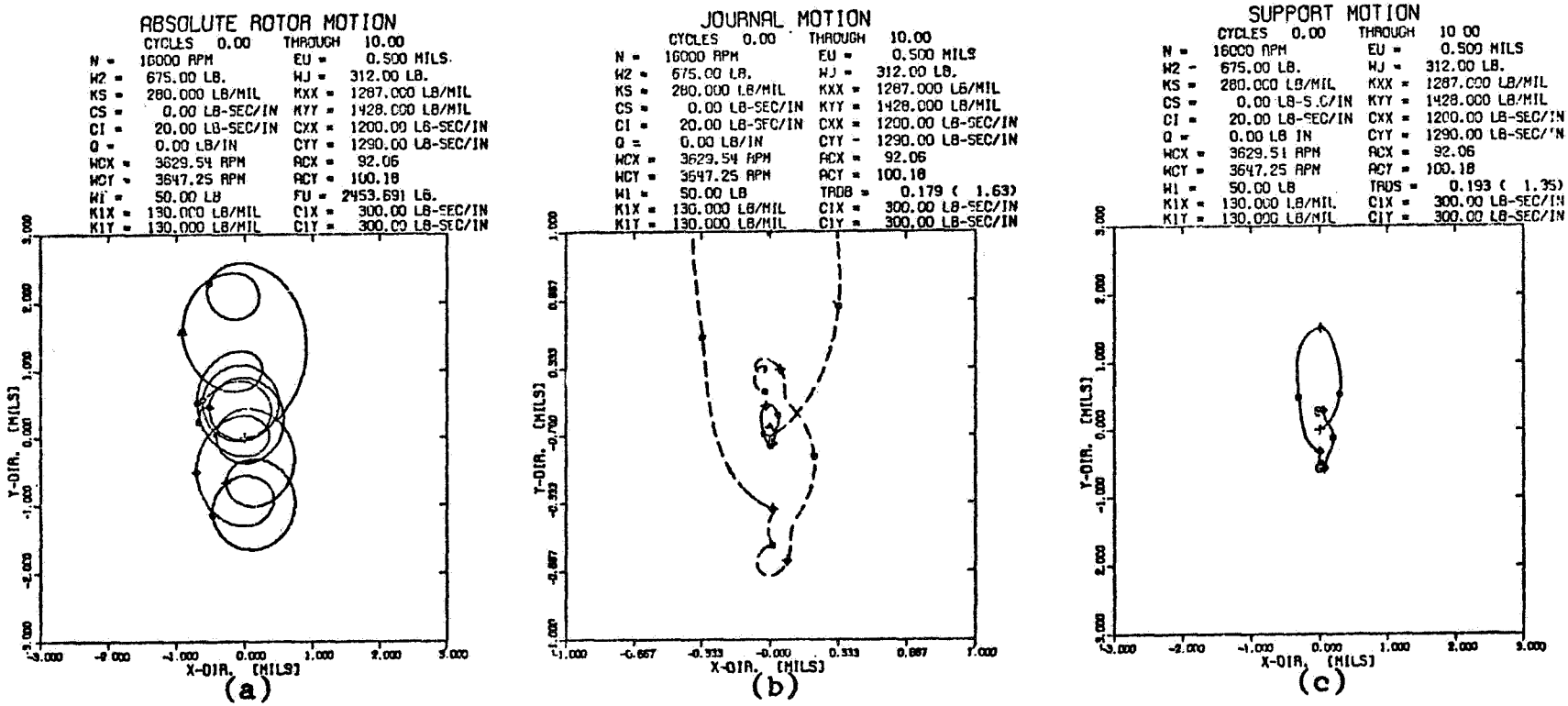

FIG. 5.10(a) ABSOLUTE ROTOR MOTION SHOWING UNBALANCE RESPONSE WITH LIGHT INTERNAL DAMPING AND MOUNTED ON FLEXIBLE, DAMPED SUPPORTS
(b) JOURNAL RELATIVE AND ABSOLUTE RESPONSE
(c) SUPPORT TRANSIENT RESPONSE FOR SUDDENLY APPLIED UNBALANCE LOAD (N=16,000)

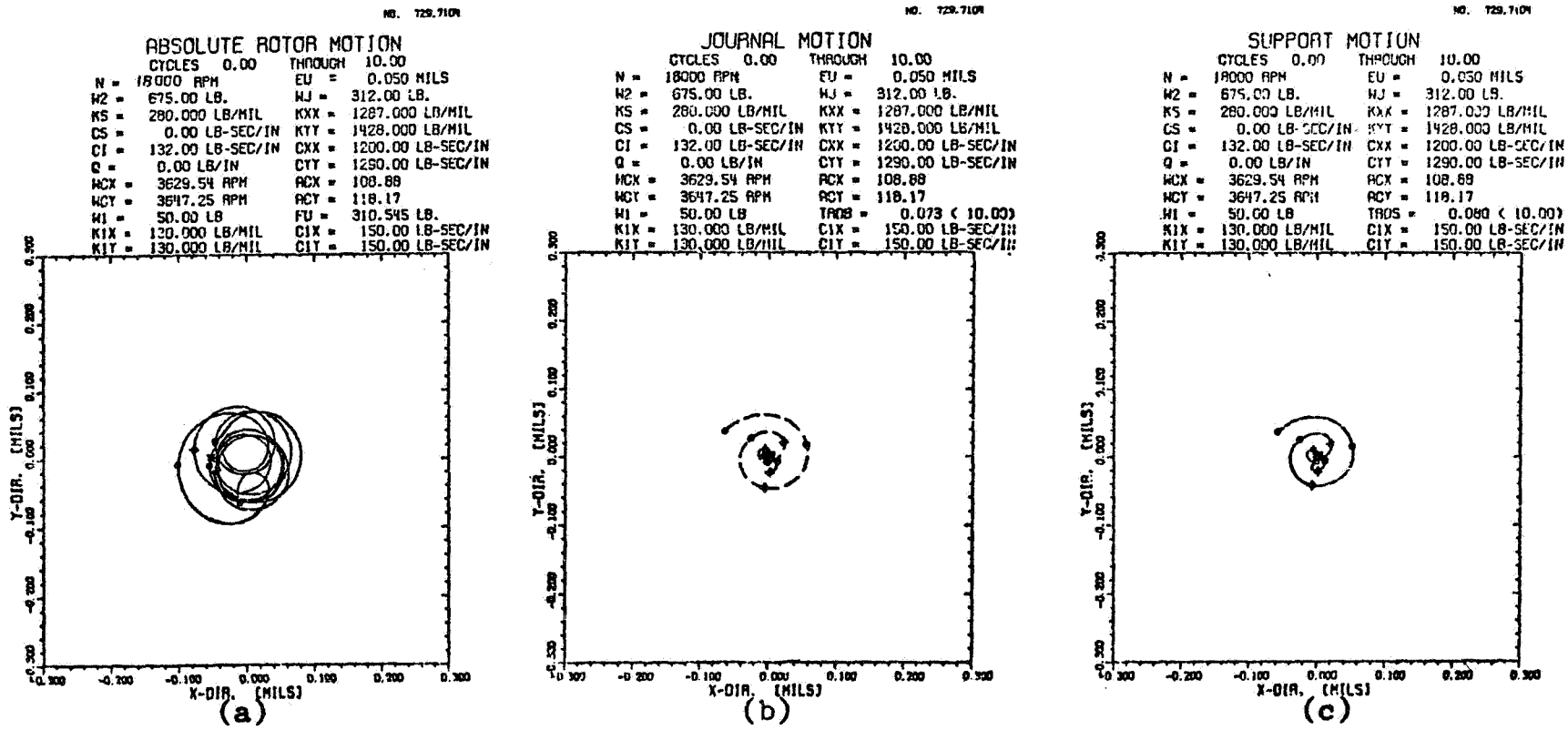

FIG. 5.11(a) ROTOR ABSOLUTE MOTION FROM STEADY-STATE RESPONSE EXCITED BY A 1.1 IMPULSE LOAD
(b) JOURNAL ABSOLUTE MOTION INDICATING UNSTABLE SUPPORT SYSTEM
(c) SUPPORT TRANSIENT RESPONSE TO IMPULSE LOAD ON ROTOR (N=18,000)

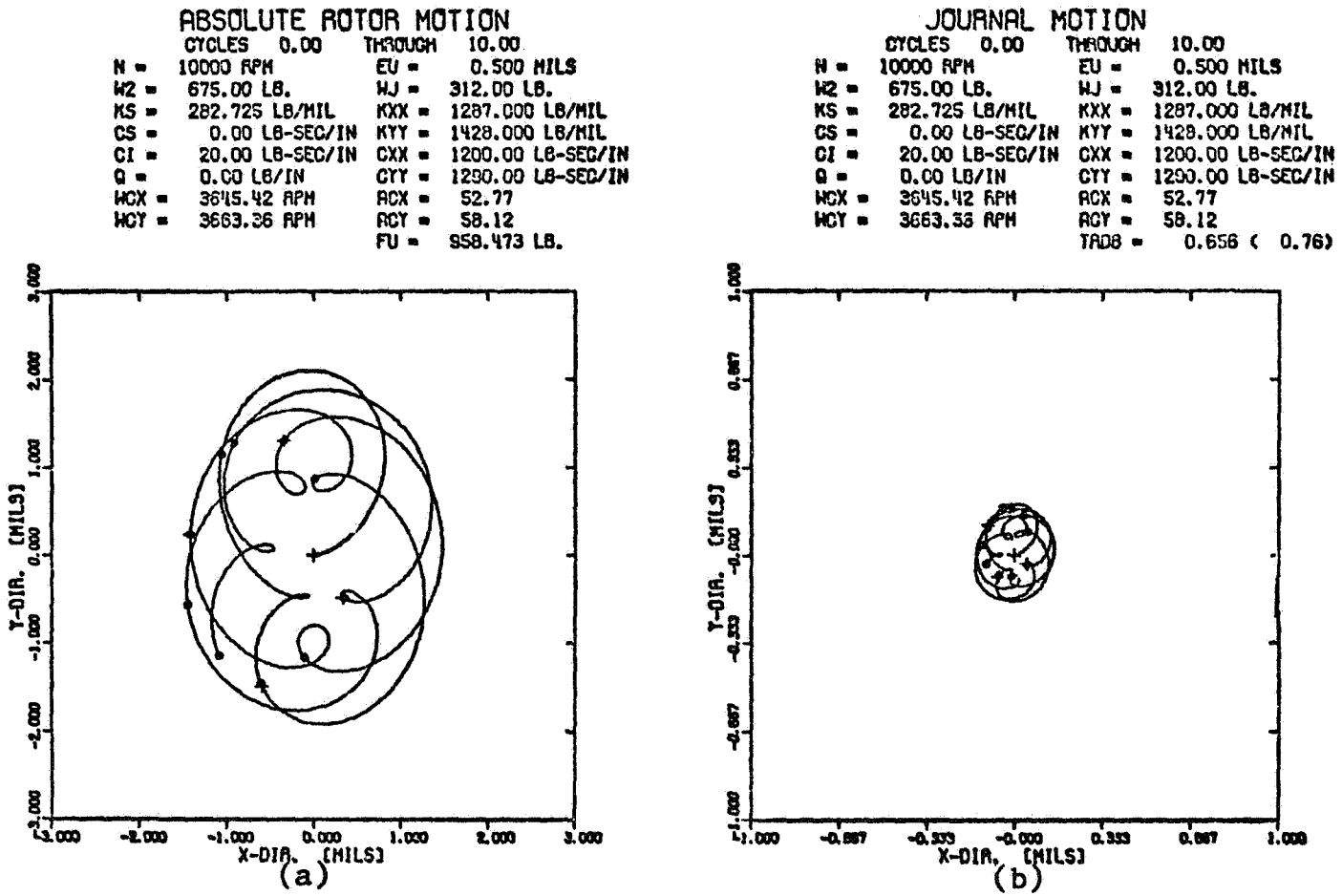

FIG. 5.12(a) ABSOLUTE ROTOR RESPONSE TO SUDDENLY APPLIED UNBALANCE LOAD (RIGID SUPPORT, 5.4OZ-IN UNBALANCE)
(b) JOURNAL TRANSIENT FOR TEN CYCLES (N=10,000)

The force occurs at 0.76 cycles of motion as indicated in parentheses following the TRDB factor.

The same rotor system was programmed for the multi-mass flexible rotor program and the results of the calculated orbits are given in Figs. 5.13(a) and 5.13(b) for five cycles of motion. The orbits are similar to Figs. 5.12(a) and 5.12(b) for the first five cycles of motion. The maximum force to the bearings is predicted by MODELJ to occur during the first cycle of motion and is given as 290 lb. for each bearing (see Table 5.1). This represents an 8% derivation in the two program on the maximum forces calculated. This is due to the fact that the 0.5 mil eccentricity is equivalent to 5.4 oz-in unbalance. The orbits of Figs. 5.13(a) and 5.13(b) were produced from an unbalance level of only 5 oz-in and explains the slight difference in the orbits and forces.

A similar comparison is now made for the flexible, damped support system having support stiffness of 130,000 lb/in and 300.0 lb-sec/in damping. The absolute rotor, journal, and support motion calculated by SMFROLS are given in Figs. 5.14(a), (b), (c). The dashed lines in Fig. 5.14(b) represents the journal absolute motion while the solid line is the relative motion. The maximum bearing force to each bearing is

$$F_{B_{max}} = \text{TRDB} \times \text{FU}/2 = 958.473 \times 0.402/2 = 193 \text{ lb.}$$

The support force is

$$F_{S_{max}} = \text{TRDS} \times \text{FU}/2 = 958.473 \times 0.429/2 = 206 \text{ lb.}$$

The orbits produced by the program MODELJ with unbalance level of 5.4 oz-in. are given in Fig. 5.15 and are in good agreement with the orbits

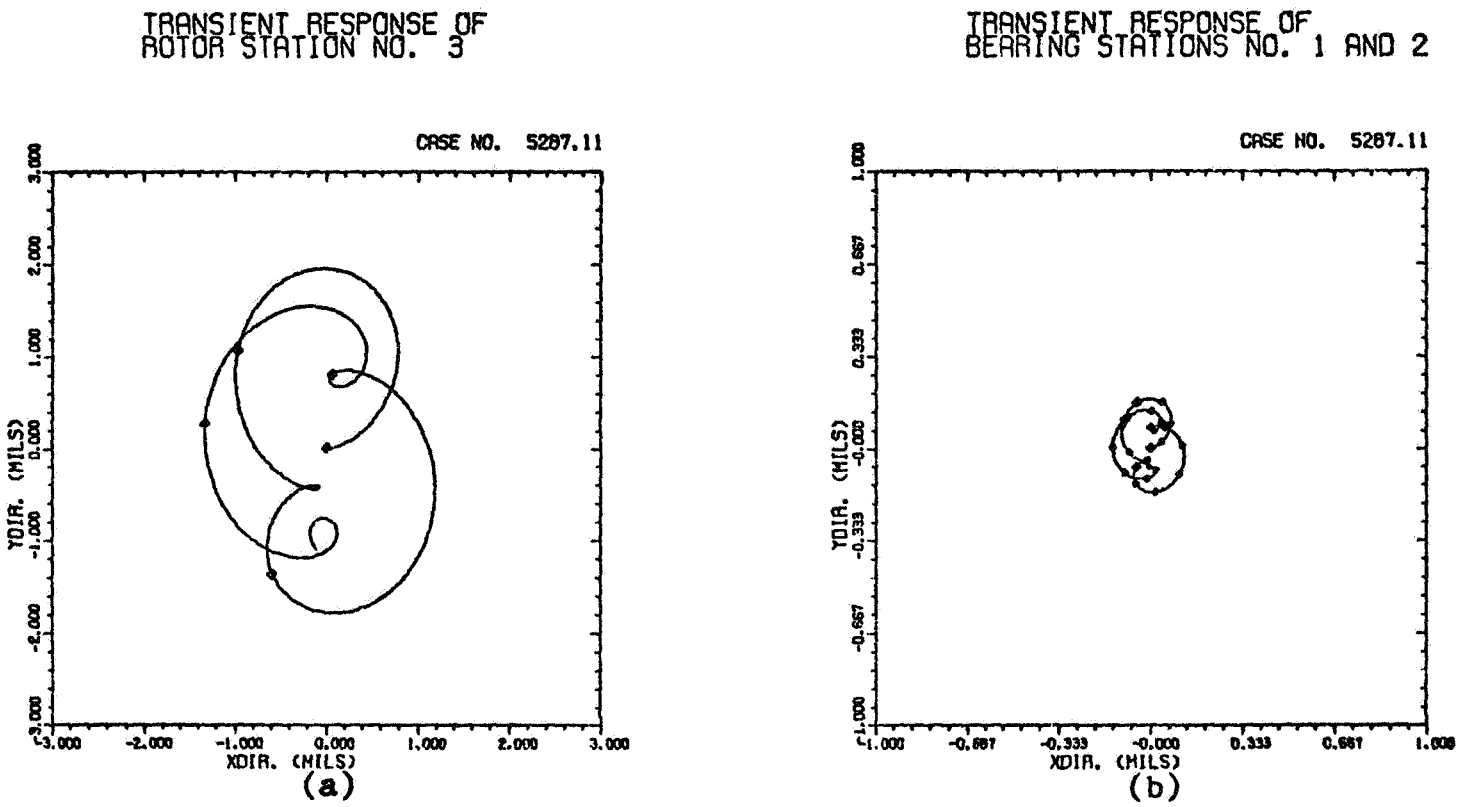

FIG. 5.13(a) TRANSIENT ROTOR RESPONSE FOR FIVE CYCLES BY PROGRAM MODELJ (5OZ-IN UNBALANCE)
(b) JOURNAL TRANSIENT RESPONSE TO IMPACT UNBALANCE LOAD OF 5 OZ-IN ON ROTOR

FLEXIBLE POINT MASS ROTOR TRANSIENT RESPONSE --BY R. GORDON KIRK--

(UNITS ARE IN.-LB.-SEC, UNLESS OTHERWISE SPECIFIED)

CASE NUMBER = 5287.11

ROTOR SHAFT SPECIFICATIONS

ROTOR ACCEL = 0.0 RPM/SEC

SECTION	LENGTH	DIAMETER	YOUNGS MODULUS	PRODUCT OF E*I	INSIDE DIAMETER
1	1.00	4.00	3.000E 07	3.770E 08	0.00
2	19.00	4.00	3.000E 07	3.770E 08	0.00
3	19.00	4.00	3.000E 07	3.770E 08	0.00
4	1.00	4.00	3.000E 07	3.770E 08	0.00

BEARING NO. 1 IS 0.00 INCHES FROM THE LEFT END, STATION NO. 1

BEARING NO. 2 IS 40.00 INCHES FROM THE LEFT END, STATION NO. 5

BEARING SPAN IS 40.00 INCHES

APPROXIMATED ROTOR SPECIFICATIONS

STATION	LENGTH FROM END	WEIGHT	MASS	STIFFNESS	DAMPING	INT. DAMP	STIFF-0	EXT. WT	EMU	PMI
3	20.00	675.014	1.7487	0.0	0.000	20.000	0.0	675.00	5.00	0.0

(EMU GIVEN IN OZ-IN UNITS)

(ALL OTHER STATIONS EXCEPT THE BEARINGS HAVE ZERO MASS)

TOTAL LENGTH OF ROTOR = 40.000 IN.
ACTUAL WEIGHT OF ROTOR = 1439.251 LBS.
TOTAL WEIGHT OF APPROXIMATE ROTOR = 1297.014 LBS.

BEARING STATION SPECIFICATIONS

NO.	STATION	LENGTH FROM END	WEIGHT	MASS	EXTERNAL WEIGHT	STIF-X	STIF-Y	DAMP-X	DAMP-Y
1	1	0.00	312.778	0.8103	311.000	1.2870E 06	1.4280E 06	1.2000E 03	1.2900E 03
2	5	40.00	312.778	0.8103	311.000	1.2870E 06	1.4280E 06	1.2000E 03	1.2900E 03

SEGMENT	N-INIT. (RPM)	ACCEL. (RPM/SEC)	N-FINAL (RPM)	T-FINAL (RAD)	FMAXB-1 LB*10-3	FMAXB-2 LB*10-3	FMAXS-1 LB*10-3	FMAXS-2 LB*10-3
1	10000.0	0.0	10000.0	6.3	0.29	0.29		
2	10000.0	0.0	10000.0	12.6	0.24	0.24		
3	10000.0	0.0	10000.0	18.8	0.26	0.26		
4	10000.0	0.0	10000.0	25.1	0.23	0.23		
5	10000.0	0.0	10000.0	31.4	0.22	0.22		

TABLE 5.1 ROTOR SPECIFICATIONS FOR UNBALANCE RESPONSE ON RIGID SUPPORT BEARINGS INDICATING MAXIMUM FORCES TO BEARING HOUSING

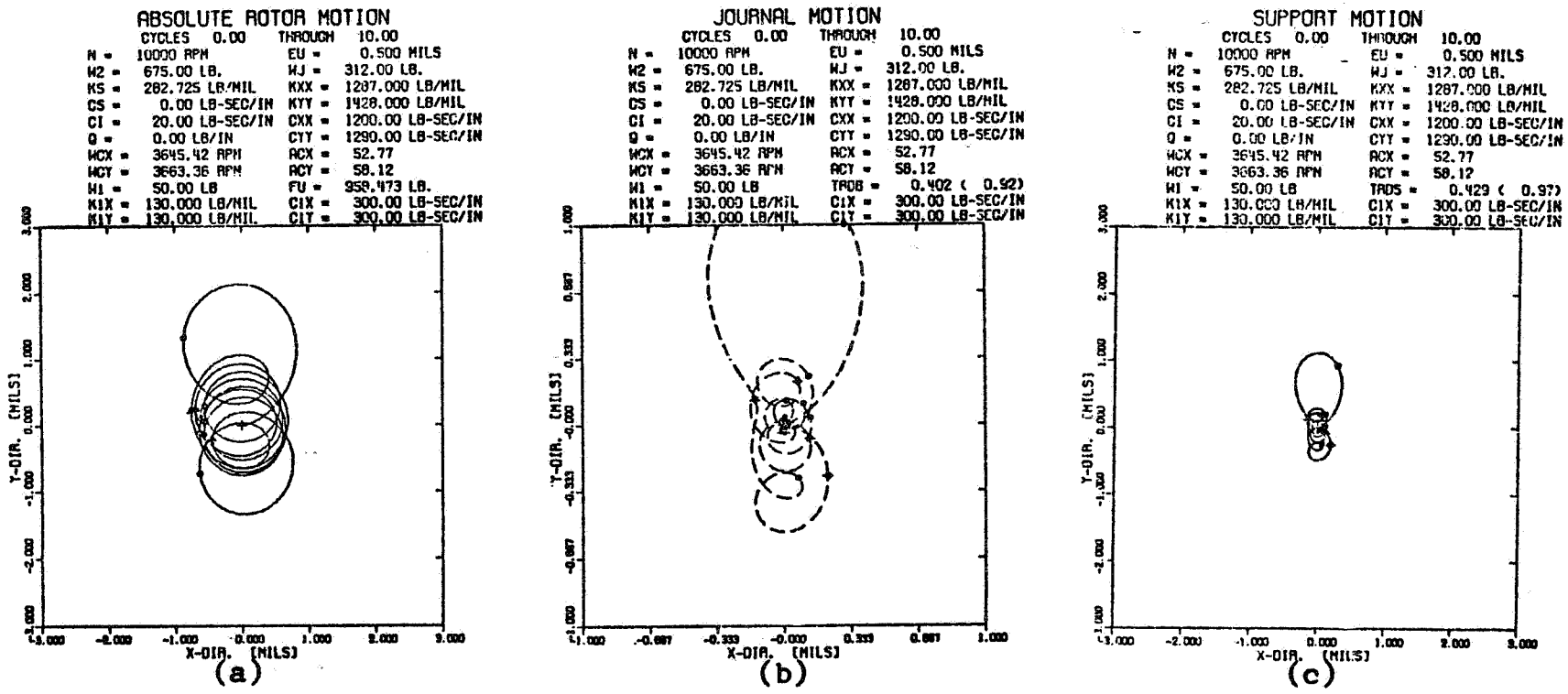

FIG. 5.14(a) ABSOLUTE ROTOR TRANSIENT RESPONSE TO IMPACT UNBALANCE LOAD FOR DAMPED ELASTIC SUPPORT SYSTEM (5.4OZ-IN UNBALANCE)
(b) JOURNAL TRANSIENT ABSOLUTE MOTION FOR TEN CYCLES
(c) SUPPORT SYSTEM TRANSIENT RESPONSE FOR TEN CYCLES (N=10,000)

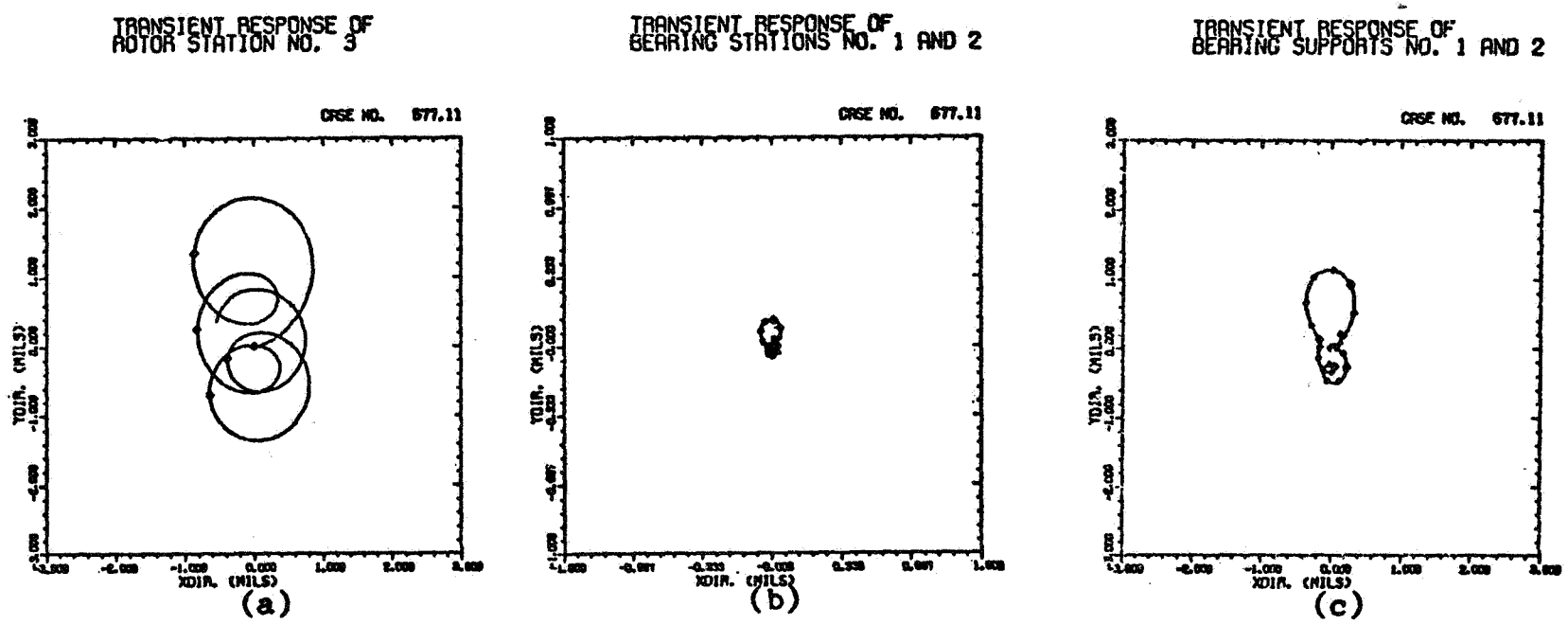

FIG. 5.15(a) ROTOR TRANSIENT RESPONSE WITH 5.4OZ-IN UNBALANCE IMPACT LOAD
(b) JOURNAL RESPONSE FOR FIVE CYCLES
(c) SUPPORT TRANSIENT MOTION FOR FIVE CYCLES (N=10,000)

FLEXIBLE POINT MASS ROTOR TRANSIENT RESPONSE --MY S. GOKHOUL KING--

(UNITS ARE IN-LB-SEC, UNLESS OTHERWISE SPECIFIED)

CASE NUMBER = 677.11

ROTOR SHAFT SPECIFICATIONS

ROTOR ACCEL = 0.0 RPM/SEC

SECTION	LENGTH	DIAMETER	YOUNGS MODULUS	PRODUCT OF E*I	INSIDE DIAMETER
1	1.00	4.00	3.000E 07	3.770E 08	0.00
2	19.00	4.00	3.000E 07	3.770E 08	0.00
3	19.00	4.00	3.000E 07	3.770E 08	0.00
4	1.00	4.00	3.000E 07	3.770E 08	0.00

BEARING NO. 1 IS 0.00 INCHES FROM THE LEFT END, STATION NO. 1

BEARING NO. 2 IS 40.00 INCHES FROM THE LEFT END, STATION NO. 5

BEARING SPAN IS 40.00 INCHES

APPROXIMATED ROTOR SPECIFICATIONS

STATION	LENGTH FROM END	WEIGHT	MASS	STIFFNESS	DAMPING	INT. DAMP	STIFF-B	EXT. WT	EMU	PHI
3	20.00	675.014	1.7487	0.0	0.000	90.000	0.0	475.00	5.40	0.0

(EMU GIVEN IN OZ-IN UNITS)

(ALL OTHER STATIONS EXCEPT THE BEARINGS HAVE ZERO MASS)

TOTAL LENGTH OF ROTOR = 40.000 IN.
ACTUAL WEIGHT OF ROTOR = 1637.291 LBS.
TOTAL WEIGHT OF APPROXIMATE ROTOR = 1287.014 LBS.

BEARING STATION SPECIFICATIONS

NO.	STATION	LENGTH FROM END	WEIGHT	MASS	EXTERNAL WEIGHT	STIF-X	STIF-Y	DAMP-X	DAMP-Y
1	1	0.00	312.778	0.8103	311.000	1.787OE 06	1.426OE 06	1.2000E 03	1.2900E 03
2	5	40.00	312.778	0.8103	311.000	1.787OE 06	1.426OE 06	1.2000E 03	1.2900E 03

BEARING PEDESTAL SPECIFICATIONS

NO.	STATION	LENGTH FROM END	WEIGHT	MASS	STIF-X	STIF-Y	DAMP-X	DAMP-Y
1	1	0.00	50.000	0.1295	1.3000E 05	1.3000E 05	3.0000E 02	3.0000E 02
2	5	40.00	50.000	0.1295	1.3000E 05	1.3000E 05	3.0000E 02	3.0000E 02

CASE NO. 677.11

SEGMENT	N-INIT. (RPM)	ACCEL. (RPM/SEC)	N-FINAL (RPM)	T-FINAL (RAD)	FMAXB-1 LB*10-3	FMAXB-2 LB*10-3	FMAXS-1 LB*10-3	FMAXS-2 LB*10-3
1	10000.0	0.0	10000.0	6.3	0.19	0.19	0.21	0.21
2	10000.0	0.0	10000.0	12.6	0.19	0.19	0.21	0.21
3	10000.0	0.0	10000.0	18.8	0.07	0.07	0.07	0.07
4	10000.0	0.0	10000.0	25.1	0.09	0.09	0.09	0.09
5	10000.0	0.0	10000.0	31.4	0.06	0.06	0.07	0.07

TABLE 5.2 ROTOR SPECIFICATIONS FOR UNBALANCE RESPONSE ON FLEXIBLE, DAMPED SUPPORTS INDICATING MAXIMUM FORCE TO BEARING AND SUPPORT HOUSINGS

of SMFROLS. Table 5.2 indicates very good agreement with the maximum forces calculated and indicates the maximum force to each bearing to be 190 lb. and the maximum force to the supports is indicated to be 210 lb. This excellent agreement of the two programs indicates that the theory of Chapter II produces results which are accurate and acceptable for study of ccmplex rotor support systems.

5.5 Stability Analysis of the Three Mass Rotor With Aerodynamic Cross Coupling and Internal Friction

If the rotor analyst is primarily concerned with the design of flexible support systems to promote stability and for the attenuation of the rotor amplitude and forces transmitted due to unbalance, it would be difficult to utilize the transient orbit program for the solution of the optimum support parameters. For example, in the case of the rotor in Example 5.1 with internal friction it would be desirable to know the range of the permissible values of the support system stiffness and damping that may be incorporated for optimum performance. It is difficult to determine from the observation of the orbits of Figs. 5.10(a) and 5.11(a) for support damping values of 300 and 150 lb.-sec./in. respectively whether the optimum damping is higher or lower or whether the support stiffness should be reduced or increased. It would be extremely expensive and time consuming to develope the necessary series of rotor orbits for all the ranges of variables required for the desired results.

For this reason it is therefor desirable to first develop stability maps showing the relationship of the various variables on rotor stability. Variables of interest would consist of support housing damping and flexibility, bearing characteristics, rotor shaft flexibility, internal

damping, and aerodynamic effects. The stability analysis for the linear system is identical to the analysis that will be presented in Chapter VI for the stability study of the nonlinear squeeze damper. The computer code SDSTB of Appendix F may be programmed for given bearing and support characteristics and hence may be used to develope stability charts for the given rotor bearing system.

For example consider the effect of the damped support on the suppression of aerodynamic instability as shown in Fig. 5.16 which has the value of the real part of the major root plotted versus the support damping for various values of support stiffness. The support mass for this example is noted to be 15 lb. with the other variables remaining the same as given for Example 5.1. This plot is for a rotor speed of 10,000 RPM and an aerodynamic cross-coupling of 20,000 lb./in. The figure indicates that there is a definite value of support damping that will promote stability for a given support stiffness. For example a damping of 500 lb-sec/in. would be optimum for the support stiffness of 50,000 lb/in. As the support stiffness increases the required optimum damping also increases and the system becomes less stable for the increased support stiffness. If the support system loses the damping then the rotor system is easily driven unstable as indicated on the left-most portion of the stability map.

The importance of the tuned support damping is even more evident for the increased level of cross-coupling given in Fig. 5.17. It is noted that the range of damping that will promote stability has been reduced considerably from a range of 100 to 10,000 for the lesser cross-coupling value to only a range of 370 to 1600 for the higher

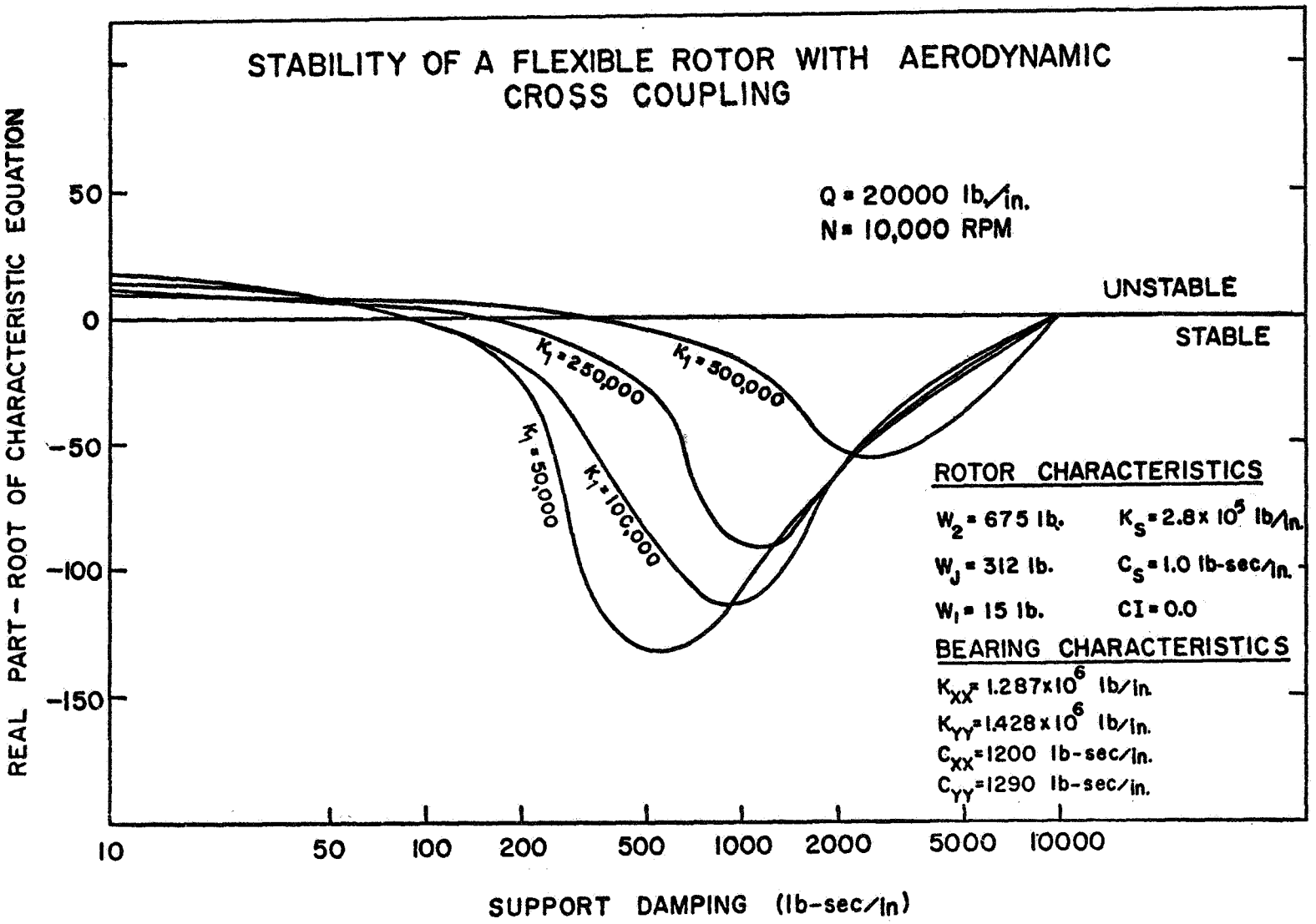

FIG. 5.16 STABILITY MAP FOR A THREE MASS FLEXIBLE ROTOR ON DAMPED FLEXIBLE SUPPORTS (Q=20,000LB/In, N=10,000RPM)

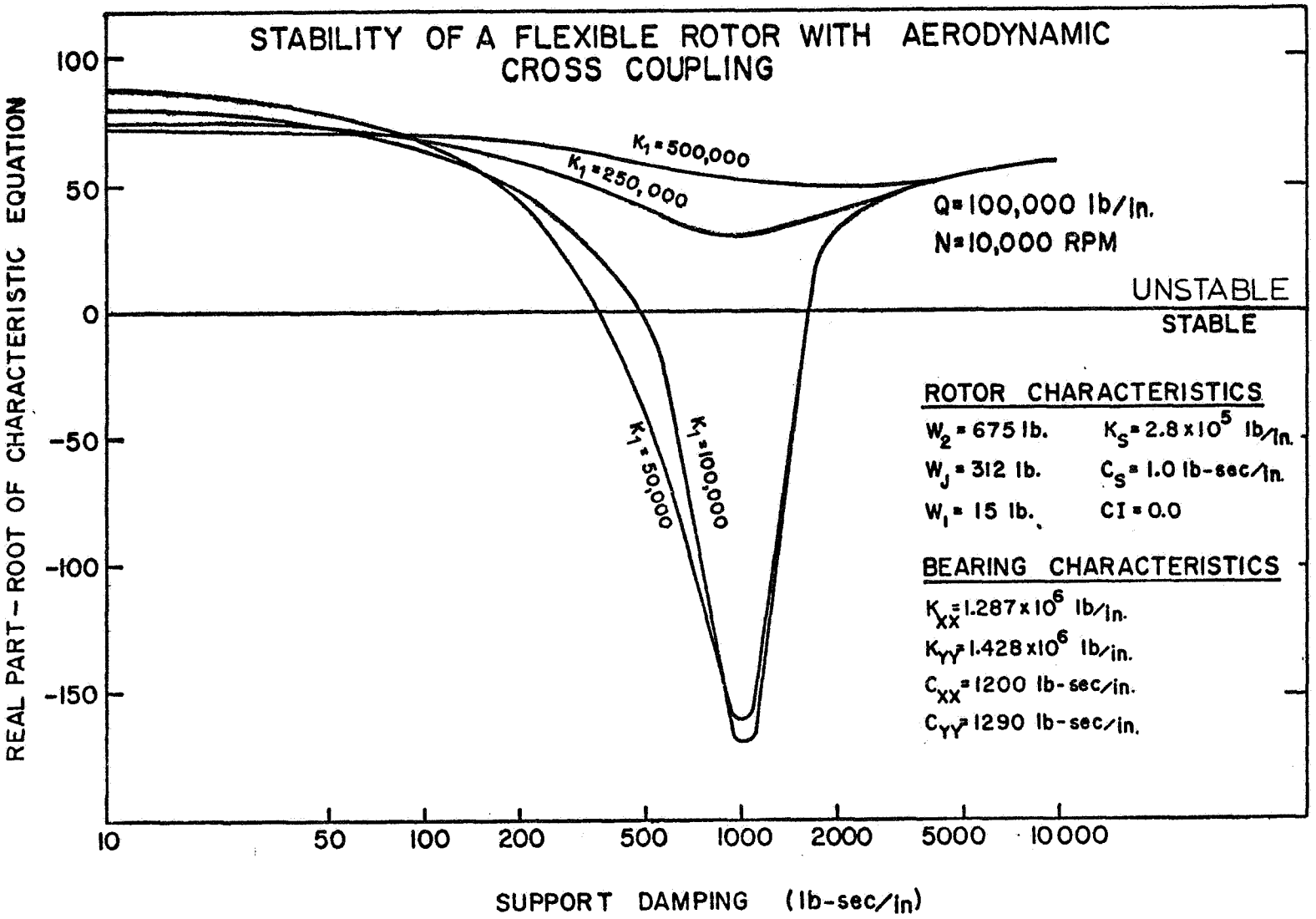

FIG. 5.17 STABILITY MAP FOR A THREE MASS FLEXIBLE ROTOR ON DAMPED FLEXIBLE SUPPORTS (Q=100,000LB/IN, N=10,000RPM)

level of aerodynamic excitation. The stiffer support systems are indicated to be unstable regardless of the damping chosen for the support system for the case of the higher aerodynamic cross-coupling.

At this point in the analysis the transient program could be used to establish the effect of unbalance and external shock loads to the support system. The transient analysis becomes of even greater importance when nonlinear system are being analyzed for stability by linear approximations. These nonlinear systems may exhibit stability for small pertubations but may also give large sustained whirl orbits for suddenly applied unbalance and impact loads. The nonlinear damper will be discussed in greater detail in the following Chapter.

CHAPTER VI

MULTI-MASS FLEXIBLE ROTOR WITH NONLINEAR SQUEEZE DAMPER SUPPORTS

This chapter will introduce the nonlinear squeeze damper support system into the model analyzed in Chapter IV with the added feature of allowing for rotor shaft flexibility. Thus the model of this chapter will be closer to real life machine performance than the linear model of the previous chapter. The inclusion of nonlinear elements in the transient analysis can be very time consuming unless approximate stability boundaries are known. A computer code to determine the stability of the rotor model described in Section 6.1 was developed and will be discussed in connection with a time transient program for the same model.

6.1 Explanation of the Rotor Bearing Model

The rotor-bearing system shown in Fig. 6.1 represents a three mass symmetric flexible rotor supported by journal bearings suspended in squeeze damper housings. The analysis will not consider the gyroscopic action of the rotor disk and hence the problem may be reduced to the study of motion in a plane. The characteristics of the fluid-film bearing have been discussed in Chapter IV and will be used to model the bearings in the present analysis. The squeeze damper supports will be derived from the same analysis. Fig. 6.2 indicates the cavitated bearing model and the fluid film damper recess.

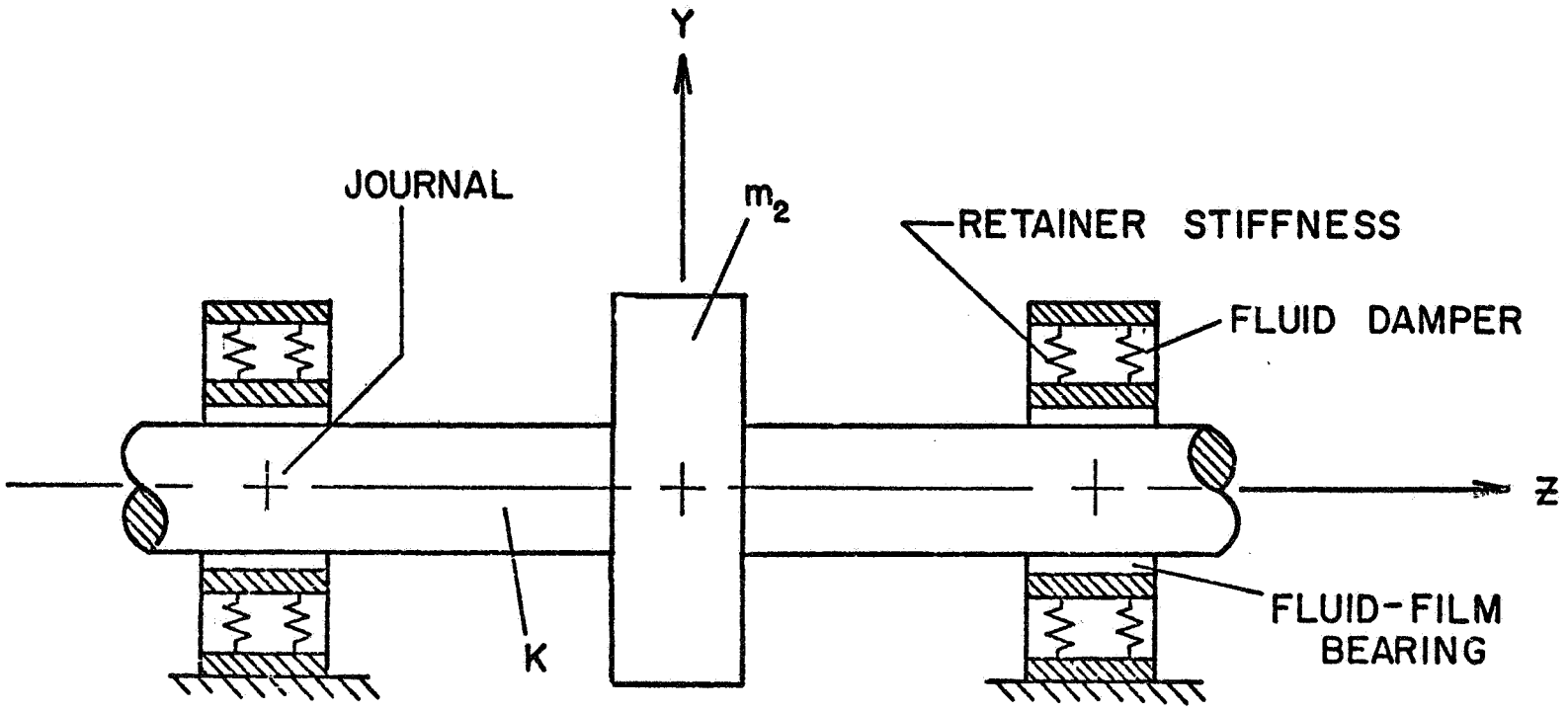

FIG. 6.1 ROTOR SYSTEM SUPPORTED ON FLUID-FILM JOURNAL BEARINGS WITH BEARING HOUSINGS SUSPENDED IN FLUID-DAMPER SUPPORTS

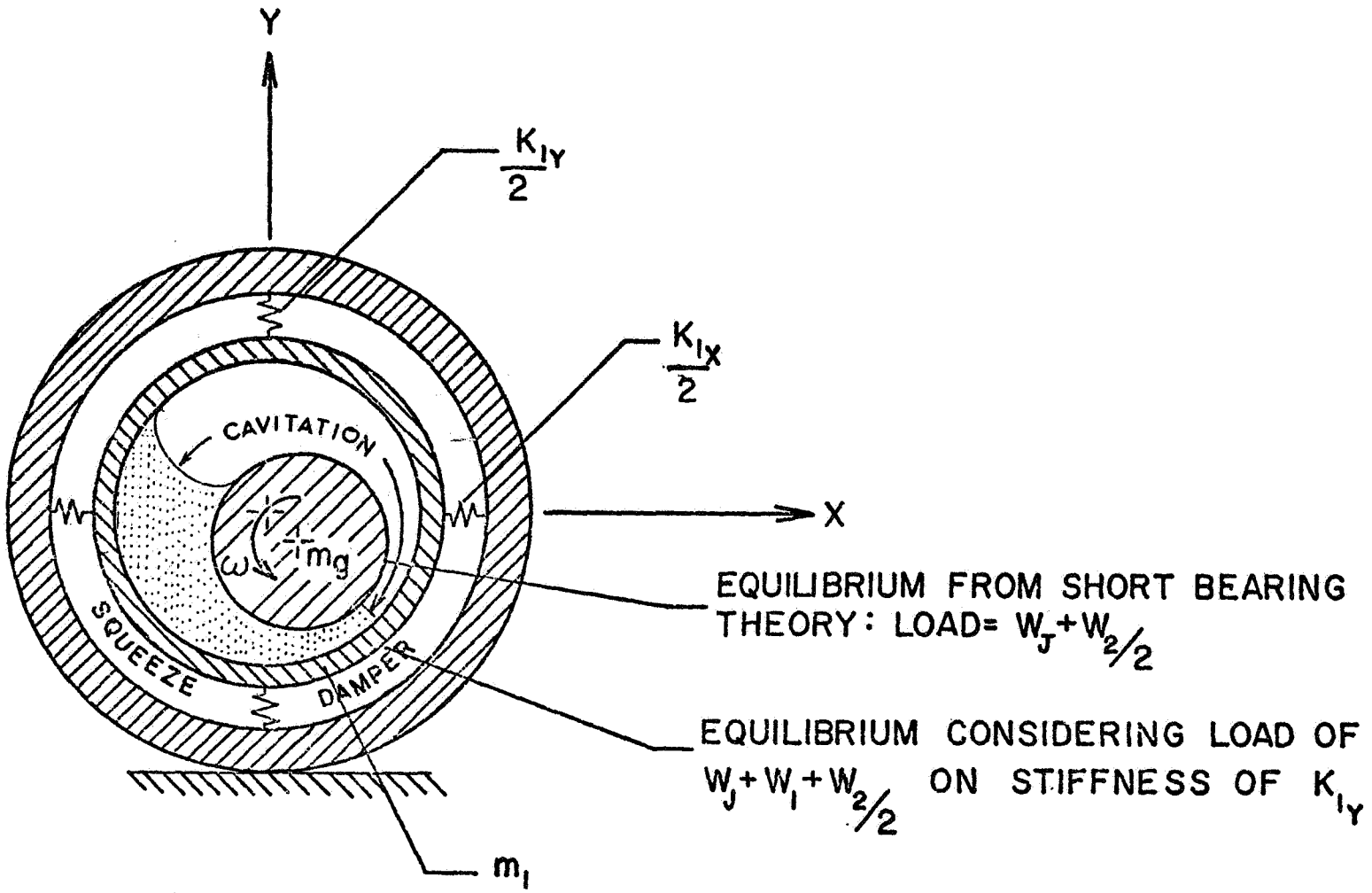

FIG. 6.2 CROSS-SECTION OF THE DAMPER STATION SHOWING JOURNAL CAVITATION AND RETAINER STIFFNESS IN THE BEARING SUPPORT HOUSING

The bearing ring has an anti-rotation pin and is suspended by assumed linear retainer springs which may have unequal stiffness characteristics for the two coordinate directions.

6.2 Equations of Motion

The equations of motion of a symmetric two bearing rotor may be written in terms of the following coordinates.

x_2, y_2 - absolute displacement of rotor mass, m_2

x_J, y_J - absolute journal displacement

x_b, y_b - bearing bush motion

The equations are easily derived considering linearized stiffness and damping terms to model the hydrodynamic bearings and squeeze bush. A simple force balance and inclusion of the internal friction components and cross coupling expressions at the rotor station produces the following equations.

Rotor Mass:

$$m_2\ddot{x}_2 + k_s(x_2 - x_J) + IC(\dot{x}_2 - \dot{x}_J) + \omega IC(y_2 - y_J) + c_s\dot{x}_2 + Q_{y2} = m_2 e_\mu \omega^2 \cos(\omega t + \phi_2) \tag{6.1}$$

$$m_2\ddot{y}_2 + k_s(y_2 - y_J) + IC(\dot{y}_2 - \dot{y}_J) - \omega IC(x_2 - x_J) + c_s\dot{y}_2 - Qx_2 = m_2 e_\mu \omega^2 \sin(\omega t + \phi_2) \tag{6.2}$$

Journal Bearings:

$$2m_J \ddot{x}_J - k_s(x_2 - x_J) - IC(\dot{x}_2 - \dot{x}_J) - \omega IC(y_2 - y_J)$$
$$+ 2k_{xx}(x_J - x_b) + 2k_{xy}(y_J - y_b) + 2c_{xx}(\dot{x}_J - \dot{x}_b)$$
$$+ 2c_{xy}(\dot{y}_J - \dot{y}_b) = 0 \qquad [6.3]$$

$$2m_J \ddot{y}_J - k_s(y_2 - y_J) - IC(\dot{y}_2 - \dot{y}_J) + \omega IC(x_2 - x_J)$$
$$+ 2k_{yy}(y_J - y_b) + 2k_{yx}(x_J - x_b) + 2c_{yy}(\dot{y}_J - \dot{y}_b)$$
$$+ 2c_{yx}(\dot{y}_J - \dot{y}_b) = 0 \qquad [6.4]$$

Bush Damper

$$2m_b\ddot{x}_b + 2k_{1xx}x_b + 2k_{1xx}x_b + 2k_{1xy}y_b + 2c_{1xx}\dot{x}_b + 2c_{1xy}\dot{y}_b$$
$$- 2k_{xx}(x_J - x_b) - 2k_{xy}(y_J - y_b) - 2c_{xx}(\dot{x}_J - \dot{x}_b)$$
$$- 2c_{xy}(\dot{y}_J - \dot{y}_b) = 0 \qquad [6.5]$$

$$2m_b\ddot{y}_b + 2k_{1yy}y_b + 2k_{1yx}x_b + 2c_{1yy}\dot{y}_b + 2c_{1yx}\dot{x}_b$$
$$- 2k_{yy}(y_J - y_b) - 2k_{yx}(x_J - x_b) - 2c_{yy}(\dot{y}_J - \dot{y}_b)$$
$$- 2c_{yx}(\dot{x}_J - \dot{x}_b) = 0 \qquad [6.6]$$

These equations are basically the same as those presented in the previous chapter. The difference is due to the absolute coordinate chosen to describe the journal motion. The methods of obtaining the

bearing characteristics have been discussed in Chapter IV and the squeeze damper characteristics will be presented in the following section.

6.3 Stability Analysis

Manufacturers are presently installing floating squeeze damper supports into their high speed machines. Tanaka and Hori (89) have recently reported on the stability of the spinning floating bush damper. They included rotor shaft flexibility but excluded the journal mass from the analysis. Several curves were presented showing that regions of instability could be passed through as rotor speed increased. Experimental results were presented and the agreement with the analytical results was satisfactory.

The major conclusions of Tanaka-Hori may be summarized as follows:

(1) Floating bush damper bearings are superior to cylindrical bearings due to the damping effect in the bush.

(2) Stability is generally improved when

a) the shaft is stiffer

b) large floating bush radius

c) large bush clearance

d) small L/D ratios

e) small oil supply pressure to allow cavitation

(3) The stability criterion is complicated and a particular case must be checked to assure best design.

As early as 1958 Hill (90) reported on the improved performance of small gas turbines running at 36,000 RPM by using slipper bearings which actually introduced a damped support system into the bearing

configuration. Dworskie (91) later reported successful use of floating sleave bearings in a 44,000 RPM gas generator.

In 1968 Orcutt and Ng (92) presented steady-state and dynamic properties of plain cylindrical floating ring bearings but the equations were reduced by the assumption of synchronous motion which limits the validity of these results since fractional frequency whirl is to be expected in the fluid-film bearings. Experimental tests indicated several different types of instabilities were possible. The journal was usually the source of instability but at times the outer film was unstable while the inner film was stable. One conclusion reached was that the amplitude of the instability was more important than a calculated stability threshold speed since low-level whirling could be tolerated in any given application.

The present analysis will consider the damper bearing as a non-spinning journal deriving damping only from the fluid film squeeze action. Considering a pure squeeze action for a velocity in the +y direction the positive film extent is from 0 to π as shown in Fig. 6.3(a). For a positive x velocity the positive film extends from $-\pi/2$ to $\pi/2$ as indicated in Fig. 6.3(b). The expression for the force is obtained from Eq. 4.1 for the case of $\omega_j = 0.0$.

$$F^{(s)}_{x,y} = \frac{\mu R L^3}{2} \int_0^{2\pi} \frac{-2(\dot{x}\cos\theta + \dot{y}\sin\theta)}{(c - x\cos\theta - y\sin\theta)^3} \begin{Bmatrix}\cos\gamma \\ \sin\theta\end{Bmatrix} d\theta \qquad [6.7]$$

Differentation of this equation produces the damping coefficients as follows:

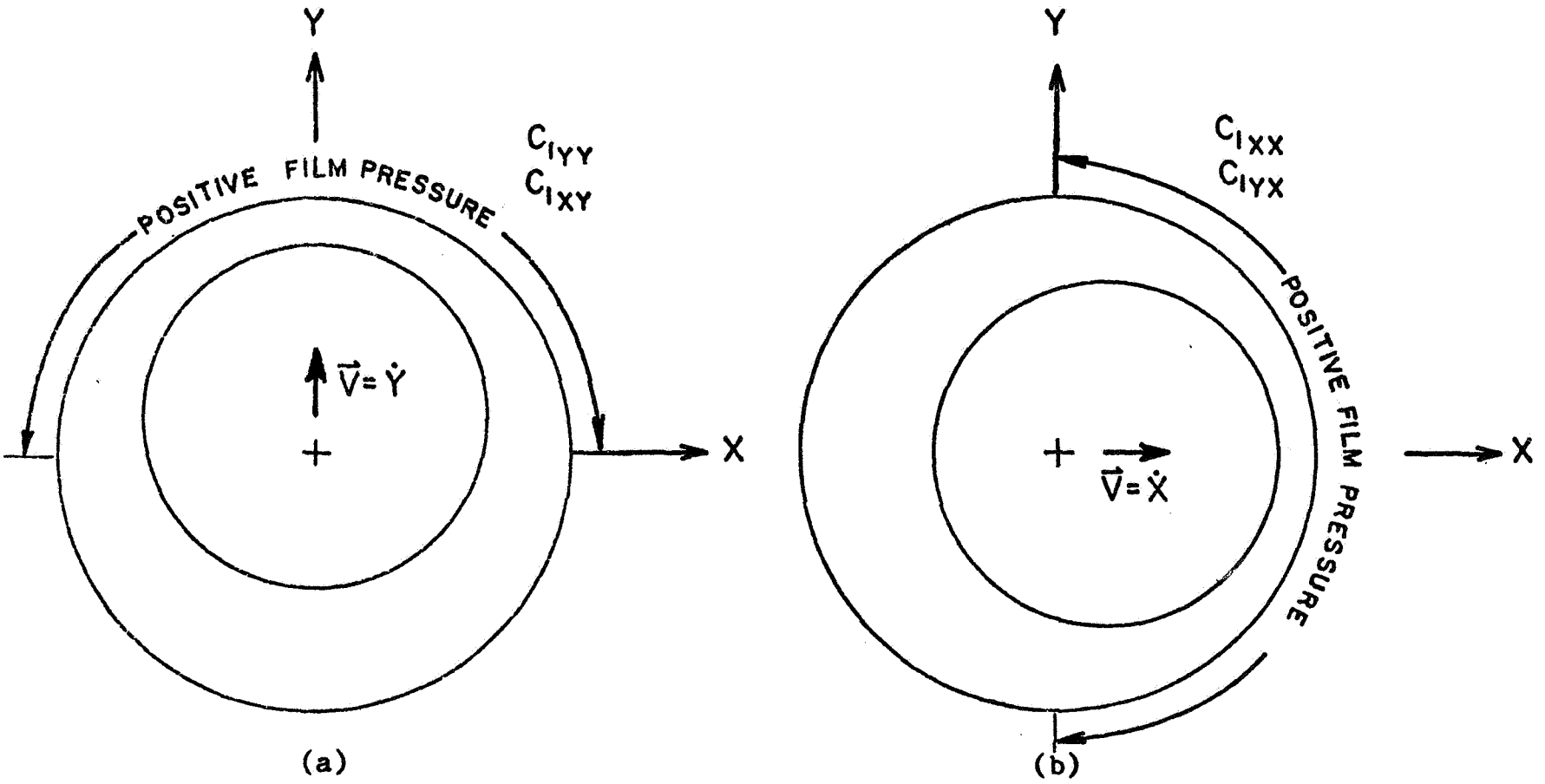

FIG. 6.3(a) INDICATION OF POSITIVE FILM EXTENT FOR A POSITIVE VERTICAL VELOCITY PERTUBATION
(b) INDICATION OF POSITIVE FILM EXTENT FOR A POSITIVE HORIZONTAL VELOCITY PERTUBATION

$$c_{1xx} = -\frac{\partial F_x(\dot{x},\dot{y}=0)}{\partial \dot{x}} = \frac{\mu R L^3}{2}\int_{-\pi/2}^{\pi/2} \frac{2\cos^2\theta}{(c - x\cos\theta - y\sin\theta)^3}\, d\theta \qquad [6.8]$$

$$c_{1yx} = -\frac{\partial F_y(\dot{x},\dot{y}=0)}{\partial \dot{x}} = \frac{\mu R L^3}{2}\int_{-\pi/2}^{\pi/2} \frac{2\cos\theta\,\sin\theta}{(c - x\cos\theta - y\sin\theta)^3}\, d\theta \qquad [6.9]$$

$$c_{1xy} = -\frac{\partial F_x(\dot{x}=0,\dot{y})}{\partial \dot{y}} = \frac{\mu R L^3}{2}\int_{0}^{\pi} \frac{2\cos\theta\,\sin\theta}{(c - x\cos\theta - y\sin\theta)^3}\, d\theta \qquad [6.10]$$

$$c_{1yy} = -\frac{\partial F_y(\dot{x}=0,\dot{y})}{\partial \dot{y}} = \frac{\mu R L^3}{2}\int_{0}^{\pi} \frac{2\sin^2\theta d\theta}{(c - x\cos\theta - y\sin\theta)^3} \qquad [6.11]$$

It is of interest to note that McGrew (93) has derived a damping expression for circular synchronous precession (short bearing solution using rotating coordinates) which is expressed as

$$C_o = \frac{\mu R L^3}{2c^2}\left[\frac{\pi}{(1-\varepsilon_o^2)^{3/2}}\right] \qquad [6.12]$$

Also by assuming $\dot{\varepsilon} = \varepsilon\omega\cos(\omega t)$ a pseudo stiffness term may be derived and is given by

$$K_o = \frac{2\mu\omega L^3 R}{c^3}\,\frac{\varepsilon_o}{(1-\varepsilon_o^2)^2} \qquad [6.13]$$

The results of the computer calculated damping coefficients are presented in Fig. 6.4(a) along with points calculated from the expression derived from McGrew's analysis. The circular synchronous damping values

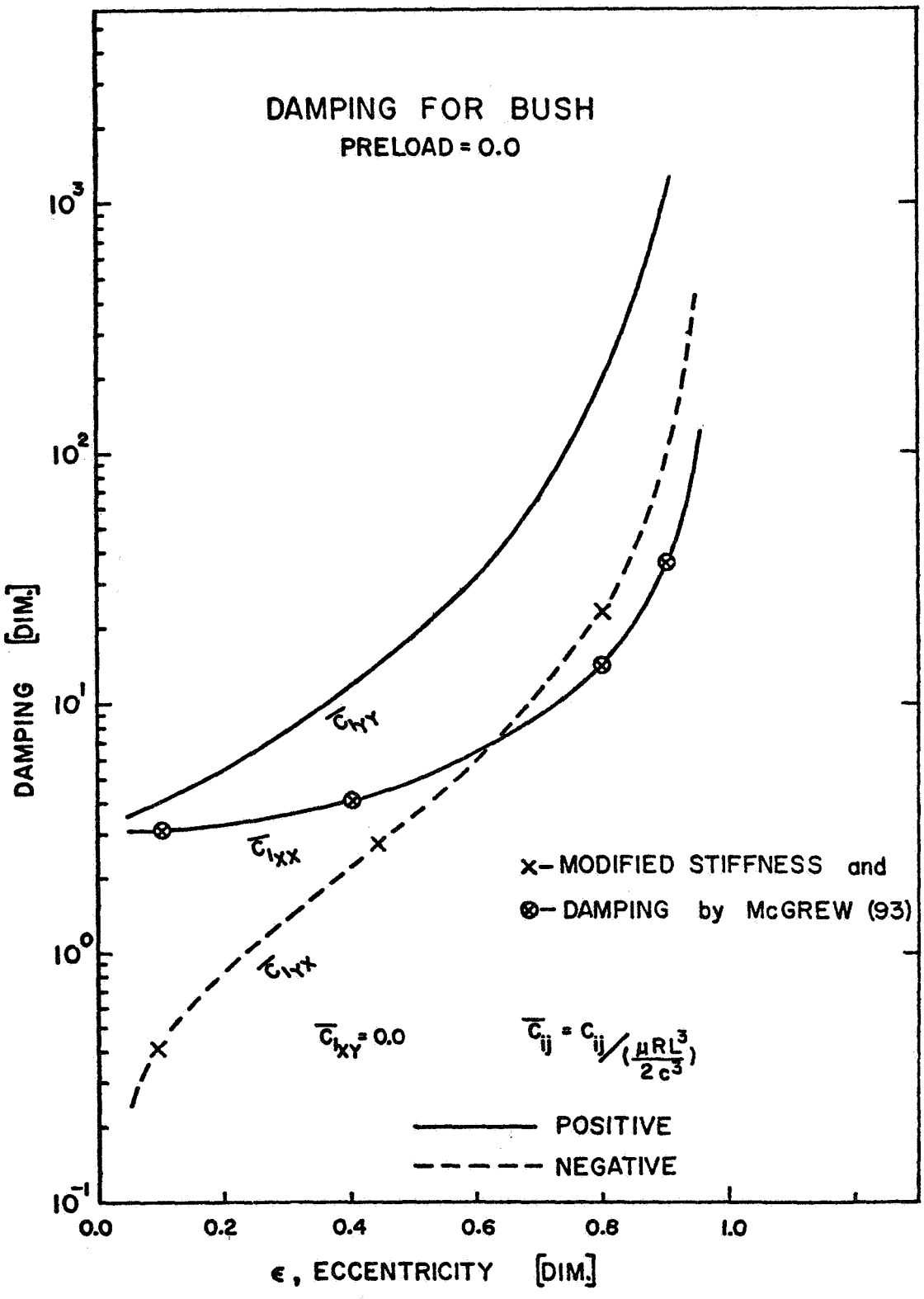

FIG. 6.4(a) FLOATING BUSH DAMPING CHARACTERISTICS VERSUS ECCENTRICITY (X=0.0, Y=ε)

are observed to equate to c_{1xx} while the stiffness term is actually a cross coupled damping force as it must be since the damper can in no instance develop a stiffness in the absolute sense.

Figures 6.4(b) and 6.4(c) indicate that preloading the damper produces damping expressions that are converging to equivalent values for the two coordinate directions. This characteristic may be very desirable when trying to design a tuned support system for optimum performance.

Figure 6.5 illustrates the effect of the additional pseudo stiffness term on the rigid rotor supported by a damper bearing with retainer spring rates of 5772 lb/in. The initial condition was given for the zero speed sag of the retainers. At the running speed of 9500 RPM the journal lifts up from the steady-state balanced equilibrium position and has a stable whirl orbit due to the unbalance level of 0.08 of the clearance. This lift of the nonlinear fluid damper must be considered when designing real machines which do have unbalance. The additional psudo stiffness (damping) contribution could shift the operating conditions with unbalance into a region where aerodynamic excitation could drive the system and produce large unstable whirl orbits.

Once the damping expressions for the floating bush and journal characteristics are known the stability analysis is easily programmed on a digital computer.

Assuming solutions of the form

$$x_i = A_i e^{\lambda t}; \; i = 1,6 \qquad [6.14]$$

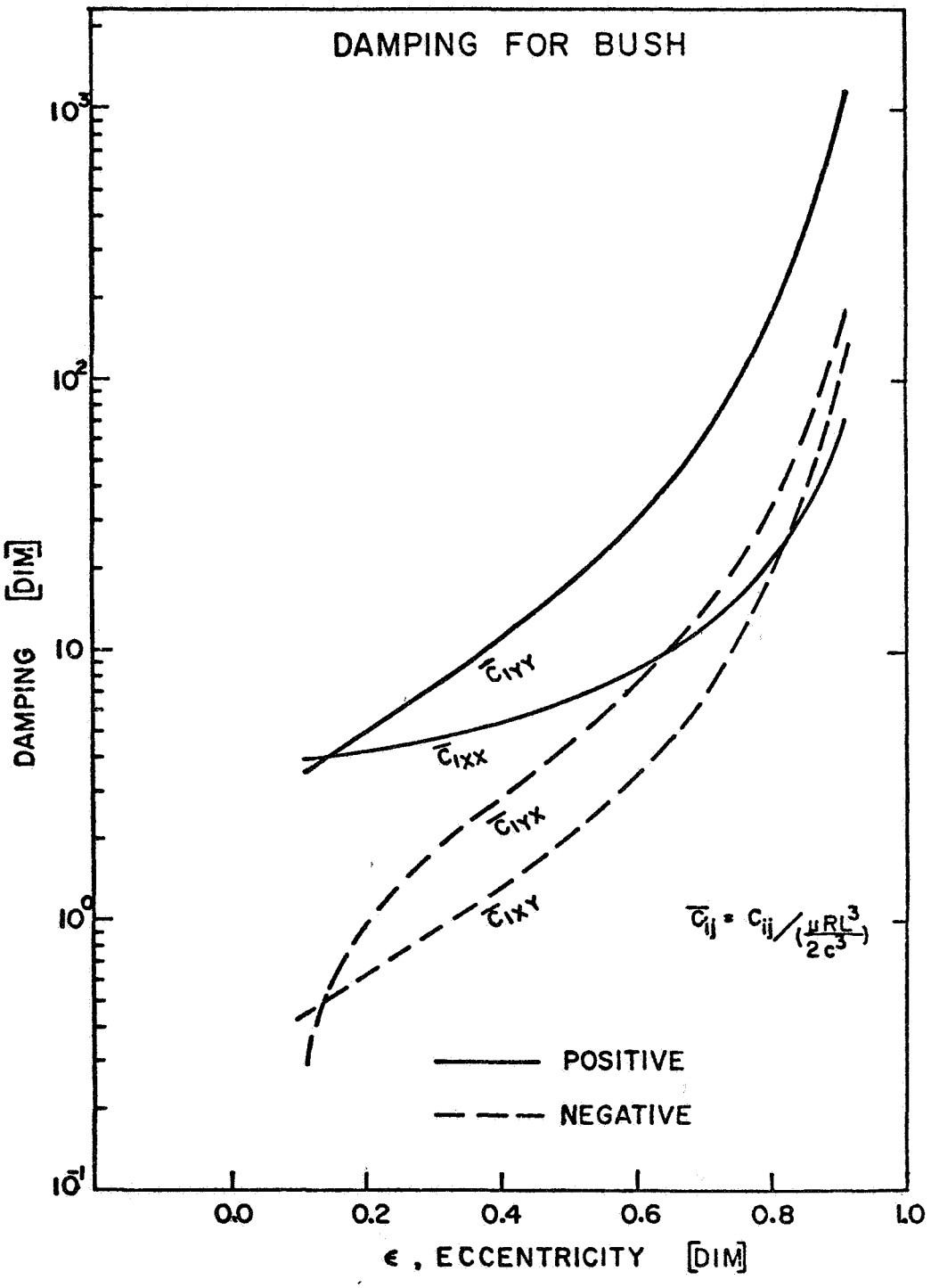

FIG. 6.4(b) FLOATING BUSH DAMPING CHARACTERISTICS VERSUS ECCENTRICITY (X=0.10)

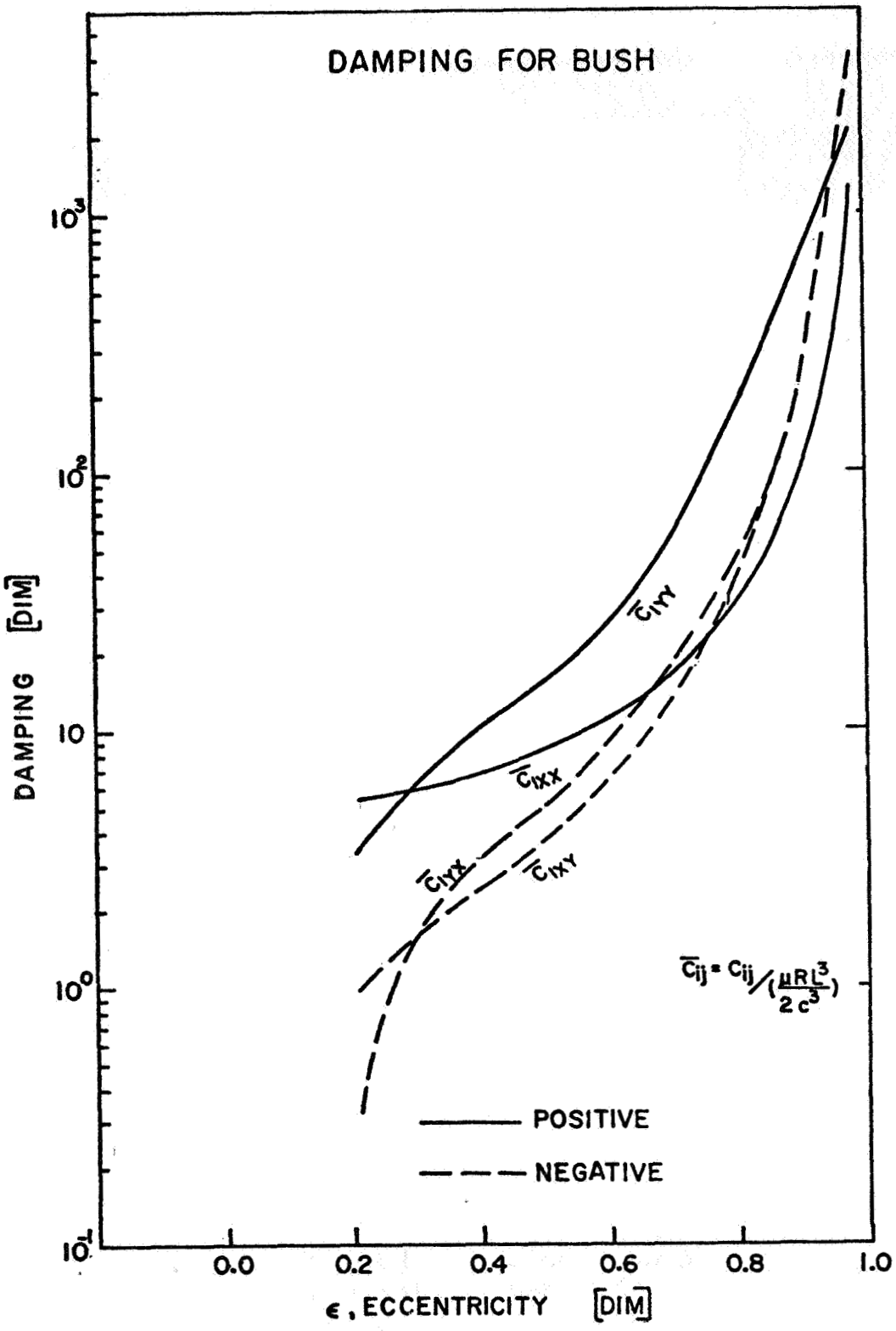

FIG. 6.4(c) FLOATING BUSH DAMPING CHARACTERISTICS VERSUS ECCENTRICITY (X=0.20)

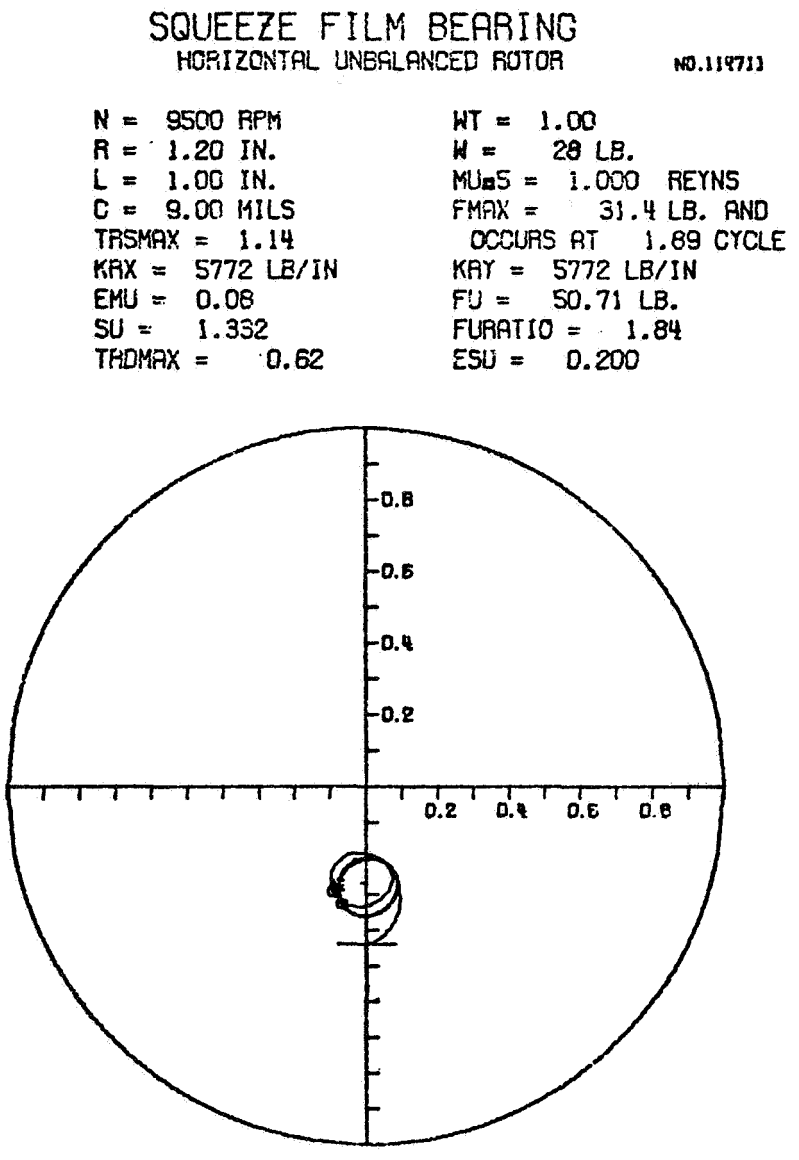

FIG. 6.5 SQUEEZE DAMPER UNBALANCE RESPONSE FOR RIGID ROTOR AND RIGID BEARINGS (N=9,500RPM, W=28LB, C=9MILS, EMU=0.08)

where

i = 1 corresponds to x_2

i = 2 corresponds to y_2

i = 3 corresponds to x_J

i = 4 corresponds to y_J

i = 5 corresponds to x_b

i = 6 corresponds to y_b

The homogeneous equations of motion may be examined for stability by determining the solutions of the characteristic equation and examining the real part for a positive value. The characteristic equation can be obtained by expanding the determinant given on the following page.

A computer code SDSTB has been developed to carry out the necessary operations to determine the stability of a given rotor-bearing system. A listing and explanation of the required input is given in Appendix F.

To demonstrate the capability of the program consider the following example case study.

Example 6.1

Rotor weight	-	40 lb.
Journal weight	-	5 lb.(each)
Bush weight	-	2.5 lb.(each)
Journal clearance	-	5 mils
Journal radius	-	1 in.
Journal length	-	1 in.
Viscosity	-	1×10^{-5} reyns
Radius of bush	-	1.2 in.

$$
\begin{array}{c}
\\
x_2: \\
\\
y_2: \\
\\
x_J: \\
\\
y_J: \\
\\
x_b: \\
\\
y_b: \\
\\
\end{array}
\begin{bmatrix}
m_2\lambda^2 & & -\lambda IC & & & \\
+(IC+cs)\lambda & Q+\omega IC & -k_s & -\omega IC & 0 & 0 \\
+k_s & & & & & \\
 & m_2\lambda^2 & & -\lambda IC & & \\
-Q-\omega IC & +(IC+cs)\lambda & \omega IC & -k_s & 0 & 0 \\
 & +k_s & & & & \\
-\lambda IC/2 & & m_J\lambda^2 & c_{xy}\lambda & -c_{xx}\lambda & -c_{xy}\lambda \\
-(k_s+\omega IC)/2 & 0 & +(c_{xx}+IC/2)\lambda & +k_{xy} & -k_{xx} & -k_{xy} \\
 & & +(k_s+\omega IC)/2 & & & \\
 & & +kxx & & & \\
 & -\lambda IC/2 & c_{yx}\lambda & m_J\lambda^2 & -c_{yx}\lambda & -c_{yy}\lambda \\
0 & -(k_s-\omega IC)/2 & +k_{yx} & +(c_{yy}+IC/2)\lambda & -k_{yx} & -k_{yy} \\
 & & & +(k_s-\omega IC)/2 & & \\
 & & & +k_{yy} & & \\
 & & -c_{xx}\lambda & -c_{xy}\lambda & m_b\lambda^2 & (c_{xy}+c_{1xy})\lambda \\
0 & 0 & -k_{xx} & -k_{xy} & +(c_{xx}+c_{1xx})\lambda & +(k_{xy}+k_{1xy}) \\
 & & & & +(k_{xx}+k_{1xx}) & \\
 & & -c_{yx}\lambda & -c_{yy}\lambda & (c_{yx}+c_{1yx})\lambda & m_b\lambda^2 \\
0 & 0 & -k_{yx} & -k_{yy} & +(k_{yx}+k_{1yx}) & +(c_{yy}+c_{1yy})\lambda \\
 & & & & & +(k_{yy}+k_{1yy})
\end{bmatrix}
\begin{bmatrix} A_1 \\ A_2 \\ A_3 \\ A_4 \\ A_5 \\ A_6 \end{bmatrix}
=
\begin{bmatrix} 0 \\ 0 \\ 0 \\ 0 \\ 0 \\ 0 \end{bmatrix}
$$

$k_{1x} = k_{1y}$ = retainer stiffness = 5772 lb/in.

The bush clearance was varied from 5 to 30 mils for each of two shaft stiffness values of 5,000 and 500,000 lb/in. These produce δ/c values of 1.6 and 0.016 respectively. The result from Ruhl's analysis (40) of the flexible rotor on short journal bearings is shown in Fig. 6.6 for reference. Comparing the above values of δ/c to the flexible rotor stability chart of Ruhl the stability of the flexible rotor (δ/c = 1.6) should be lowered considerably from that of a rigid rotor.

The results of the analysis is given in Fig. 6.7 where the stability boundaries for both shaft stiffness values are plotted. For a bush clearance of 5 mils the stability of the flexible shaft is indeed considerably reduced from the rigid rotor values. This is as predicted by Ruhl. As the bush clearance is opened up the stability boundary increases first for the flexible shaft and then for the rigid shaft. For a clearance of 12 mils the stability boundary has increased from $\frac{\omega}{\sqrt{g/c_j}}$ = (1.0, 2.54) to (8.0, 13.0) respectively for δ/c = (1.6, 0.016). As the clearance increases their is a lower region of instability which can be passed through to a region of stable operation. As the rotor speed increases the whirl reduces from 0.50 to 0.25 at 17 mils and encounters another instability of whirl frequency of approximately 0.50 as predicted by the stability program. As the clearance is opened further the lower instability region increases in width and finally converges with the upper instability boundary at higher bush clearance values (~ 28 mils for δ/c = 1.6). This plot was developed by keeping the retainer spring rate fixed and increasing the bush clearance. This

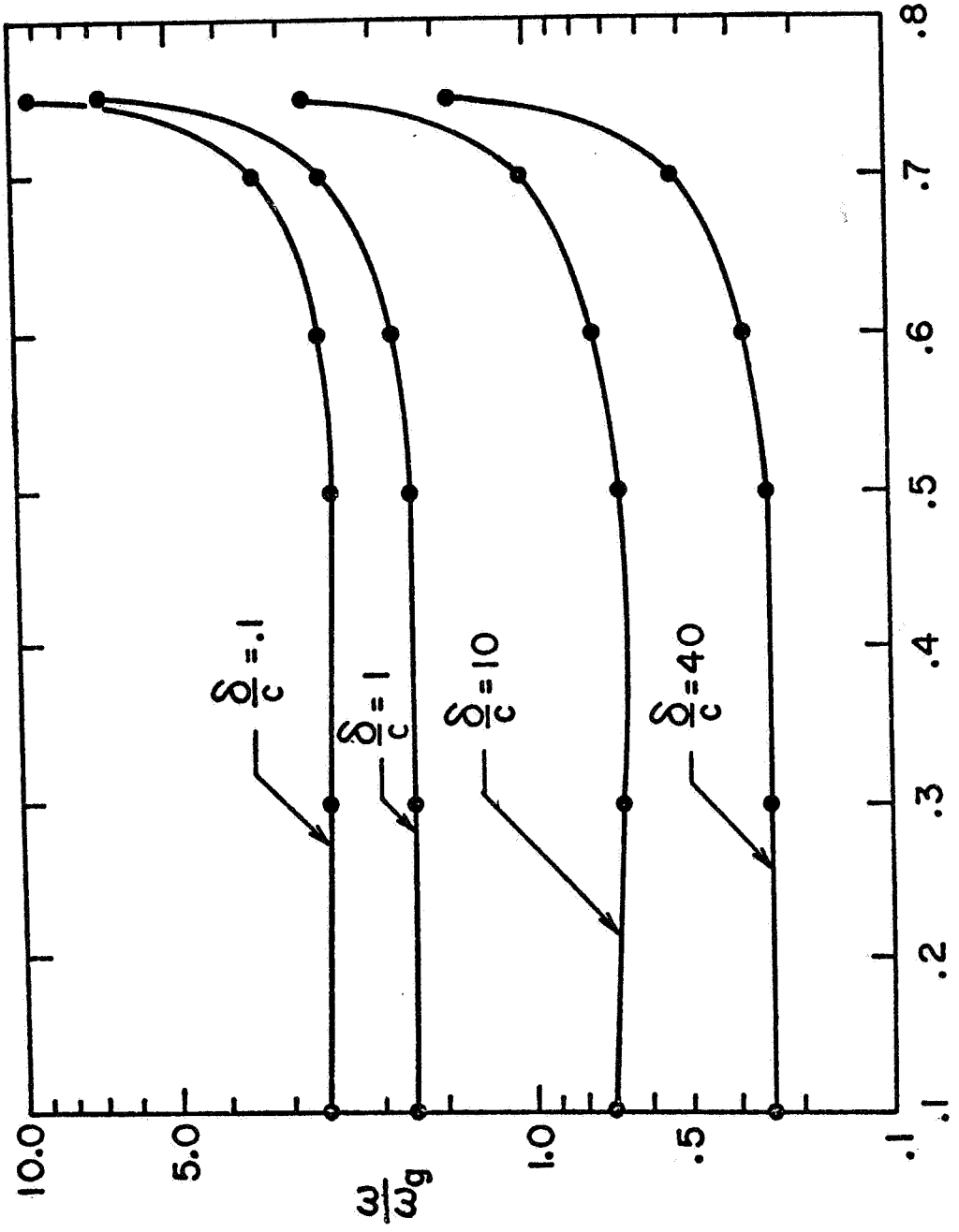

FIG. 6.6 EFFECT OF ROTOR FLEXIBILITY ON SHORT JOURNAL BEARING STABILITY (FROM RUHL (40))

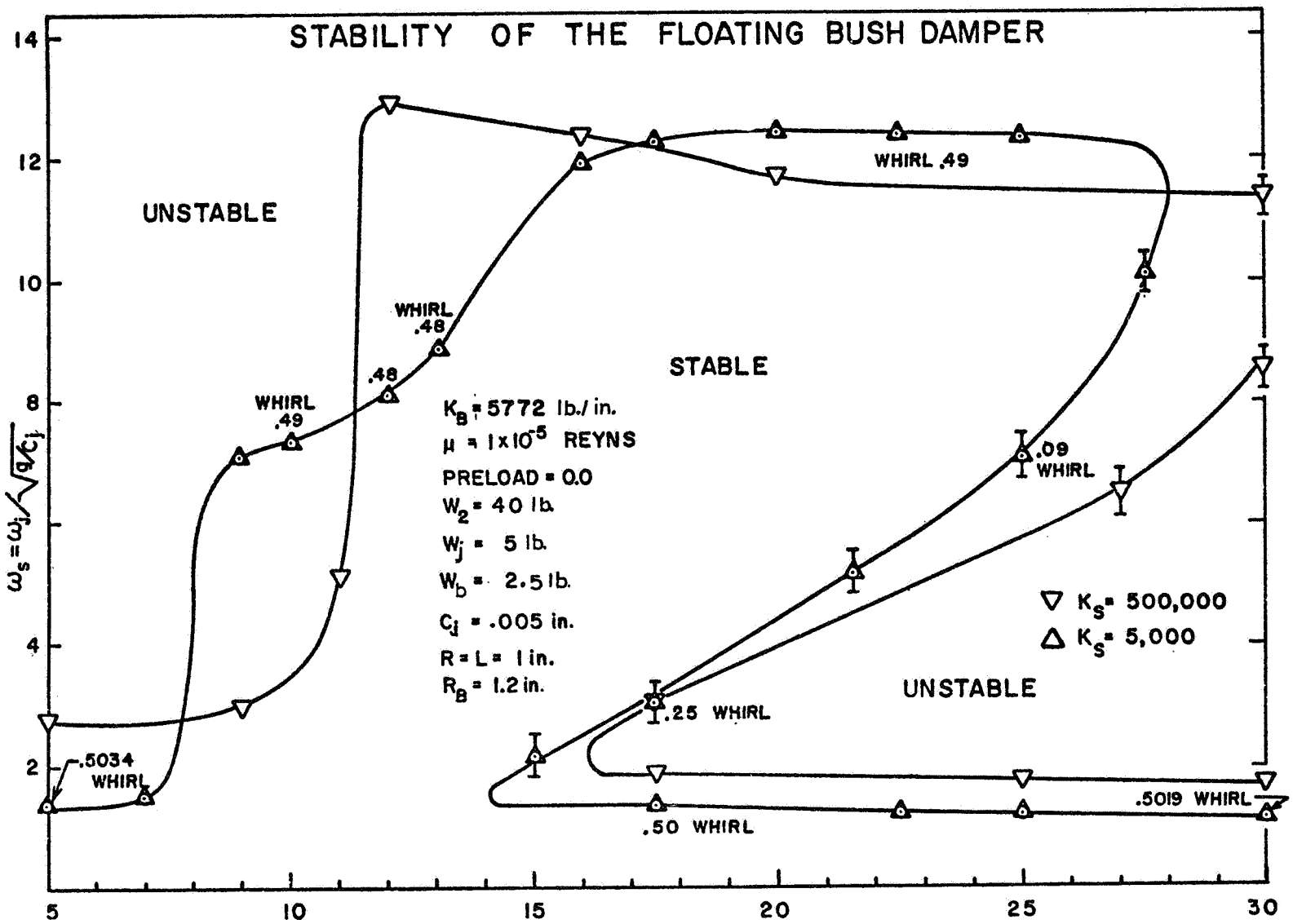

FIG. 6.7 STABILITY MAP FOR THE FLOATING BUSH DAMPER BEARING (K_B=5,772LB/IN, PRELOAD=0.0, W_2=40LB, W_J=5LB, W_b=2.5LB, K_S=5,000 and 500,000LB/IN)

of course produces results which vary from an analysis that has the bearing always centered in the bush clearance.

This phenomenon of passing through regions of instability with the damped supports has been reported in the literature for experimental results (54,74) and increases the significance of this analytical simulation results. The results of a time transient computer code to verify certain boundaries shown in Fig. 6.7 will be presented and discussed in the following section.

6.4 Transient Behavior of a Rotor Supported in a Floating Bush Damper

The equations of motion including the nonlinear journal bearings and squeeze bush damper force evaluations have been programmed for verification of the stability program SDSTB. This computer code, TMASSNL, which calculates and plots the transient solution is given in Appendix G. The equations programmed were written in terms of journal relative motion for the transient solution and are identical to Eqs. 5.37-5.42. The program has an option to use either a 4^{th} order Runge-Kutta or an Euler integration technique. The type integration chosen determines the step size necessary for a realistic whirl orbit. The step size required depends on the loading, rotor size (weight) and stiffness, and the type support chosen for the simulation. As the number of degrees of freedom increases the step size generally must be decreased to insure a valid solution.

Several cases have been computed that were chosen to verify the stability map of Fig. 6.7. Consider first the rigid rotor ($\delta/c = 0.016$) with a bush clearance of 17.5 mils. From Fig. 6.7 the system upper

stability bound is at ω_s = 12.3 or 32,000 RPM for our system. Fig. 6.8(a), (b), (c) indicates two cycles of motion at 29,000 RPM of the absolute rotor, journal relative, and support motion respectively. The system was started near the steady-state equilibrium position and the journal relative motion is approximately a half-frequency whirl and the damper is moving in a non-circular path as indicated in Fig. 6.8(c). The next series of figures continue the motion for cycles 2-5 and indicates that the rotor motion is negligible (Fig. 6.8(d)) while the journal relative motion is still whirling but decreasing as indicated by the orbit of Fig. 6.8(e). The damper motion (Fig. 6.8(d)) also indicates the motion is tending toward a stable mode of response.

For a rotor speed of 37,000 RPM the response for five cycles is given by Fig. 6.9(a) -(f). The rotor still shows a very small amplitude in comparison to the journal relative motion which is indeed unstable and spirals out in cycles two through five at an average whirl of 0.50. The damper motion is also observed to whirl at large amplitudes as compared to the motion at 29,000 RPM.

If the bush clearance is reduced to 10 mils the stability map indicates the system should be unstable. Figs. 6.10(a) - (f) give eight cycles of motion and indicate that the journal relative motion has a sustained circular whirl of 0.50 while the rotor motion is very small and the damper motion has non-circular motion but similar to the stable case of Fig. 6.8. It must be remembered that the stability chart indicates the stability at "a point". As soon as the bush motion begins the equilibrium position changes and so does the stability of the system for cases near the threshold speed. However the journal relative motion in Fig. 6.10(e)

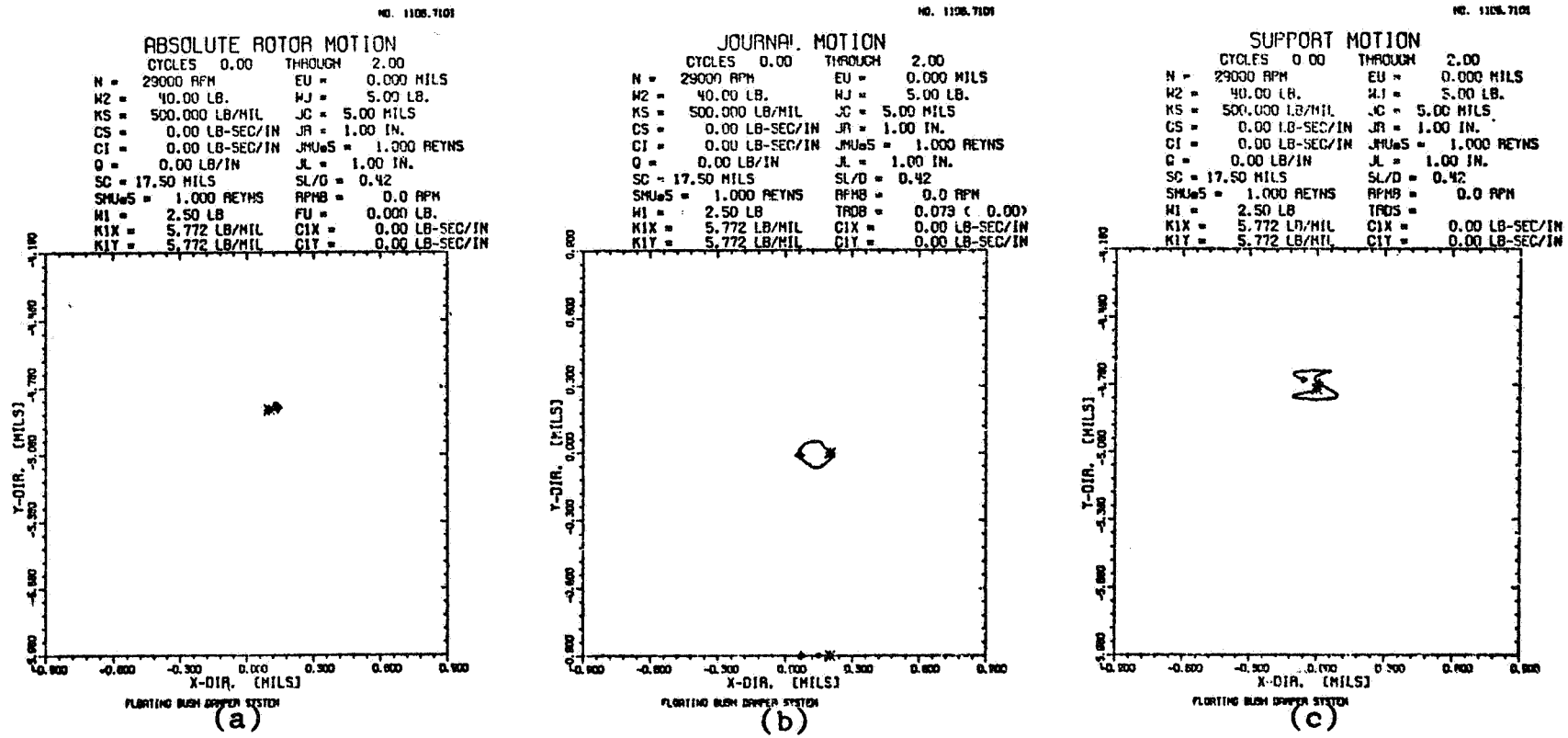

FIG. 6.8(a) ABSOLUTE ROTOR MOTION FOR TWO CYCLES (N=29,000RPM, K_S=500LB/MIL)
(b) JOURNAL RELATIVE MOTION BELOW STABILITY THRESHOLD
(c) DAMPER SUPPORT TRANSIENT RESPONSE (CLEARANCE=17.5MILS)

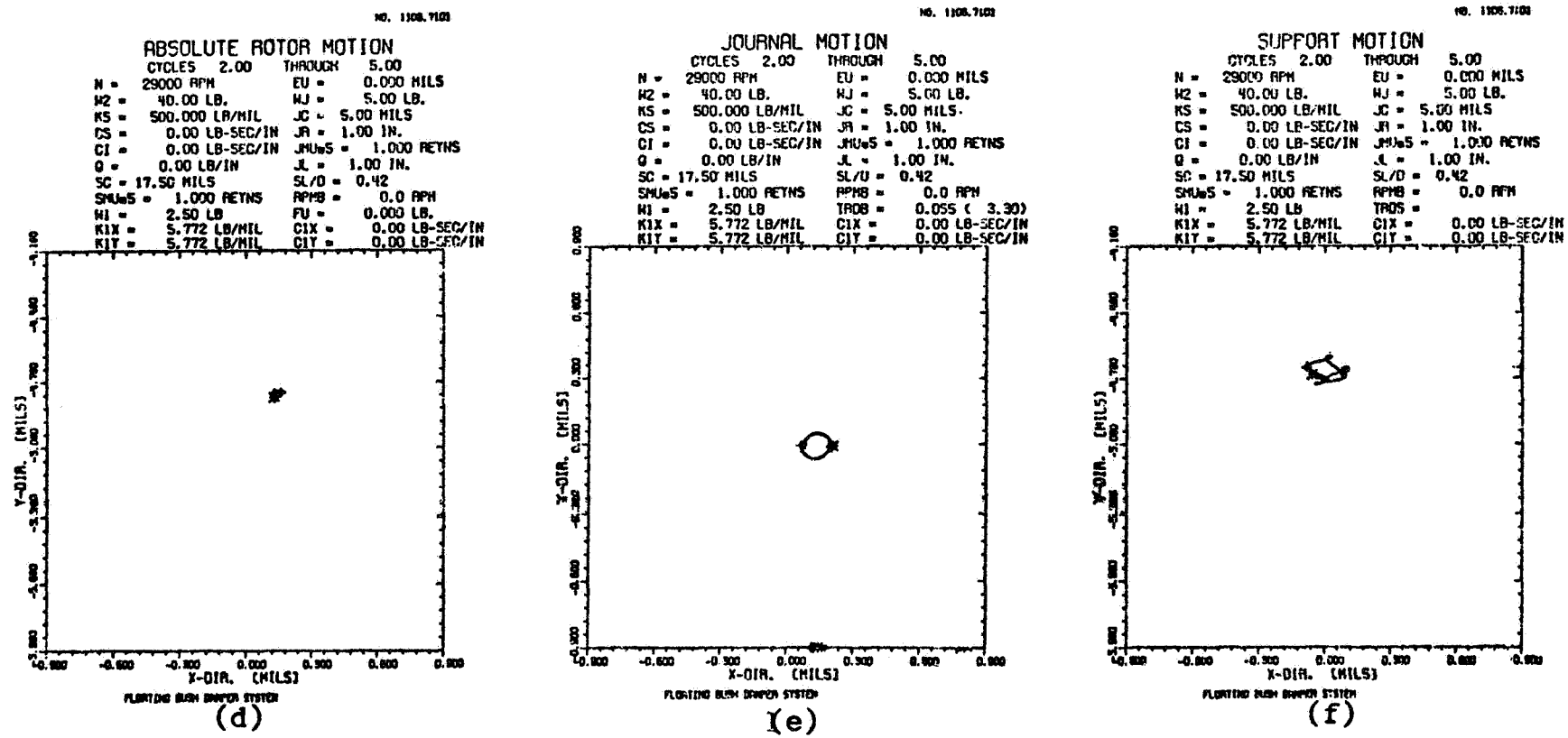

FIG. 6.8(d) ABSOLUTE ROTOR MOTION FOR CYCLES TWO THROUGH FIVE (N=29,000, K_S=500LB/MIL)
(e) JOURNAL RELATIVE MOTION
(f) DAMPER SUPPORT TRANSIENT RESPONSE (CLEARANCE=17.5MILS)

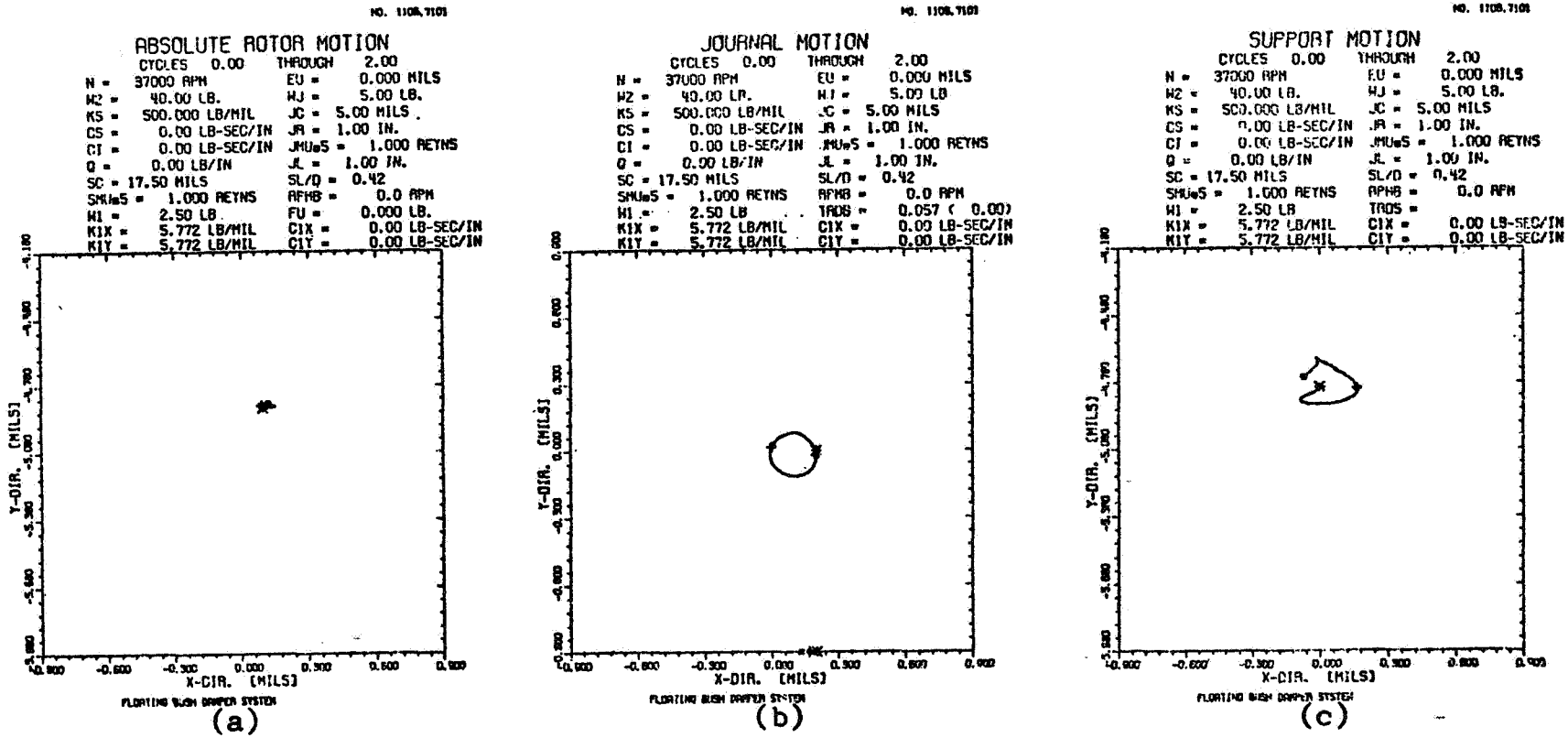

FIG. 6.9(a) ABSOLUTE ROTOR MOTION FOR TWO CYCLES (N=37,000RPM, K_S=500,000)
(b) JOURNAL RELATIVE MOTION ABOVE STABILITY THRESHOLD SHOWING HALF-FREQUENCY WHIRL
(c) DAMPER SUPPORT TRANSIENT RESPONSE (CLEARANCE=17.5MILS)

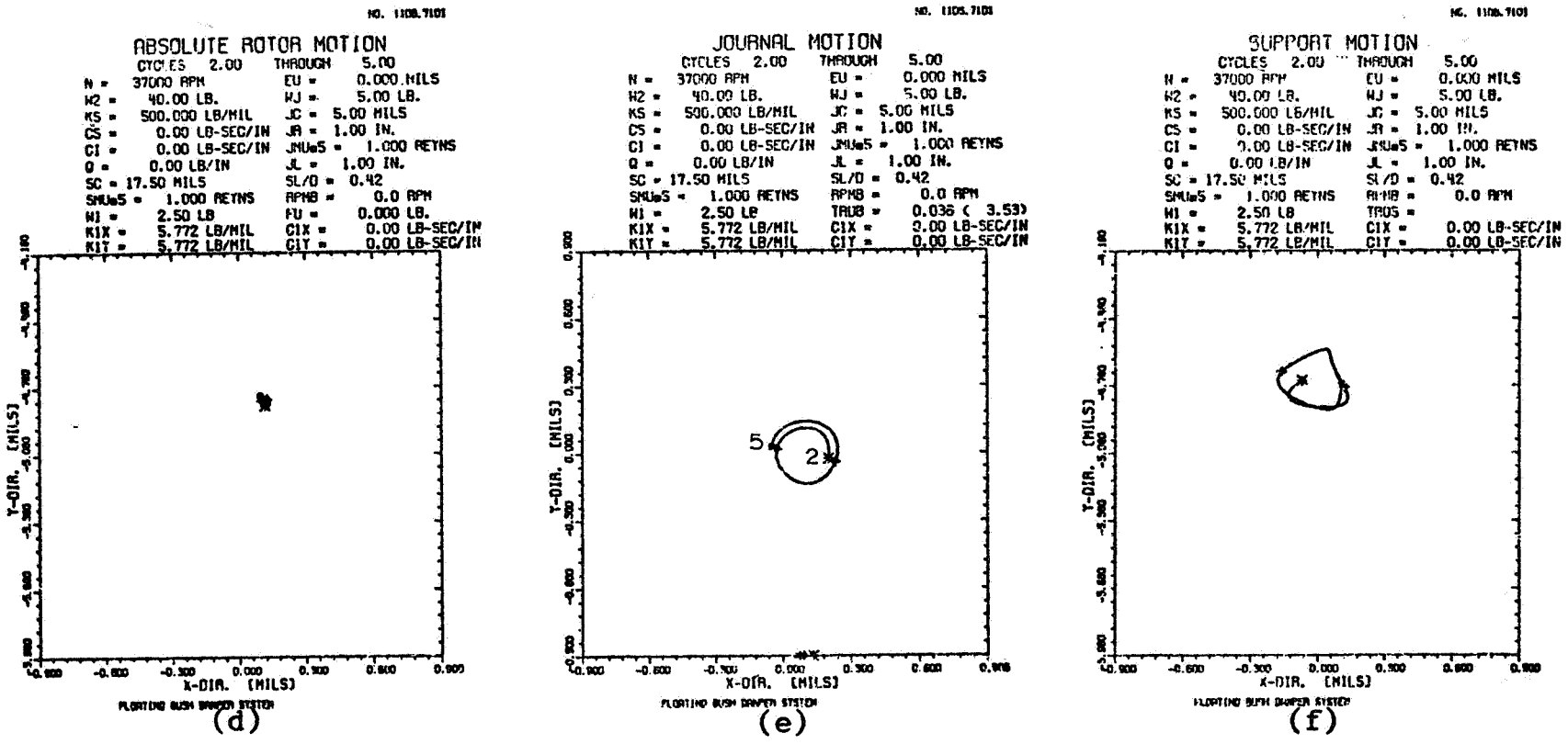

FIG. 6.9(d) ABSOLUTE ROTOR MOTION FOR CYCLES TWO THROUGH FIVE (N=37,000RPM, K_S=500LB/MIL)
(e) JOURNAL RELATIVE MOTION SHOWING UNSTABLE HALF-FREQUENCY WHIRL
(f) DAMPER SUPPORT SUSTAINED WHIRL (CLEARANCE=17.5MILS)

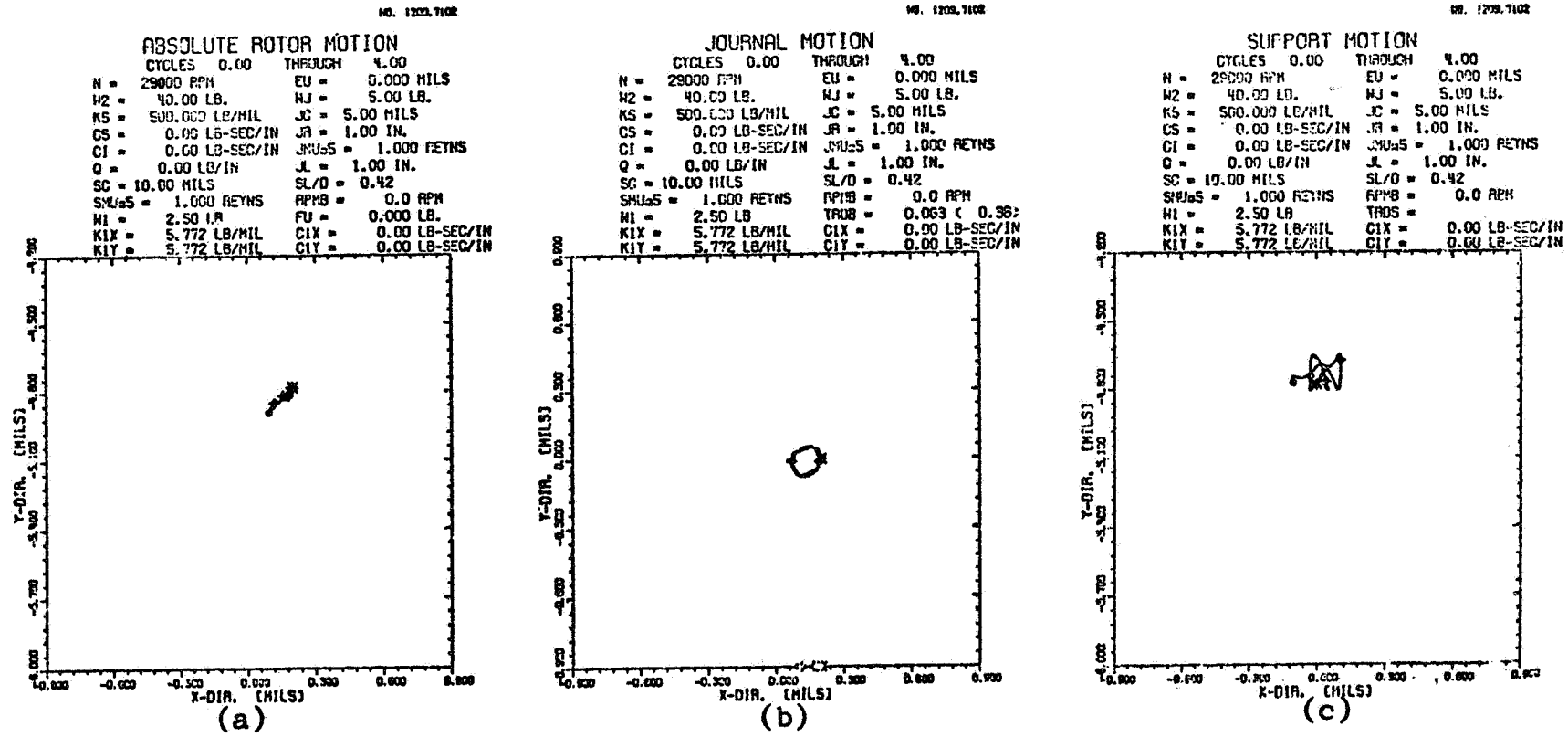

FIG. 6.10(a) ABSOLUTE ROTOR TRANSIENT FOR FOUR CYCLES (N=29,000RPM, K_S=500LB/MIL,
(b) JOURNAL RELATIVE MOTION IN UNSTABLE REGION OF STABILITY MAP
(c) DAMPER SUPPORT RESPONSE (CLEARANCE=10MILS)

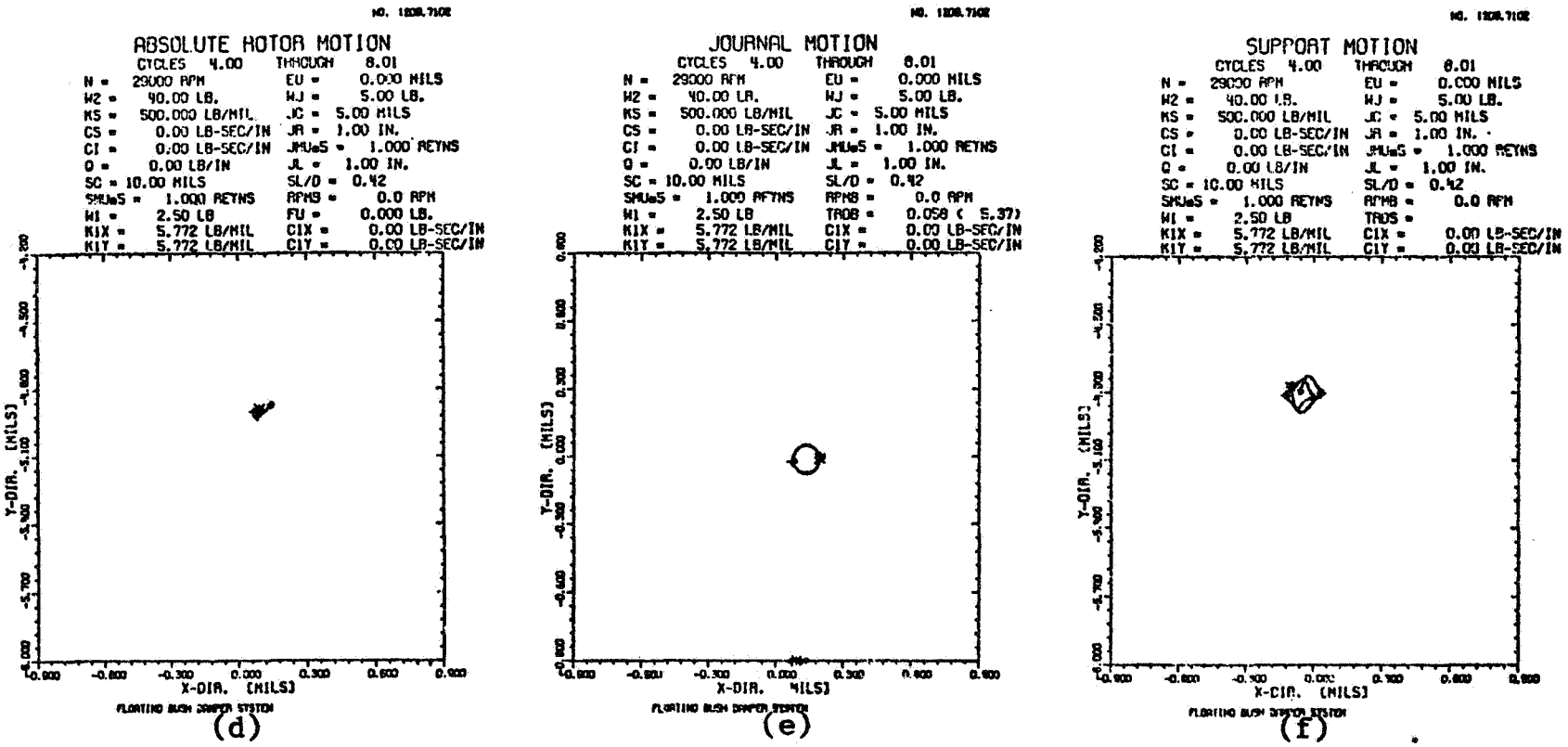

FIG. 6.10(d) ABSOLUTE ROTOR MOTION FOR CYCLES FOUR THROUGH EIGHT(N=29,000RPM, K_S=500LB/MIL)
(e) JOURNAL RELATIVE MOTION INDICATING SUSTAINED HALF-FREQUENCY WHIRL
(f) DAMPER SUPPORT RESPONSE (CLEARANCE=10MILS)

does have a sustained whirl even though the limit cycle is very small, and verifies the predicted instability.

When the bush clearance is reduced to 5 mils the same type limit cycle motion for the journal is indicated in Fig. 6.11(b) and the bush motion of 6.11(c) indicates less stability than for the 10 mil damper. To demonstrate how the damper has improved the rotor motion a rigid support case for five cycles of motion was computed (see Fig. 6.12). The rotor and journal spiral outward in a very unstable whirl orbit after the initial drop of the rotor and lift of the journal to achieve the proper rotor-journal force balance.

The flexible rotor ($\delta/c = 1.6$) has the same upper threshold as the rigid rotor for the larger clearance values. The same speeds of 29,000 and 37,000 RPM were run for four cycles beginning from the end conditions of the rigid rotor case (plus a static bow for the flexible shaft). These orbits appear in Fig. 6.13(d) - (f) where the journal relative motion is observed to go into the half-frequency whirl above the predicted threshold speed. The bush motion is considerably larger than in the rigid rotor case but the rotor is noted to be seeking another position than the one given as a starting condition. Fig. 6.14(a) and 6.14(b) indicate the unstable journal motion for rigid supports and the fact that the rotor motion has not gone unstable during these five cycles of motion. The damper support has improved the response a great deal as compared to the whirl orbit obtained on the rigid supports.

In order that the lower region of instability could be verified the 17.5 mil bush damper was tested. The system specifications appear in Table 6.1 and the information in Table 6.2 indicates an unstable whirl

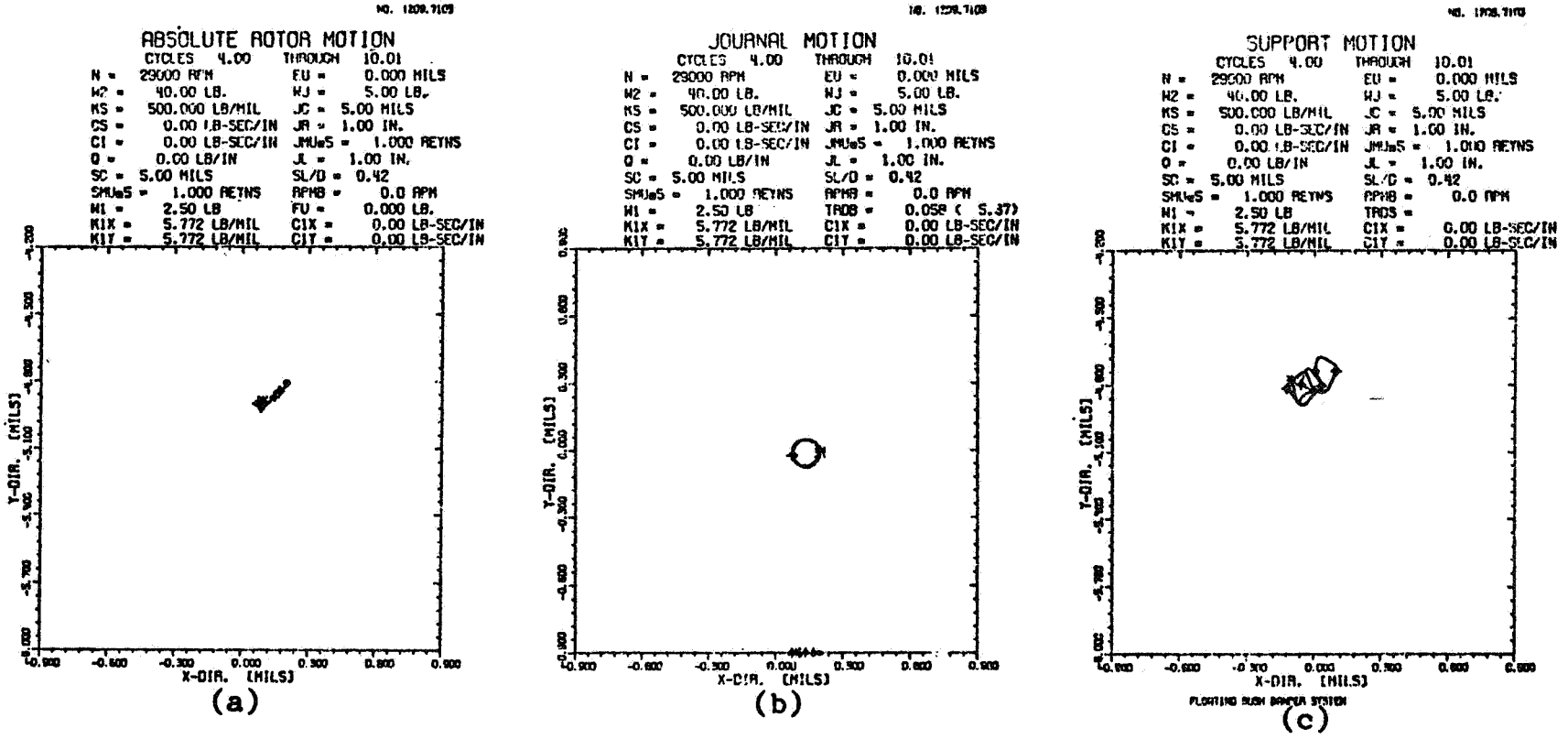

FIG. 6.11(a) ABSOLUTE ROTOR MOTION FOR CYCLES FOUR THROUGH EITHT(N=29,000RPM, K_S=500LB/MIL)
(b) JOURNAL RELATIVE MOTION
(c) DAMPER SUPPORT TRANSIENT RESPONSE (CLEARANCE=5MILS)

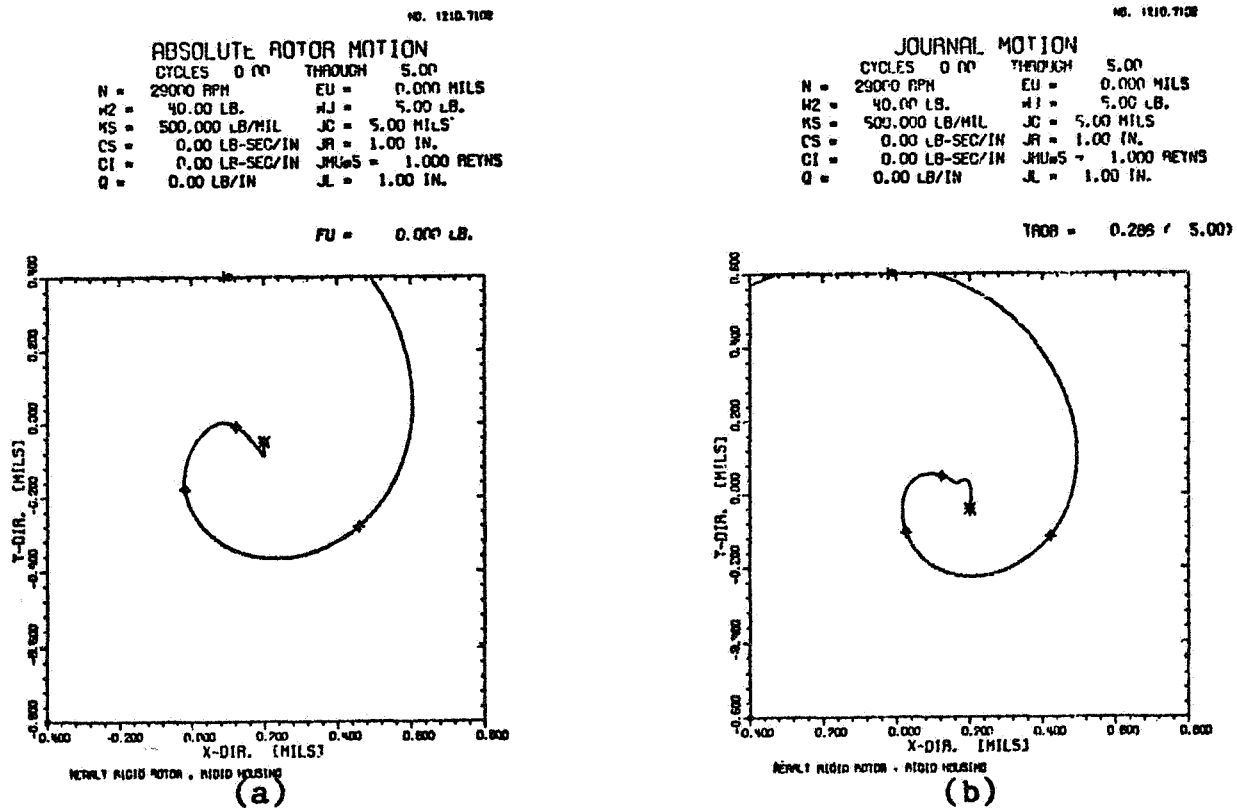

FIG. 6.12(a) ABSOLUTE ROTOR TRANSIENT FOR INITIAL DISPLACEMENT PERTUBATION (N=29,000RPM, K_S=500LB/MIL, RIGID DAMPER SUPPORT

(b) JOURNAL TRANSIENT SHOWING HIGHLY UNSTABLE SYSTEM AFTER INITIAL RESPONSE TO PERTUBATION

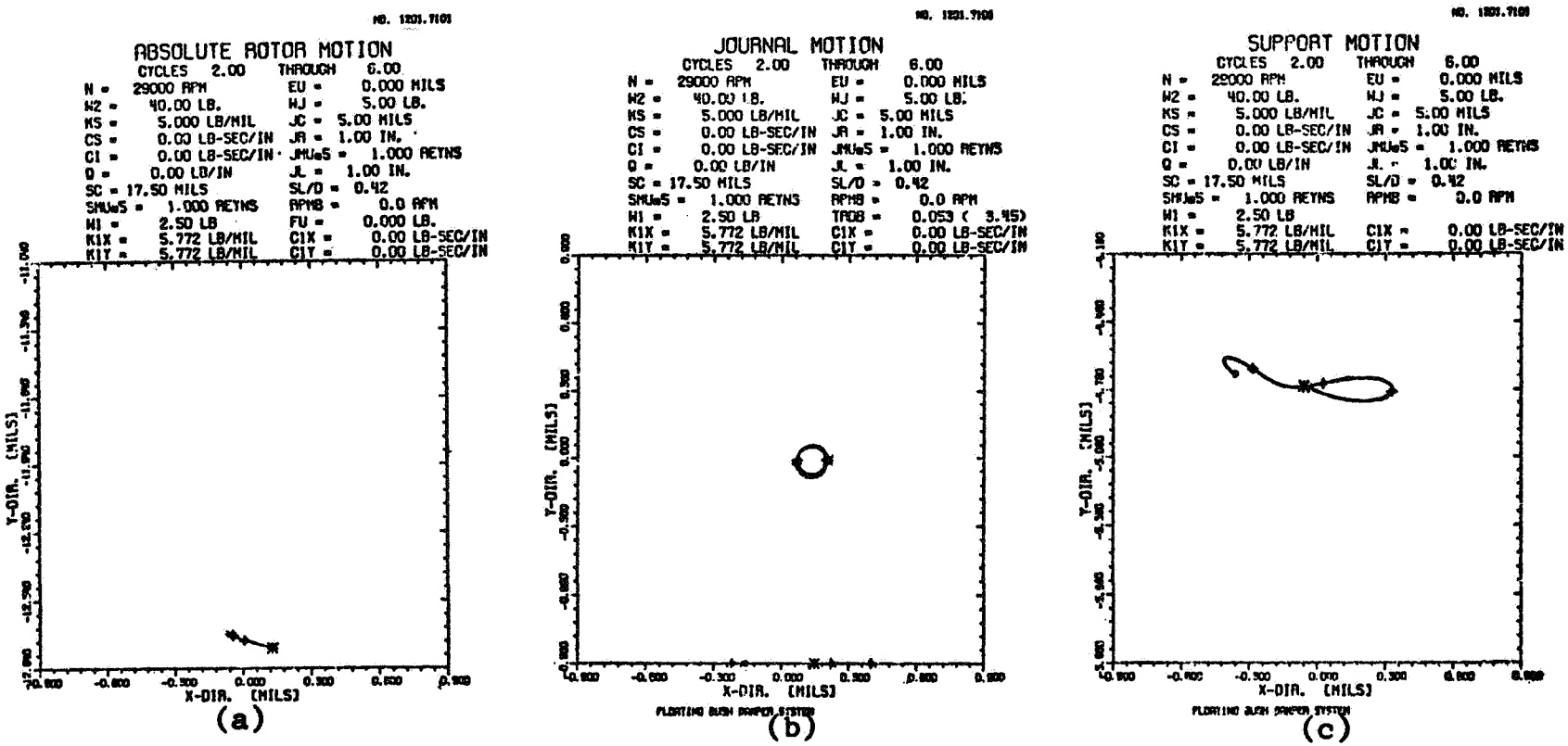

FIG. 6.13(a) ABSOLUTE ROTOR RESPONSE FOR CYCLES TWO THROUGH SIX (N=29,000RPM, K_S=5LB/MIL)
(b) JOURNAL RELATIVE MOTION FOR STABLE RESPONSE PORTION OF STABILITY MAP
(c) DAMPER SUPPORT TRANSIENT (CLEARANCE=17.5MILS)

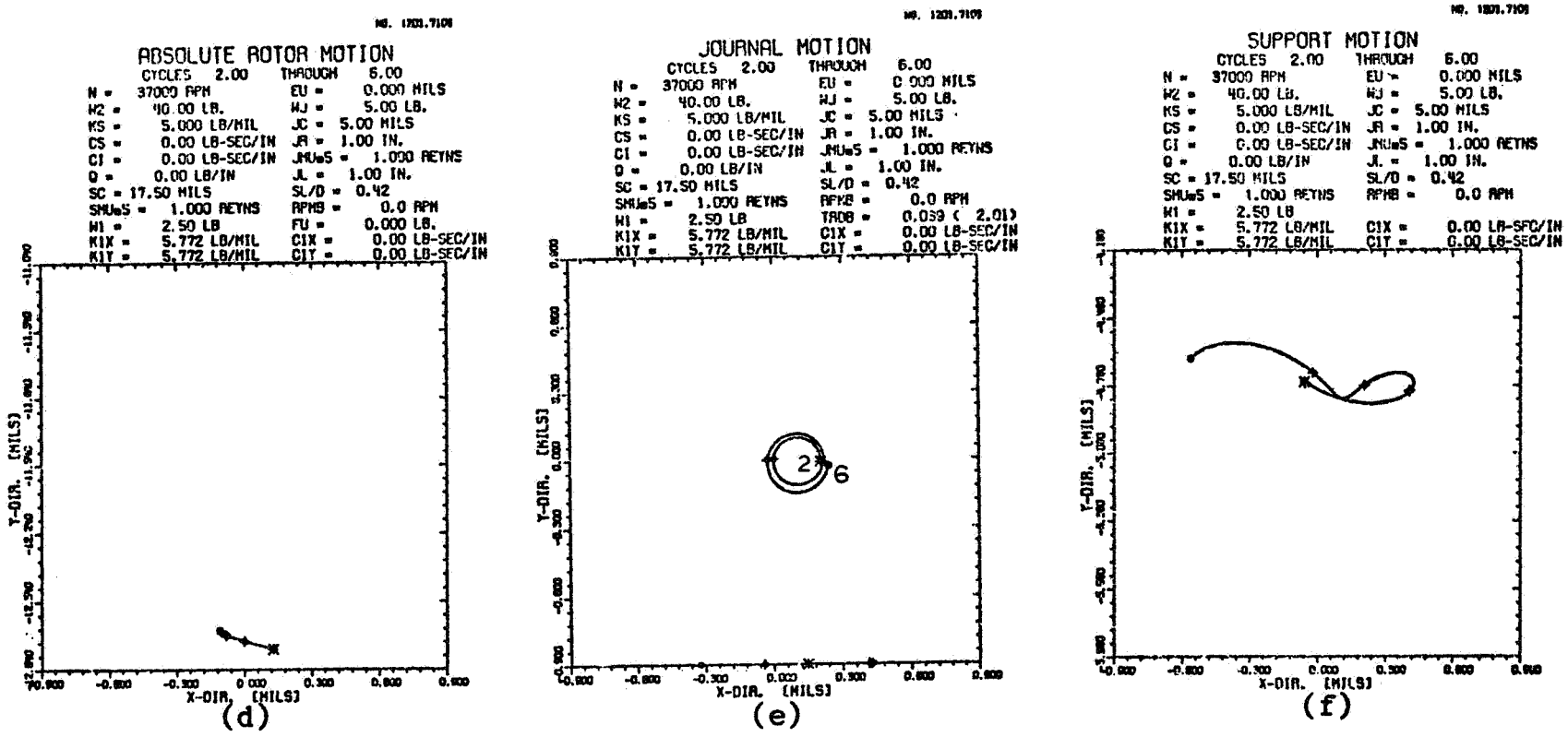

FIG. 6.13(d) ABSOLUTE ROTOR RESPONSE FOR CYCLES TWO THROUGH SIX (N=37,000RPM, K_S=5LB/MIL)
(e) JOURNAL RELATIVE MOTION INDICATING AN UNSTABLE HALF-FREQUENCY WHIRL
(f) DAMPER SUPPORT TRANSIENT RESPONSE (CLEARANCE=17.5MILS)

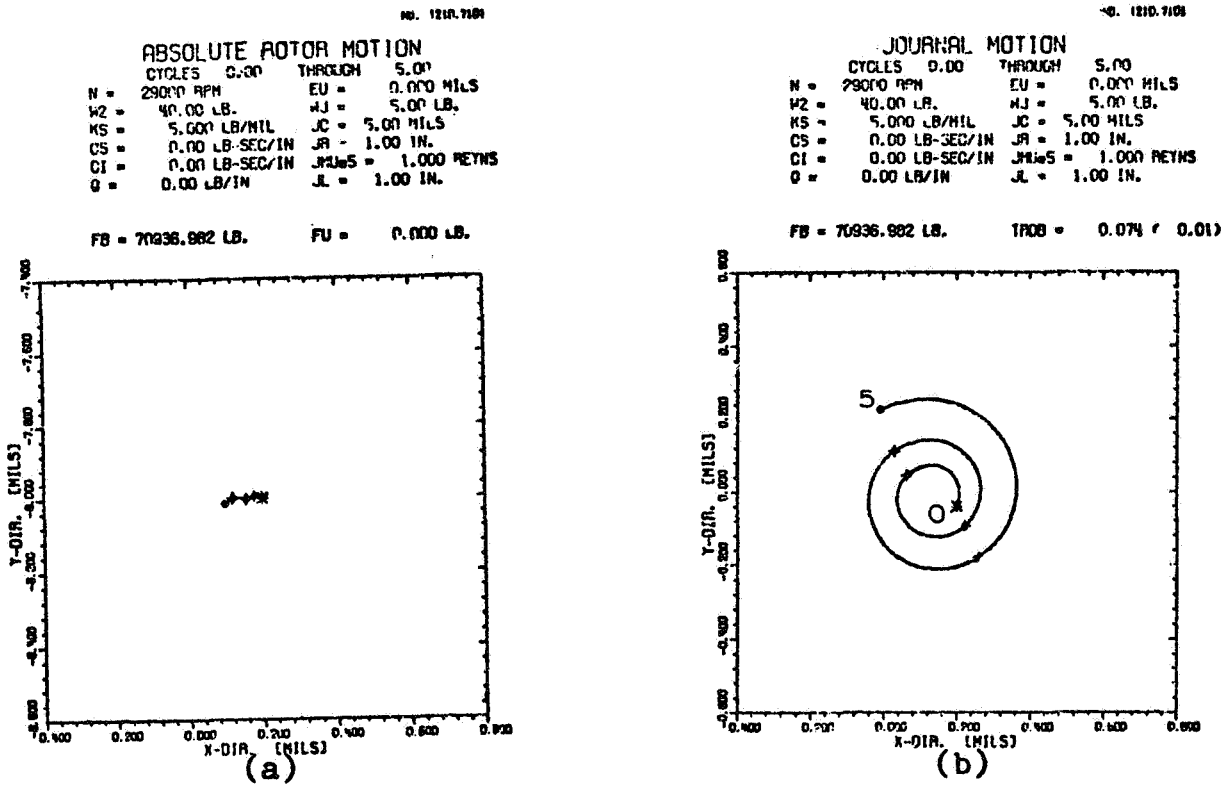

FIG. 6.14(a) ABSOLUTE ROTOR RESPONSE (N=29,000RPM, K_S=5LB/MIL, RIGID DAMPER SUPPORT)
(b) JOURNAL TRANSIENT SHOWING UNSTABLE HALF-FREQUENCY WHIRL

STABILITY ANALYSIS OF THE FLOATING BUSH DAMPER

ROTOR SPECIFICATIONS

W2 = 40.00 LB. CS = 0.00 LB-SEC/IN Q = 0.0 LB/IN

KS = 5000.0 LB/IN. IC = 0.00 LB-SEC/IN

ORDER = 12

ODR = 12

JOURNAL BEARING SPECIFICATIONS

WJ = 5.00 LB. RJ = 1.0 IN. MUJ = 1.000E-05 REYNS

CJ = .0050 IN. LJ = 1.0 IN.

FLOATING BUSH SPECIFICATIONS

WB = 2.50 LB. RB = 1.20 IN. MUB = 1.000E-05 REYNS

CB = .0175 IN. LB = 1.00 IN.

PRELOAD-X = 0.00

PRELOAD-Y = 0.00

K1XX = 5772.0 LB/IN

K1YY = 5772.0 LB/IN

STEADY-STATE POSITION

ROTOR

X2S = .7438 MILS

Y2S = -12.9096 MILS

DLTA = 1.6000

JOURNAL

XRJ = .7438 MILS

YRJ = -.1452 MILS

BUSH

XBS = 0.0000 MILS

YBS = -4.7644 MILS

CD	CD/CJ	THR.SPEED-W	W/SQRT(G/CJ)	ECCEN.-J	KONTBI	KOUNT
.0175	3.500	4774.7	1.80	.152	0	0

TABLE 6.1 FLOATING BUSH DAMPER ROTOR SYSTEM SPECIFICATIONS

MATRIX FOR SQUEEZE DAMPER

1.036270-03	0.	0.	0.	0.	0.	0.	
0.	0.	0.	0.	0.	0.	0.	
5.000000D+01	0.	-5.000000D+01	0.	0.	0.	0.	
0.	1.036270-03	0.	0.	0.	0.	0.	
0.	0.	0.	0.	0.	0.	0.	
0.	5.000000D+01	0.	-5.000000D+01	0.	0.	0.	
0.	0.	1.295340-04	0.	0.	0.	0.	
0.	0.	1.353490+00	-2.627780-01	-1.353490+00	2.627780-01		
-2.500000D+01	0.	1.532540+02	3.280320+02	-1.282540+02	-3.280320+02		
0.	0.	0.	1.295340-04	0.	0.	0.	
0.	0.	-2.627780-01	1.401760+00	2.627780-01	-1.401760+00		
0.	-2.500000D+01	-3.607790+02	9.282200+01	3.607790+02	-6.782200+01		
0.	0.	0.	0.	6.476630-05	0.		
0.	0.	-1.353490+00	2.627780-01	1.392990+00	-2.627130-01		
0.	0.	-1.282540+02	-3.280320+02	1.853740+02	3.280320+02		
0.	0.	0.	0.	0.	6.476680-05		
0.	0.	2.627780-01	-1.401760+00	-2.772670-01	1.480650+00		
0.	0.	3.607790+02	-6.782200+01	-3.607790+02	1.255420+02		

CHARACTERISTIC EQUATION
GIVEN IN FORM A0 + A1*L + A2*L**2 + ... A13*L**12)

1.058160+12	4.360740+09	9.175090+07	3.119300+05	2.684320+03	6.770450+00	2.935270-02
4.221750-05	9.366620-08	6.548040-11	8.047990-14	4.961140-16	7.558160-23	

COEFFICIENTS IN REVERSE NORMALIZED FORM

1.000000+00	6.563050+04	1.064810+09	8.663540+11	1.239270+15	5.585690+17	3.883580+20
8.957790+22	3.551550+25	4.127060+27	1.213930+30	5.769570+31	1.400030+34	

SCFA = 1.0000+02

THE ROOTS OF THE CHAR. EQ. ARE AS FOLLOWS

-9.1057342D+00	-1.7935246D+02	-1712.7 RPM.	-.3587
-9.1057342D+00	1.7935246D+02	1712.7 RPM.	.3587
-1.9423393D+02	-6.2262232D+02	-5945.6 RPM.	-1.2452
-1.9423393D+02	6.2262232D+02	5945.6 RPM.	1.2452
3.4230435D+00	-1.7412073D+02	-1662.7 RPM.	-.3482
3.4230435D+00	1.7412073D+02	1662.7 RPM.	.3482
-8.9968972D+01	-2.6193213D+02	-2501.3 RPM.	-.5239
-8.9968972D+01	2.6193213D+02	2501.3 RPM.	.5239
-9.9358807D+01	-6.5047527D+02	-6211.6 RPM.	-1.3010
-9.9358807D+01	6.5047527D+02	6211.6 RPM.	1.3010
-2.6216727D+04	0.	0.0 RPM.	0.0000
-3.8644246D+04	0.	0.0 RPM.	0.0000

TABLE 6.2 STABILITY ANALYSIS DATA FOR AN UNSTABLE DAMPER SUPPORT SYSTEM

of 0.35 when the running speed is 4775 RPM. This information was obtained from the stability program SDSTB. The transient program response plots are presented in Fig. 6.15(a) - (i) where cycles 0-2 were started from approximate steady-state conditions and show no large transients. Figs. 6.15(d), (e), (f) for cycles 2-6 indicate a large whirl developing at the rotor and support with the journal loosing some of its load capacity (Fig. 6.15(e)) due to the whirl of the bush as indicated in Fig. 6.15(f). Cycles 6 through 10 indicate a sustained whirl of the rotor and bush at slightly over one-third as shown by the timing marks (this was as predicted by SDSTB - Table 6.2). Note that the journal relative motion is actually very "stable" in this mode of operation (Fig. 6.15(h)) and is thus tracking out the same motion as the bush damper ie., ≈ 1/3 whirl rate).

For a speed ratio of 4.52 (12,000 RPM) the system is stable as indicated by Fig. 6.7. The transient response for both a large initial displacement of the journal and a very small pertubation were calculated and are given in Figs. 6.16 and 6.17. For a large pertubation the damper response is not readily reducing. The journal decreases initially (Fig. 6.16(b)) but has a sustained limit cycle due to the bush transient motion. Fig. 6.16(k) indicates that after 16 cycles the journal relative motion is very slowly reducing in amplitude whereas the rotor and bush (support) motion has a relatively large motion. However these are not in phase as they were for the case of 4775 RPM (unstable condition). Figs. 6.17(a) - (f) indicate eight cycles of motion at 12,000 RPM for a very small pertubation. The motion is considerably more stable than

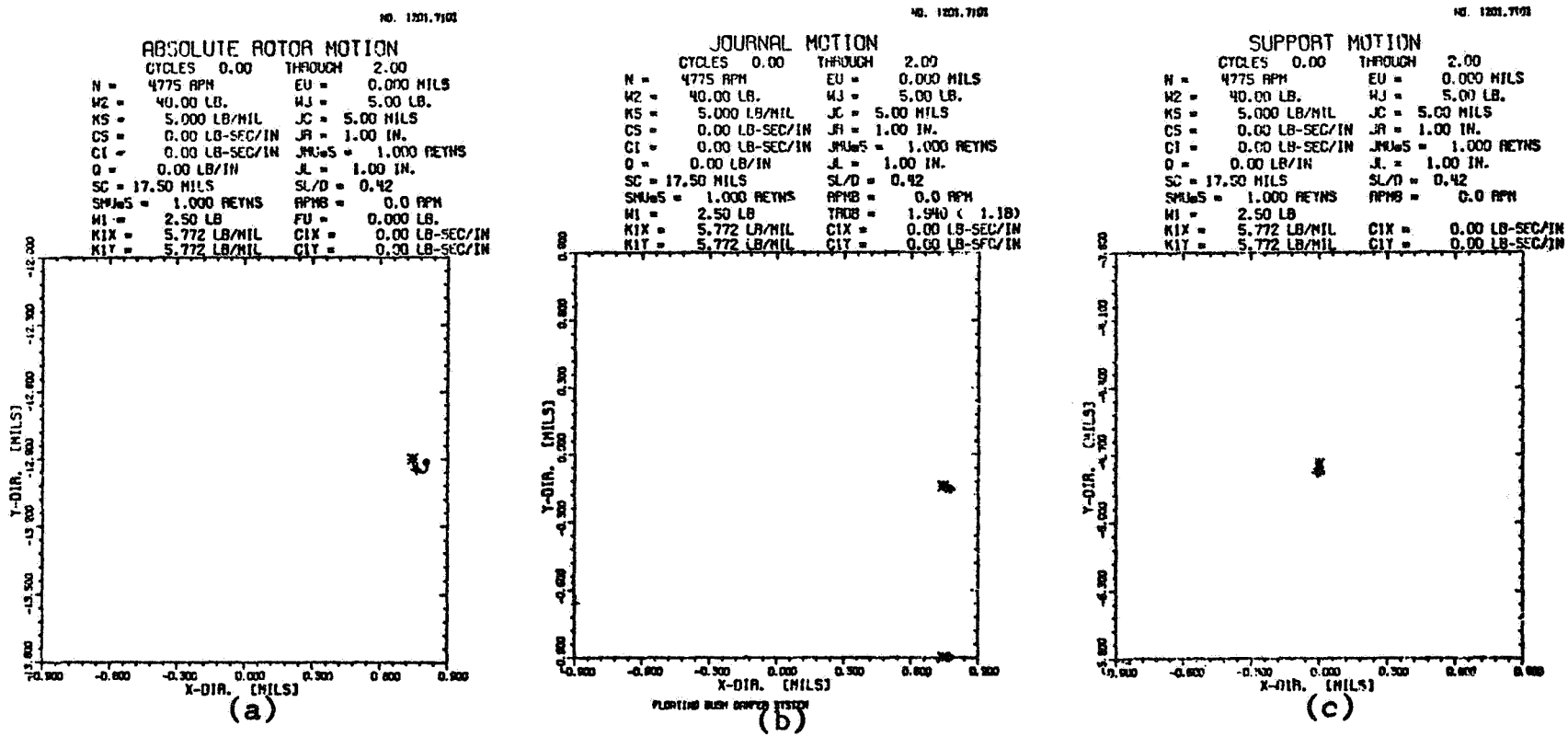

FIG. 6.15(a) ABSOLUTE ROTOR MOTION FOR TWO CYCLES (N=4,775RPM, K_S=5LB/MIL)
(b) JOURNAL TRANSIENT
(c) DAMPER SUPPORT TRANSIENT (CLEARANCE=17.5MILS)

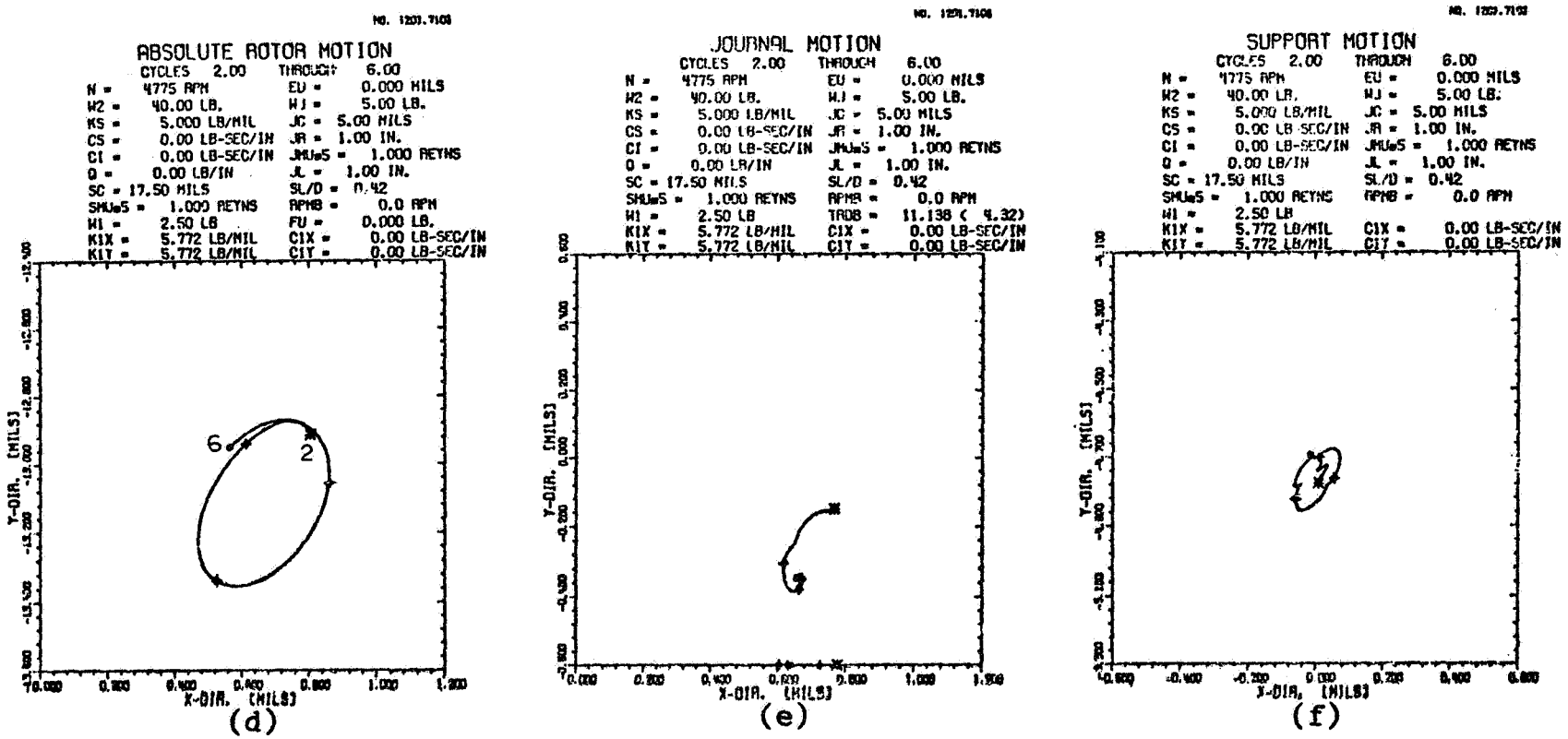

FIG. 6.15(d) ABSOLUTE ROTOR TRANSIENT WHIRL FOR CYCLES TWO THROUGH SIX (N= 4,775RPM, K_S=5LB/MIL)
(e) JOURNAL RELATIVE TRANSIENT SHOWING NEW RELATIVE EQUILIBRUM POSITION
(f) DAMPER SUPPORT TRANSIENT MOTION (CLEARANCE=17.5MILS)

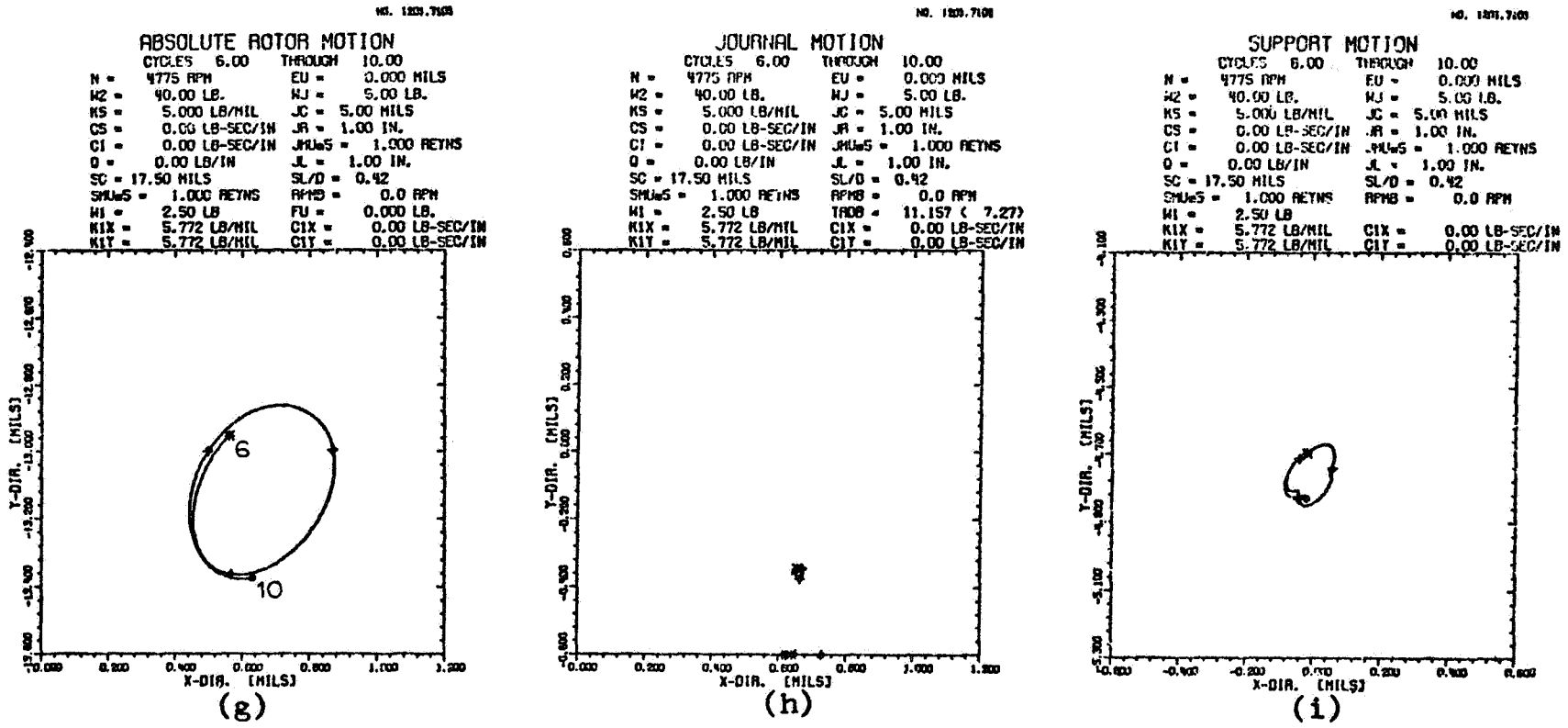

FIG. 6.15(g) ABSOLUTE ROTOR MOTION FOR CYCLES SIX THROUGH TEN (N=4,775RPM, K_S=5LB/MIL)
(h) JOURNAL RELATIVE MOTION SHOWING STABLE JOURNAL FLUID-FILM (RELATIVE TO SUPPORT)
(i) DAMPER MOTION INDICATING SUSTAINED 35% WHIRL AS PREDICTED BY STABILITY ANALYSIS

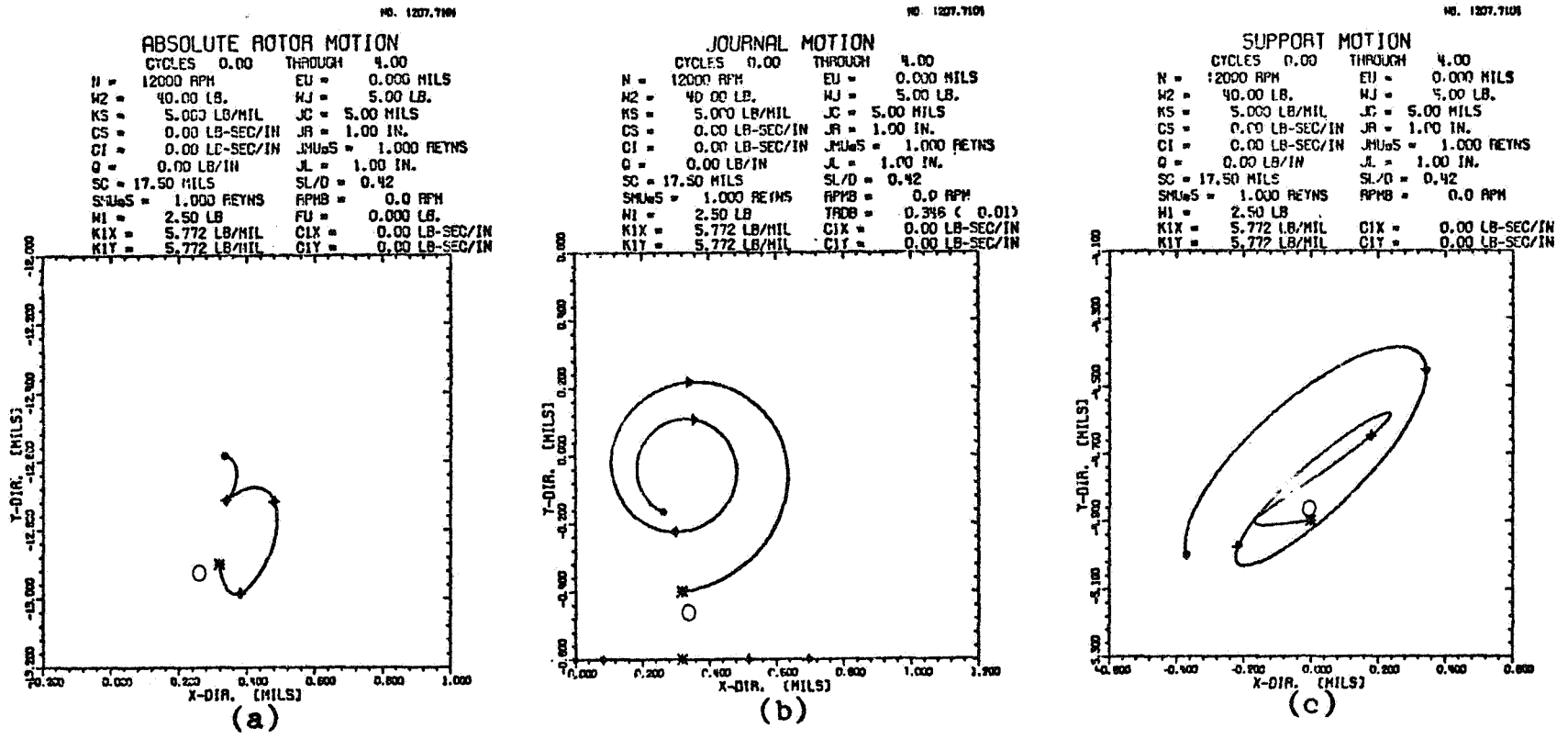

FIG. 6.16(a) ABSOLUTE ROTOR MOTION FOR FOUR CYCLES (N=12,000RPM, K_S=5LB/MIL)
(b) JOURNAL RELATIVE MOTION FOR LARGE INITIAL DISPLACEMENT PERTUBATION
(c) DAMPER TRANSIENT RESPONSE (CLEARANCE=17.5MILS)

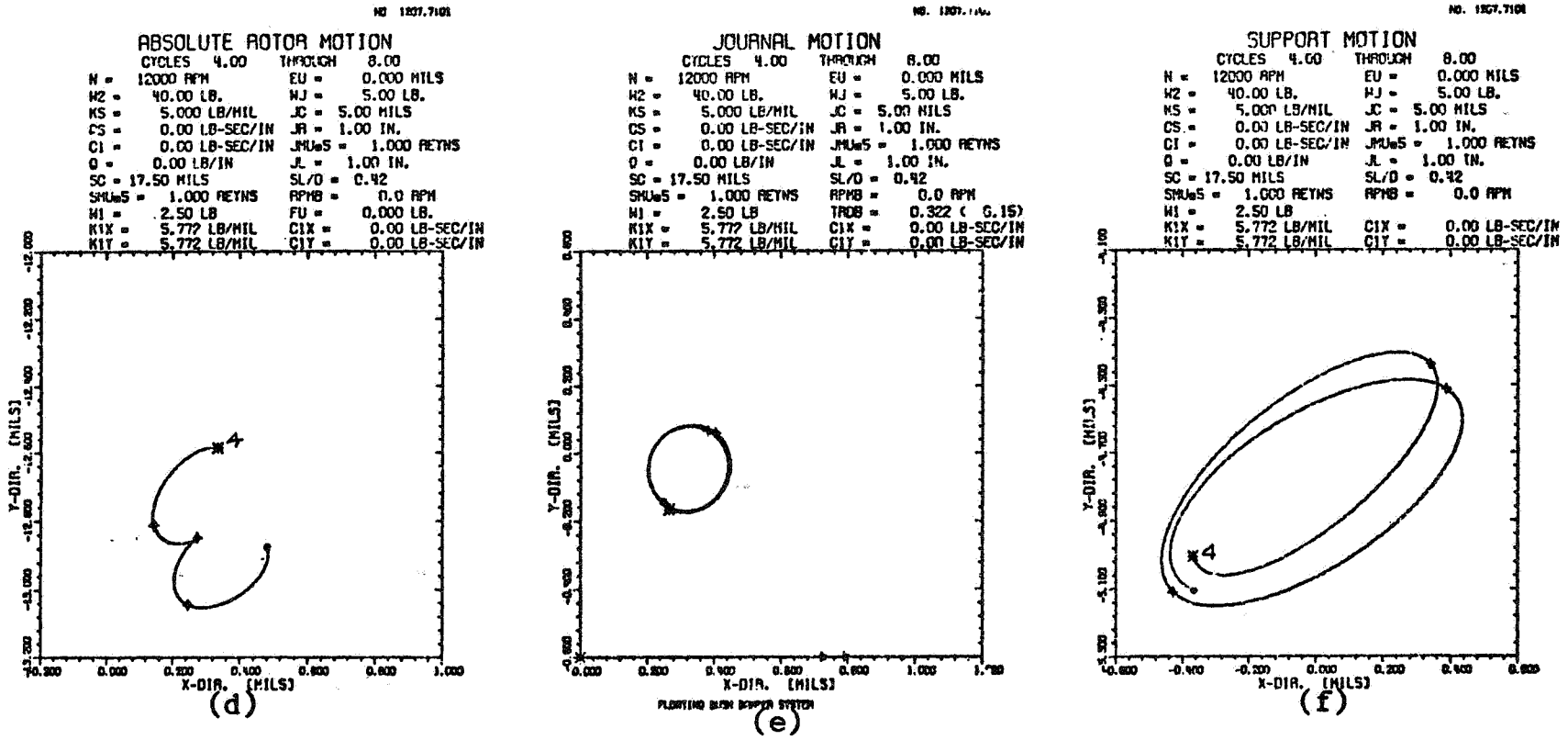

FIG. 6.16(d) ABSOLUTE ROTOR MOTION FOR CYCLES FOUR THROUGH EIGHT (N=12,000RPM, K_S=5LB/MIL)
(e) JOURNAL TRANSIENT LIMIT CYCLE INDICATING HALF-FREQUENCY WHIRL
(f) DAMPER TRANSIENT WHIRL

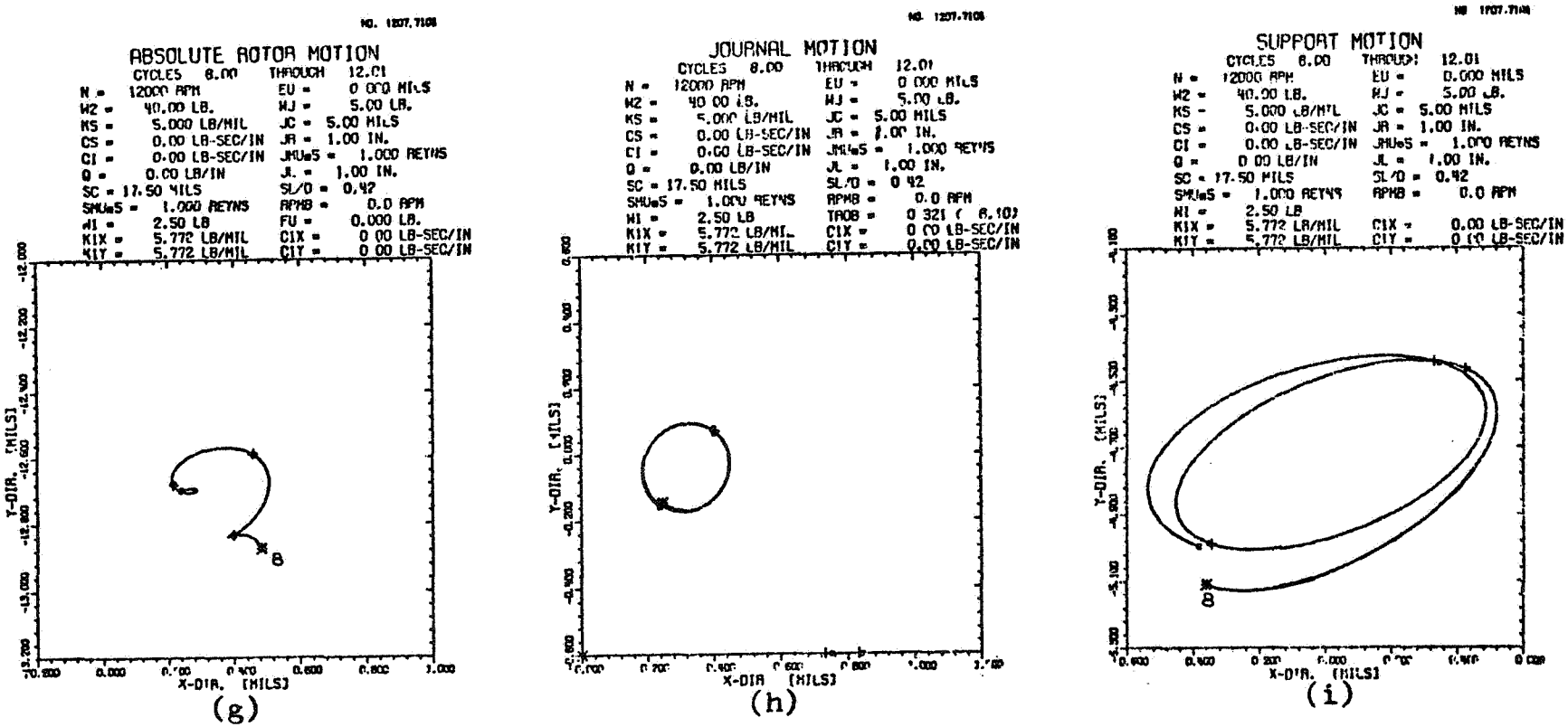

FIG. 6.16(g) ABSOLUTE ROTOR TRANSIENT FOR CYCLES EIGHT THROUGH TWELVE (N= 12,000, K_S=5LB/MIL)
(h) JOURNAL SUSTAINED LIMIT CYCLE
(i) DAMPER TRANSIENT WHIRL

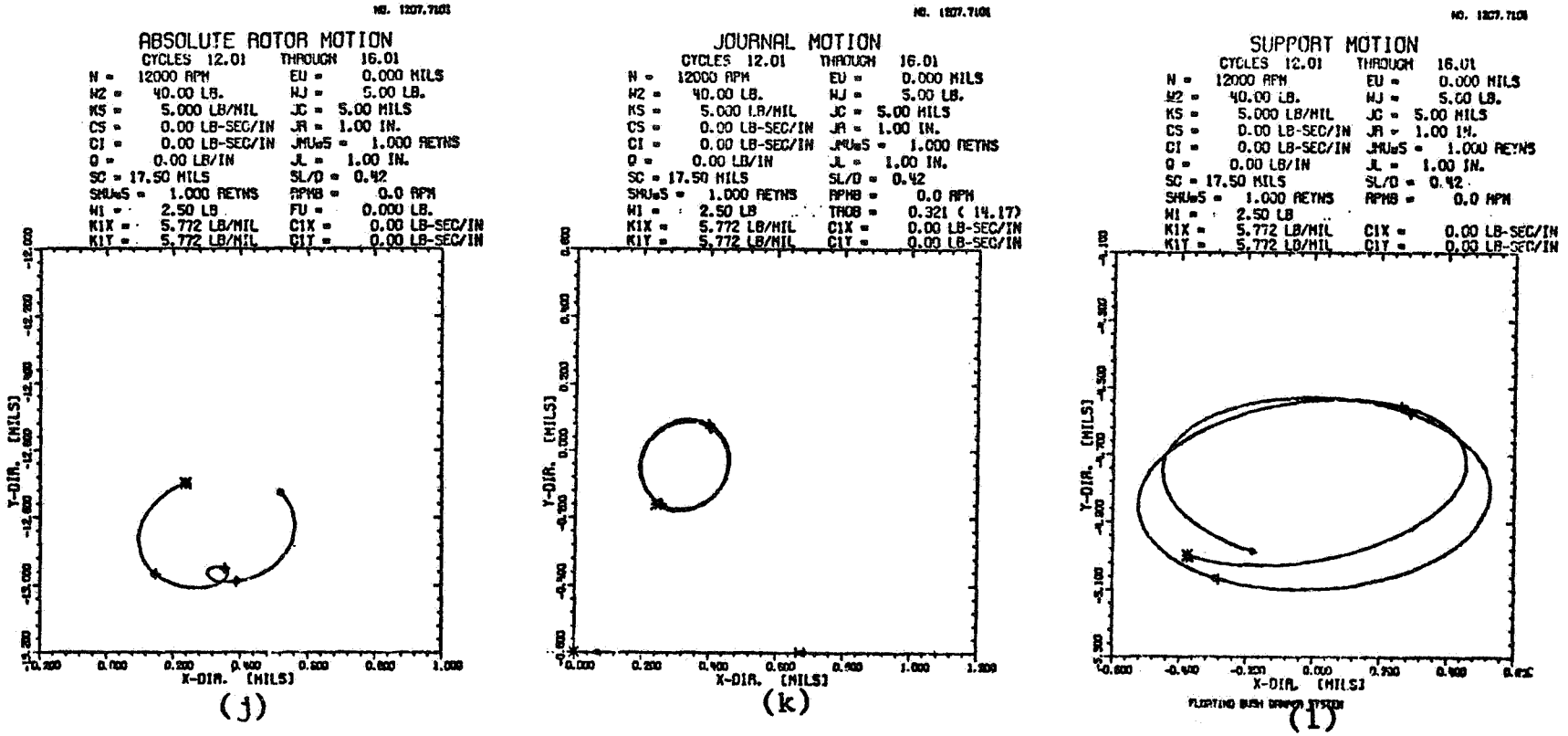

FIG. 6.16(j) ABSOLUTE ROTOR MOTION FOR CYCLES TWELVE THROUGH SIXTEEN (N= 12,000RPM, K_S=5LB/MIL)
(k) JOURNAL ORBIT
(l) DAMPER SUSTAINED WHIRL TRANSIENT MOTION

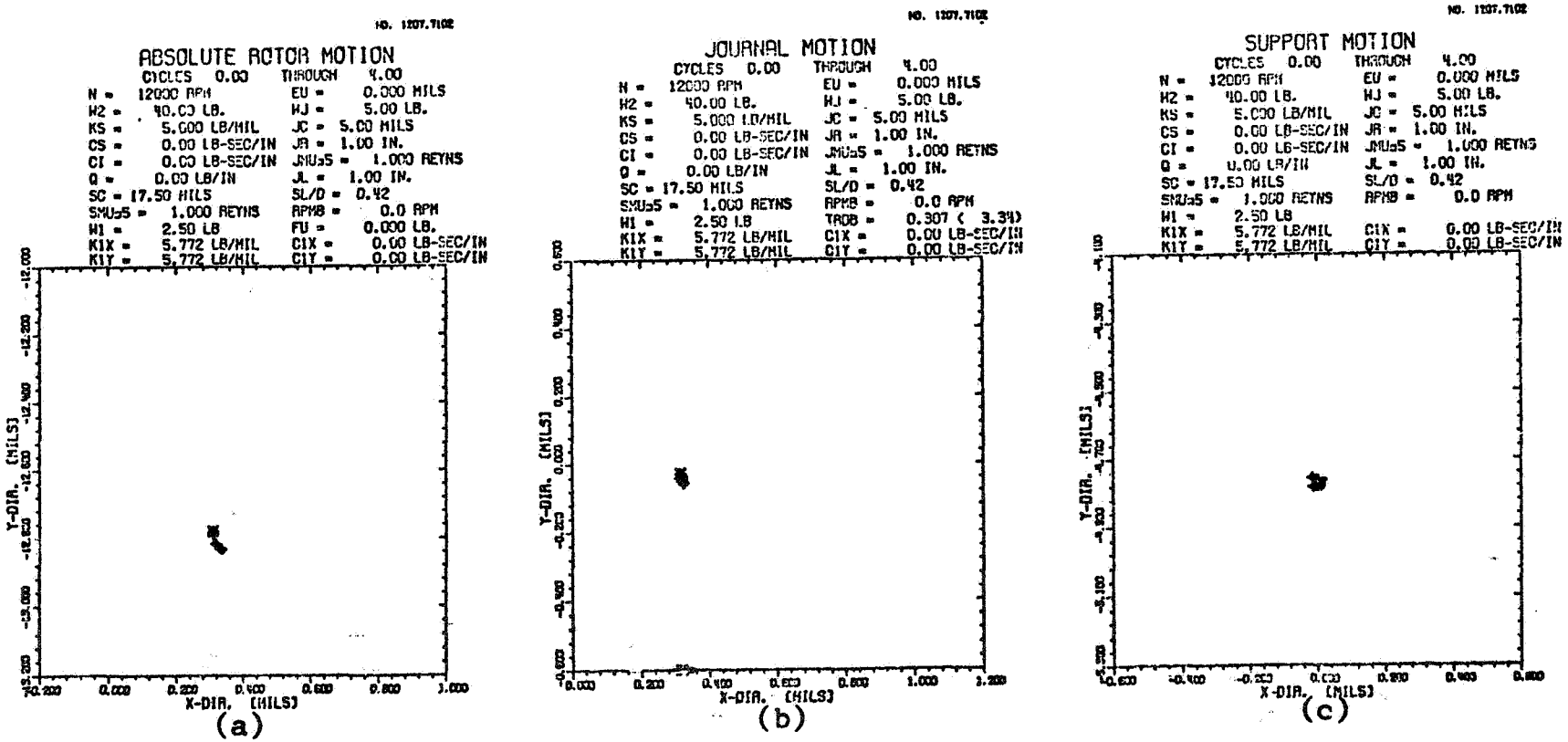

FIG. 6.17(a) ABSOLUTE ROTOR MOTION FOR FOUR CYCLES (N=12,000, K_S=5LB/MIL)
(b) JOURNAL TRANSIENT FOR SMALL INITIAL PERTUBATION
(c) DAMPER SUPPORT TRANSIENT (CLEARANCE=17.5MILS)

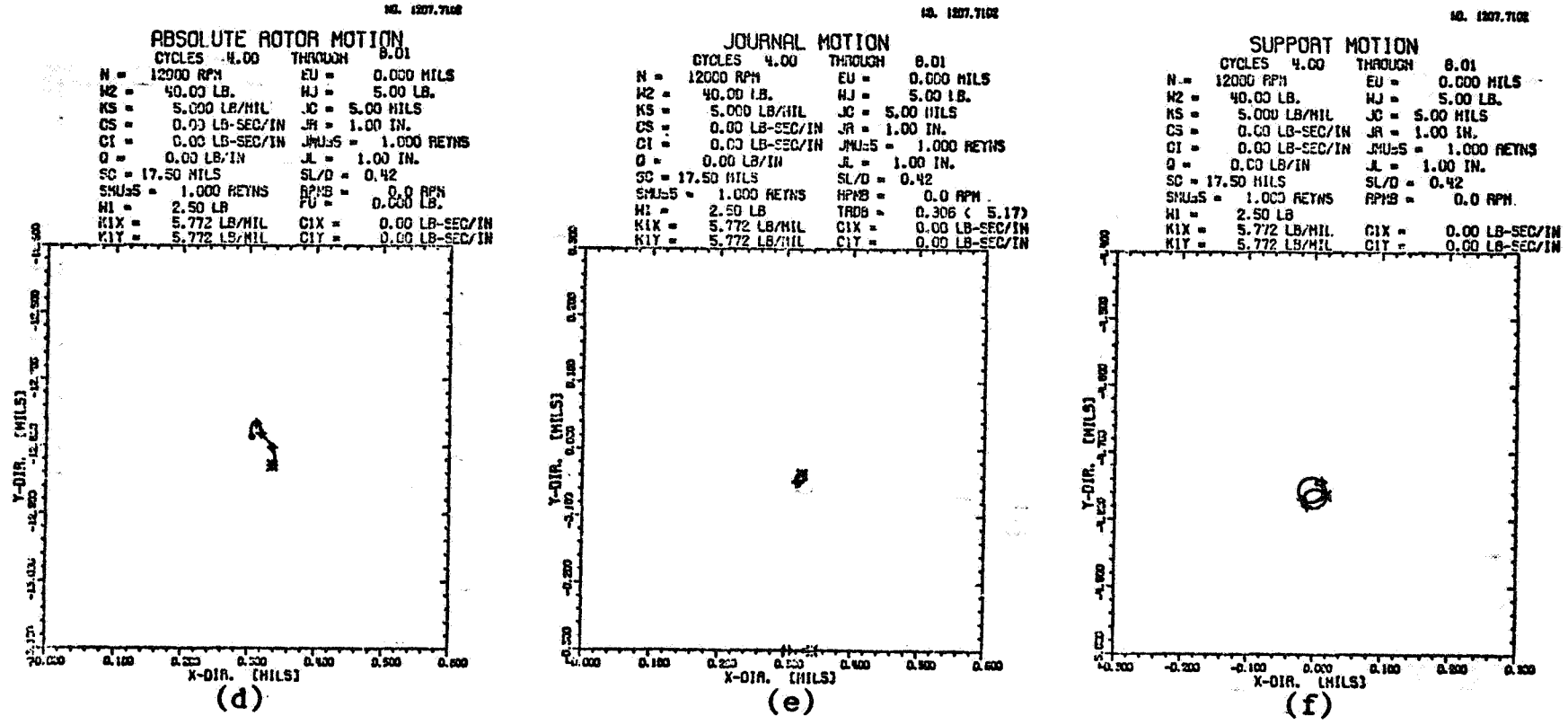

FIG. 6.17(d) ABSOLUTE ROTOR TRANSIENT FOR CYCLES FOUR THROUGH EIGHT (N= 12,000RPM, K_S=5LB/MIL)
(e) JOURNAL TRANSIENT RESPONSE
(f) DAMPER SUPPORT TRANSIENT SHOWING SMALL ORBITING DUE TO SMALL INITIAL PERTUBATION

for the large pertubation but the bush damper and rotor are giving some initial motion. The motion would eventually reduce to the steady-state equilibrium position as predicted by the stability analysis.

The sustained transient due to the large pertubation in what should be a stable system is the greatest drawback to squeeze damper design. This type of performance could be catastrophic in an actual rotor system.

CHAPTER VII

CONCLUSIONS

7.1 The Importance of Analytic Simulation

Due to the ease of manufacture and installation of plain journal bearings in pumps, transmissions, and small motors, there is need for the dispersion of information on the stability characteristics and unbalance response of plain journal bearings. Plain journal bearings operating under reduced-load conditions can exhibit large whirling and eventual failure of the bearing surface caused by the cyclic loading from the whirling journal. Isolated journal bearing performance studies can produce this much needed stability data and unbalance response information.

Manufacturers of turbine and compressors conduct test runs on actual equipment to verify the design and performance of their products. Each test unit may represent from $200,000 to in excess of a half-million dollars in hardware and instrumentation. A single bearing failure or rotor-shaft instability could destroy the entire test facility in a matter of seconds if the unit malfunction were not detected or the worst case would be if the test group could not recognize the presence of the instability and its eventual growth leading to a system failure.

The instrumentation necessary to observe the rotor shaft and housing motion is readily available and easily installed in existing test rigs. The complete shaft orbit should be observed to prevent the possibility of choosing the incorrect plane to observe the greatest motion. Systems having asymmetric bearing characteristics may exhibit instability in one

plane and stability in a plane at right angles to first. The incorporation of timing marks on the rotor orbits by the use of a reference mark on the shaft and a keyphasor probe is also of importance in the determination of the rate of whirl. Subharmonic and superharmonic whirl is easily distinguished if timing marks are placed on the whirl orbit trace.

The analytic simulation is important due to the fact that controlled excitation can be introduced in the model and the reaction observed from that isolated excitation. Combinations of external forces, unbalance, and internal damping can also be studied under controlled conditions and their response characteristics observed. In an actual system the exact form of excitation might be very hard to determine and the only information available is the response of the unit. The machine analyst must be able to infer from the performance of the machine the likely forms of excitation and the approximate magnitude. The easiest way to obtain this recognition ability is by the study of the controlled digital simulation of accurately simplified rotor-bearing models.

7.2 Summary of Major Results and Conclusions

This analysis has developed and presented results of steady-state response, transient simulation, and stability of rigid and flexible rotor models. The transient models developed included both linear and nonlinear bearing and support characteristics. The results and conclusions may be summarized as follows:

(1) Nonlinear transient analysis of complex rotor-bearing systems can be readily produced by digital computation by the approach presented in Chapter II.

(2) Simplified steady-state models of rotor systems have been presented and may be used in the design and analysis of rotating equipment in addition to providing initial conditions for the transient computer codes.

(3) Simplified rotor model transient computer codes have been developed to check the major transient program of this analysis (MODELJ) and are themselves a valuable tool to the machine analyst due to the simplicity of the input specifications.

(4) Transient simulation is necessary to verify the rate of growth of instabilities in nonlinear systems as predicted by linearized stability studies.

(5) The stability boundaries as given by Choudhury and Gunter (69) for the elastic mounted plain journal bearing have been verified by transient simulation.

(6) Unbalance was shown to be advantageous in vertical plain journal bearings having elastic support structures. This was previously reported for the rigid support vertical journal bearing.

(7) Phase angle measurements may be used in addition to amplitude response to analyze machine performance. The timing mark on elliptical orbits can be related to circular synchronous motion by graphical construction.

(8) It has been demonstrated that it is feasible to use the direct expansion approach on a 6 x 6 quadratic determinant to determine the stability of several important rotor models which had not been reported in the literature by this approach to date.

The key to time saving in the expansion is a zero check to avoid many needless operations.

(9) The phenomenon of passing through regions of instability has been demonstrated by the stability analysis of damper bearings and verified by transient simulation.

(10) It was shown that floating bush dampers indicated as stable in linearized stability criterions can have large sustained motion when large perturbations are imposed on the system.

(11) Numerous example rotors have been investigated and illustrate the versatility of the simulation approach to design and diagnosis of machine failures.

(12) Damped flexible supports can be used to increase the stable operating speed range of high-speed rotors. A properly designed support reduces the system transmissibility and maintains low level response for unbalance excitation in the stable operating speed range.

(13) Suppression of complex aerodynamic excitation can be studied for elastic mounted rotor-bearing systems by the stability program developed for the floating bush damper bearing.

(14) Timing marks on simulation orbits correspond to keyphasor timing marks placed on actual machines and are excellent means of helping to interpret the resulting orbits.

(15) The more complex transient programs are more useful for analysis of existing machine designs and evaluation of proposed system modifications than for producing extensive general design criteria.

(16) Steady-state response information will be essential for large complex rotor simulations to avoid costly undesired transient behavior. Zero initial conditions may be acceptable for impact unbalance studies but instabilities due to aerodynamic excitation, internal damping, and fluid-film bearings are best studied from steady-state initial conditions with small pertubations.

7.3 Suggestions for Future Research

This analysis has developed several computer codes for the simulation of rotor-bearing systems. Additional design criterion can be produced from the rotor models presented and will be of extreme interest to turbine and compressor manufacturers. Some of the areas that need extension are as follows:

(1) Extensive studies of rotor acceleration rates on forces transmitted and transient response.

(2) Inclusion of skewed disk excitation on the flexible rotor simulation for studies of transient behavior.

(3) Analysis of coupled lateral-torsional modes of vibration for the flexible rotor.

(4) Extensive stability maps produced showing the effect of damper supports on aerodynamic and internal friction instability.

(5) Stability and transient response of the flexible rotor-bearing system on closed-end pressurized damper supports.

(6) Verification of the response characteristics of the damped support by controlled experimental models of flexible rotor-bearing systems.

(7) Verification of the reduction of the transmissibility factors by experimental techniques.

(8) Extensive transient orbit studies of the response of the non-linear fluid-film dampers to large perturbations.

BIBLIOGRAPHY

1. Myklestad, N. O., "A New Method of Calculating Natural Modes of Uncoupled Bending Vibration of Airplane Wings and Other Types of Beams," Journal of Aeronautical Sciences, April, 1944, pp. 153-162.

2. Prohl, M. A., "A General Method for Calculating Critical Speeds of Flexible Rotors," Journal of Applied Mechanics, Sept., 1945, pp. 142-148.

3. Green, R. B., "Gyroscopic Effects on the Critical Speeds of Flexible Rotors," Journal of Applied Mechanics, December, 1948, pp. 369-376.

4. Wojnowski, R. F., and T. R. Faucett, "Critical Speeds of Two Bearing Machines with Overhung Weight," Journal of Engineering for Industry, Trans. ASME, Vol. 83, Series B, No. 4, November 1961, pp. 377-382.

5. Pilkey, W. and P. Y. Chang, "Avoiding Iterative Searches to Find Critical Speeds of Rotating Shafts With the Transfer Matrix Method," ASME Paper 71-Vibr-53.

6. Hess,M. S., "Vibration Frequencies for a Uniform Beam With Central Mass and Elastic Supports," Brief Notes, Journal of Applied Mechanics Trans. ASME, Vol. 86, Series E, September 1964, pp. 556-558.

7. Carnegie, W. and J. Thomas, "The Effects of Shear Deformation and Rotary Inertia on the Lateral Frequencies of Cantilever Beams in Bending," ASME Paper 71-Vibr-79.

8. Sorensen, A. and R. Larsen, "Determining Critical Speeds of a Crankshaft-Flywheel Assembly for An Outboard Motor," ASME Paper 71-Vibr-54.

9. Huang, T. C. and Frank C. C. Huang, "On Precession and Critical Speeds of Two-Bearing Machines With Overhung Weight," Journal of Engineering for Industry, Trans. ASME, Vol. 89, Series B, No. 4, November 1967, pp. 713-718.

10. Cunningham, B. E. and E. J. Gunter, "Critical Speeds of a Rotor in Rigidly Mounted, Externally Pressurized Air-Lubricated Bearings," NASA TN D-6350, Lewis Research Center, Cleveland, Ohio, 44135, May, 1971.

11. Yamamoto, T., "On the Critical Speeds of a Shaft," Memoirs of the Faculty of Engineering, Nagoya University, Japan, November, 1954, Vol. 6, No. 2, pp. 106-174.

12. Lund, J. W., "Rotor-Bearing Dynamics Design Technology, Part V" Technical Report AFAPL-TR-65-45, Aero Propulsion Lab, Wright-Patterson Air Force Base, Dayton, Ohio, May 1965.

13. Lund, J. W. and F. K. Orcutt, "Calculations and Experiments on the Unbalance Response of a Flexible Rotor," Journal of Engineering for Industry, Trans. ASME, Series B, Vol. 89, No. 4, November 1967, pp. 785-796.

14. Tang, T. M. and P. R. Trumpler, "Dynamics of Synchronous Precessing Turborotors with Particular Reference to Balancing; Part I, Theoretical Foundations," Journal of Applied Mechanics, March 1964.

15. Koenig, E. C., "Analysis for Calculating Lateral Vibration Characteristics of Rotating Systems With Any Number of Flexible Supports; Part I, Method of Analysis," Journal of Applied Mechanics, Trans. ASME, Vol. 28, 1961, pp. 585-590.

16. Gunter, E. J., "The Influence of Flexibly Mounted Rolling Element Bearings on Rotor Response, Part I: Linear Analysis," Journal of Lubrication Technology, Trans. ASME, pp. 59-75, January 1970.

17. Kemper, J. D. and R. S. Ayre, "Optimum Damping and Stiffness in a Nonlinear Four-Degree-of-Freedom System Subject to Shock Load," ASME Paper 70-WA/APM-18, published in Journal of Applied Mechanics.

18. Kirk, R. G. and E. J. Gunter, "Transient Journal Bearing Analysis," NASA CR-1549, Washington, D.C., June, 1970.

19. Kirk, R. G. and E. J. Gunter, "The Effect of Support Flexibility and Damping on the Synchronous Response of a Single-Mass Flexible Rotor," Journal of Engineering for Industry, Trans. ASME, Vol. 94, Series B, No. 1, February, 1972, pp. 221-232.

20. Jeffcott, H. H., "The Lateral Vibrations of Loaded Shafts in the Neighborhood of a Whirling Speed...the Effect of Want of Balance," Phil. Mag. Series 6, Vol. 37, 1919, p. 304.

21. Dunkerley, S., "On the Whirling and Vibration of Shafts," Phil. Trans. A, Vol. 185, 1894, p. 279.

22. Chree, C., "Whirling and Transverse Vibrations of Rotating Shafts," Phil. Mag. Series 6, Vol. 37, 1904, p. 304.

23. Rankine, W. A., "On the Centrifugal Force of Rotating Shafts," Engineer, London, Vol. 27, 1869, p. 249.

24. Thearle, E. L., "Dynamic Balancing of Rotating Machinery in the Field," Trans. ASME, Vol. 56, 1934, pp. 745-753.

25. Little, R. M., "The Application of Linear Programming Techniques to Balancing Flexible Rotors," Ph.D. Dissertation, University of Virginia, August 1971.

26. Church, A. H. and R. Plunkett, "Balancing Flexible Rotors," Journal of Engineering for Industry, Trans. ASME, Vol. 83, Series B, No. 4, November 1961, pp. 383-389.

27. Hundal, M. S. and R. J. Harker, "Balancing of Flexible Rotors Having Arbitrary Mass and Stiffness Distribution," Trans. ASME, Journal of Engineering for Industry, Vol. 88, Series B, May 1966, pp. 217-223.

28. Chi-Yeh, Han, "Balancing of High Speed Machinery," Trans. ASME, Journal of Engineering for Industry, Vol. 89, Series B, February 1967, pp. 111-118.

29. Goodman, T. P., "A Least-Squares Method for Computing Balance Corrections," Journal of Engineering for Industry, Trans. ASME, Vol. 86, August 1964, pp. 273-279.

30. Tessarzik, J. M., R. H. Badgley, and W. J. Anderson, "Flexible Rotor Balancing by the Exact Point-Speed Influence Method," Journal of Engineering for Industry, Trans. ASME, Vol. 94, Series B, No. 1, February 1972, pp. 148-158.

31. Lund, J. W. and J. Tonnesen, "Analysis and Experiments on Multi-Plane Balancing of a Flexible Rotor," Journal of Engineering for Industry, Trans. ASME, Vol. 94, Series B, No. 1, February 1972, pp. 233-242.

32. LeGrow, J. V., "Multiplane Balancing of Flexible Rotors - A Method of Calculating Correction Weights," ASME Paper 71-Vibr-52.

33. Kellenberger, W., "Should a Flexible Rotor Be Balanced in N or (N + 2) Planes?," Journal of Engineering for Industry, Trans ASME, Vol. 94, Series B, ASME Paper 71-Vibr-55.

34. Bishop, R. E. D. and A. G. Parkinson, "On the Use of Balancing Machines for Flexible Rotors," Journal of Engineering for Industry, Trans. ASME, Vol. 94, Series B, ASME Paper 71-Vibr-73.

35. Newkirk, B. L., "Shaft Whipping," Gen. Elec. Rev., Vol. 27, 1924, p. 169.

36. Robertson, D., "Whirling of a Journal in a Sleeve Bearing," Phil. Mag., Series 7, Vol. 15, No. 66, January 1933.

37. Newkirk, B. L. and H. D. Taylor, "Shaft Whipping Due to Oil Action in Journal Bearings," Gen. Elec. Rev., Vol. 28, 1925, pp. 559-568.

38. Hagg, A. C., "The Influence of Oil Film Journal Bearings on the Stability of Rotating Machines," Journal of Applied Mechanics, Vol. 68, 1946, p. 211.

39. Gunter, E. J., "Dynamic Stability of Rotor-Bearing Systems," NASA SP-113, 1966.

40. Ruhl, R. L., "Dynamics of Distributed Parameter Rotor Systems: Transfer Matrix and Finite," Ph.D. Dissertation, Cornell University, January, 1970.

41. Badgley, R. H., "Turborotor Instability— Dynamic Unbalance, Gyroscopic, and Variable-Speed Effects With Finite-Length, Cavitated, Fluid-Film Bearings," Ph.D. Dissertation, Cornell University, June 1967.

42. Kirk, R. G., "Transient Journal Bearing Analysis," M.M.E. Thesis, University of Virginia, June, 1967.

43. Choudhury, P. De., "Dynamic Stability of Flexible Rotor-Bearing Systems," Ph.D. Dissertation, University of Virginia, June 1971.

44. Newkirk, B. L., "Journal Bearing Instability," Inst. of Mech. Engrs., ASME International Conference on Lubrication and Wear, London, October 1957 (Review Paper, Session I, No. 2).

45. Newkirk, B. L., "Varities of Shaft Disturbances Due to Fluid Films in Journal Bearings," Trans. ASME, Vol. 78, 1956, p. 985.

46. Morrison, D. and A. N. Patterson, "Criteria for Unstable Oil-Whirl of Flexible Rotors," The Institute of Mech. Eng. Proceedings, 1964-65, Vol. 179, Part 3J, p. 45.

47. Hori, Y., "Theory of Oil Whip," Journal of Applied Mechanics, Vol. 26, Trans. ASME, Series E, Vol. 81, 1959, p. 189.

48. Holmes, R., "The Vibration of a Rigid Shaft on Short Sleeve Bearings," J. Mech. Eng. Sci., 1960, Vol. 2, p. 337.

49. Pinkus, O. and Sternlicht, B., Theory of Hydrodynamic Lubrication, McGraw-Hill Book Co., New York and London, 1961.

50. Ruhl, R. L. and J. F. Booker, "A Finite Element Model for Distributed Parameter Turborotor Systems," Journal of Engineering for Industry, Trans. ASME, Vol. 94, Series B., No. 1, February 1972, pp. 126-132.

51. Dimentberg, F. M. Flexural Vibrations of Rotating Shafts, Butterworths, London, 1961.

52. Tondl, A., Some Problems of Rotor Dynamics, Chapman Hall, London, 1965.

53. Alford, J. S., "Protecting Turbomachinery From Self-Excited Rotor Whirl," J. of Engr. for Power, Trans. ASME, Vol. 87, October 1965, pp. 333-344.

54. Kerr, J., "The Onset and Cessation of Half-Speed Whirl in Air-Lubricated Self-Pressurized Journal Bearings," Proc. Instn. Mech. Engrs., 1965-66, Vol. 180, Paper 22, pp. 145-153.

55. Jennings and Ocvirk, "The Simulation of Bearing Whirl on an Electronic-Analog Computer," Journal of Basic Engineering, Trans. ASME, Vol. 84, Series D, December, 1962, pp. 503-510.

56. Reddi, M. M. and P. R. Trumpler, "Stability of the High-Speed Journal Bearing Under Steady Load--I. The Incompressible Film," Journal of Engineering for Industry, Trans. ASME, Series B, Vol. 84, 1962, pp. 351-358.

57. Castelli, V. and J. T. McCabe, "Transient Dynamics of a Tilting Pad Gas Bearing System," Journal of Lubrication Technology, Trans. ASME, Series F, Vol. 89, No. 3, October 1967, pp. 449-509.

58. Badgley, R. H. and J. F. Booker, "Turborotor Instability: Effect of Initial Transient on Plane Motion," Journal of Lub. Tech., Trans. ASME, October, 1969, pp. 625-633.

59. Kirk, R. G. and E. J. Gunter," The Influence of Damper Supports on the Dynamic Response of a Single Mass Flexible Rotor - Part I, Linear System," RLES, No. ME-4040-105-71U, March 1971, University of Virginia for NASA Lewis Research Center, Contract NGR 47-005-050.

60. Akers, A., S. Michaelson and A. Cameron, "Stability Contours for a Whirling Finite Journal Bearing," Journal of Lub. Tech., Trans. ASME, Series F, No. 1, Vol. 93, January 1971, pp. 177-190.

61. Shapiro, W. and R. Colsher, "Implementation of Time Transient and Step-Jump Dynamic Analyses of Gas-Lubricated Bearings," Journal of Lub. Tech., Trans. ASME, Series F, Vol. 92, July 1970, pp. 518-529.

62. Falkenhagen, G. L., E. J. Gunter and E T. Schuller, "Stability and Transient Motion of a Vertical Three-Lobe Bearing System," ASME Paper 71-Vibr-76.

63. Paul, B. and D. Krajeinovic, "Computer Analysis of Machines with Planar Motion - Part 1: Kinematics," Journal of Applied Mechanics, Vol. 37, No. 3, Trans. ASME, Vol. 92, Series E, September 1970, pp. 697-702.

64. Paul, B. and D. Krajeinovic, "Computer Analysis of Machines with Planar Motion - Part 2: Dynamics," Journal of Applied Mechanics, Vol. 37, No. 3, Trans. ASME, Vol. 92, Series E, September 1970, pp. 703-712.

65. Bammert, K. and G. Krey, "Dynamic Behavior and Control of Single-Shaft Closed-Cycle Gas Turbines," Journal of Engineering for Power, Trans. ASME, Vol. 93, Series A, No. 4, October 1971, pp. 447-453.

66. Shen, F. A., "Transient Flexible-Rotor Dynamic Analysis - Part 1: Theory," ASME Paper 71-Vibr-92.

67. Childs, D. W., "A Simulation Model for Flexible Rotating Equipment," Journal of Engineering for Industry, Trans. ASME, Vol. 94, Series B, No. 1, February 1972, pp. 201-209.

68. Gunter, E. J., "The Influence of Internal Friction on the Stability of High Speed Rotors," Journal of Engineering for Industry, Trans. ASME, November 1967, pp. 683-688.

69. Choudhury, P. De and E. J. Gunter, "Dynamic Stability of Flexible Rotor-Bearing Systems," RLES, Report No. ME-4040-104-70U, University of Virginia, December 1970.

70. Gunter, E. J., Critical Speeds of Flexible Rotors, CRITSPD, Computer Program on Library, University of Virginia.

71. Langhaar, H. L., Energy Methods in Applied Mechanics, John Wiley and Sons, Inc., New York and London, 1962, pp. 255-259.

72. Poritsky, H., "Rotor Stability," Proceedings of the Fifth U.S. National Congress of Applied Mechanics, ASME, pp. 37-61, 1966.

73. Elrod, H. G., J. T. McCabe, T. Y. Chu, "Determination of Gas Bearing Stability by Response to a Step-Jump," Journal of Lub. Tech., Trans. ASME, Vol. 89, Series F, No. 4, pp. 293-494, October 1967.

74. Lund, J. W., "The Stability of an Elastic Rotor in Journal Bearings with Flexible, Damped Supports," Journal of Applied Mechanics, Trans. ASME, Series E, Vol. 87, No. 4, December 1965, pp. 911-920.

75. Powell, J. W. and M. C. Tempest, "A Study of High Speed Machines with Rubber Stabilized Air Bearings," Journal of Lub. Tech., Trans. ASME, ASME Paper No. 68-Lubs-9.

76. Marsh, H., "The Stability of Self-Acting Gas Journal Bearings With Noncircular Members and Additional Elements of Flexibility," Journal of Lub. Tech., Trans. ASME, Vol. 91, Series F, No. 1, January 1969, pp. 113-120.

77. Booker, J. F., "Dynamically-Loaded Journal Bearings: Numerical Application of the Mobility Method," Journal of Lubrication Technology, Trans. ASME, Series F, No. 1, Vol. 93, January 1971, pp. 168-176.

78. Hagg, A. C., and P. C. Warner, "Oil Whip of Flexible Rotors," Trans. ASME, Vol. 75, October, 1953, pp. 1339-1344.

79. Shawki, G. S. A., "Whirling of a Journal Bearing; Experiments Under No-Load Conditions," Engineering, Vol. 179, 1955, pp. 243-246.

80. Newkirk, B. L., and J. F. Lewis, "Oil-Film Whirl - An Investigation of Disturbances Due to Oil Films in Journal Bearings," Trans. ASME, Vol. 78, January 1956, pp. 21-27.

81. Orbeck, Finn, "Theory of Oil Whip for Vertical Rotors Supported by Plain Journal Bearings," Trans. ASME, Vol. 80, October 1958, pp. 1497-1502

82. Rentzepis, G. M., and B. Sternlicht, "On the Stability of Rotors in Cylindrical Journal Bearings," Journal of Basic Engineering, Trans. ASME, Vol. 84, Series D, December, 1962, pp. 521-532.

83. Cole, J. A., "Film Extent and Whirl in Complete Journal Bearings," Inst. Mech. Eng., 1968, Paper 59, pp. 186-189.

84. Tolle, G. C. and D. Muster, "An Analytical Solution for Whirl in a Finite Journal Bearing With a Continuous Lubricating Film," Journal of Engineering for Industry, Trans. ASME, Vol. 91, Series B, No. 4, November 1969, pp. 1189-1195.

85. Sweet, J. and J. Genin, "Squeeze Film Bearings for the Elimination of Oil Whip," Journal of Lubrication Technology, Trans. ASME, Vol. 93, Series F, No. 2, April 1971, pp. 252-261.

86. Harrison, H. L. and J. G. Bollinger, Introduction to Automatic Controls, International Textbook Company, Scranton, Penn., 1964, pp. 329-331.

87. Gunter, E. J. and P. De Choudhury, "Rigid Rotor Dynamics," NASA CR 1391, Washington, D.C., August 1969.

88. Gunter, E. J., Computer Code BALANC4 on Permanent Library, Computer Science Center, University of Virginia.

89. Tanaka, M. and Y. Hori, "Stability Characteristics of Floating Bush Bearings," Journal of Lubrication Technology, Trans. ASME, ASME Paper No. 71-Lub-9.

90. Hill, H. C., "Slipper Bearings and Vibration Control in Small Gas Turbines," Trans. ASME, Vol. 80, 1958, pp. 1756-1964.

91. Dworski, J., "High-Speed Rotor Suspension Formed by Fully Floating Hydrodynamic Radial and Thrust Bearings," Journal of Engineering for Power, Trans. ASME, Series A, Vol. 86, No. 2, April 1964, pp. 149-160.

92. Orcutt, F. K., and C. W. Ng, "Steady-State and Dynamic Properties of the Floating-Ring Journal Bearing," Journal of Lubrication Technology, Trans. ASME, Series F, Vol. 90, No. 1, January 1968, pp. 243-253.

93. McGrew, J. M., Discussion of paper by E. J. Gunter, Journal of Lubrication Technology, Trans. ASME, January 1970.

*U.S. GOVERNMENT PRINTING OFFICE: 1973-739-152/28

NATIONAL AERONAUTICS AND SPACE ADMINISTRATION
WASHINGTON, D.C. 20546

OFFICIAL BUSINESS
PENALTY FOR PRIVATE USE $300

SPECIAL FOURTH-CLASS RATE BOOK

POSTAGE AND FEES PAID
NATIONAL AERONAUTICS AND SPACE ADMINISTRATION
451

U.S.MAIL

POSTMASTER : If Undeliverable (Section 158 Postal Manual) Do Not Return

"The aeronautical and space activities of the United States shall be conducted so as to contribute . . . to the expansion of human knowledge of phenomena in the atmosphere and space. The Administration shall provide for the widest practicable and appropriate dissemination of information concerning its activities and the results thereof."

—NATIONAL AERONAUTICS AND SPACE ACT OF 1958

NASA SCIENTIFIC AND TECHNICAL PUBLICATIONS

TECHNICAL REPORTS: Scientific and technical information considered important, complete, and a lasting contribution to existing knowledge.

TECHNICAL NOTES: Information less broad in scope but nevertheless of importance as a contribution to existing knowledge.

TECHNICAL MEMORANDUMS: Information receiving limited distribution because of preliminary data, security classification, or other reasons. Also includes conference proceedings with either limited or unlimited distribution.

CONTRACTOR REPORTS: Scientific and technical information generated under a NASA contract or grant and considered an important contribution to existing knowledge.

TECHNICAL TRANSLATIONS: Information published in a foreign language considered to merit NASA distribution in English.

SPECIAL PUBLICATIONS: Information derived from or of value to NASA activities. Publications include final reports of major projects, monographs, data compilations, handbooks, sourcebooks, and special bibliographies.

TECHNOLOGY UTILIZATION PUBLICATIONS: Information on technology used by NASA that may be of particular interest in commercial and other non-aerospace applications. Publications include Tech Briefs, Technology Utilization Reports and Technology Surveys.

Details on the availability of these publications may be obtained from:

SCIENTIFIC AND TECHNICAL INFORMATION OFFICE

NATIONAL AERONAUTICS AND SPACE ADMINISTRATION

Washington, D.C. 20546